THE PROBLEM OF THE MODELING UNCERTAINTIES IN THE PARADIGM OF THE ACTIVE DISTURBANCE REJECTION CONTROL

RADOSŁAW PATELSKI, M.ENG.

DOCTORAL DISSERTATION

Faculty of Control, Robotics and Electrical Engineering
Institute of Automatic Control and Robotics
Poznan University of Technology

Supervisor: Dariusz Pazderski, Ph.D., D.Sc.

Poznań, Poland, 2023

Radosław Patelski: *The Problem of the Modeling Uncertainties in the Paradigm of the Active Disturbance Rejection Control,* Doctoral Dissertation, Poznan University of Technology, 2023

ABSTRACT

In the following dissertation, the theoretical and experimental results on the problem of modeling uncertainties in the system control within the Active Disturbance Rejection Control paradigm are presented. The considered concept proposes that, in the presence of unmodeled dynamics or unmeasurable external disturbances, it is possible to employ the Extended State Observer algorithm to online estimate a difference between the controlled plant and its assumed nominal model. It is advocated that this measure of uncertainty of the dynamics of the plant can be then used in the control law to effectively compensate for the unknown dynamics and achieve high performance without the perfect knowledge of the system.

Various examples from both academia and industry have proven the quality of such an approach. Yet, its premises are based on the assumption of a specific form of the model uncertainties and disturbances affecting the plant, which is often not satisfied in practice. In this work, the performance and robustness of the Active Disturbance Rejection Control in the presence of unmodeled dynamics which may not conform to this nominal structure are discussed. Namely, the model of the dynamics subject to the uncertainty of both input gain and assumed drift term is considered and the performance of the discussed control scheme is analyzed through the Lyapunov approach. To further extend the insights into the problem of Active Disturbance Rejection Control performance in the presence of modeling uncertainties, a series of individual and specific scenarios is also discussed, covering a wider range of control tasks which may not be consistent with the characteristics assumed in the earlier analysis.

As the possible methods of increasing the robustness of the considered control schemes to the presence of modeling uncertainties the recently proposed novel Parameter Identifying Extended State Observer and Parameter Identifying Disturbance Rejection Control are discussed. These algorithms stem from the Extended State Observer and Active Disturbance Rejection Control approaches but incorporate the adaptive terms employing the gradient adaptation law to online identify the model of the plant and fine tune the controller to best fit the dynamics of the real object. The applicability and stability conditions of the proposed approaches are discussed, and their usability is verified by extensive simulation and experimental testing. It is demonstrated that the introduction of the adaptive identification of the dynamics of the plant within the Active Disturbance Rejection

Control algorithms can significantly improve their performance by ensuring asymptotic convergence of all errors in the system.

In this thesis, particular attention is given to the application of the Active Disturbance Rejection Control and Parameter Identifying Disturbance Rejection Control approaches to robotic manipulators and autonomous mobile robots. The experimental validation of the discussed schemes is performed mainly using a robotic telescope mount designed and constructed by a team that includes the author of this work, and a mobile hovercraft robot adapted for scientific research solely by the author of this dissertation. The structure and design of these devices are also given in this paper in the scope corresponding to the involvement of the author.

STRESZCZENIE

W niniejszej rozprawie przedstawiono teoretyczne i eksperymentalne wyniki badań nad problemem niepewności modelowania w systemach sterowania opartych o paradygmat Aktywnej Kompensacji Zaburzeń (ang. Active Disturbance Rejection Control, ADRC). W ramach tego paradygmatu wnioskuje się, iż w obecności niemodelowanej dynamiki lub niemierzalnych zewnętrznych zaburzeń, możliwe jest zastosowanie Obserwatora Stanu Rozszerzonego (ang. Extended State Observer, ESO) by w czasie rzeczywistym estymować różnicę pomiędzy dynamiką sterowanego obiektu, a przyjętym modelem nominalnym. Proponuje się, by tak uzyskany wskaźnik niepewności modelu wykorzystać następnie w projekcie prawa sterowania w celu efektywnej kompensacji nieznanej dynamiki obiektu i uzyskania wysokiej jakości sterowania mimo braku dokładnej znajomości układu.

Różnorodne przykłady zastosowania, zarówno w warunkach akademickich jak i przemysłowych, wykazały wysoką skuteczność takiego rozwiązania. Teoretyczne podstawy tej metody oparte są jednak na założeniu pewnego modelu niepewności i zaburzeń oddziałowujących na układ, które często nie jest spełnione w warunkach praktycznych. W niniejszej pracy, przedstawiono wyniki badań nad skutecznością i odpornością sterowania z Aktywną Kompensacją Zaburzeń w obecności niemodelowanej dynamiki nie spełniającej tego założenia. W szczególności, rozważono układy dynamiczne z niepewnością w torze wejścia oraz dryfu i, wykorzystując podejście Lyapunova, zbadano właściwości układów sterowania opartych o metodę Aktywnej Kompensacji Zaburzeń. By poszerzyć zakres uzyskanych wyników na temat właściwości sterowania z Aktywną Kompensacją Zaburzeń w obecności niepewności modelowania, przedstawiono i zbadano także zestaw wybranych problemów z zakresu sterowania, nie objętych przez wcześniejszą analizę.

Jako potencjalną metodę zwiększenia skuteczności rozważanej metody w obliczu niepewności modelowania, w pracy przedstawiono także niedawno zaproponowane techniki Obserwatora Stanu Rozszerzonego z Identyfikacją Parametryczną (ang. Parameter Identifying Extended State Observer, PIESO) oraz Sterowania z Kompensacją Zaburzeń z Identyfikacją Parametryczną (ang. Parameter Identifying Disturbance Rejection Control, PIDRC). Algorytmy te zaproponoawne zostały w oparciu o struktury Obserwatora Stanu Rozszerzonego oraz Sterowania z Aktywną Kompensacją Zaburzeń i wzbogacone o adaptacyjne składniki wykorzystujące gradientowe prawa adaptacji w

celu identyfikacji modelu zaburzenia w czasie rzeczywistym i dopasowania struktury sterownika do rzeczywistej dynamiki obiektu. W pracy przedstawiono warunki stabilności i stosowalności zaproponowanych metod, a ich skuteczność w problemach praktycznych została zweryfikowana przez wyczerujące badania symulacyjne i eksperymentalne. Wykazano, że wprowadzenie składnika adaptacyjnego w celu identyfikacji dynamiki rzeczywistego obiektu pozwala znacząco zwiększyć skuteczność metod Aktywnej Kompensacji Zaburzeń i uzyskać asymptotyczną zbieżność wszystkich błędów w układzie regulacji.

W niniejszej rozprawie szczególną uwagę poświęcono zastosowaniom techniki Aktywnej Kompensacji Zaburzeń i Kompensacji Zaburzeń z Identyfikacją Parametryczną do sterowania robotycznymi manipulatorami oraz autonomicznymi robotami mobilnymi. Eksperymentalne badania rozważanych metod przeprowadzono w istotnej części z wykorzystaniem zrobotyzowanego montażu teleskopu astronomicznego zaprojektowanego i wykonanego przez zespół badawczy którego członkiem był autor tej rozprawy, oraz mobilnego zrobotyzowanego poduszkowca przygotowanego do celów badawczych przez autora tej rozprawy. Struktura obu tych narzędzi również została krótko omówiona w zakresie odpowiadającym zaangażowaniu autora tej rozprawy.

CONTENTS

1 INTRODUCTION

It may happen, however, that the characteristics demanded of the equalizer cannot be prescribed in advance, either because the characteristics of the associated apparatus are not known with sufficient precision, or because they vary with time.

— H. W. Bode, 1938 [31]

The hereby presented dissertation summarizes the research carried out by the author throughout the five years of his doctoral studies at the Poznan University of Technology. This work has been fully devoted to the problems of automatic control and has started as an investigation into the general problem of robustness of the Active Disturbance Rejection Control (ADRC) and Extended State Observer (ESO) to the modeling uncertainties which do not conform to the commonly accepted assumptions on the structure of the controlled system. The initial years of the doctoral studies have thus been focused on the search for different types of disruptive dynamics commonly occurring in the practical tasks in the field of automatic control and robotics, and analysis of their influence on the performance of the algorithms based on the ADRC scheme. These efforts are covered in the first half of this thesis. The findings of these studies have led the author to the formulation of the novel adaptive Parameter Identifying Extended State Observer (PIESO) and Parameter Identifying Disturbance Rejection Control (PIDRC) schemes combining the merits of the ADRC approach and indirect identification algorithms. Development, analysis, and validation of these new estimation, identification, and control approaches are presented in the second part of this dissertation.

In this chapter, the wide background of the conducted research is portrayed. Namely, the general problem of modeling uncertainties in the automatic control is defined, and some solutions to this issue as reported in the literature are recalled and shortly presented. In the further sections of this chapter, the scope, contribution, and structure of this work are precisely defined and the list of embraced nomenclature choices is formulated for a future reference.

1.1 PARAMETRIC UNCERTAINTY IN DYNAMIC SYSTEMS

Automatic control can be defined as a deliberate influence, governed by an autonomous controller device, on the evolution of a process [133]. How to design and implement such a controller apparatus

has been a subject of interest since at least the 18th century and the invention of a centrifugal governor by J. Watt. Nonetheless, the rigorous studies of the principles of automatic control have not been carried out until 1868 when J. C. Maxwell published a seminar paper describing the dynamics of the different types of governors [193], setting a cornerstone for a use of mathematical models of the process, in form of sets of differential equations, for development and analysis of control techniques. Such an approach has become the standard scientific methodology in the field of automatic control, establishing a foundation for the development of a model-based control paradigm.

The embracement of the model-based approach imposes on the designer the obligation to create and develop the mathematical description of the plant in order to design and implement the control algorithm. Unfortunately, obtaining a precise and accurate model of the physical systems is an exercise that may be time-consuming, expensive, and often even impossible to perform. These difficulties may be caused by unknown physical properties of the system, changes in environmental working conditions, or unexpected external forces affecting the plant, and may severely hinder the process of system modeling. As a result, the mathematical model of the system dynamics used in the design and synthesis of the control algorithm often deviates from the real behavior exhibited by the plant. The uncertainties affecting the dynamic systems can be categorized by taking into account various aspects of their presence.

1. On basis of the extent of possessed knowledge about the model of the system [30]
    - parametric uncertainty – the dynamics of the real plant are properly modeled by the assumed equations, save for the incorrectly chosen values of constant parameters,
    - structural uncertainty – the structure of the assumed model does not describe the real behavior of the plant with a required accuracy for any choice of constants.
2. On basis of the dependence of uncertainty on certain variables
    - input uncertainty – the unknown effects can be expressed as a function of the input variable,
    - drift uncertainty – the plant uncertainty depends on the time or momentary state of the system and is not directly dependent on the control variable.
3. On basis of the possibility to directly decouple the uncertain dynamics [20, 51]

- matched uncertainty – the uncertainty is present in the same path as the input variable and could be easily compensated for had it be known,
- unmatched uncertainty – the unknown dynamics affect the paths which are not directly controlled by the input variables.

4. On basis of the expected properties of the uncertain dynamics
   - bounded uncertainty – the unmodeled dynamics or their norm satisfy some algebraic bounds under some predefined conditions,
   - unbounded uncertainty – the disturbance present in the system may grow to arbitrarily large values at some states of the plant.
5. On basis of the predictability of the unknown dynamics [60]
   - deterministic uncertainty – the system uncertainty can be expressed as some deterministic functions and could be predicted had this function be known,
   - stochastic uncertainty – the system is affected by the uncertainty that cannot be predicted except for some of its statistical properties.

Moreover, various uncertainties not easily conforming to the proposed classification can arise in the control systems, including unmodeled time-delays [139, 310] or incorrectly assumed order of the plant [75, 128]. The proposed division of the modeling uncertainties is not an exhaustive one and other classes of disturbances could be denoted depending on the specific context of the considered system. In this work, only the systems burdened by the deterministic disturbances satisfying some boundedness properties are considered. Special consideration is given to a class of systems with matched parametric uncertainties applying to both input and drift. Some attention is also paid to specific scenarios featuring structural uncertainties concerning a drift term, an input path, and an unknown degree of the system. In the latter parts of this dissertation, a new control solution is proposed to overcome the problem of matched parametric uncertainties of the drift part of the dynamics.

The problem of modeling uncertainty is of extreme importance in both mobile and manipulation robotics due to the growing range of applications of the robotic systems and tasks they are expected to handle. According to the International Federation of Robotics, in 2020 alone almost 400 thousand new units of industrial robots were introduced worldwide which increased the global stack of such devices by ten percent. In the same year, over 19 million new service

robots, corresponding mainly to mobile robots of various types, were manufactured [307, 308]. Development of the methods of reliable control of these devices, even in the presence of imperfect modeling or disturbances, is thus a crucial task for modern robotics. Uncertainties in such systems may be caused by the changes in an unpredictable environment where the robot operates, especially in the presence of people or other devices moving in the same space, imperfection of the employed sensors, the performance of which is limited by noise and quantization, low accuracy of used actuators which are subject to wear and tear, or conscious choices on algorithmic approximations of both control schemes and mathematical models [284]. The evolution of scientific interest in these problems is visualized in Fig. 1.1.

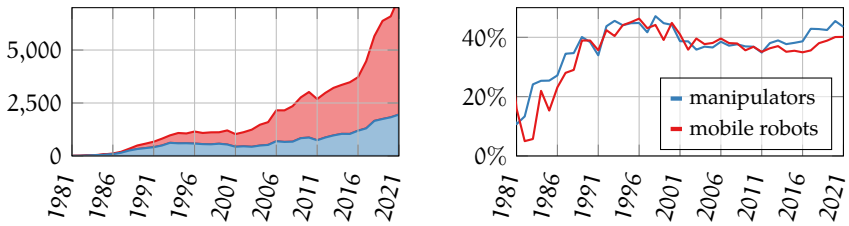

(a) Number of papers

(b) Percent of all papers

Own work based on [118]

Figure 1.1: Search results of the IEEE Xplore database for papers published in each year with terms *robot* and either *manipulator* or *mobile* containing also words *robust* or *uncertain*. In the last decades, almost half of the papers on mobile and manipulator robotics acknowledge also the problems of uncertainty and robustness.

At the basic level, the modeling of the robotic system consists of a description of its kinematics and dynamics, both of which can be affected by modeling uncertainties [289]. The kinematics of the manipulators are usually described using a model derived from a set of constant parameters unambiguously defining the relations between the positions of the joints of the robot. These representations, like the Denavit-Hartenberg model, the Sheth-Uicker model, or the so-called Unified method, require the designer to perform precise measurements of the physical dimensions of the robot. While the required measurements differ in each representation, typically the lengths and twists of the links, as well as offsets along the axes of rotation, or some quantities derived from these, are necessary to successfully generate the model of a robot [264]. The imperfection of any of these measurements, or change of these parameters e. g. due to bending of loaded links, may be a source of some modeling uncertainty. In the context of mobile robotics, the kinematic model describes the relationship between the local velocities and control variables of the robot with

its movements in the global coordinate system. Modeling errors can arise, if the model does not account for e. g. the slip of the wheels [146, 261], operation in uneven terrain [39] or if the dimensions of the robot, including a wheelbase or wheel radius, are not perfectly known [55]. The description of the dynamics of the robotic systems may contain the influence of friction effects in joints and motors, which may vary with mileage and temperature change [33, 263], or centrifugal forces, depending on the mass and inertia of the elements of the robot [213, 295]. The flexibility of the manipulator robots [45, 351] or wheel slip of the mobile robots [306] can also be perceived as a source of dynamic uncertainties. Moreover, even if the obtained nominal model accurately describes the dynamics of the plant, the robotic systems are subject to wearing and aging leading to a deterioration of the performance of the robot itself and thus to changes in its dynamics. In this context, the means to alleviate the impact of the appearing uncertainties on the performance of the system are vital to ensure the reliability and fault-free operation of the plant [1, 6]. Some common examples of modeling uncertainties in the standard control plants are given in [3]. Other instances of the robotic systems subject to certain uncertainties and disturbances are given in Fig. 1.2.

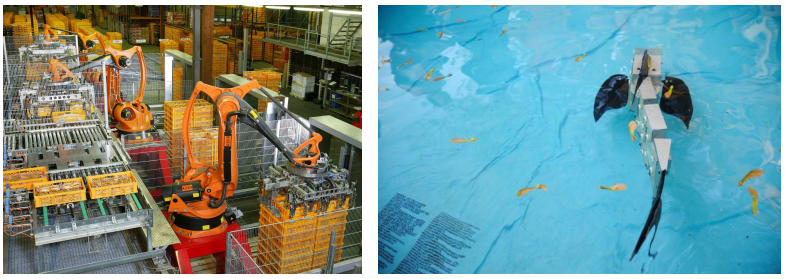

(a) Robotic manipulators (b) Swimming robot

Factory Automation by KUKA Roboter GmbH, public domain
Robot Fish by Kuba Bożanowski, CC BY 2.0

Figure 1.2: Robotic systems subject to disturbances and modeling uncertainties. Unknown properties of the load or environment may strongly impact the performance of the system.

No matter the type and source of the uncertainty that affects the system, in the presence of a difference between the mathematical description and the behavior of the real plant two kinds of problems arise that require special attention [348]:

- analysis problem – how to determine whether a given controller guarantees a satisfactory performance in the presence of certain classes of disturbances, noises, and uncertainties,

- synthesis problem – how to design a controller guaranteeing satisfactory performance in the presence of certain classes of disturbances, noises, and uncertainties.

While the two are distinct in their scope of interest, both ultimately consider the same question of whether it is possible to efficiently control the real system without explicit knowledge about parts of its dynamic model. The controller able to perform these tasks is said to be robust to the chosen class of uncertainties. The detailed reports on the history of early research on the robustness of control schemes have been published in [57, 58, 251] and are recalled here in brief.

The earliest results on the robustness of the control schemes have considered only the linear systems and propounded the frequency-domain stability margin criteria to evaluate the robustness of linear systems to uncertain gain and phase shift of the plant [32, 211]. These allow the designer to investigate the admissible uncertainty of gain and phase shift of the linear system for which the control scheme remains asymptotically stable. The later developments in the field of robustness analysis have come chiefly in the form of the small-gain theorem [105, 331] and analysis based on the Lyapunov second method [89, 92, 200] with both approaches being applicable to linear and nonlinear systems. The small-gain theorem considers the uncertain dynamic system as a set of interconnected subsystems with external inputs and says that to maintain the stability of the whole, the high gains of one subsystem have to be compensated for by the small gains of the other. From the formulation of the small-gain theorem, one can directly derive the proposition to use the high-gain feedback to overcome the parametric and structural uncertainties in nonlinear systems. The standard approach to the uncertain system analysis using a Lyapunov method is to seek a function that meets the conditions of Lyapunov second method for the undisturbed system, and then investigate its evolution in the presence of uncertainties satisfying some expected properties, e. g. being expressed by Lipschitz or bounded functions. From such an inquiry, one can establish some feasible set of uncertainties for which the system stability is maintained. Other means of robust system analysis include the singular perturbation method investigating the systems subject to small deviations of the evolution of state variables [140], approaches based on H_∞ theory treating the uncertain model as a simplified linear system with parameters varying in time [349], or passivity theorem assuming the uncertainty of the plant can be expressed as a positive-real transfer function [93]. A comprehensive overview and more details on these and other methods of robust stability analysis can be found in the recent review papers [127, 234] or modern textbooks on robust and nonlinear control [137, 302] and references therein.

Importantly, due to the character of the uncertainty, which is in its nature unknown, the methods of stability analysis of uncertain or disturbed systems are inherently conservative, and obtained results are often based on some predictions of the worst-case scenario possible for the considered class of modeling errors. There is thus a constant need for new studies investigating both more specific and more general types of uncertainties, to obtain either less conservative results or the results applicable to wider classes of the dynamic systems. In this work, the robustness and stability of the investigated control methods are established mainly through the Lyapunov-based analysis of the uncertainties which are expected to satisfy specific boundedness conditions. As auxiliary tools, the standard methods of analysis of linear systems are employed whenever they fit the character of the studied systems.

1.2 CONTROL SOLUTIONS

To answer the problem of the modeling uncertainties in dynamic systems, a wide range of control algorithms characterized by high robustness to unmodeled dynamics has been considered throughout the years. The earliest results on the robust control schemes in robotics have been summarized in [2, 197, 252], while a wide review of modern robust control schemes has been recently presented in [244]. The authors of these papers have outlined multiple approaches proposed to cope with the lack of precise knowledge of the system dynamics.

The most basic and classic approach often employed by control practitioners consists of the standard PID controller, which is de facto default solution in many practical situations, tuned to achieve a satisfying performance in the presence of some modeling uncertainty. Such tuning is often either derived from some roughly identified model of the system in the model-based approach or is iteratively obtained in an attempt to optimize some criterion function based on the input-output data in the model-free procedure [4, 34, 271]. Tuning schemes have been proposed to answer the specific requirements, including guarantee of chosen gain and phase margins in linear system [157] or compensation of time-delays [214, 262]. Despite high scientific interest in the robustification of the PID controllers, studies show that in practical applications only about a quarter of employed PID controllers offer satisfactory performance [212]. Other publications contest also the claimed robustness of this well-known algorithm [296].

Classic algorithms designed specifically to deal with the problem of modeling uncertainty include robust H_∞ controllers, algorithms employing a notion of passivity, or the sliding mode control (SMC). H_∞ algorithms, nominally designed for the linear systems, have initially

been proposed as an answer to problems of optimal control and only later evolved into a method of robust control [59]. To this end, a sensitivity function, corresponding to a transfer function of the disturbance, is incorporated into the cost function which is then optimized, what results in a proposition of a suitable control law [87, 290]. Recently, the application of this approach to systems with nonlinearities [106, 123] or time-delays [312] has also been presented. The use of the passivity theorem to design the robust controllers rely on the notion that a passive system can be easily stabilized by the control law which is itself independent of the model of the plant, even if only a weak form of passivity is exhibited by the system [132]. Thus, multiple control algorithms seeking to ensure the passivity of the uncertain systems have been proposed in the literature [136, 278]. The notion that the robustness can be ensured by the use of the controller independent of the model of the system is also used in the SMC method, where the control law is designed to force the states of the system to slide along a predefined trajectory in the phase space and does not depend on the dynamics of the plant [292]. This control law is then enhanced with terms responsible for the transition of the state of the plant from the initial condition to this sliding trajectory. The sliding mode controllers, characterized by their high robustness to system uncertainties and external disturbances, fast dynamic response, and intuitive implementation, became one of the standard solutions in the field of automatic control [141]. Multiple variants of this method have been proposed to improve its efficiency or widen its applicability [18, 77], including the Terminal SMC aimed at increasing a convergence speed [327], the Integral SMC eliminating the reaching phase and enforcing sliding movement in an entire response of the plant [221], and High Order SMC [260, 293] or SMC with an exponential reaching law [65], both seeking to limit a chattering effect caused by standard SMC approach.

The advances in the field of robust control have led also to the formulation of new algorithms, designed to offer satisfactory performance in the presence of unmodeled dynamics, in form of solutions employing the Disturbance Observers (DOB). These approaches propose the use of some kind of an observer able to online estimate the momentary impact of the system uncertainty. The disturbance can be then compensated for by the control law, thus separating the control of a nominal system, which can be performed with any suitable non-robust controller, and robust elimination of disturbing dynamics. In its standard form, the DOB scheme is designed for disturbed or uncertain linear systems and consists of a linear observer constructed based on a nominal model of the plant and some filtering transfer functions chosen by the designer [163, 259]. These results have later been extended to the class of nonlinear systems by replacing the linear

filters used in the observer design with some nonlinear dynamics [17]. Other advances in the design of DOB control include the High Order DOB offering better performance at a cost of reduced robustness [254] or Finite Time DOB proposed to achieve the disturbance compensation in the finite time horizon [160]. The methods of Uncertainty and Disturbance Estimator (UDE) [321], Generalized Proportional Integral Observer (GPIO) [191, 309], Unknown Input Observer (UIO) [95] or Active Disturbance Rejection Control (ADRC) [314, 326] may also be perceived as custom solutions within the general DOB pattern. Specifically, significant scientific interest has been in recent years given to the ADRC scheme, which estimates the disturbance affecting the plant by the means of Extended State Observer (ESO) and treats the uncertain dynamics as separate state variables describing the evolution of the system.

A different approach to the problem of system uncertainty is represented by the adaptive control schemes which, historically, have been developed as a branch of solutions independent of other robust control algorithms [153]. In opposition to the robust approaches, which primarily seek to reduce the influence of the unknown dynamics on the performance of the closed loop, the adaptive controllers are designed to online adapt their parameters and structure to produce a controller suitable for the real dynamics of the system. That is, had the dynamics of the plant been known, the non-adaptive controller could be designed with the same parameters as the ones generated by the adaptive scheme. Wide overviews of the historical results in this field have been published in [13, 256] and recently in [8]. Two distinct approaches to the adaptive control have been established in the literature. The indirect control attempts first to identify the model of the plant, and only then use it to synthesize the controller in form of some suitable non-adaptive algorithm. Alternatively, the only goal of the adaptation in the direct control is to find the controller suitable for the real system, without seeking for the real model of the plant [119, 208]. The classic solutions belonging to the group of indirect control include the parameter identification through the family of algorithms based on the Least Square Error approach [170, 246] which modifies the parameters of the controller in order to minimize the cost function defined as a square of the modeling error, or a class of algorithms employing the Gradient Method which changes the parameter values in the direction of the steepest descent of the identification error [124, 188]. Among the indirect adaptive control schemes, the greatest interest has been given to the Model Reference Adaptive Control (MRAC), designed to automatically tune the controller to guarantee that resulting closed loop dynamics correspond to some predefined reference dynamic [334]. Regardless of the chosen solution,

the adaptive algorithms are commonly characterized by the persistency of excitation (PE) condition, requiring the evolution of the plant to be rich enough to enable the proper adaptation of the controller [205]. A significant number of the existing schemes are also designed under the assumption, that the considered plant is characterized by the strictly positive-real (SPR) transfer function which enables parameter identification on the basis of the output feedback only [155]. The modern advances in the field of adaptive control are often focused on the applications to the nonlinear systems [14], employment of multiple models of the plant in the controller design [7, 207] or attempts to weaken the PE condition [198, 222].

Both in the fields of robust and adaptive control, growing interest has been lately given to solutions based on machine learning, including fuzzy controllers or algorithms employing neural networks. The surveys and tutorials on these methods can be found in [161, 168, 237, 297] with some insights on the future of such approaches discussed in [280]. The focus of this dissertation, however, is limited to the formal methods of control and attention is paid to the deterministic description of the systems. The methods involving machine learning are thus beyond the interest of this dissertation and are not discussed here in more detail. Scientific interest in the rest of the presented control solutions is visualized in Fig. 1.3. In this work, the main emphasis

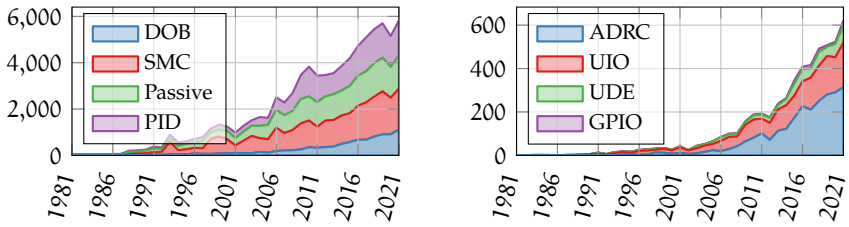

(a) Major control types

(b) Methods within DOB approach

Own work based on [118]

Figure 1.3: Search results of the IEEE Xplore database for papers published each year with terms corresponding to the chosen type of controller. In years of late, the number of papers published on DOB and ADRC schemes has rapidly increased.

is placed on the ADRC method and its recent modifications. In the second part of this dissertation, the methods of adaptive control are also recalled, and new solutions based on the combination of both ADRC and adaptive schemes are presented.

1.3 RANGE AND CONTRIBUTION

In this work, the results on the robustness and applicability of the ADRC in the presence of the modeling uncertainties are discussed. Namely, the stability and robustness of the ADRC control scheme are analyzed for the dynamic system with single input and single output which is burdened by parametric uncertainties. Uncertainties applying to both input gain and drift terms are studied under assumptions which are less restrictive than the ones commonly accepted in the literature. It is shown that the ADRC scheme ensures a convergence of the tracking and estimation errors to some boundary of the origin for a wide class of uncertain systems. In the presence of input gain uncertainty or state-dependent disturbances, this convergence is only achieved under sufficiently high tuning gains. Furthermore, from the presented analysis a conclusion is drawn that, in some cases, the performance of the ADRC controller may be improved by an increase in the modeling uncertainty. This notion is further studied with respect to the parametric uncertainty of the input gain, and it is shown that for the ADRC scheme designed in the tracking error domain, the performance of the closed-loop system is indeed improved if the nominal parameters are consciously chosen to differ from the dynamics of the real plant. Following the presented analysis, the series of experimental, simulation, and theoretical results are presented to further investigate the specific forms of the modeling uncertainties. It is shown that the ADRC is robust to some extent of various disturbances including unmodeled actuator dynamics, friction phenomenon, and harmonic disturbances. Simultaneously, it is emphasized that the quality of control increases if the proper model of these effects is included in the controller design.

In the second part of this work, the advantage is taken of the aforementioned results and a new control algorithm is proposed to cope with parametric uncertainties in the paradigm of the ADRC. To this end, a system with a disturbance modeled by a function linear in unknown parameters is considered, and an identification scheme is designed combining the ESO observer and gradient descent adaptation law. It is shown that this new observer guarantees asymptotic convergence of identification and estimation errors. The proposed algorithm is then employed in the design of a control law ensuring the convergence of tracking errors to the origin in the task of trajectory tracking. The effectiveness of this approach is validated in simulation and experiments on mobile and manipulator robots.

Lastly, this work presents also the results of engineering works undertaken by the author during his doctoral studies. In this context, the design, construction, and software implementation of the laboratory-

scale hovercraft system is presented. This device has been constructed on the basis of a commercially available off-the-shelf hovercraft model and modified to better fit the purpose of scientific research and experiments. Recent advances in the development of the astronomic telescope mounts in the SkyLab laboratory are also covered in the finishing sections of this work in the range corresponding to the involvement of the author. The author has been engaged mainly in the design and implementation of the distributed communication scheme of the telescope control system, as well as the development and tuning of the control algorithms. Both of these devices have been vital to the studies presented in this dissertation and the results of experiments performed with these systems are presented throughout this work.

The contributions and findings presented in this work may be summarized as follows:

1. Detailed stability analysis of the ADRC scheme in the presence of the modeling uncertainties.
2. Establishment of the idea of ADRC tuning by the means of conscious input gain underestimation.
3. Experimental validation of the ADRC for real uncertain systems.
4. Proposition of adaptive ESO observer able to identify the parameters of the plant and ensure asymptotic convergence.
5. Proposition of adaptive ADRC controller guaranteeing asymptotic tracking.
6. Formulation of theorems and analytical proofs of certain properties of the proposed methods.
7. Development and implementation of laboratory tools for research in automatic control.

1.4 STRUCTURE OF THE THESIS

The structure of this dissertation is as follows. In Chapter 2 the analysis of the ADRC robustness is presented. To this end, Section 2.1 recalls the background of the ADRC control and the fundamental results available in the literature. The history of this approach is recalled to show the foundation and rise of a new paradigm in control theory. The review of the most important findings in the development of this method is presented with special attention given to the publications on stability and robustness. Some publications on the possible directions of development of the ADRC scheme are also presented and a picture of the future of this paradigm is thus painted. Section 2.2 presents the

results of the research of the author on the stability of the ADRC in the general scenario of uncertain systems. A detailed investigation on the basis of the Lyapunov approach is shown and a series of theorems are formulated stating the stability properties of the ADRC method in the presence of different types of uncertainties and disturbances. The studies focused on the impact of the input gain uncertainty on the stability and performance of the ADRC system are reported in Section 2.3. By the means of numerical studies, the stability regions are formulated in terms of the extent of input gain uncertainty and feasible choices of the tuning variables. Furthermore, the influence of the incorrectly estimated input gain on the disturbance rejection ability is studied in detail. In Section 2.4 and its subsections, the studies of the author on the performance of the ADRC in the presence of specific types of uncertainties are presented. Namely, the problems of unmodeled dynamics of the input path, ignored disturbance in form of friction phenomenon, and harmonic disturbance are discussed in the context of the ADRC control. Thus, the opening chapter of this work is devoted to the analysis and discussion of the impact of the modeling uncertainties on the established ADRC schemes.

Chapter 3 presents a novel Parameter Identifying Extended State Observer (PIESO) and Parameter Identifying Disturbance Rejection Control (PIDRC) algorithms. To better establish their position among other control schemes, in Section 3.1 a wide literature review on adaptive control is carried out. Mainly, the literature on parameter identification, the persistence of excitation, and adaptive control stability are discussed in detail. The recent progresses in the analysis of the stability of adaptive systems utilizing the Lyapunov's direct method are also highlighted as a cornerstone for the examination of the new methods to be proposed. Section 3.2 introduces the PIESO identification method, describing its development on the basis of ADRC control. The two variants of the PIESO algorithm are derived for the system, depending on the extent of the available knowledge of the system. For both cases, the stability analysis is performed and convergence is proved through the use of Lyapunov functions. Results of simulation studies on PIESO approach are also presented for a wide range of dynamic systems. Beside the structures nominally conforming to the assumptions made during the design of the methods, some additional models are considered, including the two mass system and dynamics disturbed by a harmonic function of unknown frequency, to highlight the wide applicability of the proposed method. Section 3.3 builds upon the preceding content and presents the results on closed-loop PIDRC control. Both variants of PIESO observer are incorporated into corresponding control schemes, with some additional design freedoms incorporated, resulting in a total of three various PIDRC propositions.

Once again, the stability is proven by the Lyapunov approach with the global asymptotic and local exponential convergence of the tracking, estimation, and identification errors being established, and the efficiency of the method is confirmed by extensive simulations. To further validate the effectiveness and performance of the new algorithms, the results of experimental studies are presented in Section 3.4. Two applications from the field of robotics are considered, with the experiments conducted on the differentially driven mobile robot and the hovercraft system.

Chapter 4 contains the reports on the engineering works on the laboratory-scale mobile hovercraft system and robotic astronomic telescope. Works carried out by the author are presented and their importance for scientific research is highlighted. In Section 4.1 the mechanical and electrical structures of the considered hovercraft system are presented. Furthermore, a discussion is made on the communication scheme designed to facilitate the control of the system and execution of scientific experiments. Mathematical modeling of the hovercraft system is also presented. Development of the robotic astronomic mount is presented in Section 4.2, with special attention given to the design and implementation of the control and communication schemes. Some remarks on the general features and performance of this instrument are also given in this section.

The dissertation is summarized in Chapter 5. All of the presented results are once again recalled in brief and the most important findings are emphasized. Furthermore, some plans for future research are highlighted, both on the classic ADRC approach and novel PIESO and PIDRC methods.

1.5 NOMENCLATURE

Throughout this work, certain choices concerning the notation and symbol use are made to ensure the uniformity of the mathematical expressions across the work. The chosen nomenclature is, unless explicitly stated otherwise, as follows:

1. $\mathbb{R}$ represents a set of real numbers, with $\mathbb{R}_+$ standing for a set of only positive real numbers and $\mathbb{R}_-$ being a set of negative real numbers. $\mathbb{N}$ stand for the set of natural numbers.

2. $\mathcal{C}^\kappa$ is a class of κ-differentiable functions, i. e. functions with at least κ continuous derivatives.

3. All matrices are denoted with bold uppercase letters, while vectors are denoted with bold lowercase letters, e. g. $\mathbf{A}, \mathbf{b}, \boldsymbol{\beta}$. The elements of the matrices and vectors are denoted with lowercase regular letters and subscripts indicating the position of the

element within a matrix, e. g. $a_{2,1}, b_3, \beta_4$. The same notation applies to matrix-valued functions, e. g. $\mathbf{f}(t), f_1(t)$.

4. Terms $\mathbf{I}_\kappa$ and $\mathbf{0}_\kappa$ with $\kappa \in \mathbb{N}$ stand for the identity and zero matrix of size $\kappa \times \kappa$. Moreover, $\mathbf{0}_{\kappa_1 \times \kappa_2}$ stand for the zero matrix of size $\kappa_1 \times \kappa_2$ with $\kappa_1, \kappa_2 \in \mathbb{N}$.

5. The following matrices are defined for any constant $\kappa \geqslant 2 \in \mathbb{N}$:

$$\mathbf{A}_\kappa = \begin{bmatrix} \mathbf{0}_{\kappa-1\times 1} & \mathbf{I}_{\kappa-1} \\ 0 & \mathbf{0}_{1\times\kappa-1} \end{bmatrix} \in \mathbb{R}^{\kappa\times\kappa}, \ \mathbf{b}_\kappa = \begin{bmatrix} \mathbf{0}_{\kappa-1\times 1} \\ 1 \end{bmatrix} \in \mathbb{R}^\kappa,$$

$$\mathbf{c}_\kappa = \begin{bmatrix} 1 \\ \mathbf{0}_{\kappa-1\times 1} \end{bmatrix} \in \mathbb{R}^\kappa, \ \mathbf{d}_\kappa = \begin{bmatrix} \mathbf{0}_{\kappa-2\times 1} \\ 1 \\ 0 \end{bmatrix} \in \mathbb{R}^\kappa.$$

6. The hat accent is used to denote the estimate of a variable, e. g. $\hat{x}$. The tilde accent represents an error between the variable and its expected value, e. g. $\tilde{x}$. The bar accent denotes some scaling, applied either to the original variable, its error, or some other derived quantity, e. g. $\bar{x}$. The starred variables, e. g. x^*, are used to denote some other modifications of the original quantity.

7. Euclidean norm of vector $\mathbf{h}$ is denoted by $\|\mathbf{h}\|$. For matrix $\mathbf{H}$, induced euclidean norm is denoted by $\|\mathbf{H}\|$.

8. For any constant matrix or vector $\mathbf{H}$, constant $h_M = \|\mathbf{H}\| \in \mathbb{R}_+$ is denoted. For bounded varying vector or matrix $\mathbf{H}(x)$, constant $h_M \geqslant \|\mathbf{H}(\mathbf{x})\| \in \mathbb{R}_+$ for any x is defined. For any constant square matrix $\mathbf{H}$, constant $h_m = \lambda_{\min}(\mathbf{H}) \in \mathbb{R}$ is also denoted with $\lambda_{\min}(\mathbf{H})$ being the eigenvalue of $\mathbf{H}$ with the smallest real part. These constants can be defined with respect to the original variable, its error, or some other derived quantity denoted with an accent.

9. A scaling matrix is defined for any constants $\kappa \in \mathbb{N}, \omega \in \mathbb{R}_+$ as $\mathbf{\Phi}_\kappa(\omega) = \operatorname{diag}(\omega^{\kappa-1}, \omega^{\kappa-2}, \ldots, 1) \in \mathbb{R}^{\kappa\times\kappa}$.

10. The extraction matrix is defined for any constant $\kappa \in \mathbb{N}$ as $\mathbf{\Lambda}_\kappa = \begin{bmatrix} \mathbf{I}_\kappa & \mathbf{0}_{\kappa\times 1} \end{bmatrix} \in \mathbb{R}^{\kappa\times\kappa+1}$ Notably $\mathbf{\Lambda}_\kappa \mathbf{A}_{\kappa+1} = \mathbf{A}_\kappa \mathbf{\Lambda}_\kappa + \mathbf{b}_\kappa \mathbf{b}_{\kappa+1}^{\mathrm{T}}$, $\mathbf{\Lambda}_\kappa \mathbf{c}_{\kappa+1} = \mathbf{c}_\kappa$, $\mathbf{\Lambda}_\kappa \mathbf{d}_{\kappa+1} = \mathbf{b}_\kappa$ and $\mathbf{\Lambda}_\kappa \mathbf{b}_{\kappa+1} = 0$.

11. For most of the time-varying variables the time argument is presented only in the first appearances of the variable in the text. The argument is omitted for brevity in the succeeding appearances, e. g. $\mathbf{x}(t)$ and $\mathbf{x}$.

12. The custom piecewise exponentiation operator is defined as $\omega^{\kappa_1|\kappa_2} = \max(\omega^{\kappa_1}, \omega^{\kappa_2})$. for any constants $\omega, \kappa_1, \kappa_2 \in \mathbb{R}$.

2

ACTIVE DISTURBANCE REJECTION CONTROL

There is no way of assuming away intractable conditions in the real world.

— G. Leitmann, 1994 [159]

In this chapter, the research on the problem of robustness of the Active Disturbance Rejection Control (ADRC) is presented. At first, the history of the ADRC is recalled in brief, from its creation by J. Han to the rise of scientific interest and its establishment as a new design paradigm. Particular attention is given to its robustness to unmodeled dynamics present in the system. A wide review of literature results on this problem is given as an introduction to the presentation of new results obtained by the author. The theoretical considerations are followed by extensive simulation and experimental studies.

2.1 BACKGROUND AND EARLIER RESULTS

The foundations of the ADRC control lie in the general ideas of the disturbance observer control, yet its initial evolution is hard to precisely track due to the language barriers and political situation of the end of the 20th century. Some highlights on its history are given in recent papers pointing at the inspiration of the ADRC in the invariance principle which was proposed in early 19th century by J. V. Poncelet and has later gained significant interest in the Soviet Union [83, 286]. The idea of Poncelet states that if the matching disturbances acting upon the system can be measured, then this measure can be also used in the control signal to compensate for the presence of these disturbances [239]. To visualize this notion, one may consider a simple first-order dynamic system in the form of

$$\dot{x} = u + d(t), \tag{2.1}$$

where $x \in \mathbb{R}$ is a state of the system, $u \in \mathbb{R}$ is an input variable, and $d(t) \in \mathbb{R}$ represents some unknown, possibly time-varying, disturbance impacting the plant. Clearly, if $d(t)$ is known or measurable, the control signal can be chosen as

$$u = v - d(t), \tag{2.2}$$

with $v \in \mathbb{R}$ being some new control input of a system free of disturbances. By applying (2.2) to nominal system (2.1), the invariance

principle is invoked in practice, the disturbance is compensated for, and a controller can be designed by considering only the dynamics

$$\dot{x} = v. \tag{2.3}$$

This idealistic premise encounters its limitation if the disturbance does not appear in the same path as a control signal, i. e. the matching condition is not satisfied, or it is not available for direct measurement. As the disturbance may be understood as any phenomenon impacting the plant which is not modeled by the available mathematical description of the system, its measurability is seldom ensured in real-life scenarios.

Starting in the early 1970s, this constraint was treated as an incentive for the development of various control algorithms employing observers able to online estimate the momentary impact of disturbance affecting the plant. The earliest propositions in this field are represented by the papers on the Unknown Input Observer (UIO) published in 1971 [129] and the original Disturbance Observer (DOB) first developed in 1987 [291]. These notions resulted also in the idea of the Extended State Observer (ESO) which is an essential component of the ADRC control scheme. The first manuscripts by J. Han on this control algorithm were published in Chinese in the 1990s [97–100]. The method was probably presented to the Western scientific community for the first time in the year 1998 in the papers by groups of G. Feng [69] and Z. G. Hou [110] and followed by a presentation by Han himself at 14th IFAC World Congress in the year 1999 [101]. At the same time, a strikingly similar idea was independently reported by L. Praly and Z. P. Jiang in [238]. Soon other results presenting the possible applications of the ADRC have been reported in English [109, 333]. These early years of scientific interest in the ADRC are often forgotten, and it is commonly reported, that it had been presented in the West for the first time in 2001 in [84] by J. Han and his collaborators – Z. Gao and Y. Huang. In the year 2003 the simplified linear version of the ADRC controller was proposed which sparked a further increase of interest in the method [80]. The initial period of the intensified research on the ADRC has been oriented mostly on the applicability of the scheme to new practical problems. Numerous papers have been published on the use of this control algorithm in tasks of drive control [70, 283], mobile robotics [250, 273], naval ships cruise control [46, 249], power plant process control [112, 138], and many others.

The growing interest in the ADRC method combined with the high performance of this control scheme offered despite the lack of precise analytical background has led to the announcement of the rise of a new paradigm in the control theory in 2006 [81]. Two major points are

brought forward by this new archetype. First, any uncertainty of the system can be perceived as a disturbance affecting the nominal model which can be freely defined by the designer. Second, only a minimum degree of knowledge about the system is required for a successful controller design and any lack of familiarity with the dynamics of the plant can be counterbalanced by a properly designed algorithm. The ADRC paradigm thus strives to find a balance between control based on the mathematical model of the system and the empirical measurements of the momentary error in the closed loop.

Remark. *The point of view proposed by the ADRC paradigm is also embraced in this dissertation and the term disturbance may represent external disturbances, unmodeled dynamics, or any other modeling uncertainties.*

It was not until the second half of the 2000s that the focus of the researchers was redirected to the problem of stability and theoretical analysis of the foundations of the ADRC algorithm. Although some stability results for specific applications and controller structures were published as soon as in 2001 [114, 115], probably the first results on the systematic analytical approach to the question of convergence of the general ADRC were presented in 2006 by Z. Gao in [81] where Lyapunov function was proposed for linear ESO affected by bounded disturbance and was used to draw conclusions about the closed-loop stability of the linear ADRC. In the next year, G. Tian and Z. Gao used a frequency domain approach in [285], and the group of Q. Zheng gave more detailed results by once again using the Lyapunov method in [347]. This was followed in 2008 by L. B. Freidovich and H. K. Khalil who presented an analysis of closed-loop performance viewed as a singularly perturbed system [74]. Others have followed suit starting a period of analytical studies to the ADRC control. The published results on the stability of the ADRC scheme include an analysis of the performance of both single-input single-output [242] and multi-input multi-output [344] system, with respect to the chosen tuning of the controller [335] or the order of the system [5]. A better understanding of the theoretical foundations of ADRC made it possible to establish notions of equivalence between certain structures of the ADRC and other means of disturbance attenuation, including the equivalence with the GPIO and DOB observers [247], controllers based on a flatness property [266], PID controller [164] and integral observers employing the SMC approach [270]. Moreover, the explicit conditions of applicability of the ADRC have been formulated regarding the structure of the controlled system [210] or degree of feasible uncertainty [43, 319]. Advances in the analysis of ADRC have led also to the formulation of new variants of the controller able to tune its parameters in an adaptive manner [56, 220] or estimate the feedforward signal

of the time-varying reference trajectory [196, 336]. Simultaneously to these progresses, numerous tutorial papers have been published in international journals to further acquaint the global community with the ideas of the ADRC [41, 79, 82, 102]. The timeline visualizing the rise and development of the ADRC approach is presented in Fig. 2.1.

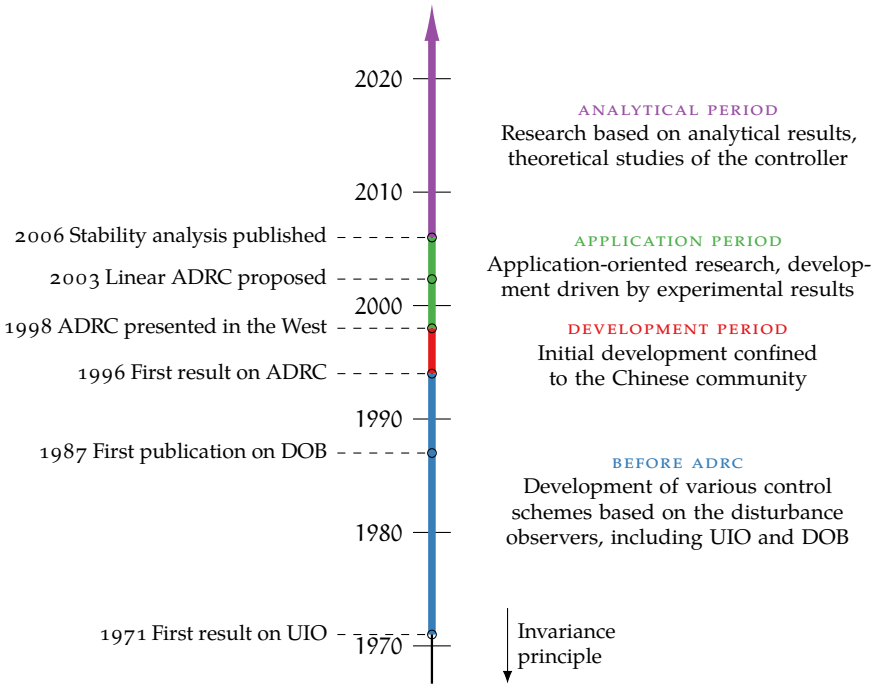

Figure 2.1: The timeline of ADRC development, current research is focused mainly on the results derived from a theoretical understanding of the method.

The cornerstone of control schemes built upon the DOB approach, and in particular upon the ADRC paradigm, is the notion that the fundamental difficulty in the application of the invariance principle – the unmeasurability of the disturbance dynamics – can be overcome by means of some observer structure able to recover the information about the disturbance from measurements of the available input-output data. If such an estimation is possible, the control law akin to (2.2) can be designed on the basis of the estimate produced by the observer. A schematic view of general control scheme consistent with this approach is given in Fig. 2.2. The ADRC method gives a specific structure compliant with this notion to answer the question of how to synthesize the observer to effectively estimate both the disturbance and the state of the system.

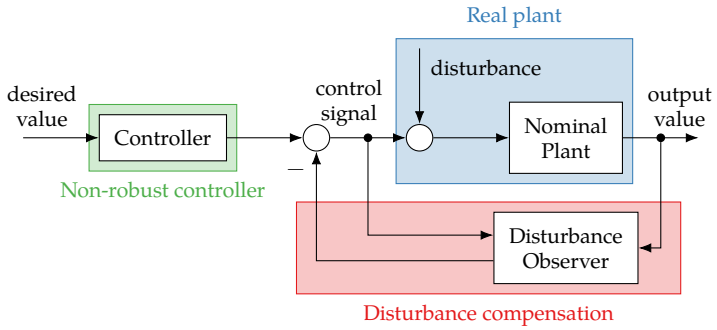

Figure 2.2: The simplified graphical illustration of the general DOB or ADRC approach. The disturbance is understood as any deviation from the nominal model.

Following the first English paper of J. Han on the ADRC [101], consider the system similar to (2.1) given by

$$\begin{aligned} \dot{\mathbf{x}} &= \mathbf{A}_n \mathbf{x} + \mathbf{b}_n \left(bu + d(t, \mathbf{x}) \right), \\ y &= \mathbf{c}_n^T \mathbf{x}, \end{aligned} \tag{2.4}$$

where $\mathbf{x} = \begin{bmatrix} x_1 & \dots & x_n \end{bmatrix}^T \in \mathbb{R}^n$ is the state of the system, $y \in \mathbb{R}$ is the measurable output, $u \in \mathbb{R}$ is the control variable, and $d(t, \mathbf{x}) \in \mathbb{R}$ stands for the unknown disturbance affecting the plant. Parameter $b \in \mathbb{R} \setminus \{0\}$ represents the input gain of the system. Constant matrices $\mathbf{A}_n, \mathbf{b}_n$ and $\mathbf{c}_n$ are as defined in Section 1.5. It is of major importance to note, that the specific form of disturbance $d(t, \mathbf{x})$ is not declared here, and it can represent both external factors impacting the plant and internal uncertainties. Namely, disturbance $d(t, \mathbf{x})$ represents any components by which the real plant differs from the undisturbed nominal system. This disturbing term is thus denoted as *total disturbance* which is to be overcome by the properly designed control algorithm. According to the ADRC methodology, the nominal system can be rewritten by employing the notion of an *extended state*. Let $\mathbf{z} = \begin{bmatrix} z_1 & \dots & z_m \end{bmatrix}^T \in \mathbb{R}^m$ represent the extended state of the system and be defined as $\mathbf{z} = \begin{bmatrix} \mathbf{x}^T & \delta \end{bmatrix}^T$ with $m = n + 1$ and δ being a new representation of the total disturbance affecting the system. The distinction between $d(t, \mathbf{x})$ as a physical phenomenon affecting the real system and δ as a conceptual total disturbance is made here to increase the unambiguity of the notation. The system dynamics expressed in terms of extended state $\mathbf{z}$ takes the form of

$$\begin{aligned} \dot{\mathbf{x}} &= \mathbf{A}_n \mathbf{x} + \mathbf{b}_n \left(bu + \delta \right), \\ \dot{\delta} &= \frac{d}{dt} d(t, \mathbf{x}), \\ y &= \mathbf{c}_n^T \mathbf{x}, \end{aligned} \tag{2.5}$$

or equivalently can be expressed in compact matrix notation as

$$\begin{aligned} \dot{\boldsymbol{z}} &= \boldsymbol{A}_m \boldsymbol{z} + \boldsymbol{d}_m b u + \boldsymbol{b}_m \frac{d}{dt} d(t, \boldsymbol{\Lambda}_n \boldsymbol{z}), \\ y &= \boldsymbol{c}_m^T \boldsymbol{z} \end{aligned} \tag{2.6}$$

with the constant matrix $\boldsymbol{d}_m$ and the extraction matrix $\boldsymbol{\Lambda}_n$ as defined in Section 1.5. Notably, while (2.4) and (2.6) define two distinct dynamic systems, these representations both describe the same physical plant, if the proper initial conditions are chosen for the extended system. Thus the equality $\boldsymbol{x} = \boldsymbol{\Lambda}_n \boldsymbol{z}$ is satisfied. Due to such reformulation of the system dynamics, the problem of disturbance measurement can be perceived as one of the state estimation. As the system expressed by (2.6) is inherently observable, a suitable estimation algorithm can be designed [41]. In the original development of the ADRC scheme, the following Nonlinear Extended State Observer (Nonlinear ESO, NESO) has been proposed to estimate the extended state of the system,

$$\dot{\hat{\boldsymbol{z}}} = \boldsymbol{A}_m \hat{\boldsymbol{z}} + \boldsymbol{d}_m b u + \boldsymbol{\phi}(y - \boldsymbol{c}_m^T \hat{\boldsymbol{z}}), \tag{2.7}$$

where $\hat{\boldsymbol{z}} = \begin{bmatrix} \hat{z}_1 & \dots & \hat{z}_m \end{bmatrix}^T \in \mathbb{R}^m$ is the estimate of the extended state and $\boldsymbol{\phi}(\cdot) = \begin{bmatrix} \phi_1(\cdot) & \dots & \phi_m(\cdot) \end{bmatrix}^T \in \mathbb{R}^m$ is a nonlinear vector-valued function with elements given as

$$\phi_i(e) = \begin{cases} l_i e \beta_i^{\alpha_i - 1} & |e| \leqslant \beta_i, \\ l_i |e|^{\alpha_i} \operatorname{sgn}(e) & |e| > \beta_i \end{cases} \tag{2.8}$$

with $\alpha_i, \beta_i, l_i \in \mathbb{R}$ for $i \in \{1, \dots, m\}$ being the tuning parameters the choice of which is given to the designer. The term $y - \boldsymbol{c}_m^T \hat{\boldsymbol{z}}$ is the estimation error calculated on the basis of the measurable output of the system. In order to achieve the efficient stabilization of system (2.4), the following nonlinear feedback set-point controller has been proposed to accompany the nonlinear observer,

$$u = \frac{\sum_{i=1}^{n} \phi_{ci}(x_{ri} - \hat{z}_i) - \hat{z}_m}{b} \tag{2.9}$$

with $\phi_{ci}(\cdot)$ defined analogously to $\phi_i(\cdot)$ of the observer and $\boldsymbol{x}_r = \begin{bmatrix} x_{r1} & \dots & x_{rn} \end{bmatrix}^T \in \mathbb{R}^n$ being a constant set-point to be achieved by the state of the plant. The control law in such a form consists of two fundamental terms. At first, the state error feedback term is used to drive the system in the direction of the desired reference state. While the feedback is here formulated on the basis of the state estimate, this may be replaced with real state values if the state of the system is measurable. The second part, being a crucial component of the ADRC scheme, is an estimate of the total disturbance and is supposed to

compensate for the presence of uncertainties in the system. The disturbance decoupling performed on the basis of the disturbance estimate can be perceived as a tool of *indirect linearization* [187]. In the perfect case, the system after the disturbance compensation behaves like the nominal linear system. The nonlinear ADRC discussed here presents certain difficulties with theoretical analysis of stability and dynamic properties and can be deemed cumbersome in implementation – in particular, the definition of nonlinear functions $\boldsymbol{\phi}(\cdot)$ requires a conditional operations, the use of a discontinuous signum operation is often problematic in the presence of measurement noise, and proper tuning of α_i, β_i, and l_i for the observer and controller requires a choice of a total of $3m + 3n$ parameters what is time-consuming and prone to cause the stability issues.

To overcome the drawbacks of the original nonlinear ESO, the simplified Linear Extended State Observer (Linear ESO, LESO) has been proposed in the literature and gained significant attention. The schemes derived from this simplified method are the main focus of this dissertation. The comparison of scientific interest of the linear and nonlinear variants of the ESO observer is given in Fig. 2.3 The

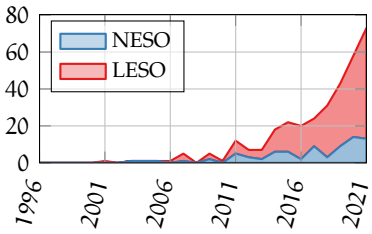

Own work based on [118]

Figure 2.3: Search results of the IEEE Xplore database for papers published each year on *nonlinear extended state observer* or *NESO* and *linear extended state observer* or *LESO*. Increased interest in the simplified linear scheme is visible, although many papers do not explicitly state the type of employed ESO (cf. number of papers on ADRC in Fig. 1.3)

linear ESO algorithm abandons troublesome $\boldsymbol{\phi}(\cdot)$ functions in favor of simple constant gain coefficients. Due to such a change, the LESO takes the form of a classic Luenberger observer designed for a system (2.6) by ignoring the unknown disturbing dynamics, and is given by

$$\dot{\hat{\mathbf{z}}} = \mathbf{A}_m \hat{\mathbf{z}} + \mathbf{d}_m b u + \mathbf{l}\left(y - \mathbf{c}_m^T \hat{\mathbf{z}}\right), \tag{2.10}$$

where $\mathbf{l} = \begin{bmatrix} l_1 & \dots & l_m \end{bmatrix}^T \in \mathbb{R}_+^m$ are the constant positive observer gains chosen to ensure the desired dynamics of the state estimates.

Following the linear structure of the observer, the control law itself is reformulated as

$$u = \frac{\mathbf{k}^T (\mathbf{x}_r - \boldsymbol{\Lambda}_n \hat{\mathbf{z}}) - \mathbf{b}_m^T \hat{\mathbf{z}}}{b} \tag{2.11}$$

with $\mathbf{k} = \begin{bmatrix} k_1 & \dots & k_n \end{bmatrix}^T \in \mathbb{R}_+^n$ being constant feedback gains.

In contrast to the sophisticated NESO tuning, the LESO is characterized by only n of controller gains and m of observer gains. The tuning process is further simplified by the application of *bandwidth parametrization*, consisting of the controller and observer gains chosen on the basis of the standard root-locus procedure. The method, initially employed in [80], takes advantage of the notion that the observer is designed on basis of a hypothetical undisturbed system. The choice of the parameters of the controller is thus done on the basis of the dynamics of simple linear system. Consider the system in form of (2.6) and denote the estimation error between the output of observer (2.10) and the state of the plant as $\tilde{\mathbf{z}} = \mathbf{z} - \hat{\mathbf{z}}$. The dynamics of the estimation error are considered by ignoring the disturbance and are thus given as

$$\dot{\tilde{\mathbf{z}}}\Big|_{d=0} = \left(\boldsymbol{\Lambda}_m - \mathbf{l}\mathbf{c}_m^T\right) \tilde{\mathbf{z}}, \tag{2.12}$$

what is stable if the real parts of the roots of the characteristic equation of the resultant matrix are negative. Observer tuning in the form of

$$l_i = \bar{l}_i \omega_o^i, \quad i \in \{1, m\}, \tag{2.13}$$

ensures the satisfaction of this condition if the elements of the observer gain vector $\bar{\mathbf{l}} = \begin{bmatrix} \bar{l}_1 & \dots & \bar{l}_m \end{bmatrix}^T \in \mathbb{R}_+^m$ are chosen as coefficients of a Hurwitz polynomial. The positive parameter $\omega_o \in \mathbb{R}_+$ determines the *observer bandwidth*. Similarly, stabilization error can be considered by ignoring the estimation errors. The dynamics of the control errors $\tilde{\mathbf{x}} = \mathbf{x}_r - \mathbf{x}$ are then given by

$$\dot{\tilde{\mathbf{x}}}\Big|_{\tilde{z}=0} = \left(\boldsymbol{\Lambda}_n - \mathbf{b}_n \mathbf{k}^T\right) \tilde{\mathbf{x}}. \tag{2.14}$$

The choice of controller gains as

$$k_i = \bar{k}_i \omega_c^{n+1-i}, \quad i \in \{1, n\}, \tag{2.15}$$

with elements of $\bar{\mathbf{k}} = \begin{bmatrix} \bar{k}_1 & \dots & \bar{k}_n \end{bmatrix}^T \in \mathbb{R}_+^n$ chosen as coefficients of a Hurwitz polynomial, guarantees that all roots of the resultant matrix in (2.14) are Hurwitz and thus the system is stable. The constant parameter $\omega_c \in \mathbb{R}_+$ defines a *controller bandwidth* and is a new tuning variable. In practical scenarios the scaled gains $\bar{\mathbf{l}}$ and $\bar{\mathbf{k}}$ are often chosen to ensure that the eigenvalues of the matrices in (2.12) and (2.14) are

located in $-\omega_o$ and $-\omega_c$ respectively. Such a decision leads to the choice of scaled gains on the basis of the order of the system only, with values of tuning parameters as given in Tab. 2.1. Under such a tuning

n	m	$\bar{\mathbf{l}}$	$\bar{\mathbf{k}}$
1	2	$\begin{bmatrix}2 & 1\end{bmatrix}^T$	$\begin{bmatrix}1\end{bmatrix}^T$
2	3	$\begin{bmatrix}3 & 3 & 1\end{bmatrix}^T$	$\begin{bmatrix}1 & 2\end{bmatrix}^T$
3	4	$\begin{bmatrix}4 & 6 & 4 & 1\end{bmatrix}^T$	$\begin{bmatrix}1 & 3 & 3\end{bmatrix}^T$
4	5	$\begin{bmatrix}5 & 10 & 10 & 5 & 1\end{bmatrix}^T$	$\begin{bmatrix}1 & 4 & 6 & 4\end{bmatrix}^T$
5	6	$\begin{bmatrix}6 & 15 & 20 & 15 & 6 & 1\end{bmatrix}^T$	$\begin{bmatrix}1 & 5 & 10 & 10 & 5\end{bmatrix}^T$

Table 2.1: Values of $\bar{\mathbf{l}}$ and $\bar{\mathbf{k}}$ under the common bandwidth parametrization for chosen orders of dynamic systems.

bandwidths ω_o, ω_c remain the only parameters to be chosen by the designer and can be easily set on the basis of an intuitive expectation that an increase of bandwidths corresponds to faster convergence at the cost of stronger noise amplification and potential stability issues in discrete digital implementations.

In order to further expand the scope of applicability of the ADRC method, the problem of tracking of the time-varying trajectory can be considered instead of the simple set-point stabilization. While this improvement can be incorporated into both linear and nonlinear ADRC, only the linear approach is discussed here. Specifically, for system (2.4), the observer given by (2.10) is employed without any modifications, but the control law is reformulated as

$$u = \frac{\mathbf{k}^T(\mathbf{x}_r - \mathbf{\Lambda}_n\hat{\mathbf{z}}) + \mathbf{b}_n^T\dot{\mathbf{x}}_r - \mathbf{b}_m^T\hat{\mathbf{z}}}{b}. \tag{2.16}$$

This control law differs from (2.11) by the presence of the feedforward signal, enabling the system to successfully track the time-varying reference trajectory. Such a combination of the LESO and control law with feedback, feedforward and disturbance compensation term constitues a basis for majority of further considerations of this work. Fig. 2.4 presents the graphical interpretation of the linear control scheme given by (2.4), (2.10) and (2.16). The performance of the linear ADRC controller is illustrated by a simulation example.

Simulation 2.1. *Consider the second order* $n = 2$ *system with* $b = 1$ *and subject to a time varying disturbance expressed by* $d = \sin(4t)$. *The problem of tracking of the reference trajectory in the form of* $\mathbf{x}_r(t) = \begin{bmatrix}\sin(2t) & 2\cos(2t)\end{bmatrix}^T$ *is investiaged and the LARDC controller as given by* (2.10) *and* (2.16) *is designed to control the plant. The tuning gains of the algorithm are chosen according to* (2.13), (2.15) *and Tab. 2.1 with* $\omega_o = 100, \omega_c = 1$. *The response of the system is shown in Fig. 2.5 where*

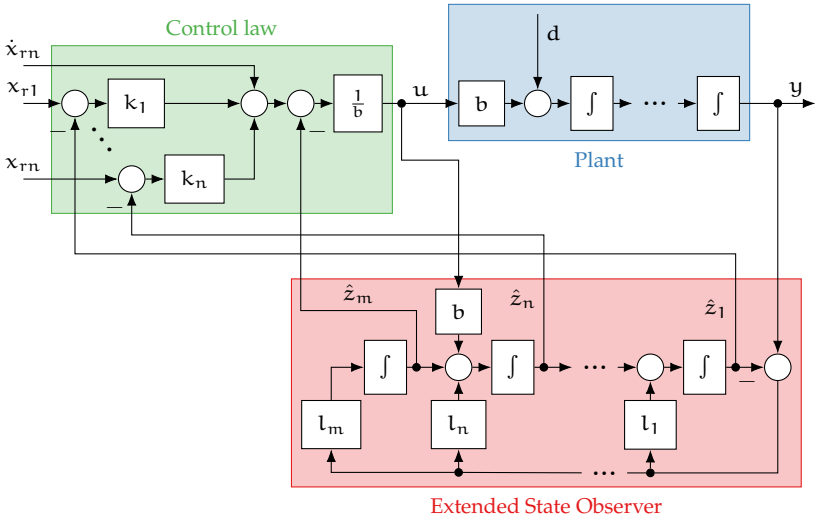

Figure 2.4: The detailed graphical illustration of the linear ADRC controller. Increased order of the observer and the disturbance compensation scheme are visible.

the evolution of the state of the plant and the estimates produced by the observer, as well as tracking and estimation error, are presented. For comparison, the tracking errors produced by the standard state feedback algorithm without disturbance estimation (i. e. with $\omega_o = 0$, $\hat{z}_m = 0$, and the state measurements instead of estimates used in the control law) are also presented.

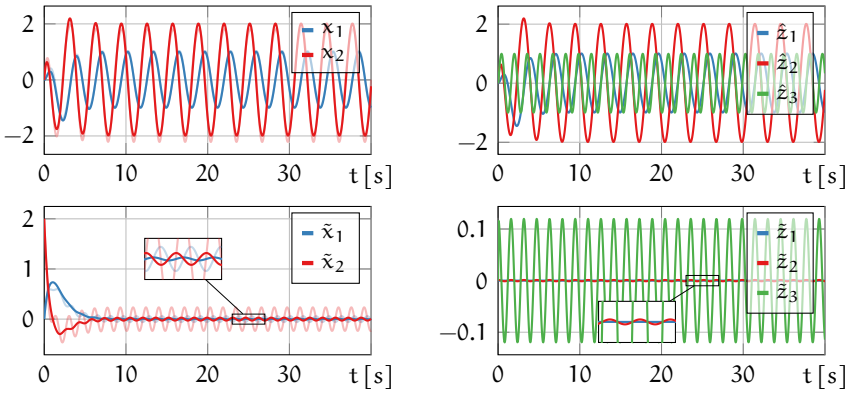

Figure 2.5: Time responses of the second order system under the linear ADRC controller. Results of the simulation without disturbance estimation are shown by transparent plots of x and $\tilde{x}$.

One can notice the correct estimation of both state variables and disturbance term, as well as efficient trajectory tracking thanks to the disturbance compensation. Simultaneously, it is clear that the conventional ADRC algorithm does not offer asymptotic stability of the system in the presence of disturbances and only convergence of the errors to some boundaries is achieved in the considered scenario. Nonetheless, a significant improvement of the control quality in com-

parison with the standard approach without disturbance rejection is offered by the scheme employing the ESO observer.

One of the significant modifications of the ADRC scheme has been developed by applying the ESO observer to the closed-loop error dynamics, instead of the nominal dynamics of the plant. This error-domain ADRC (EADRC) has been proposed independently by M. M. Michałek in [196] and H. Zheng in [336], and has since been a subject of active research [156, 182, 184]. Consider once again system (2.4) with the task of tracking of $\mathbf{x}_r(t)$ reference trajectory. Without any specific choice of the control law, the dynamics of the control errors $\tilde{\mathbf{x}} = \mathbf{x}_r - \mathbf{x}$ are given as

$$\dot{\tilde{\mathbf{x}}} = \mathbf{A}\tilde{\mathbf{x}} - \mathbf{b}_n \left(bu - \dot{x}_{rn} + d(t, \mathbf{x}_r - \tilde{\mathbf{x}}) \right), \tag{2.17}$$

what, in its general structure, resembles the nominal system (2.4) disturbed additionally by derivative of the reference trajectory. Thus, the idea to apply the ADRC scheme to this resultant dynamics arises intuitively. To this end, the extended state is defined as $\mathbf{z} = \begin{bmatrix} \tilde{\mathbf{x}}^T & \delta \end{bmatrix}^T \in \mathbb{R}^m$ with dynamics

$$\dot{\mathbf{z}} = \mathbf{A}_m \mathbf{z} - \mathbf{d}_m bu - \mathbf{b}_m \frac{d}{dt} \left(d(t, \mathbf{x}_r - \mathbf{\Lambda}_n \mathbf{z}) - \dot{x}_{rn} \right) \tag{2.18}$$

and the linear extended state observer designed in the error domain takes the form of

$$\dot{\hat{\mathbf{z}}} = \mathbf{A}_m \hat{\mathbf{z}} - \mathbf{d}_m bu + \mathbf{l} \left(\mathbf{c}_n^T \tilde{\mathbf{x}} - \mathbf{c}_m^T \hat{\mathbf{z}} \right). \tag{2.19}$$

The structure of the error domain ESO is the same as the standard ESO and, due to the embraced definition of tracking error $\tilde{\mathbf{x}}$, differs in the sign of input gain only. The previously discussed tuning and stability conditions are thus directly applicable also to this modified scheme. The control law is proposed on the basis of the error estimates as

$$u = \frac{\mathbf{k}^T \mathbf{\Lambda}_n \hat{\mathbf{z}} + \mathbf{b}_m^T \hat{\mathbf{z}}}{b}. \tag{2.20}$$

The graphical interpretation of the EADRC approach is given in Fig. 2.6. Importantly, the EADRC control law (2.20) does not necessarily include explicit feedforward term which constitutes part of the standard ADRC controller. This term is considered here as a part of the total disturbance and is actively estimated by the ESO observer. Thus, the application of the ADRC scheme in the error domain alleviates the need for analytical calculation of the higher derivatives of the reference trajectory which may increase the applicability of this algorithm in practical scenarios.

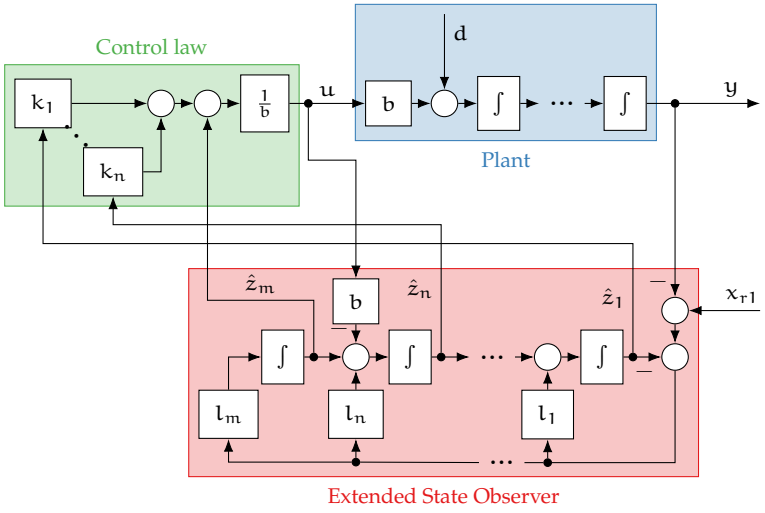

Figure 2.6: The detailed graphical illustration of the error-domain EADRC controller. The estimates are generated on the basis of control error measurement.

Simulation 2.2. *The practical illustration of the performance offered by the EADRC scheme is given in Fig. 2.7 where the results of simulations akin to these of Sim. 2.1 are given.*

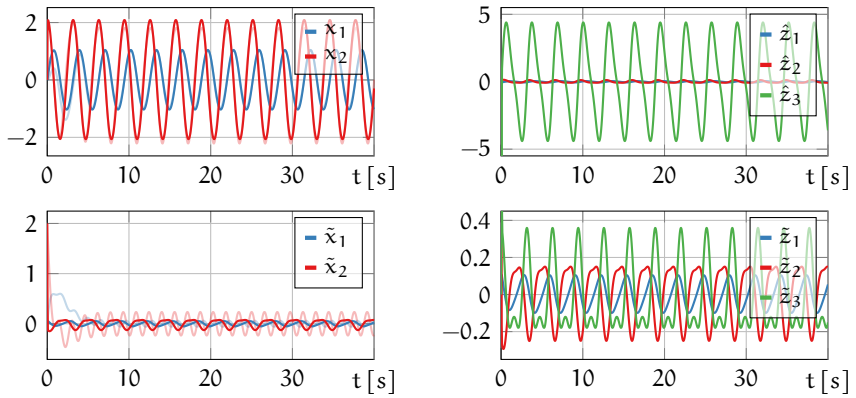

Figure 2.7: Time responses of the second order system under the linear EADRC controller. Results of the simulation without disturbance estimation are shown by transparent plots of $\mathbf{x}$ and $\tilde{\mathbf{x}}$.

It can be noted that due to the inclusion of the reference trajectory derivative in the disturbance signal the estimate of this term is significantly greater than in the standard ADRC approach as given in Fig. 2.5. In the consequence, the disturbance estimation quality is decreased in comparison with the conventional ADRC controller. Nonetheless, the resultant tracking errors are smaller than in the case of classic state feedback control. This increase in performance in comparison with the algorithm devoid of disturbance estimation could be further enhanced by the choice of greater controller and observer bandwidths. Thus the

EADRC scheme proves its usefulness if the derivative of the reference trajectory is not available.

No matter the choice of the precise form of ESO observer, the control law, or the tuning of the parameters, both (2.7) and (2.10) are designed by omitting the unknown disturbing term $\frac{d}{dt}d(\cdot)$. Thus, the observer is inherently ill-formed, and the presence of any non-constant disturbance inevitably deteriorates its performance. The ability of the standard ESO to perfectly estimate the constant disturbances, and thus compensate for their presence in the ADRC scheme, has been observed and analyzed already at the early stages of research on these methods [114]. The systematic studies on the impact of different types of uncertainties on the convergence and performance of the ESO and ADRC algorithms were started in 2007 with [285], where the authors used the frequency response analysis to prove the high robustness of the controller to the system uncertainties. It was shown that the stability margins are almost invariant to the changes in the parameters of the plant if high gains are used in the employed ESO.

The major advance in the understanding of the ADRC method has been done in [347] which was further extended in [346]. The authors considered linear ADRC structure with bandwidth parametrized gains, and analyzed the convergence of the estimation and tracking errors by employing the Lyapunov methods. It was shown that if the structure of the system is perfectly known the errors converge to the origin, while the presence of unknown disturbance characterized by boundedness of its derivative leads to convergence to the boundary of the origin only. These results were obtained under the conditions that ω_o and ω_c have to be chosen greater than some predefined thresholds. Using a singular perturbation approach these results have been at first confirmed [350] and then significantly extended in [74] by showing, that such a convergence of the errors to the boundary of the origin can also be achieved if the input gain b is not precisely given and is only known to be greater than some minimum value. The feasible class of disturbances for which convergence to the neighborhood of the origin is guaranteed has been expanded to include the bounded disturbances with unbounded derivatives in [322]. The analytical results were further validated by simulation of the system with disturbances in form of a square wave for which the satisfactory performance of the controller was achieved.

Results established for the linear ESO have been later also confirmed valid for the custom proposition of the nonlinear observer in [91]. Attention has been also given to the systems with an unknown degree, and it has been shown that the ADRC offers satisfactory performance even if the relative degree of the SISO system is not known [337–339]. The analysis in the frequency domain was employed under the as-

sumption that the upper bound of the uncertain relative degree is known. The same approach has been employed in [316] to confirm the robustness of the ADRC method. The stability of ADRC has been also analyzed for multi-input multi-output systems. The conditions on the stability of the MIMO systems with linear ADRC have been presented at first in [315] and further investigated in [318]. The applicability of the nonlinear ADRC to the MIMO systems has been studied in [90]. The results on the control of the MIMO plants of unknown orders have been presented in [340] on the basis of the analysis akin to the one employed earlier for the SISO systems. In [317] the performance of ADRC in the presence of uncertainties with unbounded derivatives and unknown input gain has been further studied. It was proved that the convergence to the origin is maintained if the discontinuities of the disturbance are all of the first kind. Moreover, the conditions on the range of feasible input gain uncertainty were strongly weakened in comparison with earlier studies. Multiple studies confirming the earlier results have also been reported in the literature. In [64] the studies on the convergence of nonlinear ADRC applied to the undisturbed plant with nonlinearities have been presented and convergence to some stable surface in the phase-space was proved. A reformulation of the closed-loop system into a perturbed Lurie model has been presented in [243] and Lyapunov-based analysis with the use of the Sylvester equation has been shown in [5]. In [258] the analysis by the singular perturbation method has been revisited, and in [320] the studies based on the linear system theory have been reported.

The stability and a peaking phenomenon present in the ADRC have been studied in the context of nonlinear systems in [345]. It was shown that the use of time-varying gains may successfully attenuate the peaking of the estimates. In the paper [42], the conditions of applicability and stability of the ADRC for the systems with unmatched and unobservable uncertainties have been given and discussed. It was shown that the ESO can be successfully employed to transform some class of individually unmatched and unobservable disturbances into a single, combined total disturbance satisfying a matching and observability conditions, and thus enabling the output regulation through the ADRC controller. A further weakening of the assumptions on the form of disturbances has been achieved in [48] where the disturbance with derivative which is unbounded, but Lipschitz was studied on the example of the simplified first-order system. In [300] the impact of the input uncertainty on the closed-loop system has been studied in more detail, while in [44] the necessary and sufficient conditions of the input gain uncertainty for the open-loop estimation with ESO have been established in place of earlier conservative results. The surveys on the studies on stability analysis of the ADRC have been published

first in the year 2014 [116] and then in 2017 [71]. A summary of studies on the problem of stability, performance, and applicability of the ESO and ADRC is presented in Tab. 2.2.

Study	Subject method	Analysis	Input gain
[114]	NESO	Lyapunov, SSR	known
[285]	LADRC	frequency	known
[5, 346, 347]	LADRC	Lyapunov	known
[74]	LADRC	s. perturbation	approx.
[350]	LADRC	s. perturbation	known
[322]	LESO	integration	known
[337–339]	LADRC	frequency	approx.
[91]	NESO	Lyapunov	known
[315, 318]	LADRC	Lyapunov	approx.
[90, 344]	NADRC	s. perturbation, Lyapunov	approx.
[317]	LADRC	*no proof*	approx.
[316]	LADRC	frequency	approx.
[64]	NADRC	Lyapunov	known
[345]	NADRC	s. perturbation	approx.
[42]	LADRC	*no proof*	approx.
[243]	NADRC	Lyapunov	approx.
[258]	LADRC	s. perturbation	known
[340]	LADRC	frequency	approx.
[48]	LADRC	Lyapunov	known
[44]	LESO	integration	approx.
[300]	LADRC	Lyapunov	approx.
[71, 116]	Review papers		

Table 2.2: Survey of publications on the stability of ADRC. Types of the considered method, employed analysis tools, and assumed knowledge about the system are given.

The general conclusions about the stability of the ADRC systems can be drawn from the aforementioned studies. It has been shown that the ADRC schemes with both linear and nonlinear structure, as given by (2.7)–(2.9) and (2.10)–(2.16), offer asymptotic convergence only if the total disturbance is either constant or vanishes with time. The asymptotic convergence can be extended to some other classes of disturbances (e. g. linear or polynomial) by further extending the state of the system. In the general case, only the convergence of the errors to some neighborhood of the origin can be ensured. The most conservative results assume that the total derivative of the disturbance has to be bounded by some constant values in order to achieve such a performance. More detailed studies have shown that the convergence of the errors to the neighborhood can be also guaranteed if the disturbance has discontinuities of the first type or depends linearly on

certain variables in the system. One of the most important notions given by the analytical studies of the ADRC is that in the presence of the unknown disturbances, the neighborhood to which the errors converge can be made arbitrarily small by the increase of the observer and controller bandwidths. Thus, even if the asymptotic stability is not achieved, the satisfactory performance of the system can be accomplished in practical scenarios. Moreover, research has confirmed the earlier observations that the performance of the ADRC is not significantly deteriorated even if the input gain of the system is unknown. The precise range of feasible input gain uncertainty, for which the system can be stabilized by a choice of high enough observer bandwidth, has been recently established. It has been furthermore shown that both linear and nonlinear algorithms exhibit similar stability properties, and these properties apply to both SISO and MIMO systems under certain conditions.

2.2 STABILITY OF A CLASS OF UNCERTAIN SYSTEMS

Due to its robustness to modeling uncertainties, external disturbances, and changes in the parameters of the system, the ADRC method has been recently employed in the growing number of problems in the field of robotics. Numerous publications have reported successful applications of this control paradigm to the manipulator robots [167, 240, 287], including systems as sophisticated as flexible manipulators [68, 117], soft continuum robots [103], or even wearable robots [103]. Other publications highlight the effectiveness of the ADRC in the tasks of mobile robotics [40, 179, 265]. A wide review of the recent results on the applicability of the ADRC to the tasks of robotics has also been published in [67].

With the thriving interest in the applications of the ADRC in robotics, there also arises the need for a detailed theoretical analysis of the stability and performance of the controller, tailored for the characteristics of the robotic systems. In this section, some results on this topic are presented. Namely, by the means of Lyapunov analysis, the robustness of the ADRC scheme applied to the system corresponding to the dynamics subject to parametric uncertainties is investigated. To this end, the analysis presented in [225] is extended and reformulated in more detail. Due to the employment of the original form of the state extension proposed recently by the author, the unified analysis is presented for the SISO system with and without uncertainties. On the basis of this study, a series of theorems is formulated to unveil the impact of different forms of uncertainties on the stability of the ADRC control scheme. Importantly, the conducted investigation does not require any assumptions on the behavior of the system or the disturbances

(such as boundedness of the trajectories or disturbances) which are commonly accepted in the studies presented in the literature. In their stead, only the assumptions on the reference trajectory and the general properties (such as satisfaction of the Lipschitz property) of the disturbances are considered. Thus the analysis presented in this chapter is based on assumptions which are significantly easier to verify and have stronger practical foundations. The stability conditions of the closed-loop system are formulated on the basis of the parametrized observer and controller gains and the feasible range of the input gain uncertainty. The theoretical analysis is performed for the systems of the arbitrary order which further increases its applicability in various practical scenarios.

Consider the dynamic system

$$\begin{aligned} \dot{x}_1 &= x_2, \\ &\vdots \\ \dot{x}_n &= bu + \psi(t,x)\theta + d(t,x), \\ y &= x_1, \end{aligned} \tag{2.21}$$

where $x = \begin{bmatrix} x_1 & \dots & x_n \end{bmatrix}^T \in \mathbb{R}^n$ corresponds to the state of the system, $u \in \mathbb{R}$ is a control input, and $b \in \mathbb{R} \setminus \{0\}$, $\theta = \begin{bmatrix} \theta_1 & \dots & \theta_k \end{bmatrix}^T \in \mathbb{R}^k$ are constant unknown parameters of the system. Terms $\psi(t,x) = \begin{bmatrix} \psi_1(t,x) & \dots & \psi_k(t,x) \end{bmatrix} \in \mathbb{R}^{1\times k}$ and $d(t,x) \in \mathbb{R}$ stand for the fully known and unknown dynamics, correspondingly. The output of the system is denoted by $y \in \mathbb{R}$. A system in such a form may, for example, represent the robotic manipulator with a single degree of freedom controlled on the level of torques (for $n = 2$) or motor voltages (for $n = 3$).

Assumption 2.1. *Let* $\psi(t,x)$ *and* $d(t,x)$ *be Lipschitz, i.e. let*

$$\begin{aligned} \|\psi(t,x_a) - \psi(t,x_b)\| &\leqslant \psi_L \|x_a - x_b\|, \\ \|\psi(t_a,x) - \psi(t_b,x)\| &\leqslant \psi_L \|t_a - t_b\|, \\ \|d(t,x_a) - d(t,x_b)\| &\leqslant d_L \|x_a - x_b\|, \\ \|d(t_a,x) - d(t_b,x)\| &\leqslant d_L \|t_a - t_b\|, \end{aligned} \tag{2.22}$$

for some constant $\psi_L, d_L \in \mathbb{R}_+$ *and any* $x_a, x_b \in \mathbb{R}^n$ *and* $t_a, t_b \in \mathbb{R}$.

Corollary 2.1. *For any Lipschitz function* $f(x)$ *satisfying*

$$\|f(x_a) - f(x_b)\| \leqslant f_L \|x_a - x_b\| \tag{2.23}$$

for some positive constant $f_L \in \mathbb{R}_+$ *and any* $\mathbf{x}_a, \mathbf{x}_b$*, the inequality*

$$\left\| \frac{\partial}{\partial \mathbf{x}} f(\mathbf{x}) \right\| \leqslant f_L \tag{2.24}$$

is also satisfied for any $\mathbf{x}$*.*

The extended state $z = \begin{bmatrix} \mathbf{x}^T & \delta \end{bmatrix}^T = \begin{bmatrix} z_1 & \dots & z_m \end{bmatrix}^T \in \mathbb{R}^m$, with $m = n + 1$, for system (2.21) can be defined as

$$\begin{aligned} \dot{z}_1 &= z_2, \\ &\vdots \\ \dot{z}_n &= \hat{b} u + \boldsymbol{\psi}(t, \boldsymbol{\Lambda}_n z)\theta - \boldsymbol{\psi}(t, \mathbf{x}_r)\left(\theta - \hat{\theta}\right) + z_m, \\ \dot{z}_m &= \frac{d}{dt}\left(\left(b - \hat{b}\right) u + \boldsymbol{\psi}(t, \mathbf{x}_r)\left(\theta - \hat{\theta}\right) + d(t, \boldsymbol{\Lambda}_n z)\right), \end{aligned} \tag{2.25}$$

which incorporates the impact of the drift parameter estimation error within the total disturbance. On the basis of the dynamics of the extended system, the ESO which employs only the available or measurable signals can be easily formulated in its standard form as

$$\begin{aligned} \dot{\hat{z}}_1 &= \hat{z}_2 + l_1 (z_1 - \hat{z}_1), \\ &\vdots \\ \dot{\hat{z}}_n &= \hat{b} u + \boldsymbol{\psi}(t, \boldsymbol{\Lambda}_n \hat{z})\hat{\theta} + \hat{z}_m + l_n (z_1 - \hat{z}_1), \\ \dot{\hat{z}}_m &= l_m (z_1 - \hat{z}_1), \end{aligned} \tag{2.26}$$

where $\hat{z} = \begin{bmatrix} \hat{\mathbf{x}}^T & \hat{\delta} \end{bmatrix}^T = \begin{bmatrix} \hat{z}_1 & \dots & \hat{z}_m \end{bmatrix}^T \in \mathbb{R}^m$ is the estimate of the extended state. Equations (2.21), (2.25) and (2.26) can be rewritten in an equivalent compact form as

$$\begin{aligned} \dot{\mathbf{x}} &= \mathbf{A}_n \mathbf{x} + \mathbf{b}_n \left(b u + \boldsymbol{\psi}(t, \mathbf{x})\theta + d(t, \mathbf{x})\right), \\ \dot{z} &= \mathbf{A}_m z + \mathbf{d}_m \left(\hat{b} u + \boldsymbol{\psi}(t, \boldsymbol{\Lambda}_n z)\theta - \boldsymbol{\psi}(t, \mathbf{x}_r)\left(\theta - \hat{\theta}\right)\right) \\ &\quad + \mathbf{b}_m \frac{d}{dt}\delta, \\ \dot{\hat{z}} &= \mathbf{A}_m \hat{z} + \mathbf{d}_m \left(\hat{b} u + \boldsymbol{\psi}(t, \boldsymbol{\Lambda}_n \hat{z})\hat{\theta}\right) + \mathbf{l}\mathbf{c}_m^T (z - \hat{z}), \end{aligned} \tag{2.27}$$

with

$$\delta = \left(b - \hat{b}\right) u + \boldsymbol{\psi}(t, \mathbf{x}_r)\left(\theta - \hat{\theta}\right) + d(t, \boldsymbol{\Lambda}_n z). \tag{2.28}$$

Such formulation of the extended state seems unorthodox but is a valid solution for the analysis of the system with modeling uncertainties. Specifically, in the presence of modeling uncertainty, the model description introduced here allows one to assume, that even if the estimation error vanishes, the dynamics of the plant are still disturbed

by the uncertainty of the drift term due to the tracking errors. Thus the proposed form of the extended state imposes a stronger separation between the tracking and estimation errors and the ESO is expected to accommodate only the former, while the task of compensating for the latter is laid on the controller only. Importantly, if the term θ is known then the extended state in form of (2.25) is simplified to the form suitable for the analysis of the undisturbed systems. Moreover, such an approach is vital to the analysis presented in the later sections of this work and is thus employed here for clarity.

Remark 2.1. *The extended state may be defined differently than* (2.27) *to facilitate the analysis of various aspects of the closed-loop system dynamics, e. g. ability of the observer to estimate the disturbance or the ability of control law to compensate for the transient estimation errors. In particular, one may consider the system given by*

$$\begin{aligned} \dot{\boldsymbol{z}} &= \boldsymbol{A}_m \boldsymbol{z} + \boldsymbol{d}_m \left(\hat{b} u + \boldsymbol{\psi}(t, \boldsymbol{\Lambda}_n \boldsymbol{z}) \hat{\theta} \right) + \boldsymbol{b}_m \frac{d}{dt} \delta, \\ \delta &= \left(b - \hat{b} \right) u + \boldsymbol{\psi}(t, \boldsymbol{\Lambda}_n \boldsymbol{z}) \left(\theta - \hat{\theta} \right) + d(\boldsymbol{\Lambda}_n \boldsymbol{z}), \end{aligned} \tag{2.29}$$

which simplifies the forthcoming analysis, but does not yield such a clear separation of the tracking and estimation errors. Alternatively, the state extension of

$$\begin{aligned} \dot{\boldsymbol{z}} &= \boldsymbol{A}_m \boldsymbol{z} + \boldsymbol{d}_m \left(\hat{b} u + \boldsymbol{\psi}(t, \boldsymbol{\Lambda}_n \hat{\boldsymbol{z}}) \hat{\theta} \right) + \boldsymbol{b}_m \frac{d}{dt} \delta, \\ \delta &= \left(b - \hat{b} \right) u - \boldsymbol{\psi}(t, \boldsymbol{\Lambda}_n \hat{\boldsymbol{z}}) \hat{\theta} + \boldsymbol{\psi}(t, \boldsymbol{\Lambda}_n \boldsymbol{z}) \theta + d(\boldsymbol{\Lambda}_n \boldsymbol{z}) \end{aligned} \tag{2.30}$$

or

$$\begin{aligned} \dot{\boldsymbol{z}} = {} & \boldsymbol{A}_m \boldsymbol{z} + \boldsymbol{d}_m \left(\hat{b} u + \boldsymbol{\psi}(t, \boldsymbol{\Lambda}_n \hat{\boldsymbol{z}}) \hat{\theta} + \left(\frac{b}{\hat{b}} - 1 \right) \boldsymbol{b}_m^\top (\boldsymbol{z} - \hat{\boldsymbol{z}}) \right) \\ & + \boldsymbol{b}_m \frac{d}{dt} \delta, \\ \delta = {} & \left(b - \hat{b} \right) u - \boldsymbol{\psi}(t, \boldsymbol{\Lambda}_n \hat{\boldsymbol{z}}) \hat{\theta} + \boldsymbol{\psi}(t, \boldsymbol{\Lambda}_n \boldsymbol{z}) \theta \\ & + d(\boldsymbol{\Lambda}_n \boldsymbol{z}) - \left(\frac{b}{\hat{b}} - 1 \right) \boldsymbol{b}_m^\top (\boldsymbol{z} - \hat{\boldsymbol{z}}) \end{aligned} \tag{2.31}$$

may be considered. These are designed to accommodate, within the total disturbance, for the state estimation error impacting the evaluation of the known $\boldsymbol{\psi}$ term. Importantly, for the extended systems defined in such ways, even in the presence of the nonzero estimation errors, the control law fully decouples the dynamics of the nominal plant in the latter case and omits only the impact of the disturbance estimation in the former. Thus, in these approaches, the total disturbances are expected to partially or fully accommodate for the effects directly caused by the imperfect estimation of this disturbance. Some results

obtained through the analysis using the latter dynamics are presented in [225]. Notably, all of these representations correspond to the same dynamics of the underlying physical system and yield the same observer design.

By taking advantage of the state and disturbance estimates produced by the observer, the control law is proposed in the form of standard ADRC control enhanced by the estimated value of the partially known dynamics

$$u = \frac{1}{\hat{b}} \left(v - \hat{\delta} - \boldsymbol{\psi}(t, \boldsymbol{\Lambda}_n \hat{\boldsymbol{z}}) \hat{\theta} \right), \tag{2.32}$$

with $v \in \mathbb{R}$ being a new input, which can be used to define some internal control law designed to cope with a specific control task. Here, the inner control law is designed as

$$v = \mathbf{k}^T (\boldsymbol{x}_r - \hat{\boldsymbol{x}}) + x_r^{(n)} \tag{2.33}$$

and consists of the state feedback evaluated on the state estimate and feedforward generated on the basis of the derivative of the reference trajectory which is defined as

$$\boldsymbol{x}_r = \begin{bmatrix} x_{r1} & \dots & x_{rn} \end{bmatrix}^T = \begin{bmatrix} x_r^{(0)}(t) & \dots & x_r^{(n-1)}(t) \end{bmatrix}^T \in \mathbb{R}^n, \tag{2.34}$$

with $x_r(t) \in \mathbb{R}$ being some function of time chosen freely by the designer. The internal control law v can be defined differently depending on the availability of the state measurements. In (2.33) the most restrictive variant of the controller is assumed, and the control law is synthesized fully on the basis of the state estimates. Importantly, by solving (2.28) and (2.32) for u, the control law can be expressed as

$$\begin{aligned} u = \frac{1}{b} \Big(& v + (\delta - \hat{\delta}) - \boldsymbol{\psi}(t, \boldsymbol{x}_r) \left(\theta - \hat{\theta} \right) \\ & - \boldsymbol{\psi}(t, \boldsymbol{\Lambda}_n \hat{\boldsymbol{z}}) - d(t, \boldsymbol{\Lambda}_n \boldsymbol{z}) \Big), \end{aligned} \tag{2.35}$$

what visualizes that the control law defined on the basis of the estimated input gain value corresponds to the control law for the nominal system incorporating the estimation error dynamics. Thus, as the estimation progresses and $\delta - \hat{\delta} \approx 0$, the input gain uncertainty may be correctly compensated for due to the total disturbance estimation. Hence, if the estimation errors are small enough, the obtained control law becomes almost indistinguishable from the controller designed with a full knowledge of the input gain parameter. In conclusion, even in the presence of the input gain uncertainty, the ADRC does not require the designer to manually compensate for the unknown input

gain, for example by scaling the controller gains or the feedforward signal, as the disturbance rejection should drive the control signal close to the form suitable for the true value of the input gain. The

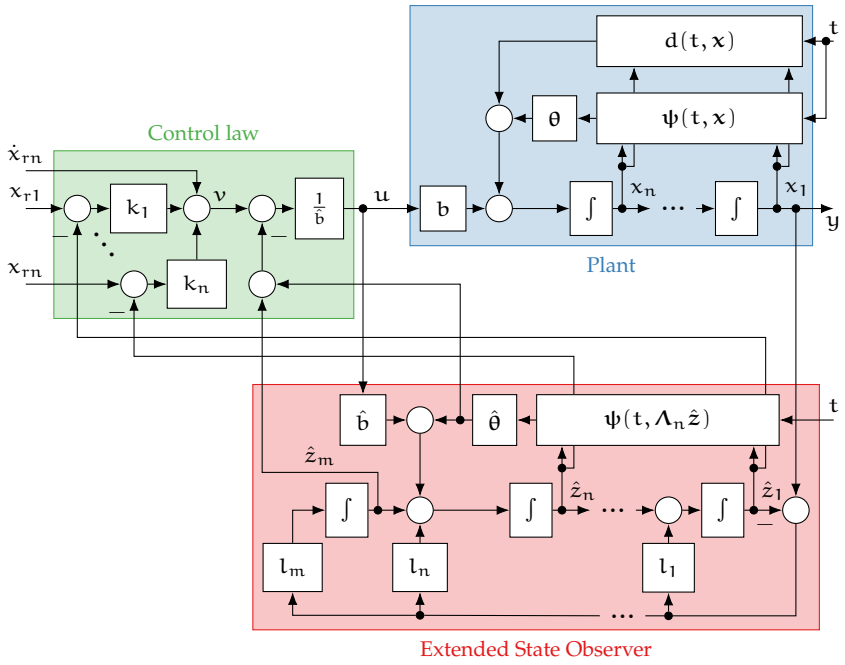

Figure 2.8: The detailed graphical illustration of the considered ADRC controller. The state-dependent disturbance and drift dynamics, as well as employed estimates of drift parameters and input gain, are visible.

detailed scheme of the considered control system is given in Fig. 2.8.

Assumption 2.2. *Let the reference trajectory belong to the class C^m, i. e. let derivative $x_r^{(m)}$ exist and be continuous.*

Assumption 2.3. *Let the reference trajectory be chosen such that its derivative is bounded, i. e.*

$$\|\dot{x}_r(t)\| \leqslant x_M \tag{2.36}$$

for some constant $x_M \in \mathbb{R}_+$ and any t.

Denote the tracking errors $\tilde{x} = x_r - x = \begin{bmatrix} \tilde{x}_1 & \dots & \tilde{x}_n \end{bmatrix}^T$ and estimation errors $\tilde{z} = z - \hat{z} = \begin{bmatrix} \tilde{z}_1 & \dots & \tilde{z}_m \end{bmatrix}^T$. By taking advantage of

(2.32) and analytically calculating the time derivative of u, the error dynamics can be then derived directly from (2.27) as

$$\begin{aligned}
\dot{\tilde{z}} &= \mathbf{H}\tilde{z} + \mathbf{d}_m\Big(\psi(t,\boldsymbol{\Lambda}_n z)\theta - \psi(t,x_r)\left(\theta-\hat{\theta}\right) \\
&\quad - \psi(t,\boldsymbol{\Lambda}_n\hat{z})\hat{\theta}\Big) + \mathbf{b}_m\Big(\dot{\psi}(t,x_r)\left(\theta-\hat{\theta}\right) \\
&\quad - \left(\frac{b}{\hat{b}}-1\right)\left(\dot{\psi}(t,\boldsymbol{\Lambda}_n\hat{z})\hat{\theta}-\dot{\nu}\right) + \dot{d}(t,\boldsymbol{\Lambda}_n z)\Big), \\
\dot{\tilde{x}} &= \mathbf{G}\tilde{x} - \boldsymbol{W}\tilde{z} + \mathbf{b}_n\Big(\psi(t,x_r)\left(\theta-\hat{\theta}\right) + \psi(t,\boldsymbol{\Lambda}_n\hat{z})\hat{\theta} \\
&\quad - \psi(t,\boldsymbol{\Lambda}_n z)\theta\Big),
\end{aligned} \tag{2.37}$$

with $\mathbf{H} = \boldsymbol{\Lambda}_m - \left(\mathbf{I}_m + \left(\frac{b}{\hat{b}}-1\right)\mathbf{b}_m\mathbf{b}_m^\top\right)\mathbf{l}\mathbf{c}_m^\top$, $\mathbf{G} = \boldsymbol{\Lambda}_n - \mathbf{b}_n\mathbf{k}^\top$ and $\boldsymbol{W} = \mathbf{b}_n\mathbf{k}^\top\boldsymbol{\Lambda}_n + \mathbf{b}_n\mathbf{b}_m^\top$. The term ν is as in (2.33). The time derivative of the internal control law can be obtained analytically from (2.33) in the form of

$$\dot{\nu} = \mathbf{k}^\top\mathbf{G}\tilde{x} + \mathbf{k}^\top\left(\boldsymbol{\Lambda}_n\mathbf{H} - \boldsymbol{W}\right)\tilde{z} + x_r^{(m)}. \tag{2.38}$$

Furthermore, denoting $d = d(t,\boldsymbol{\Lambda}_n z)$ and $\psi = \psi(t,\boldsymbol{\Lambda}_n z)$, $\hat{\psi} = \psi(t,\boldsymbol{\Lambda}_n\hat{z})$, $\psi_r = \psi(t,x_r)$, the time derivatives of the known and unknown drift terms present in (2.37) are expressed by

$$\begin{aligned}
\dot{\hat{\psi}} &= \frac{\partial\hat{\psi}}{\partial\left(\boldsymbol{\Lambda}_n\hat{z}\right)}\left(\left(\boldsymbol{\Lambda}_n\mathbf{l}\mathbf{c}_m^\top - \mathbf{G}\boldsymbol{\Lambda}_n\right)\tilde{z} - \mathbf{G}\tilde{x} + \dot{x}_r\right) + \frac{\partial\hat{\psi}}{\partial t}, \\
\dot{d} &= \frac{\partial d}{\partial\left(\boldsymbol{\Lambda}_n z\right)}\Big(\boldsymbol{W}\tilde{z} - \mathbf{G}\tilde{x} + \dot{x}_r + \mathbf{b}_n\Big(\psi\theta - \psi_r\left(\theta-\hat{\theta}\right) \\
&\quad - \hat{\psi}\hat{\theta}\Big)\Big) + \frac{\partial d}{\partial t}.
\end{aligned} \tag{2.39}$$

The detailed deriviations of these expressions are given in Appendix A.1. The precise form of matrices $\mathbf{H}, \mathbf{G}, \boldsymbol{W}$ are given by

$$\mathbf{H} = \begin{bmatrix} -l_1 & 1 & 0 & \cdots & 0 \\ -l_2 & 0 & 1 & \ddots & 0 \\ \vdots & \vdots & \ddots & \ddots & \vdots \\ -l_n & 0 & 0 & \ddots & 1 \\ -\frac{b}{\hat{b}}l_m & 0 & 0 & \cdots & 0 \end{bmatrix},\ \mathbf{G} = \begin{bmatrix} 0 & 1 & \cdots & 0 \\ \vdots & \vdots & \ddots & \vdots \\ 0 & 0 & \ddots & 1 \\ -k_1 & -k_2 & \cdots & -k_n \end{bmatrix},$$

$$\boldsymbol{W} = \begin{bmatrix} 0 & 0 & \cdots & 0 & 0 \\ \vdots & \vdots & & \vdots & \vdots \\ 0 & 0 & \cdots & 0 & 0 \\ k_1 & k_2 & \cdots & k_n & 1 \end{bmatrix}. \tag{2.40}$$

Matrices $\mathbf{H}$ and $\mathbf{G}$ are respectively the state matrices of the undisturbed estimation and control errors dynamics, while matrix $\boldsymbol{W}$ corresponds to the influence of the state estimation errors on the control law.

Remark 2.2. *Importantly, matrix $\boldsymbol{W}$ is associated with the use of state estimates in the control law to formulate the feedback signal. If the measurability of at least part of the state vector can be ensured in a considered specific scenario then the control law may be formulated on the basis of the measured state variables. Matrix $\boldsymbol{W}$ is then strongly simplified. In the extreme case of measurability of entire state $\mathbf{x}$, matrix $\boldsymbol{W}$ is reduced to $\mathbf{b}_m \mathbf{b}_m^T$ and becomes independent of the choice of gains $\mathbf{k}$. The significance of such a change is discussed in more detail in further parts of this dissertation.*

To facilitate the study of the closed-loop system stability, consider the choice of the tuning parameters according to the bandwidth parametrization as given in Section 2.1. Let thus the elements of $\mathbf{l}, \mathbf{k}$ be chosen as

$$\begin{aligned} l_i &= \bar{l}_i \omega_o^i, && i \in \{1, m\}, \\ k_j &= \bar{k}_j \omega_c^{n+1-j}, && j \in \{1, n\}, \end{aligned} \tag{2.41}$$

with $\omega_o, \omega_c \in \mathbb{R}_+$ being new tuning parameters of the algorithm and $\bar{\mathbf{l}} = \begin{bmatrix} \bar{l}_1 & \dots & \bar{l}_m \end{bmatrix}^T \in \mathbb{R}_+^m$ and $\bar{\mathbf{k}} = \begin{bmatrix} \bar{k}_1 & \dots & \bar{k}_n \end{bmatrix}^T \in \mathbb{R}_+^n$ being constant parameters chosen to detemine the dynamic properties of the observer and controller. Introduce also an auxiliary scaling of the estimation and tracking errors in the form of

$$\begin{aligned} \bar{z}_i &= \omega_o^{m-i} \tilde{z}_i, && i \in \{1, m\}, \\ \bar{x}_j &= \omega_c^{n-j} \tilde{x}_j, && j \in \{1, n\}. \end{aligned} \tag{2.42}$$

The proposed tuning choice and error scaling may be expressed in a matrix form as

$$\begin{aligned} \mathbf{l} &= \omega_o^m \boldsymbol{\Phi}_o^{-1} \bar{\mathbf{l}}, \\ \mathbf{k} &= \omega_c \boldsymbol{\Phi}_c \bar{\mathbf{k}}, \\ \bar{\boldsymbol{z}} &= \boldsymbol{\Phi}_o \tilde{\boldsymbol{z}}, \\ \bar{\mathbf{x}} &= \boldsymbol{\Phi}_c \tilde{\mathbf{x}}. \end{aligned} \tag{2.43}$$

where $\boldsymbol{\Phi}_o = \boldsymbol{\Phi}_m(\omega_o)$ and $\boldsymbol{\Phi}_c = \boldsymbol{\Phi}_n(\omega_c)$ are the scaling operators defined as $\boldsymbol{\Phi}_\kappa(\omega) = \operatorname{diag}(\omega^{\kappa-1}, \omega^{\kappa-2}, \dots, 1) \in \mathbb{R}^{\kappa \times \kappa}$ as given in

Section 1.5. The dynamics of these new scaled errors are derived from (2.37) as

$$\begin{aligned}
\dot{\bar{z}} &= \omega_o \bar{H}\bar{z} + \omega_o \mathbf{d}_m \Big(\boldsymbol{\psi}(t, \boldsymbol{\Lambda}_n z)\theta - \boldsymbol{\psi}(t, x_r)\left(\theta - \hat{\theta}\right) \\
&\quad - \boldsymbol{\psi}(t, \boldsymbol{\Lambda}_n \hat{z})\hat{\theta} \Big) + \mathbf{b}_m \Big(\dot{\boldsymbol{\psi}}(t, x_r)\left(\theta - \hat{\theta}\right) \\
&\quad - \left(\frac{b}{\hat{b}} - 1\right)\left(\dot{\boldsymbol{\psi}}(t, \boldsymbol{\Lambda}_n \hat{z})\hat{\theta} - \dot{v}\right) + \dot{d}(t, \boldsymbol{\Lambda}_n z) \Big), \\
\dot{\bar{x}} &= \omega_c \bar{G}\bar{x} - \left(\mathbf{b}_n \bar{k}^T \omega_c \boldsymbol{\Phi}_c \boldsymbol{\Lambda}_n \boldsymbol{\Phi}_o^{-1} + \mathbf{b}_n \mathbf{b}_m^T\right)\bar{z} \\
&\quad + \mathbf{b}_n \Big(\boldsymbol{\psi}(t, x_r)\left(\theta - \hat{\theta}\right) + \boldsymbol{\psi}(t, \boldsymbol{\Lambda}_n \hat{z})\hat{\theta} - \boldsymbol{\psi}(t, \boldsymbol{\Lambda}_n z)\theta \Big),
\end{aligned} \tag{2.44}$$

The time derivative of the internal control law is transformed by substituting (2.43) into (2.38) what yields

$$\begin{aligned}
\dot{v} &= \omega_c \bar{k}^T \Big(\omega_o \boldsymbol{\Phi}_c \boldsymbol{\Lambda}_n \boldsymbol{\Phi}_o^{-1} \bar{H} - \mathbf{b}_n \bar{k}^T \omega_c \boldsymbol{\Phi}_c \boldsymbol{\Lambda}_n \boldsymbol{\Phi}_o^{-1} \\
&\quad - \mathbf{b}_n \mathbf{b}_m^T \Big)\bar{z} + \omega_c^2 \bar{k}^T \bar{G}\bar{x} + x_r^{(m)}.
\end{aligned} \tag{2.45}$$

The derivatives of the drift and disturbance dynamics expressed in terms of the new scaled state variables take the form of

$$\begin{aligned}
\dot{\hat{\psi}} &= \frac{\partial \hat{\psi}}{\partial\left(\boldsymbol{\Lambda}_n \hat{z}\right)} \Big(\boldsymbol{\Lambda}_n \omega_o \boldsymbol{\Phi}_o^{-1} \bar{l} c_n^T - \boldsymbol{A}_n \boldsymbol{\Lambda}_n \boldsymbol{\Phi}_o^{-1} \\
&\quad + \mathbf{b}_n \bar{k}^T \omega_c \boldsymbol{\Phi}_c \boldsymbol{\Lambda}_n \boldsymbol{\Phi}_o^{-1} \bar{z} \\
&\quad + \omega_c \left(\mathbf{b}_n \bar{k}^T - \boldsymbol{A}_n \boldsymbol{\Phi}_c^{-1} \omega_c^{-1}\right)\bar{x} + \dot{x}_r \Big) + \frac{\partial \hat{\psi}}{\partial t}, \\
\dot{d} &= \frac{\partial d}{\partial\left(\boldsymbol{\Lambda}_n z\right)} \Big(\omega_c \left(\mathbf{b}_n \bar{k}^T - \boldsymbol{A}_n \boldsymbol{\Phi}_c^{-1} \omega_c^{-1}\right)\bar{x} \\
&\quad + \mathbf{b}_n \left(\bar{k}^T \omega_c \boldsymbol{\Phi}_c \boldsymbol{\Lambda}_n \boldsymbol{\Phi}_o^{-1} + \mathbf{b}_m^T\right)\bar{z} \\
&\quad + \dot{x}_r + \mathbf{b}_n \left(\boldsymbol{\psi}\theta - \boldsymbol{\psi}_r\left(\theta - \hat{\theta}\right) - \hat{\boldsymbol{\psi}}\hat{\theta}\right) \Big) + \frac{\partial d}{\partial t}.
\end{aligned} \tag{2.46}$$

Due to the embracement of the bandwidth parametrization, scaled matrices $\bar{\mathbf{H}}, \bar{\mathbf{G}}$ are independent of the choice of the observer and controller bandwidths and are given by

$$\bar{\mathbf{H}} = \begin{bmatrix} -\bar{l}_1 & 1 & 0 & \cdots & 0 \\ -\bar{l}_2 & 0 & 1 & \ddots & 0 \\ \vdots & \vdots & \ddots & \ddots & \vdots \\ -\bar{l}_n & 0 & 0 & \ddots & 1 \\ -\frac{b}{\hat{b}}\bar{l}_m & 0 & 0 & \cdots & 0 \end{bmatrix}, \ \bar{\mathbf{G}} = \begin{bmatrix} 0 & 1 & \cdots & 0 \\ \vdots & \vdots & \ddots & \vdots \\ 0 & 0 & \ddots & 1 \\ -\bar{k}_1 & -\bar{k}_2 & \cdots & -\bar{k}_n \end{bmatrix}. \tag{2.47}$$

Importantly, as matrix $\bar{\mathbf{H}}$ explicitly depends on the values of b and $\hat{b}$ the choice of tuning gains $\bar{\mathbf{l}}$ has to consider this dependence. Thus, the feasible choice of the observer gains directly depends on the unknown error of the input gain estimation. This is a crucial limitation imposed on the applicability of the ADRC by the presence of the modeling uncertainties. Consider now the tuning of the controller and observer such that the following is satisfied.

Assumption 2.4. *Let the scaled observer and controller gains $\bar{\mathbf{l}}, \bar{\mathbf{k}}$ be chosen such that matrices $\bar{\mathbf{H}}$ and $\bar{\mathbf{G}}$ are Hurwitz.*

Following [178], if Assumption 2.4 is satisfied then there exist positive definite matrices $\mathbf{P} \in \mathbb{R}^{m\times m}$ and $\mathbf{R} \in \mathbb{R}^{n\times n}$ satisfying the Lyapunov equations $\bar{\mathbf{H}}^T\mathbf{P} + \mathbf{P}\bar{\mathbf{H}} = -\mathbf{I}_m$ and $\bar{\mathbf{G}}^T\mathbf{R} + \mathbf{R}\bar{\mathbf{G}} = -\mathbf{I}_n$. The investigation into the stability properties of the considered control scheme can be performed on the basis of the following function of the scaled tracking and estimation errors

$$V_2(\bar{z}, \bar{x}) = \frac{1}{2}\bar{z}^T\mathbf{P}\bar{z} + \frac{1}{2}c_0\bar{x}^T\mathbf{R}\bar{x}, \tag{2.48}$$

with $c_0 \in \mathbb{R}_+$ being some positive constant. Due to the positive definiteness of matrices $\mathbf{P}, \mathbf{R}$ implied by Assumption 2.4, the proposed function satisfies

$$V_2(\bar{z}, \bar{x}) \geqslant \frac{1}{2}p_m \|\bar{z}\|^2 + c_0\frac{1}{2}r_m \|\bar{x}\|^2, \tag{2.49}$$

with $p_m = \lambda_{\min}(\mathbf{P}) \in \mathbb{R}_+$ and $r_m = \lambda_{\min}(\mathbf{R}) \in \mathbb{R}_+$, where $\lambda_{\min}(\cdot)$ stands for the smallest eigenvalue of a matrix. Thus $V_2(\bar{z}, \bar{x}) > 0$ for

any nonzero $\bar{z}, \bar{x}$ with $V_2(\bar{z}, \bar{x}) = 0$ only for $\bar{z}, \bar{x}$ equal zero. The time derivative of (2.48) along the trajectories of the system is given by

$$\begin{aligned}\dot{V}_2(\bar{z}, \bar{x}) = & -\frac{1}{2}\omega_o \bar{z}^T \bar{z} + \omega_o \bar{z}^T \mathbf{P} \mathbf{d}_m \left(\psi\theta - \psi_r\left(\theta - \hat{\theta}\right) - \hat{\psi}\hat{\theta}\right) \\ & + \bar{z}^T \mathbf{P} \mathbf{b}_m \Bigg(\left(\frac{b}{\hat{b}} - 1\right) \dot{v} + \dot{\psi}_r \left(\theta - \hat{\theta}\right) - \left(\frac{b}{\hat{b}} - 1\right) \dot{\hat{\psi}}\hat{\theta} \\ & + \dot{d}\Bigg) - \frac{1}{2} c_0 \omega_c \bar{x}^T \bar{x} - c_0 \bar{x}^T \mathbf{R} \mathbf{b}_n \Big(\bar{k}^T \omega_c \mathbf{\Phi}_c \mathbf{\Lambda}_n \mathbf{\Phi}_o^{-1} \\ & + \mathbf{b}_m^T \Big) \bar{z} + c_0 \bar{x}^T \mathbf{R} \mathbf{b}_n \left(\psi_r \left(\theta - \hat{\theta}\right) + \hat{\psi}\hat{\theta} - \psi\theta\right),\end{aligned} \tag{2.50}$$

with $\psi = \psi(t, \mathbf{\Lambda}_n z), \hat{\psi} = \psi(t, \mathbf{\Lambda}_n \hat{z})$ and $\psi_r = \psi(t, x_r)$ denoted for brevity. By substituting $\dot{v}$ from (2.45), expanding $\dot{\hat{\psi}}$ and $\dot{d}$ as in (2.46), and finally adding and subtrackting term $\psi\hat{\theta}$ to take advantage of the Lipschitz property of ψ, the explicit form of $\dot{V}_2(\bar{z}, \bar{x})$ can be written as

$$\begin{aligned}\dot{V}_2 = & -\frac{1}{2}\omega_o \bar{z}^T \bar{z} + \omega_o \bar{z}^T \mathbf{P} \mathbf{d}_m \left((\psi - \psi_r)\left(\theta - \hat{\theta}\right) + \left(\psi - \hat{\psi}\right)\hat{\theta}\right) \\ & + \bar{z}^T \mathbf{P} \mathbf{b}_m \Bigg(\left(\frac{\partial \psi_r}{\partial x_r}\dot{x}_r + \frac{\partial \psi_r}{\partial t}\right)\left(\theta - \hat{\theta}\right) + \left(\frac{b}{\hat{b}} - 1\right)\left(x_r^{(m)}\right. \\ & - \frac{\partial \hat{\psi}}{\partial \hat{x}}\Big(\omega_c \left(\mathbf{b}_n \bar{k}^T - \mathbf{A}_n \mathbf{\Phi}_c^{-1} \omega_c^{-1}\right)\bar{x} + \left(\mathbf{\Lambda}_n \omega_o \mathbf{\Phi}_o^{-1} \bar{l} \mathbf{c}_m^T \right. \\ & \left. - \mathbf{A}_n \mathbf{\Lambda}_n \mathbf{\Phi}_o^{-1} + \mathbf{b}_n \bar{k}^T \omega_c \mathbf{\Phi}_c \mathbf{\Lambda}_n \mathbf{\Phi}_o^{-1}\Big)\bar{z} + \dot{x}_r\Big)\hat{\theta} - \frac{\partial \hat{\psi}}{\partial t}\hat{\theta} \\ & + \omega_c^2 \bar{k}^T \bar{G} \bar{x} + \omega_c \bar{k}^T \Big(\omega_o \mathbf{\Phi}_c \mathbf{\Lambda}_n \mathbf{\Phi}_o^{-1} \bar{H} - \mathbf{b}_n \mathbf{b}_m \\ & - \mathbf{b}_n \bar{k}^T \omega_c \mathbf{\Phi}_c \mathbf{\Lambda}_n \mathbf{\Phi}_o^{-1}\Big)\bar{z}\Big) + \frac{\partial d}{\partial x}\Big(\mathbf{b}_n \Big(\bar{k}^T \omega_c \mathbf{\Phi}_c \mathbf{\Lambda}_n \mathbf{\Phi}_o^{-1} \\ & + \mathbf{b}_m^T\Big)\bar{z} + \omega_c \left(\mathbf{b}_n \bar{k}^T - \mathbf{A}_n \mathbf{\Phi}_c^{-1} \omega_c^{-1}\right)\bar{x} + \dot{x}_r \\ & + \mathbf{b}_n \left((\psi - \psi_r)\left(\theta - \hat{\theta}\right) + \left(\psi - \hat{\psi}\right)\hat{\theta}\right)\Big) + \frac{\partial d}{\partial t}\Big) \\ & - \frac{1}{2} c_0 \omega_c \bar{x}^T \bar{x} + c_0 \bar{x}^T \mathbf{R} \mathbf{b}_n \Big((\psi_r - \psi)\left(\theta - \hat{\theta}\right) \\ & + \left(\hat{\psi} - \psi\right)\hat{\theta} - \left(\bar{k}^T \omega_c \mathbf{\Phi}_c \mathbf{\Lambda}_n \mathbf{\Phi}_o^{-1} + \mathbf{b}_m^T\right)\bar{z}\Big).\end{aligned} \tag{2.51}$$

The derivative of $V_2(\bar{z}, \bar{x})$ expressed as in (2.51) unveils some important stability properties of the uncertain disturbed systems working under the ADRC principle. The major notions are as follows.

1. The major influence of the input gain uncertainty is clearly visible due to the presence of the term

$$\bar{z}^T \mathbf{P} \mathbf{b}_m \left(\frac{b}{\hat{b}} - 1 \right) \Big(\omega_c^2 \bar{k}^T \bar{G} \bar{x} + \omega_c \bar{k}^T \Big(\omega_o \Phi_c \Lambda_n \Phi_o^{-1} \bar{H} - \mathbf{b}_n \mathbf{b}_m - \mathbf{b}_n \bar{k}^T \omega_c \Phi_c \Lambda_n \Phi_o^{-1} \Big) \bar{z} + x_r^{(m)} - \frac{\partial \hat{\psi}}{\partial t} \hat{\theta} - \frac{\partial \hat{\psi}}{\partial \hat{x}} \Big(\omega_c \left(\mathbf{b}_n \bar{k}^T - \mathbf{A}_n \Phi_c^{-1} \omega_c^{-1} \right) \bar{x} + \Big(\Lambda_n \omega_o \Phi_o^{-1} \bar{l} \mathbf{c}_m^T - \mathbf{A}_n \Lambda_n \Phi_o^{-1} + \mathbf{b}_n \bar{k}^T \omega_c \Phi_c \Lambda_n \Phi_o^{-1} \Big) \bar{z} + \dot{x}_r \Big) \hat{\theta} \Big).$$

   While the preliminary impact of $\hat{b}$ was already established by Assumption 2.4, from (2.51) it can be stated that the estimation error of parameter b amplifies the effects of ψ function estimation and of the higher derivatives of the reference trajectory on the convergence of the system. Specifically, the term $\frac{b}{\hat{b}} - 1$ is nonzero if the input gain is not perfectly known. In this aspect, the input gain uncertainty negatively impacts the performance of the controller and leads to the growth of the neighborhood to which the errors converge. The presence of multiple expressions quadratic in the tracking and estimation errors shows also that the uncertainty of the input gain may disturb the basic stability properties of the plant and the convergence to any neighborhood may not be guaranteed even if Assumption 2.4 is satisfied.

2. The impact of the uncertainty of θ parameters can be seen mainly in the presence of the term

$$\bar{z}^T \mathbf{P} \mathbf{b}_m \Big(\left(\frac{\partial \psi_r}{\partial x_r} \dot{x}_r + \frac{\partial \psi_r}{\partial t} \right) \left(\theta - \hat{\theta} \right) \Big).$$

   and

$$\omega_o \bar{z}^T \mathbf{P} \mathbf{d}_m \left((\psi - \psi_r) \left(\theta - \hat{\theta} \right) + \left(\psi - \hat{\psi} \right) \hat{\theta} \right),$$
$$c_0 \bar{x}^T \mathbf{R} \mathbf{b}_n \Big((\psi_r - \psi) \left(\theta - \hat{\theta} \right) + \left(\hat{\psi} - \psi \right) \hat{\theta} \Big),$$
$$\bar{z}^T \mathbf{H} \mathbf{b}_m \left(\frac{\partial d}{\partial x} \left((\psi - \psi_r) \left(\theta - \hat{\theta} \right) + \left(\psi - \hat{\psi} \right) \hat{\theta} \right) \right),$$

   The first of the recalled terms stands for the direct influence of θ uncertainty on the regressor dynamics and affects the boundedness property of the errors. Specifically, the modeling error present in this term affects the system in the same manner as the unmodeled disturbances d. The latter of these represent the indirect impact of parametric uncertainty on the evolution of the

system, exhibited as the state of the plant deviates from the nominal trajectories of the undisturbed system. Due to the explicit presence of tracking and estimation errors and Lipschitzness property of ψ function, these directly disturb the stability of the closed-loop dynamics. Notably, the separation between the impact of the tracking and estimation errors is visible here. It can be concluded that such an impact of the parametric uncertainty is exhibited only when the plant is not on the reference trajectory. Had the tracking errors been reduced, the system would evolve as if it were indeed charactertized by the assumed values of the parameters. Importantly, some of these are further amplified by the choice of observer bandwidth.

3. The dynamics of the system represented as either modeled term ψ or unmodeled d are scaled by both $\mathbf{P}$ and the term $\frac{b}{\hat{b}} - 1$. Specifically, the term

$$\begin{aligned}
&\bar{z}^{\top}\mathbf{P}\mathbf{b}_m\Bigg(\frac{\partial d}{\partial \mathbf{x}}\Bigg(\omega_c\left(\mathbf{b}_n\bar{k}^{\top} - \mathbf{A}_n\mathbf{\Phi}_c^{-1}\omega_c^{-1}\right)\bar{x}\\
&+\mathbf{b}_n\left(\bar{k}^{\top}\omega_c\mathbf{\Phi}_c\mathbf{\Lambda}_n\mathbf{\Phi}_o^{-1} + \mathbf{b}_m^{\top}\right)\bar{z} + \dot{x}_r\\
&+\mathbf{b}_n\left((\psi - \psi_r)\left(\theta - \hat{\theta}\right) + \left(\psi - \hat{\psi}\right)\hat{\theta}\right)\Bigg) + \frac{\partial d}{\partial t}\Bigg),
\end{aligned}$$

as well as the expressions

$$\begin{aligned}
&\omega_o\bar{z}^{\top}\mathbf{P}\mathbf{d}_m\left((\psi - \psi_r)\left(\theta - \hat{\theta}\right) + \left(\psi - \hat{\psi}\right)\hat{\theta}\right),\\
&\bar{z}^{\top}\mathbf{P}\mathbf{b}_m\left(\left(\frac{\partial \psi_r}{\partial \mathbf{x}_r}\dot{x}_r + \frac{\partial \psi_r}{\partial t}\right)\left(\theta - \hat{\theta}\right)\right)
\end{aligned}$$

and

$$\begin{aligned}
&\bar{z}^{\top}\mathbf{P}\mathbf{b}_m\left(\frac{b}{\hat{b}} - 1\right)\Bigg(\frac{\partial\hat{\psi}}{\partial\hat{x}}\Bigg(\Big(\mathbf{\Lambda}_n\omega_o\mathbf{\Phi}_o^{-1}\bar{l}\mathbf{c}_m^{\top} - \mathbf{A}_n\mathbf{\Lambda}_n\mathbf{\Phi}_o^{-1}\\
&+\mathbf{b}_n\bar{k}^{\top}\omega_c\mathbf{\Phi}_c\mathbf{\Lambda}_n\mathbf{\Phi}_o^{-1}\Big)\bar{z} + \omega_c\left(\mathbf{b}_n\bar{k}^{\top} - \mathbf{A}_n\mathbf{\Phi}_c^{-1}\omega_c^{-1}\right)\bar{x}\\
&+\dot{x}_r\Big)\hat{\theta} + \frac{\partial\hat{\psi}}{\partial t}\hat{\theta}\Bigg),
\end{aligned}$$

may deteriorate the performance of the algorithm. The last one is scaled by both $\mathbf{P}$ and $\frac{b}{\hat{b}} - 1$, while the remaining expressions are affected by $\mathbf{P}$ only. Imporantly, the expressions scaled by $\frac{b}{\hat{b}} - 1$ depend directly on ψ but do not contain unmodeled disturbance d. While both $\mathbf{P}$ and $\frac{b}{\hat{b}} - 1$ are the functions of the estimate of the input gain, the norm of the former grows quickly in the presence of the input gain underestimation, while the characteristics of the latter are more ambiguous. It may be thus advised to forfeit

the term ψ in the design of the observer to avoid deterioration of the tracking quality if the input gain of the system is unknown.

4. Due to the presence of the expression satisfying Lipschitz condition, the inclusion of ψ in the design of the observer also generates quadratic-like terms in the derivative of $V(\bar{z}, \bar{x})$ function. Specifically, the terms

$$\omega_o \bar{z}^T \mathbf{P} \mathbf{d}_m \left((\psi - \psi_r) \left(\theta - \hat{\theta} \right) + \left(\psi - \hat{\psi} \right) \hat{\theta} \right),$$
$$c_0 \bar{x}^T \mathbf{R} \mathbf{b}_n \left((\psi_r - \psi) \left(\theta - \hat{\theta} \right) + \left(\hat{\psi} - \psi \right) \hat{\theta} \right),$$
$$\bar{z}^T \mathbf{P} \mathbf{b}_m \left(\frac{\partial d}{\partial x} \left((\psi - \psi_r) \left(\theta - \hat{\theta} \right) + \left(\psi - \hat{\psi} \right) \hat{\theta} \right) \right)$$

are upper bounded by some quadratic functions of the norms of $\bar{x}$ and $\bar{z}$. Notably, all of these are dependent on the characteristics of ψ and do not fully vanish even if the parameters of the system are prefectly known. Thus the incorporation of the known dynamics of the model in the synthesis of the ADRC controller does not alleviate the limitations on the choice of bandwidths ω_o, ω_c imposed by the presence of the state-dependent drift. This property is caused by the dependence of ψ on the estimate of the state which induces a requirement for sufficiently high speed of the state estimation.

5. The presence of ψ and d depending on the state of the system introduces the expressions scaled by both the observer and controller bandwidths. Specifically, the expression

$$\bar{z}^T \mathbf{P} \mathbf{b}_m \left(\frac{b}{\hat{b}} - 1 \right) \left(\omega_c \bar{k}^T \left(\omega_o \mathbf{\Phi}_c \mathbf{\Lambda}_n \mathbf{\Phi}_o^{-1} \bar{H} \right.\right.$$
$$\left.\left. - \mathbf{b}_n \bar{k}^T \omega_c \mathbf{\Phi}_c \mathbf{\Lambda}_n \mathbf{\Phi}_o^{-1} \right) \bar{z} - \frac{\partial \hat{\psi}}{\partial \hat{x}} \mathbf{b}_n \bar{k}^T \omega_c \mathbf{\Phi}_c \mathbf{\Lambda}_n \mathbf{\Phi}_o^{-1} \bar{z} \hat{\theta} \right)$$

and the term

$$\bar{z}^T \mathbf{P} \mathbf{b}_m \frac{\partial d}{\partial x} \mathbf{b}_n \bar{k}^T \omega_c \mathbf{\Phi}_c \mathbf{\Lambda}_n \mathbf{\Phi}_o^{-1} \bar{z}$$

grow with the increase of ω_c and shrink with the increase of ω_o. This leads to the significant dependence of feasible observer bandwidths on the chosen controller bandwidth. Thus, with the increase of ω_c, higher choice of ω_o is also required. Such phenomenon is absent if ψ and d are independent of the state

of the system. While the same property is also exhibited by the term

$$c_0 \bar{x}^\top \mathbf{R} \mathbf{b}_n \bar{k}^\top \omega_c \mathbf{\Phi}_c \mathbf{\Lambda}_n \mathbf{\Phi}_o^{-1} \bar{z},$$

it can be attenuated by proper choice of c_0 constant.

To facilitate the further studies of the stability of the closed-loop system and simplify the upcoming analysis, denote the custom piecewise exponentiation operator

$$\omega^{\kappa_1|\kappa_2} = \max(\omega^{\kappa_1}, \omega^{\kappa_2}). \tag{2.52}$$

Notably, the operator is monotonic in its argument ω if κ_1 and κ_2 are of the same sign. If κ_1 or κ_2 is equal 0, the result of the operator is equal 1 in some range and monotonic in the remaining domain. The norms of some expressions from (2.51) can be expressed in terms of this operator. Specifically,

$$\begin{aligned} \left\| \omega_c \mathbf{\Phi}_c \mathbf{\Lambda}_n \mathbf{\Phi}_o^{-1} \right\| &= \left(\frac{\omega_c}{\omega_o} \right)^{n|1}, \\ \left\| \omega_o \mathbf{\Phi}_c \mathbf{\Lambda}_n \mathbf{\Phi}_o^{-1} \right\| &= \left(\frac{\omega_c}{\omega_o} \right)^{n-1|0}, \end{aligned} \tag{2.53}$$

and

$$\begin{aligned} \left\| \mathbf{\Lambda}_n \mathbf{\Phi}_o^{-1} \right\| &= \omega_o^{-n|-1}, & \left\| \mathbf{\Phi}_c^{-1} \omega_c^{-1} \right\| &= \omega_c^{-n|-1}, \\ \left\| \omega_o \mathbf{\Lambda}_n \mathbf{\Phi}_o^{-1} \right\| &= \omega_c^{-n+1|0}, & \left\| \mathbf{\Phi}_c^{-1} \right\| &= \omega_c^{-n+1|0}. \end{aligned} \tag{2.54}$$

Notably, the bounds of the expressions in (2.53) increase with the growth of ω_c and decrease with the growth of ω_o. The bounds of the remaining expressions in (2.54) are nonincreasing with the growth of their respective bandwidths. To further simplify the notation denote also $\bar{b} = \left\| \frac{b}{\hat{b}} - 1 \right\| \in \mathbb{R}_+$, $\bar{\theta} = \left\| \theta - \hat{\theta} \right\| \in \mathbb{R}_+$, as well as $\theta_M = \max(\left\| \theta \right\|, \left\| \hat{\theta} \right\|) \in \mathbb{R}_+$.

The structure of $\dot{V}_2(\bar{z}, \bar{x})$ obtained in (2.51) enables the formulation of the several notions tailored for different scenarios of the ADRC implementation. A selection of such results is presented in the following theorems. At first, the application of the discussed control scheme to the system with perfect knowledge of the input gain and the drift terms independent of the state of the plant or to some constant value is considered. Multiple results on the stability of such systems have been already established in the literature and are here independently obtained on the basis of the uniform framework proposed for the stability analysis.

Theorem 2.1. *For system* (2.21) *with* $\boldsymbol{\psi} = \text{const}$ *or* $\boldsymbol{\psi} = \boldsymbol{\psi}(t)$ *and constant disturbances,* $d = \text{const}$*, observer* (2.26) *and control law* (2.32)–(2.33) *designed without any modeling uncertainty (i.e.* $\hat{b} = b$*,* $\hat{\theta} = \theta$*), guarantee the global exponential asymptotic convergence of errors* $\bar{z}, \bar{x}$ *to the origin under the tuning proposed by Assumption 2.4 for any choice of* ω_o, ω_c*.*

Proof. *Under the conditions stated in Theorem 2.1, the derivative of* $V_2(\bar{z}, \bar{x})$ *takes the form of*

$$\dot{V}_2 \Big|_{\substack{\psi=\psi(t) \\ d=\text{const} \\ \hat{b}=b \\ \hat{\theta}=\theta}} = -\frac{\omega_o}{2}\bar{z}^T\bar{z} - \frac{\omega_c}{2}c_0\bar{x}^T\bar{x} - c_0\bar{x}^T\mathbf{R}\mathbf{b}_n\left(\bar{k}^T\omega_c\boldsymbol{\Phi}_c\boldsymbol{\Lambda}_n\boldsymbol{\Phi}_o^{-1} + \mathbf{b}_m^T\right)\bar{z} \tag{2.55}$$

and satisfies inequality

$$\dot{V}_2 \leqslant -\frac{\omega_o}{2}\|\bar{z}\|^2 - \frac{\omega_c}{2}c_0\|\bar{x}\|^2 + c_0\|\bar{x}\| r_M\left(k_M\left(\frac{\omega_c}{\omega_o}\right)^{n|1} + 1\right)\|\bar{z}\|, \tag{2.56}$$

with $r_M = \|\mathbf{R}\| \in \mathbb{R}_+$ *and* $k_M = \|\bar{k}\| \in \mathbb{R}_+$*. The obtained inequality is further expressed as*

$$\dot{V}_2 \leqslant -\frac{1}{2}\left(\omega_o - \frac{c_0}{\varepsilon}r_M^2\left(k_M\left(\frac{\omega_c}{\omega_o}\right)^{n|1} + 1\right)^2\right)\|\bar{z}\|^2 - c_0\frac{1}{2}(\omega_c - \varepsilon)\|\bar{x}\|^2 \tag{2.57}$$

for any positive constant $\varepsilon \in \mathbb{R}_+$*. For any choice of* ω_o *and* ω_c *bandwidths, the negativity of the second term can be guaranteed by setting* ε *small enough. Then, choosing* c_0 *small enough ensures also the negativity of the first term. Function* $V_2(\bar{z}, \bar{x})$ *thus satisfies the conditions of the Lyapunov function.*

Remark. *The conclusion formulated for the case of system disturbed by a constant disturbance only fully satisfies the separation principle and thus the design and tuning of the observer and control law can be considered as separated issues. This property does not hold in some of the subsequent cases.*

Theorem 2.2. *For system* (2.21) *with state-dependent known term* $\boldsymbol{\psi} = \boldsymbol{\psi}(t, \mathbf{x})$ *satisfying Assumption 2.1 and constant disturbances,* $d = \text{const}$*, observer* (2.26) *and control law* (2.32)–(2.33) *designed without any modeling uncertainty (i.e.* $\hat{b} = b$*,* $\hat{\theta} = \theta$*), guarantee the global exponential asymptotic convergence of errors* $\bar{z}, \bar{x}$ *to the origin under the tuning proposed by Assumption 2.4 for* ω_o, ω_c *chosen high enough.*

Proof. *Under the conditions stated in Theorem 2.2, the time derivative of* $V_2(\bar{z},\bar{x})$ *takes the form of*

$$\begin{aligned}\dot{V}_2\Big|_{\substack{\psi=\psi(t,x)\\ \dot{d}=const\\ \hat{b}=b\\ \hat{\theta}=\theta}} = &-\frac{1}{2}\omega_o\bar{z}^T\bar{z}+\omega_o\bar{z}^T\mathbf{P}\mathbf{d}_m\left(\left(\psi-\hat{\psi}\right)\hat{\theta}\right)\\ &-\frac{1}{2}c_0\omega_c\bar{x}^T\bar{x}-c_0\bar{x}^T\mathbf{R}\mathbf{b}_n\Bigg(\left(\bar{k}^T\omega_c\mathbf{\Phi}_c\mathbf{\Lambda}_n\mathbf{\Phi}_o^{-1}\right.\\ &\left.+\mathbf{b}_m^T\right)\bar{z}-\left(\hat{\psi}-\psi\right)\hat{\theta}\Bigg)\end{aligned} \tag{2.58}$$

and satisfies inequality

$$\begin{aligned}\dot{V}_2 \leqslant &-\frac{\omega_o}{2}\left\|\bar{z}\right\|^2+\omega_o\left\|\bar{z}\right\|p_M\psi_L\left\|\mathbf{\Lambda}_n\mathbf{\Phi}_o^{-1}\bar{z}\right\|\theta_M\\ &-\frac{\omega_c}{2}c_0\left\|\bar{x}\right\|^2+c_0\left\|\bar{x}\right\|r_M\left(k_M\left(\frac{\omega_c}{\omega_o}\right)^{n|1}+1\right)\left\|\bar{z}\right\|\\ &+c_0\left\|\bar{x}\right\|r_M\psi_L\left\|\mathbf{\Lambda}_n\mathbf{\Phi}_o^{-1}\bar{z}\right\|\theta_M,\end{aligned} \tag{2.59}$$

where $p_M=\left\|\mathbf{P}\right\|\in\mathbb{R}_+$. *The obtained inequality is further expressed as*

$$\begin{aligned}\dot{V}_2 \leqslant &-\frac{1}{2}\Bigg(\omega_o-2p_M\psi_L\omega_c^{-n+1|0}\theta_M\\ &-\frac{1}{\varepsilon_1}c_0r_M\left(k_M\left(\frac{\omega_c}{\omega_o}\right)^{n|1}+1\right)^2\\ &-\frac{1}{\varepsilon_2}c_0r_M\psi_L\left(\omega_o^{-n|-1}\right)^2\theta_M\Bigg)\left\|\bar{z}\right\|^2\\ &-\frac{1}{2}c_0\left(\omega_c-\varepsilon_1r_M-\varepsilon_2r_M\psi_L\theta_M\right)\left\|\bar{x}\right\|^2\end{aligned} \tag{2.60}$$

for any positive constants $\varepsilon_1,\varepsilon_2\in\mathbb{R}_+$. *The negativity of* $\left\|\bar{x}\right\|^2$ *coefficient can be ensured by the choice of* ω_c *high enough or* $\varepsilon_1,\varepsilon_2$ *small enough. Setting* ω_o *high enough with* c_0 *small enough guarantees then the negativity of the coefficient of* $\left\|\bar{z}\right\|^2$. *Function* $V_2(\bar{z},\bar{x})$ *thus satisfies the conditions of the Lyapunov function.*

Theorem 2.3. *For system* (2.21) *with* $\psi=\text{const}$ *or* $\psi=\psi(t)$ *and time-varying disturbance* $d=d(t)$ *satisfying Assumption 2.1, observer* (2.26) *and control law* (2.32)–(2.33) *designed without any modeling uncertainty (i.e.* $\hat{b}=b$, $\hat{\theta}=\theta$*), guarantee the global convergence of errors* $\bar{z},\bar{x}$ *to some neighborhood of the origin under the tuning proposed by Assumption 2.4 for any choice of* ω_o,ω_c.

Proof. *Under the conditions stated in Theorem 2.3, the derivative of* $V_2(\bar{z}, \bar{x})$ *takes the form of*

$$\dot{V}_2\Big|_{\substack{\psi=\psi(t)\\ d=d(t)\\ \hat{b}=b\\ \hat{\theta}=\theta}} = -\frac{\omega_o}{2}\bar{z}^T\bar{z} + \bar{z}^T\mathbf{P}\mathbf{b}_m\frac{\partial d}{\partial t} - \frac{\omega_c}{2}c_0\bar{x}^T\bar{x} - c_0\bar{x}^T\mathbf{R}\mathbf{b}_n\left(\bar{k}^T\omega_c\mathbf{\Phi}_c\mathbf{\Lambda}_n\mathbf{\Phi}_o^{-1} + \mathbf{b}_m^T\right)\bar{z} \tag{2.61}$$

and satisfies inequality

$$\dot{V}_2 \leqslant -\frac{\omega_o}{2}\|\bar{z}\|^2 + p_M d_L\|\bar{z}\| - \frac{\omega_c}{2}c_0\|\bar{x}\|^2 + c_0 r_M\left(k_M\left(\frac{\omega_c}{\omega_o}\right)^{n|1} + 1\right)\|\bar{x}\|\,\|\bar{z}\|, \tag{2.62}$$

which can be further expressed as

$$\dot{V}_2 \leqslant -\frac{1}{2}\left(\omega_o - \frac{c_0}{\varepsilon}r_M^2\left(k_M\left(\frac{\omega_c}{\omega_o}\right)^{n|1} + 1\right)^2\right)\|\bar{z}\|^2 - c_0\frac{1}{2}(\omega_c - \varepsilon)\|\bar{x}\|^2 + p_M d_L\|\bar{z}\| \tag{2.63}$$

for any positive constant $\varepsilon \in \mathbb{R}_+$*. For any choice of* ω_o *and* ω_c *bandwidths, the negativity of the second term can be guaranteed by setting* ε *small enough. Then, choosing* c_0 *small enough ensures also the negativity of the first term.*

Define the concatenated errors in the system as $\xi = \begin{bmatrix}\bar{x}^T & \bar{z}^T\end{bmatrix}^T \in \mathbb{R}^{n+m}$*. Expression* (2.61) *is reformulated in the terms of* ξ *as*

$$\dot{V}_2\Big|_{\substack{\psi=\psi(t)\\ d=d(t)\\ \hat{b}=b\\ \hat{\theta}=\theta}} = -\frac{1}{2}\xi^T\mathbf{N}\xi + \begin{bmatrix}0_{n\times 1} & \mathbf{b}_m^T\mathbf{P}\frac{\partial d}{\partial t}\end{bmatrix}\xi, \tag{2.64}$$

where

$$\mathbf{N} = \begin{bmatrix}\omega_c c_0\mathbf{I}_n & n_{2,2}\\ n_{2,2}^T & \omega_o\mathbf{I}_m\end{bmatrix} \in \mathbb{R}^{n+m\times n+m} \tag{2.65}$$

with $n_{2,2} = -c_0\mathbf{R}\mathbf{b}_n\left(\bar{k}^T\omega_c\mathbf{\Phi}_c\mathbf{\Lambda}_n\mathbf{\Phi}_o^{-1} - \mathbf{b}_m^T\right)$*. Matrix* $\mathbf{N}$ *is positive definite if aforestated conditions are satisfied. Derivative* (2.64) *thus satisfies*

$$\dot{V}_2 \leqslant -\frac{1}{2}n_m\|\xi\|^2 + p_M d_L\|\xi\| \tag{2.66}$$

with $n_m = \lambda_{\min}(\mathbf{N})$*, where* $\lambda_{\min}(\cdot)$ *stand for smallest eigenvalue of a matrix. The neighborhood of the origin to which errors* ξ *converge is thus defined by*

$$\|\xi\| \leqslant 2p_M d_L n_m^{-1}. \tag{2.67}$$

Notably, n_m^{-1} *can be made arbitrarily small by increase of* ω_c *and* ω_o*.*

Remark. *Evaluation of final error bounds is omitted in the subsequent proofs but could be trivially conducted following the approach presented here.*

Theorem 2.4. *For system* (2.21) *with* $\psi = \text{const}$ *or* $\psi = \psi(t)$ *and time-varying, state-dependent disturbance* $d = d(t, x)$ *satisfying Assumption 2.1, observer* (2.26) *and control law* (2.32)–(2.33) *designed with input gain perfectly known (i. e.* $\hat{b} = b$*), guarantee the global convergence of errors* $\bar{z}, \bar{x}$ *to some neighborhood of the origin under the tuning proposed by Assumption 2.4 for* ω_o, ω_c *chosen high enough.*

Proof. *Under the conditions stated in Theorem 2.4, the derivative of* $V_2(\bar{z}, \bar{x})$ *takes the form of*

$$\begin{aligned}\dot{V}_2\Big|_{\substack{\psi=\psi(t)\\ d=d(t,x)\\ \hat{b}=b\\ \hat{\theta}=\theta}} = &-\frac{\omega_o}{2}\bar{z}^T\bar{z} + \bar{z}^T P b_m\Bigg(\frac{\partial d}{\partial x}\Bigg(\omega_c\Big(b_n\bar{k}^T \\ &- A_n\Phi_c^{-1}\omega_c^{-1}\Big)\bar{x} + b_n\Big(\bar{k}^T\omega_c\Phi_c\Lambda_n\Phi_o^{-1} \\ &+ b_m^T\Phi_o^{-1}\Big)\bar{z} + \dot{x}_r\Bigg) + \frac{\partial d}{\partial t}\Bigg) - \frac{\omega_c}{2}c_0\bar{x}^T\bar{x} \\ &- c_0\bar{x}^T R b_n\left(\bar{k}^T\omega_c\Phi_c\Lambda_n\Phi_o^{-1} + b_m^T\right)\bar{z}\end{aligned} \tag{2.68}$$

and satisfies inequality

$$\begin{aligned}\dot{V}_2 \leqslant &-\frac{\omega_o}{2}\|\bar{z}\|^2 + p_M d_L\omega_c\left(k_M + \omega_c^{-n|-1}\right)\|\bar{x}\|\,\|\bar{z}\| \\ &+ p_M d_L\left(k_M\left(\frac{\omega_c}{\omega_o}\right)^{n|1} + \omega_o^{-n|-1}\right)\|\bar{z}\|^2 \\ &+ p_M d_L x_M\|\bar{z}\| + p_M d_L\|\bar{z}\| - \frac{\omega_c}{2}c_0\|\bar{x}\|^2 \\ &+ c_0 r_M\left(k_M\left(\frac{\omega_c}{\omega_o}\right)^{n|1} + 1\right)\|\bar{x}\|\,\|\bar{z}\|,\end{aligned} \tag{2.69}$$

which can be further expressed as

$$\begin{aligned}\dot{V}_2 \leqslant &-\frac{1}{2}\Bigg(\omega_o - 2p_M d_L\left(k_M\left(\frac{\omega_c}{\omega_o}\right)^{n|1} + \omega_o^{-n|-1}\right) \\ &- \frac{1}{\varepsilon_2}c_0 r_M\left(k_M\left(\frac{\omega_c}{\omega_o}\right)^{n|1} + 1\right)^2 - \frac{1}{\varepsilon_1}\omega_c^2 p_M d_L\Big(k_M \\ &+ \omega_c^{-n|-1}\Big)^2\Bigg)\|\bar{z}\|^2 - \frac{1}{2}\Big(\omega_c c_0 - \varepsilon_1 p_M d_L - \varepsilon_2 c_0 r_M\Big)\|\bar{x}\|^2 \\ &+ p_M d_L(x_M + 1)\|\bar{z}\|\end{aligned} \tag{2.70}$$

for any positive constant $\varepsilon_1, \varepsilon_2 \in \mathbb{R}_+$*. The negativity of* $\|\bar{x}\|^2$ *coefficient can be ensured by the choice of* ω_c *high enough and then* ω_o *high enough guarantees the negativity of the coefficient of* $\|\bar{z}\|^2$*. Function* $V_2(\bar{z}, \bar{x})$ *thus*

satisfies the conditions of the Lyapunov function for errors $\bar{x}, \bar{z}$ large enough what implies the ultimate boundedness of the errors.

Theorem 2.5. *For system* (2.21) *with state-dependent and time-varying known term $\psi = \psi(t, x)$ and disturbance $d = d(t, x)$ satisfying Assumption 2.1 , observer* (2.26) *and control law* (2.32)–(2.33) *designed with parameters of the model perfectly known (i.e. $\hat{b} = b$, $\hat{\theta} = \theta$), guarantee the global convergence of errors $\bar{z}, \bar{x}$ to some neighborhood of the origin under the tuning proposed by Assumption 2.4 for ω_o, ω_c chosen high enough.*

Proof. *Under the conditions stated in Theorem 2.5, the derivative of $V_2(\bar{z}, \bar{x})$ takes the form of*

$$\begin{aligned}
\dot{V}_2 \Big|_{\substack{\psi=\psi(t,x)\\ d=d(t,x)\\ \hat{b}=b\\ \hat{\theta}=\theta}} = & -\frac{1}{2}\omega_o \bar{z}^T \bar{z} + \omega_o \bar{z}^T \mathbf{P} \mathbf{d}_m \left(\psi - \hat{\psi}\right) \hat{\theta} \\
& + \bar{z}^T \mathbf{P} \mathbf{b}_m \Bigg(\frac{\partial d}{\partial x} \Bigg(\omega_c \left(\mathbf{b}_n \bar{k}^T - \mathbf{A}_n \mathbf{\Phi}_c^{-1} \omega_c^{-1} \right) \bar{x} \\
& + \mathbf{b}_n \left(\bar{k}^T \omega_c \mathbf{\Phi}_c \mathbf{\Lambda}_n \mathbf{\Phi}_o^{-1} + \mathbf{b}_m^T \mathbf{\Phi}_o^{-1} \right) \bar{z} + \dot{x}_r \\
& + \mathbf{b}_n \left(\psi - \hat{\psi} \right) \hat{\theta} \Bigg) + \frac{\partial d}{\partial t} \Bigg) - \frac{1}{2} c_0 \omega_c \bar{x}^T \bar{x} \\
& + c_0 \bar{x}^T \mathbf{R} \mathbf{b}_n \Bigg(- \left(\bar{k}^T \omega_c \mathbf{\Phi}_c \mathbf{\Lambda}_n \mathbf{\Phi}_o^{-1} + \mathbf{b}_m^T \right) \bar{z} \\
& + \left(\hat{\psi} - \psi \right) \hat{\theta} \Bigg)
\end{aligned} \tag{2.71}$$

and satisfies inequality

$$\begin{aligned}
\dot{V}_2 \leqslant & -\frac{1}{2}\omega_o \|\bar{z}\|^2 + \omega_o \|\bar{z}\| \, p_M \psi_L \left\| \mathbf{\Lambda}_n \mathbf{\Phi}_o^{-1} \bar{z} \right\| \theta_M \\
& + \|\bar{z}\| \, p_M d_L \Bigg(\omega_c \left(k_M + \omega_c^{-n|-1} \right) \|\bar{x}\| + \left(k_M \left(\frac{\omega_c}{\omega_o} \right)^{n|1} \right. \\
& \left. + 1 \right) \|\bar{z}\| + x_M + \psi_L \left\| \mathbf{\Lambda}_n \mathbf{\Phi}_o^{-1} \bar{z} \right\| \theta_M + 1 \Bigg) - \frac{1}{2} c_0 \omega_c \|\bar{x}\|^2 \\
& + c_0 \|\bar{x}\| \, r_M \Bigg(\left(k_M \left(\frac{\omega_c}{\omega_o} \right)^{n|1} + 1 \right) \|\bar{z}\| \\
& + \psi_L \left\| \mathbf{\Lambda}_n \mathbf{\Phi}_o^{-1} \bar{z} \right\| \theta_M \Bigg),
\end{aligned} \tag{2.72}$$

which can be further expressed as

$$\begin{aligned}\dot{V}_2 \leqslant & -\frac{1}{2}\Bigg(\omega_o - 2\omega_c^{-n+1|0} p_M \psi_L \theta_M - 2 p_M d_L \psi_L \omega_o^{-n|-1}\theta_M \\ & - 2 p_M d_L \left(k_M \left(\frac{\omega_c}{\omega_o}\right)^{n|1} + 1\right) - \frac{1}{\varepsilon_1}\omega_c^2 p_M d_L \Big(k_M \\ & + \omega_c^{-n|-1}\Big)^2 - \frac{1}{\varepsilon_2} c_0 r_M \left(k_M \left(\frac{\omega_c}{\omega_o}\right)^{n|1} + 1\right)^2 \\ & - \frac{1}{\varepsilon_3} c_0 r_M \psi_L \left(\omega_o^{-n|-1}\right)^2 \theta_M\Bigg) \|\bar{z}\|^2 - \frac{1}{2}\Bigg(c_0\omega_c - \varepsilon_1 p_M d_L \\ & - \varepsilon_2 c_0 r_M - \varepsilon_3 c_0 r_M \psi_L \theta_M\Bigg) \|\bar{x}\|^2 + p_M d_L (x_M + 1)\|\bar{z}\|\end{aligned} \tag{2.73}$$

for any positive constant $\varepsilon_1, \varepsilon_2, \varepsilon_3 \in \mathbb{R}_+$. The negativity of $\|\bar{x}\|^2$ coefficient can be ensured by the choice of ω_c high enough or setting $\varepsilon_1, \varepsilon_2, \varepsilon_3$ small enough. The choice of ω_o high enough guarantees then the negativity of the coefficient of $\|\bar{z}\|^2$. Function $V_2(\bar{z}, \bar{x})$ thus satisfies the conditions of the Lyapunov function for errors $\bar{x}, \bar{z}$ large enough what implies the ultimate boundedness of the errors.

The aforementioned theorems are in line with the results presented in the earlier literature on the subject of the stability of the ADRC schemes. The applicability of these results may be further extended by considering the systems with the modeling uncertainties, i. e. $\hat{b} \neq b$ and $\hat{\theta} \neq \theta$.

Theorem 2.6. *For system* (2.21) *with* $\psi = \text{const}, d = \text{const}$, *observer* (2.26) *and control law* (2.32)–(2.33) *designed with only the input gain uncertainty (i. e.* $\hat{b} \neq b, \hat{\theta} = \theta$*), guarantee the global convergence of errors $\bar{z}, \bar{x}$ to some neighborhood of the origin under the tuning proposed by Assumption 2.4 for ω_o, ω_c chosen high enough.*

Proof. *Under the conditions stated in Theorem 2.6, the derivative of $V_2(\bar{z}, \bar{x})$ takes the form of*

$$\begin{aligned}\dot{V}_2\Big|_{\substack{\psi=\text{const}\\ d=\text{const}\\ \hat{b}\neq b\\ \hat{\theta}=\theta}} = & -\frac{\omega_o}{2}\bar{z}^T\bar{z} - c_0\bar{x}^T\mathbf{R}\mathbf{b}_n\left(\bar{k}^T\omega_c\mathbf{\Phi}_c\mathbf{\Lambda}_n\mathbf{\Phi}_o^{-1} + \mathbf{b}_m^T\right)\bar{z} \\ & - \frac{\omega_c}{2}c_0\bar{x}^T\bar{x} + \bar{z}^T\mathbf{P}\mathbf{b}_m\left(\frac{b}{\hat{b}} - 1\right)\Big(\omega_c^2\bar{k}^T\bar{\mathbf{G}}\bar{x} + x_r^{(m)} \\ & + \omega_c\bar{k}^T\Big(\omega_o\mathbf{\Phi}_c\mathbf{\Lambda}_n\mathbf{\Phi}_o^{-1}\bar{\mathbf{H}} - \mathbf{b}_n\bar{k}^T\omega_c\mathbf{\Phi}_c\mathbf{\Lambda}_n\mathbf{\Phi}_o^{-1} \\ & - \mathbf{b}_n\mathbf{b}_m\Big)\bar{z}\Big)\end{aligned} \tag{2.74}$$

and satisfies inequality

$$\begin{aligned}\dot{V}_2 \leqslant & -\frac{\omega_o}{2}\|\bar{z}\|^2 + c_0 r_M\left(k_M\left(\frac{\omega_c}{\omega_o}\right)^{n|1}+1\right)\|\bar{x}\|\,\|\bar{z}\| \\ & -\frac{\omega_c}{2}c_0\|\bar{x}\|^2 + \omega_c^2\bar{b}p_M k_M g_M\|\bar{z}\|\,\|\bar{x}\| \\ & +\bar{b}p_M x_M\|\bar{z}\| + \omega_c\bar{b}p_M k_M\left(\left(\frac{\omega_c}{\omega_o}\right)^{n-1|0} h_M\right. \\ & \left.+k_M\left(\frac{\omega_c}{\omega_o}\right)^{n|1}+1\right)\|\bar{z}\|^2,\end{aligned} \tag{2.75}$$

where $h_M = \left\|\bar{\mathbf{H}}\right\| \in \mathbb{R}_+$ *and* $g_M = \left\|\bar{\mathbf{G}}\right\| \in \mathbb{R}_+$. *Moreover, a constant measure of the input gain deviation is as defined earlier* $\bar{b} = \left\|b\hat{b}^{-1} - 1\right\|$. *Notably, this term is bounded for any feasible choice of* $\hat{b}$. *The above boundary can be expressed as*

$$\begin{aligned}\dot{V}_2 \leqslant & -\frac{1}{2}\Bigg(\omega_o - 2\omega_c\bar{b}p_M k_M\left(\left(\frac{\omega_c}{\omega_o}\right)^{n-1|0} h_M\right. \\ & \left.+k_M\left(\frac{\omega_c}{\omega_o}\right)^{n|1}+1\right) - \frac{1}{\varepsilon_1}\omega_c^4\bar{b}p_M k_M g_M \\ & -\frac{1}{\varepsilon_2}c_0 r_M\left(k_M\left(\frac{\omega_c}{\omega_o}\right)^{n|1}+1\right)^2\Bigg)\|\bar{z}\|^2 - \frac{1}{2}\Big(\omega_c c_0 \\ & -\varepsilon_1\bar{b}p_M k_M g_M - \varepsilon_2 c_0 r_M\Big)\|\bar{x}\|^2 + \bar{b}p_M x_M\|\bar{z}\|\end{aligned} \tag{2.76}$$

for any positive constants $\varepsilon_1, \varepsilon_2 \in \mathbb{R}_+$. *For any choice of* c_0 *the coefficient of* $\|\bar{x}\|^2$ *can be made negative by setting* $\varepsilon_1, \varepsilon_2$ *small enough or* ω_c *high enough. Then the negativity of the coefficient of* $\|\bar{z}\|^2$ *is ensured by choosing* ω_o *high enough. Function* $V_2(\bar{z}, \bar{x})$ *satisfies conditions of the Lyapunov function for errors* $\bar{x}, \bar{z}$ *large enough and* $\hat{b}$ *chosen to satisfy Assumption 2.4, guaranteeing the ultimate boundedness of the errors.*

Remark. *In the general case presented in the theorem, only the convergence to some neighborhood of the origin can be ensured. Analysis of the proof unveils that if the reference trajectory is chosen such that* $x_r^{(m)}$ *is equal to* 0 *or vanishes with time, the term* $\bar{b}p_M x_M\|\bar{z}\|$ *in* (2.76) *also vanishes. The asymptotic convergence to the origin can thus be ensured by proper choice of bandwidths. In other cases, the ultimate boundedness is ensured and the bound depends on the chosen bandwidths, reference trajectory, and the extent of input gain uncertainty. Such a possbility to achieve the asymptotic convergence is lost if some time-varying model of the known dynamics is included in the observer design as shown by Theorem 2.7*

Theorem 2.7. *For system* (2.21) *with* $\psi = \psi(t), d = \text{const}$, *observer* (2.26) *and control law* (2.32)–(2.33) *designed with only input gain uncertainty (i.e.* $\hat{b} \neq b$, $\hat{\theta} = \theta$*), guarantee the global convergence of errors* $\bar{z}, \bar{x}$ *to some*

neighborhood of the origin under the tuning proposed by Assumption 2.4 for ω_o, ω_c *chosen high enough.*

Proof. *Under the conditions stated in Theorem 2.7, the derivative of* $V_2(\bar{z}, \bar{x})$ *takes the form of*

$$\begin{aligned}\dot{V}_2\Big|_{\substack{\psi=\psi(t)\\ d=\text{const}\\ \hat{b}\neq b\\ \hat{\theta}=\theta}} = &-\frac{\omega_o}{2}\bar{z}^T\bar{z} - c_0\bar{x}^T\mathbf{R}\mathbf{b}_n\left(\bar{k}^T\omega_c\mathbf{\Phi}_c\mathbf{\Lambda}_n\mathbf{\Phi}_o^{-1} + \mathbf{b}_m^T\right)\bar{z}\\ &-\frac{\omega_c}{2}c_0\bar{x}^T\bar{x} + \bar{z}^T\mathbf{P}\mathbf{b}_m\left(\frac{b}{\hat{b}} - 1\right)\Bigg(\omega_c^2\bar{k}^T\bar{\mathbf{G}}\bar{x} - \frac{\partial\psi}{\partial t}\hat{\theta}\\ &+ x_r^{(m)} + \omega_c\bar{k}^T\Big(\omega_o\mathbf{\Phi}_c\mathbf{\Lambda}_n\mathbf{\Phi}_o^{-1}\bar{\mathbf{H}} - \mathbf{b}_n\mathbf{b}_m\\ &- \mathbf{b}_n\bar{k}^T\omega_c\mathbf{\Phi}_c\mathbf{\Lambda}_n\mathbf{\Phi}_o^{-1}\Big)\bar{z}\Bigg)\end{aligned} \tag{2.77}$$

and satisfies inequality

$$\begin{aligned}\dot{V}_2 \leqslant &-\frac{\omega_o}{2}\|\bar{z}\|^2 + c_0 r_M\left(k_M\left(\frac{\omega_c}{\omega_o}\right)^{n|1} + 1\right)\|\bar{x}\|\,\|\bar{z}\| \qquad (2.78)\\ &-\frac{\omega_c}{2}c_0\|\bar{x}\|^2 + \omega_c^2\bar{b}p_M k_M g_M\|\bar{z}\|\,\|\bar{x}\|\\ &+\bar{b}p_M\psi_L\theta_M\|\bar{z}\| + \omega_c\bar{b}p_M k_M\Bigg(\left(\frac{\omega_c}{\omega_o}\right)^{n-1|0}h_M\\ &+k_M\left(\frac{\omega_c}{\omega_o}\right)^{n|1} + 1\Bigg)\|\bar{z}\|^2 + \bar{b}p_M x_M\|\bar{z}\|.\end{aligned}$$

The above boundary can be expressed as

$$\begin{aligned}\dot{V}_2 \leqslant &-\frac{1}{2}\Bigg(\omega_o - 2\omega_c\bar{b}p_M k_M\Bigg(\left(\frac{\omega_c}{\omega_o}\right)^{n-1|0}h_M\\ &+k_M\left(\frac{\omega_c}{\omega_o}\right)^{n|1} + 1\Bigg) - \frac{1}{\varepsilon_2}c_0 r_M\left(k_M\left(\frac{\omega_c}{\omega_o}\right)^{n|1} + 1\right)^2\\ &-\frac{1}{\varepsilon_1}\omega_c^4\bar{b}p_M k_M g_M\Bigg)\|\bar{z}\|^2 - \frac{1}{2}\Big(\omega_c c_0 - \varepsilon_1\bar{b}p_M k_M g_M\\ &-\varepsilon_2 c_0 r_M\Big)\|\bar{x}\|^2 + \bar{b}p_M(x_M + \psi_L\theta_M)\|\bar{z}\|\end{aligned} \tag{2.79}$$

for any positive constants $\varepsilon_1, \varepsilon_2 \in \mathbb{R}_+$*. For any choice of* c_0 *the coefficient of* $\|\bar{x}\|^2$ *can be made negative by setting* $\varepsilon_1, \varepsilon_2$ *small enough or* ω_c *high enough. Then the negativity of the coefficient of* $\|\bar{z}\|^2$ *is ensured by choosing* ω_o *high enough. Function* $V_2(\bar{z}, \bar{x})$ *satisfies conditions of the Lyapunov function for errors* $\bar{x}, \bar{z}$ *large enough and* $\hat{b}$ *chosen to satisfy Assumption 2.4, guaranteeing the ultimate boundedness of the errors.*

Theorem 2.8. *For system* (2.21) *with* $\psi = \psi(t, x), d = \text{const}$*, observer* (2.26) *and control law* (2.32)–(2.33) *designed with only parameter uncer-*

tainty (i.e. $\hat{b} = b$, $\hat{\theta} \neq \theta$*), guarantee the global convergence of errors* $\bar{z}, \bar{x}$ *to some neighborhood of the origin under the tuning proposed by Assumption 2.4 for* ω_o, ω_c *chosen high enough.*

Proof. *Under the conditions stated in Theorem 2.8, the derivative of* $V_2(\bar{z}, \bar{x})$ *takes the form of*

$$\begin{aligned}\dot{V}_2\Big|_{\substack{\psi=\psi(t,x)\\ \dot{d}=const\\ \dot{\hat{b}}=b\\ \dot{\hat{\theta}}\neq\theta}} = &-\frac{1}{2}\omega_o\bar{z}^T\bar{z} + \omega_o\bar{z}^T\mathbf{P}\mathbf{d}_m\Big(\left(\psi-\psi_r\right)\left(\theta-\hat{\theta}\right)\\ &+\left(\psi-\hat{\psi}\right)\hat{\theta}\Big) - \frac{1}{2}c_0\omega_c\bar{x}^T\bar{x} + \bar{z}^T\mathbf{P}\mathbf{b}_m\Big(\Big(\frac{\partial\psi_r}{\partial x_r}\dot{x}_r\\ &+\frac{\partial\psi_r}{\partial t}\Big)\left(\theta-\hat{\theta}\right)\Big) + c_0\bar{x}^T\mathbf{R}\mathbf{b}_n\Big(\left(\hat{\psi}-\psi\right)\hat{\theta}\\ &+\left(\psi_r-\psi\right)\left(\theta-\hat{\theta}\right) - \Big(\bar{k}^T\omega_c\mathbf{\Phi}_c\mathbf{\Lambda}_n\mathbf{\Phi}_o^{-1}\\ &+\mathbf{b}_m^T\Big)\bar{z}\Big)\end{aligned} \tag{2.80}$$

and satisfies inequality

$$\begin{aligned}\dot{V}_2 \leqslant &-\frac{1}{2}\omega_o\left\|\bar{z}\right\|^2 + \omega_o\left\|\bar{z}\right\|p_M\Big(\psi_L\left\|\mathbf{\Lambda}_n\mathbf{\Phi}_o^{-1}\bar{z}\right\|\theta_M\\ &+\psi_L\left\|\mathbf{\Phi}_c^{-1}\bar{x}\right\|\bar{\theta}\Big) + \left\|\bar{z}\right\|p_M\psi_L\left(x_M+1\right)\bar{\theta} - \frac{1}{2}c_0\omega_c\left\|\bar{x}\right\|^2\\ &+c_0\left\|\bar{x}\right\|r_M\Big(\left(k_M\left(\frac{\omega_c}{\omega_o}\right)^{n|1}+1\right)\left\|\bar{z}\right\| + \psi_L\left\|\mathbf{\Phi}_c^{-1}\bar{x}\right\|\bar{\theta}\\ &+\psi_L\left\|\mathbf{\Lambda}_n\mathbf{\Phi}_o^{-1}\bar{z}\right\|\theta_M\Big).\end{aligned} \tag{2.81}$$

By assigning $c_0 = \omega_o$ *the above boundary can be expressed as*

$$\begin{aligned}\dot{V}_2 \leqslant &-\frac{1}{2}\Big(\omega_o\Big(1-\varepsilon_1 p_M\psi_L\omega_c^{-n+1|0}\bar{\theta}\\ &-\varepsilon_2 r_M\left(k_M\left(\frac{\omega_c}{\omega_o}\right)^{n|1}+1\right)^2 - \varepsilon_3 r_M\psi_L\left(\omega_o^{-n|-1}\right)^2\theta_M\Big)\\ &-2p_M\psi_L\omega_c^{-n+1|0}\theta_M\Big)\left\|\bar{z}\right\|^2 - \frac{1}{2}\omega_o\Big(\omega_c\\ &-\frac{1}{\varepsilon_1}p_M\psi_L\omega_c^{-n+1|0}\bar{\theta} - \frac{1}{\varepsilon_2}r_M - \frac{1}{\varepsilon_3}r_M\psi_L\theta_M\\ &-2r_M\psi_L\omega_c^{-n+1|0}\bar{\theta}\Big)\left\|\bar{x}\right\|^2 + p_M\psi_L\left(x_M+1\right)\bar{\theta}\left\|\bar{z}\right\|\end{aligned} \tag{2.82}$$

for any positive constants $\varepsilon_1, \varepsilon_2, \varepsilon_3 \in \mathbb{R}_+$*. At first, the positiveness of the coefficient associated with* ω_o *can be achieved by setting* $\varepsilon_1, \varepsilon_2, \varepsilon_3$ *small*

enough and ensuring that $\omega_o \geqslant \omega_c$. *The negativeness of the coefficient of* $\left\|\bar{\mathbf{x}}\right\|^2$ *can be reached by setting* ω_c *high enough and choice of* ω_o *high enough ensures the negativeness of the coefficient of* $\left\|\bar{\mathbf{z}}\right\|^2$. *Function* $V_2(\bar{\mathbf{z}}, \bar{\mathbf{x}})$ *thus satisfies conditions of the Lyapunov function for errors* $\bar{\mathbf{x}}, \bar{\mathbf{z}}$ *large enough, guaranteeing the ultimate boundedness of the errors.*

Theorem 2.9. *For system* (2.21) *with* $\boldsymbol{\psi} = \boldsymbol{\psi}(t, \mathbf{x})$, $d = d(t, \mathbf{x})$, *observer* (2.26) *and control law* (2.32)–(2.33) *designed with the parameter and input gain uncertainty (i.e.* $\hat{b} \neq b$, $\hat{\boldsymbol{\theta}} \neq \boldsymbol{\theta}$*), guarantee the global convergence of errors* $\bar{\mathbf{z}}, \bar{\mathbf{x}}$ *to some neighborhood of the origin under the tuning proposed by Assumption 2.4 for* ω_o, ω_c *chosen high enough.*

Proof. *Under the conditions stated in Theorem 2.9, the derivative of* $V_2(\bar{\mathbf{z}}, \bar{\mathbf{x}})$ *takes the form given by* (2.51) *and satisfies inequality*

$$
\begin{aligned}
\dot{V}_2 \leqslant & -\frac{1}{2}\omega_o \left\|\bar{\mathbf{z}}\right\|^2 + \omega_o \left\|\bar{\mathbf{z}}\right\| p_M \psi_L \Bigg(\left\|\boldsymbol{\Lambda}_n \boldsymbol{\Phi}_o^{-1} \bar{\mathbf{z}}\right\| \theta_M \\
& + \left\|\boldsymbol{\Phi}_c^{-1} \bar{\mathbf{x}}\right\| \bar{\theta} \Bigg) + \left\|\bar{\mathbf{z}}\right\| p_M \Bigg(\psi_L \left(x_M + 1\right) \bar{\theta} \\
& + \bar{b} \Bigg(\omega_c k_M \Bigg(\left(\frac{\omega_c}{\omega_o}\right)^{n-1|0} h_M + k_M \left(\frac{\omega_c}{\omega_o}\right)^{n|1} + 1 \Bigg) \left\|\bar{\mathbf{z}}\right\| \\
& + \omega_c^2 k_M g_M \left\|\bar{\mathbf{x}}\right\| + \psi_L \Bigg(x_M + \Bigg(\omega_c^{-n+1|0} l_M + \omega_o^{-n|-1} \\
& + k_M \left(\frac{\omega_c}{\omega_o}\right)^{n|1} \Bigg) \left\|\bar{\mathbf{z}}\right\| + \omega_c \left(k_M + \omega_c^{-n|-1} \right) \left\|\bar{\mathbf{x}}\right\| \Bigg) \theta_M \\
& + \psi_L \theta_M + x_M \Bigg) \Bigg) + \left\|\bar{\mathbf{z}}\right\| p_M \Bigg(d_L \Bigg(\omega_c \left(k_M + \omega_c^{-n|-1} \right) \left\|\bar{\mathbf{x}}\right\| \\
& + \left(k_M \left(\frac{\omega_c}{\omega_o}\right)^{n|1} + 1 \right) \left\|\bar{\mathbf{z}}\right\| + x_M + \Big(\psi_L \left\|\boldsymbol{\Phi}_c^{-1} \bar{\mathbf{x}}\right\| \bar{\theta} \\
& + \psi_L \left\|\boldsymbol{\Lambda}_n \boldsymbol{\Phi}_o^{-1} \bar{\mathbf{z}}\right\| \theta_M \Big) \Bigg) + d_L \Bigg) - \frac{1}{2} c_0 \omega_c \left\|\bar{\mathbf{x}}\right\|^2 \\
& + c_0 \left\|\bar{\mathbf{x}}\right\| r_M \Bigg(\left(k_M \left(\frac{\omega_c}{\omega_o}\right)^{n|1} + 1 \right) \left\|\bar{\mathbf{z}}\right\| \\
& + \psi_L \left\|\boldsymbol{\Phi}_c^{-1} \bar{\mathbf{x}}\right\| \bar{\theta} + \psi_L \left\|\boldsymbol{\Lambda}_n \boldsymbol{\Phi}_o^{-1} \bar{\mathbf{z}}\right\| \theta_M \Bigg),
\end{aligned}
\tag{2.83}
$$

where $l_M = \|\bar{l}\| \in \mathbb{R}_+$. *By assigning* $c_0 = \omega_o$ *the above boundary can be expressed as*

$$\begin{aligned}
\dot{V}_2 \leqslant & -\frac{1}{2}\Bigg(\omega_o\Bigg(1-\varepsilon_1 p_M \psi_L \bar{\theta} - \varepsilon_2 r_M \psi_L \left(\omega_o^{-n|-1}\right)^2 \theta_M \\
& - \varepsilon_3 r_M \left(k_M \left(\frac{\omega_c}{\omega_o}\right)^{n|1} + 1\right)^2\Bigg) - \omega_c^4 p_M \bar{b} k_M g_M \\
& - 2\omega_c p_M \bar{b} k_M \left(\left(\frac{\omega_c}{\omega_o}\right)^{n-1|0} h_M + k_M \left(\frac{\omega_c}{\omega_o}\right)^{n|1} + 1\right) \\
& - 2p_M \psi_L \theta_M \Bigg(\bar{b}\left(\omega_c^{-n+1|0} l_M + \omega_o^{-n|-1} + k_M \left(\frac{\omega_c}{\omega_o}\right)^{n|1}\right) \\
& + d_L \omega_o^{-n|-1} + \omega_c^{-n+1|0}\Bigg) - 2p_M d_L \left(k_M \left(\frac{\omega_c}{\omega_o}\right)^{n|1} + 1\right) \\
& - \omega_c^2 p_M \left(\bar{b}\psi_L \theta_M + d_L\right)\left(k_M + \omega_c^{-n|-1}\right)^2 \\
& - d_L p_M \psi_L \bar{\theta}\Bigg)\|\bar{z}\|^2 - \frac{1}{2}\Bigg(\omega_o\Bigg(\omega_c - \frac{1}{\varepsilon_1} p_M \psi_L \bar{\theta}\left(\omega_c^{-n+1|0}\right)^2 \\
& - \frac{1}{\varepsilon_2} r_M \psi_L \theta_M - \frac{1}{\varepsilon_3} r_M - 2 r_M \psi_L \omega_c^{-n+1|0} \bar{\theta}\Bigg) - p_M \bar{b} k_M g_M \\
& - p_M \bar{b} \psi_L \theta_M - p_M d_L - d_L p_M \psi_L \left(\omega_c^{-n+1|0}\right)^2 \bar{\theta}\Bigg)\|\bar{x}\|^2 \\
& + p_M \Bigg(\left(\psi_L x_M + \psi_L\right)\bar{\theta} + \bar{b}\left(\psi_L x_M \theta_M + \psi_L \theta_M + x_M\right) \\
& + d_L x_M + d_L\Bigg)\|\bar{z}\|
\end{aligned} \tag{2.84}$$

for any positive constants $\varepsilon_1, \varepsilon_2, \varepsilon_3 \in \mathbb{R}_+$. *At first, the positiveness of the coefficient associated with* $\omega_o\|\bar{z}\|^2$ *can be achieved by setting* $\varepsilon_1, \varepsilon_2, \varepsilon_3$ *small enough and ensuring that* $\omega_o \geqslant \omega_c$. *The negativeness of the coefficient of* $\|\bar{x}\|^2$ *can be reached by setting* ω_c *high enough and choice of* ω_o *high enough ensures the negativeness of the coefficient of* $\|\bar{z}\|^2$. *Function* $V_2(\bar{z}, \bar{x})$ *thus satisfies conditions of the Lyapunov function for errors* $\bar{x}, \bar{z}$ *large enough and* $\hat{b}$ *chosen to satisfy Assumption 2.4, guaranteeing the ultimate boundedness of the errors.*

The presented theorems unveil a wide range of behaviors exhibited by the systems working under the ADRC controllers. It is presented that in the nominal case of the simple system without any varying disturbances the asymptotic convergence is guaranteed for any choice of the observer and controller bandwidths. In line with the results presented in the literature, it is shown that in the presence of unknown varying disturbances only the ultimate boundedness of the errors is ensured and additional requirements on the choice of bandwidths are

imposed if the disturbance directly depends on the state of the plant. The incorporation of the known terms of the plant dynamics in the observer and controller design enables successful compensation and recovery of the asymptotic stability, but the limitations of the choice of the tuning variables are also imposed if the modeled dynamics are expressed as a function of the state of the system. The uncertainties present in the considered system further erode the performance of the controller. The parametric uncertainty of the varying drift of the plant used in the observer design makes it impossible to achieve the asymptotic convergence of the errors and strengthens the limitations imposed on the choice of the tuning parameters requiring an increase of the observer and controller bandwidths. In the presence of the input gain uncertainty, an asymptotic convergence can be ensured by an increase of the bandwidths only in the most basic scenario of a system free of any known or unknown varying disturbances if the reference trajectory satisfies certain conditions. In other cases, the unknown input gain bolsters the negative effects of the structure of the system increasing the size of the ultimate bound of the system and requirements for the choice of the higher values of the tuning variables. Regardless of the considered scenario, Assumption 2.4 remains the fundamental requirement for the presented stability analysis and unveils the direct dependence of the feasible observer tuning values on the extent of the input gain uncertainty. This assumption, together with Theorem 2.6, is in line with the results presented in the manuscript by the group of S. Chen [44] where the stability of matrix $\bar{\mathbf{H}}$ is stated as the necessary and sufficient condition for the existence of ω_o high enough to stabilize the closed-loop dynamics. Here, similar results are independently developed on the basis of the straightforward Lyapunov analysis. The performance of the ADRC controller in different scenarios is summarized in Tab. 2.3 where the results which can be obtained by the analysis of (2.51) are presented.

2.3 IMPACT OF THE INPUT GAIN UNCERTAINTY

The analysis presented in Section 2.2 unveiled some major properties of the ADRC control scheme working in the presence of the modeling uncertainties. Specifically, the satisfaction of Hurwitz condition by matrix $\bar{\mathbf{H}}$ according to Assumption 2.4 is used as a cornerstone for the stability analysis. Further study of the dynamics of the closed-loop system showed that this property is not a sufficient condition for the stability of the system, as in the presence of the uncertainty of the input gain of the plant, additional requirements are imposed concerning the choice of the tuning variables, as given by Theorem 2.6. Due to the presence of matrix $\mathbf{P}$ in (2.51), the input gain uncertainty affects

	$\hat{b} = b$ $\hat{\theta} = \theta$	$\hat{b} \neq b$ $\hat{\theta} = \theta$	$\hat{b} = b$ $\hat{\theta} \neq \theta$	$\hat{b} \neq b$ $\hat{\theta} \neq \theta$
$\psi = \text{const}, d = \text{const}$	asymp., any ω	bound*., high ω	asymp., any ω	bound*., high ω
$\psi = \psi(t), d = \text{const}$	asymp., any ω	bound., high ω	bound., high ω	bound., high ω
$\psi = \psi(t, x), d = \text{const}$	asymp., high ω	bound., high ω	bound., high ω	bound., high ω
$\psi = \text{const}, d = d(t)$	bound., any ω	bound., high ω	bound., any ω	bound., high ω
$\psi = \psi(t), d = d(t)$	bound., any ω	bound., high ω	bound., high ω	bound., high ω
$\psi = \psi(t, x), d = d(t)$	bound., high ω	bound., high ω	bound., high ω	bound., high ω
$\psi = \text{const}, d = d(t, x)$	bound., high ω	bound., high ω	bound., high ω	bound., high ω
$\psi = \psi(t), d = d(t, x)$	bound., high ω	bound., high ω	bound., high ω	bound., high ω
$\psi = \psi(t, x), d = d(t, x)$	bound., high ω	bound., high ω	bound., high ω	bound., high ω

* depending on the chosen reference trajectory, possible asymptotic convergence

Table 2.3: Performance of the ADRC control and required bandwidths in different scenarios. Cases covered by the theorems explicitly presented in this work are given in color. All uncovered scenarios can be seen as special cases of the discussed examples.

also the ability of the controller to compensate for the unmodeled disturbances. The term P is derived by the Lyapunov equation directly from $\bar{H}$ which in turn depends explicitly on the ratio between the real value of the input gain of the plant and its estimated approximation. The relation between P and $\bar{H}$ is a nonlinear one, and thus the exact impact of the modeling uncertainty on the performance of the controller is not immediately clear from the analysis of (2.51). These observations suggest the need for a more detailed study aimed at finding the feasible range of the observer and controller gains, as well as their impact on the overall performance of the algorithm, for the systems subject to input gain uncertainty.

In this section, some results on this problem are presented on the basis of the findings reported in [228, 233]. Namely, the dynamics of the tracking and estimation errors as given by (2.37) are recalled and investigated in more detail. The explicit form of the error dynamics is given for various propositions of the internal control law ν and, on their basis, the numerical studies are conducted to explicitly determine the stability conditions of the closed-loop system depending on the extent of uncertainty and the chosen tuning of the algorithm.

Numerical simulations are also employed to investigate the impact of the input gain uncertainty on the rejection of the disturbance by the ADRC controller. It is found that the underestimation of the input gain of the plant introduces more strict requirements concerning the choice of the tuning bandwidths but simultaneously may lead to an increase in the performance of the system. This improvement is significantly more considerable if the controller is designed in the error domain according to (2.17)–(2.20). Moreover, it is shown that the need for the choice of higher gains imposed by the presence of the input gain uncertainty can be alleviated if at least some of the state variables are measurable. As a result of this phenomenon, the stability of $\bar{H}$ is not the necessary condition for the stability of the closed-loop system if the entire state of the system is available for measurement.

While the main focus of this section considers only the problem of static uncertainty in the input path, some results on the stability of the ADRC scheme in the presence of unmodelled dynamics governing the input of the plant are also given on the basis of [226, 227]. It is shown that if the degree of the plant is higher than assumed during the controller synthesis and the input path is governed by some stable dynamics, the overall closed loop system maintains the stability if the input path dynamics are fast enough. This general conclusion is formulated through the analytical investigation. Additional numerical studies supporting this result unveil also that the increase of input phase lag rapidly hinders the stabilization of the system and strongly limits the feasible choice of the controller bandwidth.

2.3.1 *Stability of the system*

Consider the system discussed in Section 2.2 and assume, to facilitate further analysis, that $\psi(t,\mathbf{x}) = 0$ and $d(t,\mathbf{x}) = d(t)$, what yields

$$\dot{\mathbf{x}} = \mathbf{A}_n\mathbf{x} + \mathbf{b}_n\left(b\mathbf{u} + d(t)\right), \tag{2.85}$$

where $\mathbf{x} \in \mathbb{R}^n$ is the state of the plant, $b \in \mathbb{R}\setminus\{0\}$ is the control input and $d(t) \in \mathbb{R}$ is some unknown disturbance affecting the system. Recall the state extension (2.25) and (2.28) in the form of

$$\begin{aligned} \dot{\mathbf{z}} &= \mathbf{A}_m\mathbf{z} + \mathbf{d}_m\hat{b}u + \mathbf{b}_m\frac{d}{dt}\delta, \\ \delta &= \left(b - \hat{b}\right)u + d(t) \end{aligned} \tag{2.86}$$

with $z \in \mathbb{R}^m$ being extended state, where $m = n + 1$, and $\delta \in \mathbb{R}$ being the total disturbance in the system. For such a system, observer (2.26) is given by

$$\dot{\hat{z}} = \mathbf{A}_m \hat{z} + \mathbf{d}_m \hat{b} u + \mathbf{l} \mathbf{c}_m^T (z - \hat{z}) \tag{2.87}$$

with $\hat{z} \in \mathbb{R}^m$ being the extended state estimate. The control law in the form of (2.32) and (2.33) is designed as

$$\begin{aligned} u &= \frac{1}{\hat{b}} \left(\nu - \hat{\delta} \right), \\ \nu &= \mathbf{k}^T (\mathbf{x}_r - \hat{\mathbf{x}}) + x_r^{(n)}. \end{aligned} \tag{2.88}$$

Note, that some of the state variables of the plant may be measurable and different forms of the internal control law ν may thus be designed. To consider this issue, define the auxiliary mixed extended state vector $z_\eta^* \in \mathbb{R}^m$ consisting of the combination of η measurable states variables and estimates of the remaining signals, with η being some nonnegative constant integer representing the number of measurable states available for control law design.

Remark 2.3. *Even though the degree of measurability η can be equal to 0, the observer design requires at least one state variable to be measurable. Yet, constant η refers only to the number of state variables directly included in the control law and not to their factual measurability and thus the observer can be succesfully synthesized even if $\eta = 0$.*

The explicit form of this auxiliary vector is given by

$$z_\eta^* = (\mathbf{I}_m - \mathbf{\Pi}_{m,\eta}) z + \mathbf{\Pi}_{m,\eta} \hat{z} \tag{2.89}$$

with the mixing matrix defined as $\mathbf{\Pi}_{m,\eta} = \operatorname{diag}(\mathbf{0}_\eta, \mathbf{I}_{m-\eta}) \in \mathbb{R}^{m \times m}$ for any constant nonnegative integer η satisfying $\eta \leqslant m - 1$. By taking advantage of this notation the internal control law incorporating measurable state variables in the feedback loop is redesigned as

$$\nu_\eta = \mathbf{k}^T \left(\mathbf{x}_r - \mathbf{\Lambda}_n z_\eta^* \right) + x_r^{(n)}. \tag{2.90}$$

Note that the control law considered in Section 2.2 and given by (2.33) is a specific case of the more general controller (2.90) obtained by setting $\eta = 0$. The studies of this section are thus wider in scope than previous investigations. Simultaneously, one can observe that $\left\| \mathbf{\Pi} \right\| \leqslant 1$ and thus the analytical solutions given in the preceding section are conservatively valid also for the system considered here, as introduction of $\mathbf{\Pi}$ does not invalidate the Lyapunov analysis of the stability of the closed-loop system. By employing the control law

based on the mixed extended state vector, the error dynamic, originally given by (2.37), take the generalized form of

$$\begin{aligned}\dot{\tilde{z}} &= \mathbf{H}\tilde{z} + \mathbf{b}_m \left(\left(\frac{b}{\hat{b}} - 1 \right) \dot{v} + \dot{d} \right), \\ \dot{\tilde{x}} &= \mathbf{G}\tilde{x} - \mathbf{W}\mathbf{\Pi}_{m,\eta}\tilde{z}.\end{aligned} \tag{2.91}$$

The change in the dynamics of the tracking error introduced by the use of mixed extended state is consistent with predictions of Remark 2.2. The dynamics of the inner control law, expressed in terms of the tracking and estimation errors, are given as

$$\dot{v}_\eta = \mathbf{k}^T \mathbf{G}\tilde{x} + \mathbf{k}^T \left(\mathbf{\Lambda}_n \mathbf{\Pi}_{m,\eta} \mathbf{H} - \mathbf{W}\mathbf{\Pi}_{m,\eta} \right) \tilde{z} + x_r^{(m)}. \tag{2.92}$$

Consider the concatenated errors ξ consisting of both tracking and estimation errors and defined as $\xi = \begin{bmatrix} \tilde{z}^T & \tilde{x}^T \end{bmatrix}^T \in \mathbb{R}^{m+n}$. By substituting (2.92) into (2.91) the dynamics of ξ are expressed in the compact form of

$$\dot{\xi} = \mathbf{N}\xi + \begin{bmatrix} \mathbf{b}_m^T & \mathbf{0}_{n\times 1}^T \end{bmatrix}^T \left(\dot{d} + \left(\frac{b}{\hat{b}} - 1 \right) x_r^{(m)} \right), \tag{2.93}$$

where $\mathbf{N} \in \mathbb{R}^{m+n\times m+n}$ is a constant matrix dependent on the choice of gains $\mathbf{k}$ and $\mathbf{l}$, uncertainty of the input gain b and the degree of measurability η, and is given as

$$\mathbf{N} = \begin{bmatrix} \mathbf{H} + \tilde{b}\mathbf{b}_m \mathbf{k}^T \left(\mathbf{\Lambda}_n \mathbf{\Pi}_{m,\eta} \mathbf{H} - \mathbf{W}\mathbf{\Pi}_{m,\eta} \right) & \tilde{b}\mathbf{b}_m \mathbf{k}^T \mathbf{G} \\ -\mathbf{W}\mathbf{\Pi}_{m,\eta} & \mathbf{G} \end{bmatrix} \tag{2.94}$$

with $\tilde{b} = \frac{b}{\hat{b}} - 1$. The term $\bar{b}$ is defined as in Section 2.2 and thus satisfies $\bar{b} = \left\| \tilde{b} \right\|$. The dynamics given above have the form of a simple disturbed linear system and its stability can be concluded on the basis of matrix $\mathbf{N}$. Despite the straightforward form of this equation, a direct analytical formulation of stability conditions for the system of arbitrary order is a nontrivial task due to the dependency of matrix $\mathbf{N}$ on $\mathbf{k}$, $\mathbf{l}$, $\hat{b}$, and η. The explicit solution to this problem has not yet been found.

In this chapter numerical analysis is employed to unveil some properties of matrix $\mathbf{N}$ for the system of chosen order. To this end, the second order ($n = 2$) system in the form of (2.85) is considered as the commonly investigated exemplary dynamics. By denoting $\tilde{\beta} = \frac{b}{\hat{b}}$,

the exact forms of matrix $\mathbf{N}$ for different choices of $\eta \in \{0,1,2\}$ are obtained as follows,

$$\mathbf{N}\Big|_{\substack{n=2\\ \eta=0}} = \left[\begin{array}{ccc|c} -l_1 & 1 & 0 & \\ -l_2 & 0 & 1 & \tilde{b}\mathbf{b}_m\mathbf{k}^T\mathbf{G} \\ n_{3,1} & \tilde{b}\left(k_1-k_2^2\right) & 0 & \\ \hline 0 & 0 & 0 & \\ -k_1 & -k_2 & -1 & \mathbf{G} \end{array}\right],$$

$$\mathbf{N}\Big|_{\substack{n=2\\ \eta=1}} = \left[\begin{array}{ccc|c} -l_1 & 1 & 0 & \\ -l_2 & 0 & 1 & \tilde{b}\mathbf{b}_m\mathbf{k}^T\mathbf{G} \\ -\tilde{\beta}l_3-\tilde{b}k_2l_2 & -\tilde{b}k_2^2 & 0 & \\ \hline 0 & 0 & 0 & \\ 0 & -k_2 & -1 & \mathbf{G} \end{array}\right], \tag{2.95}$$

$$\mathbf{N}\Big|_{\substack{n=2\\ \eta=2}} = \left[\begin{array}{ccc|c} -l_1 & 1 & 0 & \\ -l_2 & 0 & 1 & \tilde{b}\mathbf{b}_m\mathbf{k}^T\mathbf{G} \\ -\tilde{\beta}l_3 & 0 & -\tilde{b}k_2 & \\ \hline 0 & 0 & 0 & \\ 0 & 0 & -1 & \mathbf{G} \end{array}\right]$$

with

$$\begin{aligned} n_{3,1} &= -\tilde{\beta}l_3 - \tilde{b}\left(k_2\left(k_1+l_2\right)+k_1l_1\right), \\ \tilde{b}\mathbf{b}_m\mathbf{k}^T\mathbf{G} &= \begin{bmatrix} 0 & 0 \\ 0 & 0 \\ -\tilde{b}k_1k_2 & \tilde{b}\left(k_1-k_2^2\right) \end{bmatrix}, \ \mathbf{G} = \begin{bmatrix} 0 & 1 \\ -k_1 & -k_2 \end{bmatrix}. \end{aligned} \tag{2.96}$$

In order to investigate the impact of the modeling uncertainty on the stability and convergence of the closed-loop system working under the ADRC controller, numerical evaluation of the Hurwitz criterion for each variant of $\mathbf{N}$ matrix can be considered. To enable such analysis some parametrization of the observer and controller gain is required and thus the tuning proposed in Tab. 2.1 is embraced here, leading to the tuning variables chosen as

$$\mathbf{l} = \begin{bmatrix} 3\omega_o & 3\omega_o^2 & \omega_o^3 \end{bmatrix}^T, \ \mathbf{k} = \begin{bmatrix} \omega_c^2 & 2\omega_c \end{bmatrix}^T. \tag{2.97}$$

For such a choice of tuning variables matrix $\bar{\mathbf{H}}$ takes the form of

$$\bar{\mathbf{H}} = \begin{bmatrix} -3 & 1 & 0 \\ -3 & 0 & 1 \\ -\tilde{\beta} & 0 & 0 \end{bmatrix} \tag{2.98}$$

and is stable for any $\tilde{\beta} \in (0,9)$. The presented representation of the dynamics of the system is an alternative to (2.37) which used (2.47) as a starting point for the stability analysis. The stability conditions of

matrix $\bar{\mathbf{H}}$ can be compared with the stability of entire $\mathbf{N}$ to investigate whether Assumption 2.4 is necessary for the convergence of the ADRC system. The results of the numerical evaluation of the stability of matrix $\mathbf{N}$ are given in Fig. 2.9 as a function of ω_o, ω_c and $\tilde{\beta}$.

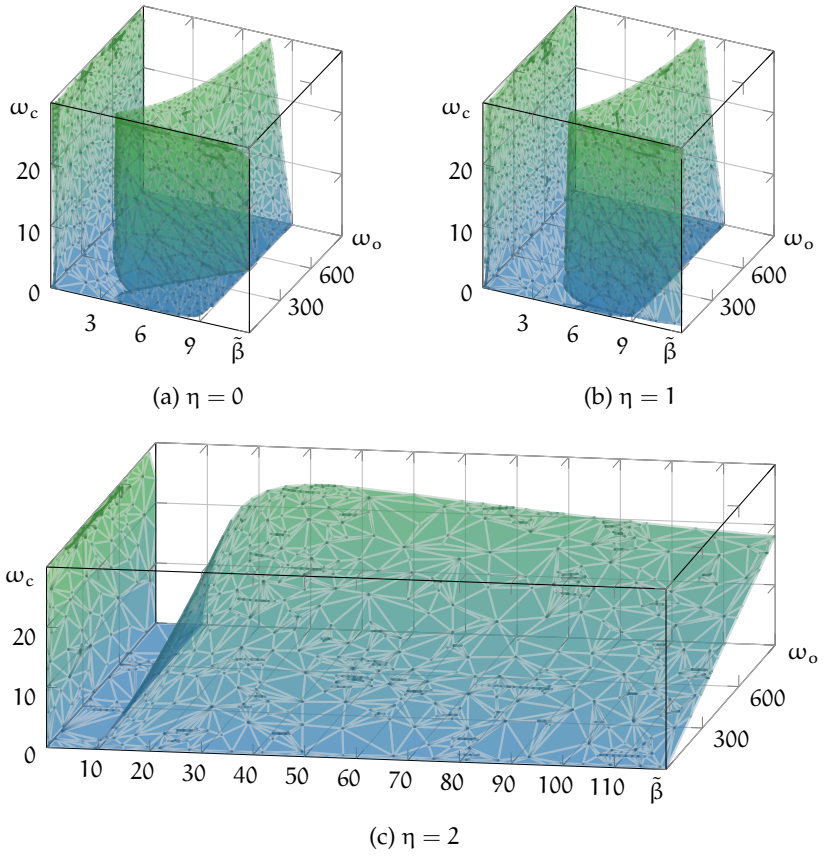

Figure 2.9: Borders of stability regions of $\mathbf{N}$ for different values of η parameter. Stable regions correspond to the areas above the surface.

Produced results show that for $\eta = 0$ and $\eta = 1$ the stability of $\bar{\mathbf{H}}$ is indeed the necessary condition for the stability of the system for a wide range of tuning bandwidths. Yet, the numerical evaluation of the stability conditions of $\mathbf{N}$ matrices reveals that for small values of the observer bandwidth the stability of the closed-loop system can be achieved even if matrix $\bar{\mathbf{H}}$ is not itself stable, what has not been noticed and reported in [44] or other earlier papers. Nonetheless, for any greater value of ω_o the system is not stabilizable for $\tilde{\beta} > 9$. An increase of the modeling uncertainty $\tilde{\beta}$ enforces also the choice of higher ω_o to maintain the stability of the closed-loop system, what is in line with the results presented in the literature. In accordance with the notions made on the basis of (2.51), higher choices of the observer bandwidth are also necessary to stabilize the system if the higher values of ω_c are chosen. The introduction of a single measurable state variable does not significantly change the character of the stability

conditions of the plant, save for a slight increase in the range of observer bandwidths feasible to stabilize the system in the presence of significant input gain uncertainty. Only once the entire state vector is available for the control law design and the observer is used only to produce the estimate of the total disturbance acting upon the plant, the dynamics of the plant undergo a fundamental change. In such a case, the stability of $\bar{\mathbf{H}}$ is no longer an important condition for the stability of the closed-loop system and the convergence of the errors can be ensured even in the presence of significantly greater modeling uncertainties. Despite multiple attempts (search up to $\tilde{\beta} = 10^4$), no ultimate value of $\tilde{\beta}$ for which it would be impossible to ensure the stability of the system was found. Moreover, once a certain threshold is crossed by the value of $\tilde{\beta}$ its further increase does not lead to higher requirements concerning the choice of ω_o and ω_c but instead increases the range of feasible bandwidth choices.

Further insights into the stability properties of $\mathbf{N}$ matrix can be provided by the analysis of the explicit forms of the Routh-Hurwitz table $\mathbf{RH}$ associated with this matrix and expressed as follows,

$$\mathbf{RH}\Big|_{n=2} = \begin{bmatrix} 1 & \rho_{2,1} & \rho_{3,1} \\ \rho_{1,2} & \rho_{2,2} & \rho_{3,2} \\ \rho_{1,3}\rho_{1,2}^{-1} & \rho_{2,3} & 0 \\ \rho_{1,4}\rho_{1,3}^{-1} & \rho_{2,4} & 0 \\ \rho_{1,5}\rho_{1,4}^{-1} & 0 & 0 \\ \rho_{1,6} & 0 & 0 \end{bmatrix}. \tag{2.99}$$

By embracing the tuning given by (2.97), the exact values of the elements of $\mathbf{RH}$ table can be derived independently for each of the matrices from (2.95). The elements for matrix $\mathbf{N}$ with $\eta = 0$ are

$$\begin{aligned} \rho_{1,2} &= 3\omega_o + 2\omega_c, \\ \rho_{1,3} &= \left(9-\tilde{\beta}\right)\omega_o^3 + 6\left(4-\tilde{\beta}\right)\omega_o^2\omega_c + 3\left(5-\tilde{\beta}\right)\omega_o\omega_c^2 - 2\omega_c^3, \\ \rho_{1,4} &= \left(9-\tilde{\beta}\right)\tilde{\beta}\omega_o^6 + 12\left(5-\tilde{\beta}\right)\tilde{\beta}\omega_o^5\omega_c \\ &\quad + 6\left(23-7\tilde{\beta}\right)\tilde{\beta}\omega_o^4\omega_c^2 + 2\left(61-18\tilde{\beta}\right)\tilde{\beta}\omega_o^3\omega_c^3 \\ &\quad + 9\left(5-\tilde{\beta}\right)\tilde{\beta}\omega_o^2\omega_c + 6\tilde{\beta}\omega_o\omega_c^5, \end{aligned}$$

$$\begin{aligned}
\rho_{1,5} = & -\tilde{\beta}\omega_o^3\omega_c^2\left(3\omega_o+2\omega_c\right)\left(3\omega_o^2+6\omega_o\omega_c+\omega_c^2\right)^2 \\
& -\tilde{\beta}^3\omega_o^4\omega_c\left(2\omega_o+3\omega_c\right)\left(\omega_o^2+6\omega_o\omega_c+3\omega_c^2\right)^2 \\
& +2\tilde{\beta}^2\omega_o^3\omega_c\Big(9\omega_o^6+75\omega_o^5\omega_c+243\omega_o^4\omega_c^2+358\omega_o^3\omega_c^3 \\
& +243\omega_o^2\omega_c^4+75\omega_o\omega_c^5+9\omega_c^6\Big), \\
\rho_{1,6} = & \tilde{\beta}\omega_o^3\omega_c^2,
\end{aligned} \tag{2.100}$$

and

$$\begin{aligned}
\rho_{2,1} = & 3\tilde{\beta}\omega_o^2+6\omega_o\omega_c+4\omega_c^2-3\tilde{\beta}\omega_c^2, \\
\rho_{2,2} = & \left(10\tilde{\beta}-9\right)\omega_o^3+6\left(2\tilde{\beta}-1\right)\omega_o^2\omega_c \\
& +3\left(3-2\tilde{\beta}\right)\omega_o\omega_c^2-6\left(\tilde{\beta}-1\right)\omega_c^3, \\
\rho_{2,3} = & -\frac{6\omega_c\left(\omega_o+\omega_c\right)}{3\omega_o+2\omega_c}\Big(\left(9-10\tilde{\beta}\right)\omega_o^3+\left(2\tilde{\beta}-3\right)\omega_o^2\omega_c \\
& +5\left(\tilde{\beta}-1\right)\omega_o\omega_c^2+\left(\tilde{\beta}-1\omega_c^3\right)\Big), \\
\rho_{2,4} = & \left(10\tilde{\beta}-9\right)\omega_o^3\omega_c^2+9\left(1-\tilde{\beta}\right)\omega_o\omega_c^4, \\
\rho_{3,1} = & 2\left(10\tilde{\beta}-9\right)\omega_o^3\omega_c+3\left(2\tilde{\beta}-1\right)\omega_o^2\omega_c^2 \\
& -18\left(\tilde{\beta}-1\right)\omega_o\omega_c^3-3\left(\tilde{\beta}-1\right)\omega_c^4, \\
\rho_{3,2} = & \left(10\tilde{\beta}-9\right)\omega_o^3\omega_c^2-9\left(\tilde{\beta}-1\right)\omega_o\omega_c^4.
\end{aligned} \tag{2.101}$$

The inclusion of some measurable state variables in the control law significantly simplifies the Routh-Hurwitz table. Assuming $\eta = 1$ leads to the terms of the table given as

$$\begin{aligned}
\rho_{1,2} = & 3\omega_o+2\omega_c, \\
\rho_{1,3} = & \left(9-\tilde{\beta}\right)\omega_o^3+6\left(4-\tilde{\beta}\right)\omega_o^2\omega_c \\
& +12\omega_o\omega_c^2+2\tilde{\beta}\omega_c^3, \\
\rho_{1,4} = & \left(9-\tilde{\beta}\right)\tilde{\beta}\omega_o^6+12\left(5-\tilde{\beta}\right)\tilde{\beta}\omega_o^5\omega_c \\
& +3\left(45-13\tilde{\beta}\right)\tilde{\beta}\omega_o^4\omega_c^2+2\left(51-8\tilde{\beta}\right)\tilde{\beta}\omega_o^3\omega_c^3 \\
& +12\left(2+\tilde{\beta}\right)\tilde{\beta}\omega_o^2\omega_c+6\tilde{\beta}^2\omega_o\omega_c^5,
\end{aligned}$$

$$
\begin{aligned}
\rho_{1,5} = & -9\tilde{\beta}\omega_o^5\omega_c^2\left(\omega_o+2\omega_c\right)^2\left(3\omega_o+2\omega_c\right)\\
& +6\tilde{\beta}^2\omega_o^4\omega_c\Big(3\omega_o^5+25\omega_o^4\omega_c+8-\omega_o^3\omega_c^2-108\omega_o^2\omega_c^3\\
& +55\omega_o\omega_c^4+8\omega_c^5\Big)+\tilde{\beta}^3\omega_o^3\omega_c\Big(2\omega_o^6+27\omega_o^5\omega_c\\
& +114\omega_o^4\omega_c^2+148\omega_o^3\omega_c^3+18\omega_o^2\omega_c^4-48\omega_o\omega_c^5-16\omega_c^6\Big),\\
\rho_{1,6} = & \tilde{\beta}\omega_o^3\omega_c^2,
\end{aligned}
\tag{2.102}
$$

as well as

$$
\begin{aligned}
\rho_{2,1} &= 3\omega_o^2+6\omega_o\omega_c+\tilde{\beta}\omega_c^2,\\
\rho_{2,2} &= \tilde{\beta}\left(\omega_o^3+6\omega_o^2\omega_c+3\omega_o\omega_c^2\right),\\
\rho_{2,3} &= \frac{6\tilde{\beta}\omega_o^2\omega_c}{3\omega_o+2\omega_c}\left(\omega_o+\omega_c\right)^2,\\
\rho_{2,4} &= \tilde{\beta}\omega_o^3\omega_c^2.
\end{aligned}
\tag{2.103}
$$

Finally, assigning $\eta = 2$ and designing a control law on the basis of the fully measurable state of the plant yields

$$
\begin{aligned}
\rho_{1,2} = & \ 3\omega_o+2\tilde{\beta}\omega_c,\\
\rho_{1,3} = & \ \left(9-\tilde{\beta}\right)\omega_o^3+18\tilde{\beta}\omega_o^2\omega_c+12\tilde{\beta}^2\omega_o\omega_c^2+2\tilde{\beta}^2\omega_c^3,\\
\rho_{1,4} = & \ \left(9-\tilde{\beta}\right)\tilde{\beta}\omega_o^6+12\left(3+\tilde{\beta}\right)\tilde{\beta}\omega_o^5\omega_c\\
& +3\left(1+27\tilde{\beta}+4\tilde{\beta}^2\right)\tilde{\beta}\omega_o^4\omega_c^2+2\left(10+33\tilde{\beta}\right)\tilde{\beta}^2\omega_o^3\omega_c^3\\
& +36\tilde{\beta}^3\omega_o^2\omega_c^4+6\tilde{\beta}^3\omega_o\omega_c^5,\\
\rho_{1,5} = & -27\tilde{\beta}\omega_o^8\omega_c^2+2\Big(9\omega_o^3+51\omega_o^2\omega_c+6\omega_o\omega_c^2\\
& +4\omega_c^3\Big)\tilde{\beta}^2\omega_o^6\omega_c+\Big(-2\omega_o^4+21\omega_o^3\omega_c+204\omega_o^2\omega_c^2\\
& +144\omega_o\omega_c^3+42\omega_c^4\Big)\tilde{\beta}^3\omega_o^5\omega_c+2\Big(12\omega_o^4+84\omega_o^3\omega_c\\
& +99\omega_o^2\omega_c^2+48\omega_o\omega_c^3+8\omega_c^4\Big)\tilde{\beta}^4\omega_o^3\omega_c^3,\\
\rho_{1,6} = & \ \tilde{\beta}\omega_o^3\omega_c^2,
\end{aligned}
\tag{2.104}
$$

with

$$\begin{aligned}
\rho_{2,1} &= 3\omega_o^2 + 6\tilde{\beta}\omega_o\omega_c + \tilde{\beta}\omega_c^2,\\
\rho_{2,2} &= \tilde{\beta}\omega_o\left(\omega_o^2 + 6\omega_o\omega_c + 3\omega_c^2\right),\\
\rho_{2,3} &= \frac{2\tilde{\beta}\omega_o^2\omega_c}{3\omega_o + 2\tilde{\beta}\omega_c}\left(3\omega_o^2 + 2\left(2+\tilde{\beta}\right)\omega_o\omega_c + 3\tilde{\beta}\omega_c^2\right),\\
\rho_{2,4} &= \tilde{\beta}\omega_o^3\omega_c^2,\\
\rho_{3,1} &= \tilde{\beta}\omega_o^2\omega_c\left(2\omega_o + 3\omega_c\right),\\
\rho_{3,2} &= \tilde{\beta}\omega_o^3\omega_c^3.
\end{aligned} \tag{2.105}$$

Some further conclusions, compatible with the results of numerical calculations, can be drawn by analysis of the elements of **RH** tables given by (2.100)–(2.105). The extensive presence of the terms in form of the polynomials of input gain estimation error $\tilde{\beta}$ can be noticed, especially of the first order terms given by $\left(\rho_0 - \tilde{\beta}\right)$ where ρ_0 is some positive constant. Clearly, such terms work toward the destabilization of the system once the input gain estimate is chosen such that $\tilde{\beta} > \rho_0$. The presence of multiple such expressions in the Routh-Hurwitz tables of the systems with $\eta = 0$ and $\eta = 1$ is associated with the destabilization of these systems in the presence of significant modeling uncertainties as shown in Fig. 2.9. In contrast, in **RH** table for $\eta = 2$ such term appears only once with $\rho_0 = 9$. Such a change is also coherent with numerical results which showed that the system with a measurable state is stable for almost any $\tilde{\beta} < 9$. The terms $\rho_{1,5}$ for all variants of the system suggest that the dynamics may not be stable for very small values of $\tilde{\beta}$ and certain choices of the controller and observer bandwidths which is also coherent with the results of the numerical evaluations.

In order to generalize and confirm the notions made on the basis of the second order system, the numerical evaluation of the stability of the third order system is presented in Fig. 2.10. For the purposes of this investigation, the tuning and parametrization as proposed in Tab. 2.1 is once again employed. Under such a tuning matrix $\bar{\mathbf{H}}$ takes the form of

$$\bar{\mathbf{H}}\Big|_{n=3} = \begin{bmatrix} -4 & 1 & 0 & 0\\ -6 & 0 & 1 & 0\\ -4 & 0 & 0 & 1\\ -\tilde{\beta} & 0 & 0 & 0 \end{bmatrix}, \tag{2.106}$$

which is Hurwitz for any input gain uncertainty satisfying $\tilde{\beta} \in (0, 5)$. The numerical evaluation of the stability of the system is conducted in the same manner as for the second-order plant. The results presented in the plots confirm the notions made in this section on the basis of

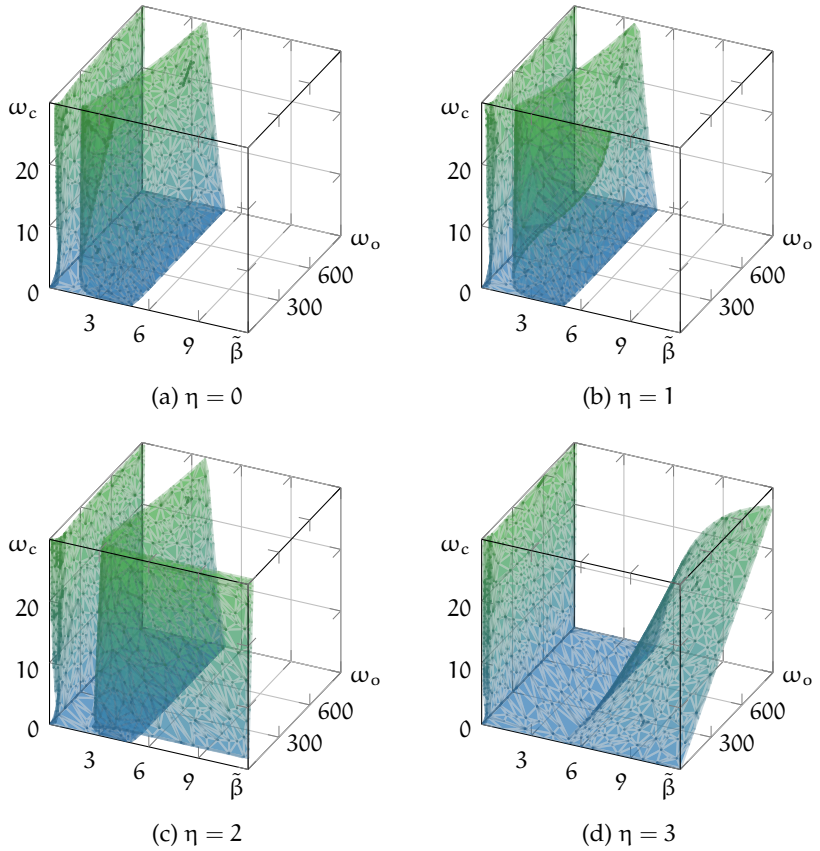

(a) $\eta = 0$ (b) $\eta = 1$

(c) $\eta = 2$ (d) $\eta = 3$

Figure 2.10: Borders of stability regions of $\mathbf{N}$ for the third order system and different values of η parameter.

the second-order system. Namely, it is possible to stabilize the system for the small values of the observer bandwidth even with the unstable matrix $\bar{\mathbf{H}}$. Nonetheless, if not all state variables are available for the control law design the stability of $\bar{\mathbf{H}}$ stands as a crucial precondition for an easy stabilization of the closed-loop system in a wider range of observer and controller tuning values. The inclusion of a fully measurable state in the control law causes the system to undergo a fundamental change in its stability properties and the convergence of the errors may be guaranteed for arbitrarily uncertain plants by proper choice of the bandwidths of the algorithm. Notably, the Lyapunov analysis of Section 2.2 is not applicable if such a tuning is embraced, as it is based on the assumption of stability of $\bar{\mathbf{H}}$ matrix. The numerical trials performed for the system of the third order shows also some difficulties to stabilize the system in the presence of very small values of $\tilde{\beta}$. These notions significantly extend the results presented hitherto in the literature and can be summarized by the following conjectures.

Conjecture 2.1. *For system* (2.21) *with* $\psi = 0, d = 0$, *observer* (2.26) *and control law* (2.32)–(2.33) *under the tuning given by* (2.13)–(2.15) *and with*

$\eta < n$ *the closed-loop system can be stabilized for* $\tilde{\beta}$ *such that Assumption 2.4 is satisfied by choice of* ω_o *high enough. For some other values of* $\tilde{\beta}$ *the system may be stabilizable by choice of* ω_o *small enough.*

Conjecture 2.2. *For system* (2.21) *with* $\psi = 0, d = 0$*, observer* (2.26) *and control law* (2.32)–(2.33) *under the tuning given by* (2.13)–(2.15) *and with* $\eta = n$ *the closed-loop system can be stabilized for* $\tilde{\beta}$ *such that Assumption 2.4 is satisfied for any choice of* ω_o*. For all other values of* $\tilde{\beta}$ *the system is stabilizable by choice of* ω_c *high enough.*

2.3.2 *Performance and disturbance attenuation*

While the presented analysis answers some questions concerning the impact of the input gain uncertainty on the stability of the closed-loop system working under the ADRC paradigm, further investigation has to be carried out in order to investigate how the modeling uncertainty influences the performance of the closed-loop system in terms of convergence speed and disturbance rejection. Some insights into these properties are here obtained on the basis of the numerical simulations of the response of the closed-loop system.

Simulation 2.3. *Series of simulations are performed for the nominal second-order (*$n = 2$*) system with dynamics corresponding to* (2.91) *and no external disturbances affecting the plant (i. e.* $d = 0$*). The real input gain of the system is set to* $b = 1$*. The controller and observer tuning are chosen according to* (2.97) *for coherence with the earlier results and the reference trajectory to be tracked by the system is chosen as a simple sine wave function given by* $x_r(t) = \sin(2t)$*. Each simulation is carried out for a different value of the input gain estimate* $\hat{b}$ *and measurability parameter* η*. The quality factor* $E(\tilde{\beta})$ *is then calculated for each run as*

$$E(\tilde{\beta}) = \frac{1}{t_1 - t_0} \int_{t_0}^{t_1} \|\mathbf{x}_r - \mathbf{x}\| \, dt, \tag{2.107}$$

where $t_0 = 20\,s, t_1 = 40\,s$ *stand for the initial and final time instants of the integration chosen to eliminate the influence of transient states on the evaluation of the controller performance. The resulting values of* $E(\tilde{\beta})$ *obtained in the simulations are given in Fig. 2.11.*

The plots confirm the existence of some feasible range of input gain uncertainty outside of which the system does not maintain its stability, as indicated by the rapid growth of calculated $E(\tilde{\beta})$ factor for simulations with $\tilde{\beta}$ larger than some threshold value. As shown already by Fig. 2.9, this limiting value grows with an increase of ω_o and decrease of ω_c, and converges toward the value of 9 if not all state variables are available for measurement. It is also visible that if

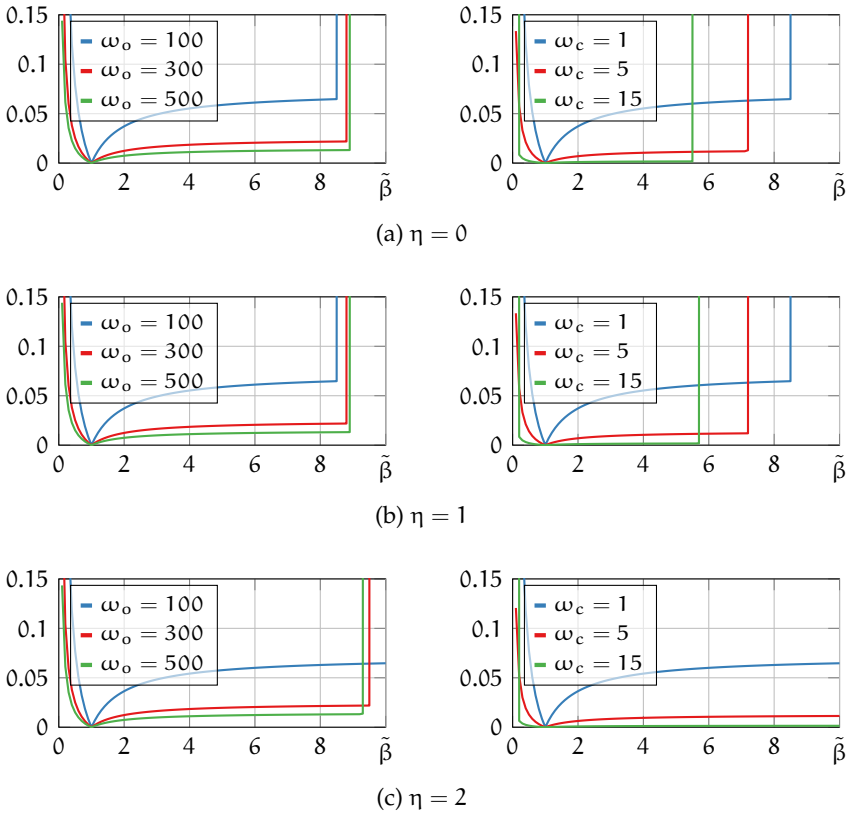

(a) $\eta = 0$

(b) $\eta = 1$

(c) $\eta = 2$

Figure 2.11: Values of the performance criterion $E(\tilde{\beta})$ for the undisturbed system with various measurability degrees. Gains are chosen as $\omega_c = 1$ in the left plots and $\omega_o = 100$ in the right plots.

state x of the plant is directly employed in the control formula this threshold grows significantly, especially in trials with the increased controller bandwidth ω_c, which is also in line with the earlier numerical results. Noteworthy, the simulations performed with $\eta = 0$ and $\eta = 1$ provided results that are visually identical and no significant difference in the response of the plant can be noted. This property would be possibly lost had some state variables used in the control law be burdened by measurement noise. The products of the simulations unveil also the impact of the input gain uncertainty on the overall performance of the system. It is shown that, in accordance with intuitive notions, the highest performance of the ADRC controller in the system without any disturbances is achieved with the input gain perfectly known and deviations from its nominal value lead to a decrease in the tracking quality. Importantly, the deterioration of the performance of the controller is significantly greater if the input gain used for the controller synthesis is overestimated, leading to $\tilde{\beta} < 1$, than if this parameter is underestimated, which corresponds to $\tilde{\beta} > 1$. In the latter case, the performance decrease seems to be limited by some boundary and further increase of $\tilde{\beta}$ does not apparently lead

to the accelerated increase of $E(\tilde{\beta})$ criterion up until the destabilizing boundary is reached. On the contrary, the accumulated value of $E(\tilde{\beta})$ factor rapidly grows with the increase of input gain overestimation. This observation may lead to a conclusion that if the input gain is not perfectly known, the choice of the smaller values of its estimate, and thus greater $\tilde{\beta}$ may be advisable in practical scenarios. This proposition is formulated here only on the basis of the results obtained for the undisturbed double integrator system, and further research into the impact of the input gain uncertainty on the ability of the controller to estimate and reject disturbances affecting the system is required in order to generalize this notion.

From the dynamics given by (2.51) it can be noted that majority of disturbing terms are scaled by the solution $\mathbf{P}$ of the Lyapunov equation which varies with the change of unknown term $\tilde{\beta}$ present in $\bar{\mathbf{H}}$ matrix. The analytical solution of the Lyapunov equation $\bar{\mathbf{H}}^{\mathsf{T}}\mathbf{P} + \mathbf{P}\bar{\mathbf{H}} = -\mathbf{I}_m$ can be obtained by taking advantage of the Kronecker product [107]. $\mathbf{P}$ is given by properly reshaping the solution of the equation

$$\operatorname{vec}(\mathbf{P}) = -\left(\mathbf{I}_m \otimes \bar{\mathbf{H}}^{\mathsf{T}} + \bar{\mathbf{H}}^{\mathsf{T}} \otimes \mathbf{I}_m\right)^{-1} \operatorname{vec}(\mathbf{I}_m), \tag{2.108}$$

where $\otimes$ is the Kronecker product operator and $\operatorname{vec}(\cdot)$ stands for the operation of matrix vectorization. For the second order system the explicit form of the solution of the Lyapunov equation takes the form of

$$\mathbf{P}\Big|_{n=2} = \begin{bmatrix} p_{1,1} & -\frac{1}{2} & \frac{1+12\omega_o^2+3\tilde{\beta}\omega_o^4}{2\left(\tilde{\beta}-9\right)\omega_o^3} \\ -\frac{1}{2} & p_{2,2} & -\frac{1}{2} \\ \frac{1+12\omega_o^2+3\tilde{\beta}\omega_o^4}{2\left(\tilde{\beta}-9\right)\omega_o^3} & -\frac{1}{2} & p_{3,3} \end{bmatrix} \tag{2.109}$$

with

$$\begin{aligned} p_{1,1} &= \frac{3+3\left(3+\tilde{\beta}\right)\omega_o^2+\tilde{\beta}^2\omega_o^4}{2\left(9-\tilde{\beta}\right)\omega_o}, \\ p_{2,2} &= \frac{1+12\omega_o^2+3\tilde{\beta}\omega_o^4}{2\left(9-\tilde{\beta}\right)\omega_o^3}, \\ p_{3,3} &= \frac{3+\left(27+\tilde{\beta}\right)\omega_o^2+3\left(9+2\tilde{\beta}\right)\omega_o^4}{2\left(\tilde{\beta}-9\right)\tilde{\beta}\omega_o^5}. \end{aligned} \tag{2.110}$$

Due to the dependence of (2.51) on $\mathbf{P}$, some general conclusions about the ability of the controller to suppress the impact of disturbances can be drawn from the numerical analysis of the norm of this matrix in the function of the observer bandwidth and the input gain uncertainty. The

derivative of function $V_2(\bar{z}, \bar{x})$ as given by (2.51) contains numerous terms scaled by $\mathbf{P}$ matrix. More specifically, the expression

$$\begin{aligned}
&\bar{z}^T \mathbf{P} \mathbf{b}_m \Bigg(\left(\frac{\partial \psi_r}{\partial x_r} \dot{x}_r + \frac{\partial \psi_r}{\partial t} \right) \left(\theta - \hat{\theta} \right) + \left(\frac{b}{\hat{b}} - 1 \right) \left(x_r^{(m)} \right. \\
&- \frac{\partial \hat{\psi}}{\partial \hat{x}} \Bigg(\omega_c \left(\mathbf{b}_n \bar{k}^T - \mathbf{A}_n \Phi_c^{-1} \omega_c^{-1} \right) \bar{x} + \Big(\Lambda_n \omega_o \Phi_o^{-1} \bar{l} \mathbf{c}_m^T \\
&- \mathbf{A}_n \Lambda_n \Phi_o^{-1} + \mathbf{b}_n \bar{k}^T \omega_c \Phi_c \Lambda_n \Phi_o^{-1} \Big) \bar{z} + \dot{x}_r \Bigg) \hat{\theta} - \frac{\partial \hat{\psi}}{\partial t} \hat{\theta} \\
&+ \omega_c^2 \bar{k}^T \bar{G} \bar{x} + \omega_c \bar{k}^T \Big(\omega_o \Phi_c \Lambda_n \Phi_o^{-1} \bar{H} - \mathbf{b}_n \mathbf{b}_m \\
&- \mathbf{b}_n \bar{k}^T \omega_c \Phi_c \Lambda_n \Phi_o^{-1} \Big) \bar{z} \Bigg) + \frac{\partial d}{\partial x} \Bigg(\mathbf{b}_n \Big(\bar{k}^T \omega_c \Phi_c \Lambda_n \Phi_o^{-1} \\
&+ \mathbf{b}_m^T \Big) \bar{z} + \omega_c \left(\mathbf{b}_n \bar{k}^T - \mathbf{A}_n \Phi_c^{-1} \omega_c^{-1} \right) \bar{x} + \frac{\partial d}{\partial t} + \dot{x}_r \\
&+ \mathbf{b}_n \left((\psi - \psi_r) \left(\theta - \hat{\theta} \right) + \left(\psi - \hat{\psi} \right) \hat{\theta} \right) \Bigg) \Bigg)
\end{aligned}$$

accommodate majority of the dynamic effect impacting the evolution of the closed-loop system and is scaled by $\mathbf{P}\mathbf{b}_m$ what stands for the last column $\mathbf{P}$ matrix only. Since, in the practical scenarios, the extent of the disturbance estimation errors is commonly significantly greater than that of the state estimation errors (see Fig. 2.5), the last element of this column, equal to $\mathbf{b}_m^T \mathbf{P} \mathbf{b}_m$, is expected to have a predominant role in shaping the evolution of the system. Differences in the character of the state and disturbance estimations have also been highlighted by the earlier finding of this section. In Fig. 2.12 the norms of both $\mathbf{P}\mathbf{b}_m$ and $\mathbf{b}_m^T \mathbf{P} \mathbf{b}_m$ are shown for different values of ω_o and $\tilde{\beta}$. The values are presented only in the range in which $\bar{H}$ maintains stability, as the analytical studies presented in the previous sections have no meaningful interpretation outside of this domain.

The presented results show that while the norm of $\mathbf{P}\mathbf{b}_m$ increases with the growth of $\tilde{\beta}$ term, the interpretation of the properties of the term $\mathbf{b}_m^T \mathbf{P} \mathbf{b}_m$ is less straightforward and its norm grows as $\tilde{\beta}$ approaches both 0 and 9. Importantly, none of these expressions has a minimum at $\tilde{\beta} = 1$ which corresponds to the perfect knowledge of the input gain of the plant. Thus, it may be expected that in some scenarios the choice of input gain estimate according to its real value may not lead to the best disturbance rejection capabilities. Yet the properties of $\mathbf{P}$ matrix alone cannot serve as a sole basis of conclusions on the disturbance rejection capabilities of the algorithm in the presence of the input gain uncertainties, as its performance inherently depends also on the character of $\mathbf{N}$ matrix as shown by simulations in Fig. 2.11. It is thus justified to seek to establish some notions on this problem on

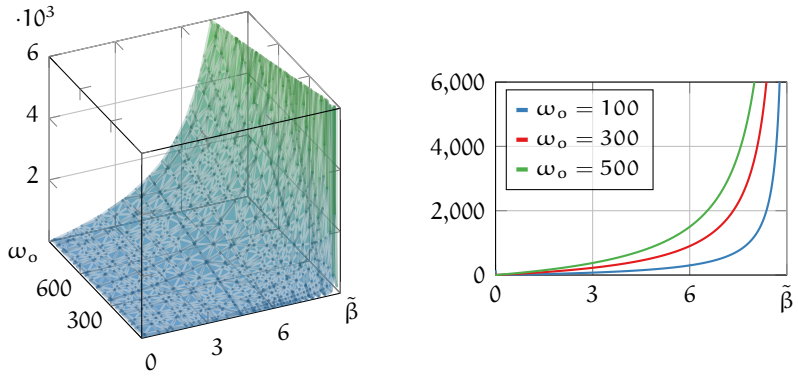

(a) Norm of $\mathbf{P}\mathbf{b}_m$

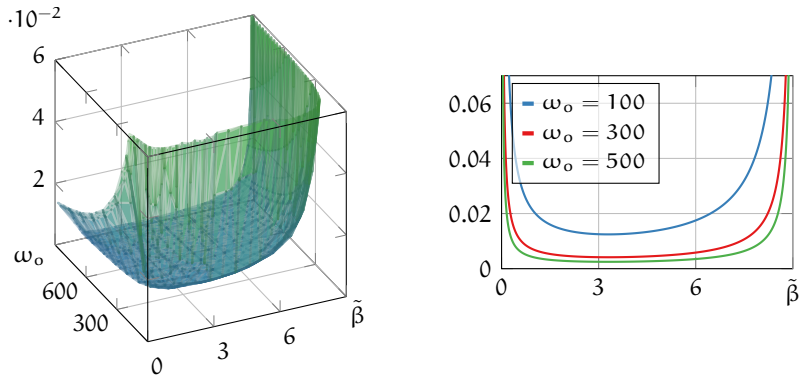

(b) Norm of $\mathbf{b}_m^T\mathbf{P}\mathbf{b}_m$

Figure 2.12: Norms of the solution of the Lyapunov equation

the basis of numerical simulations of the responses of the disturbed system.

Simulation 2.4. *The system with dynamics* (2.91) *and various forms of disturbances affecting the plant is considered. The conditions of the trials are chosen as in Sim. 2.3 with real input gain fixed as* $b = 1$ *and value of performance criterion* $E(\tilde{\beta})$ *calculated for each run with different values of* $\hat{b}$*. The algorithm is tuned with bandwidths* $\omega_o = 100, \omega_c = 1$*. The following scenarios are considered to investigate the performance of the ADRC controller for uncertain disturbed systems:*

1. *state independent disturbance* $d = \sigma \sin(4t)$,
2. *state dependent disturbance* $d = \sigma(x_1 + x_2)$,

where parameter σ *is a scaling factor varying across the simulations. The results of these trials for varying degrees of measurability* η *are given in Fig. 2.13.*

The plots show an important, yet counterintuitive, notion that the growth of $\tilde{\beta}$ factor leads to an increase in the disturbance rejection abilities of the ADRC algorithm. For the disturbances large enough

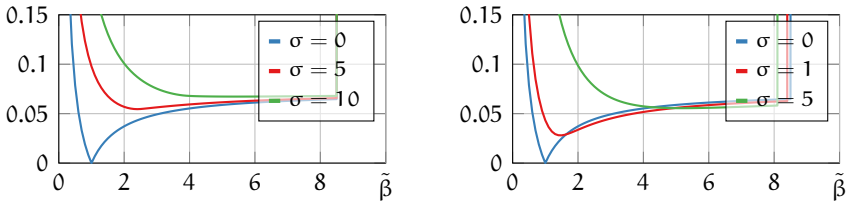

(a) $\eta = 0$

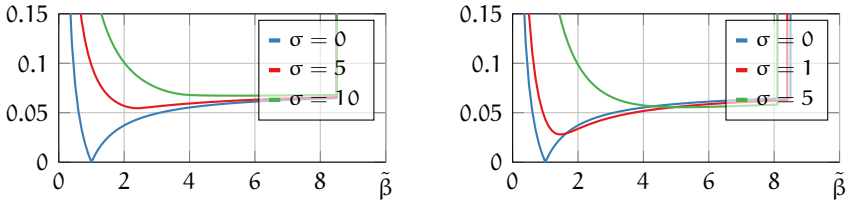

(b) $\eta = 1$

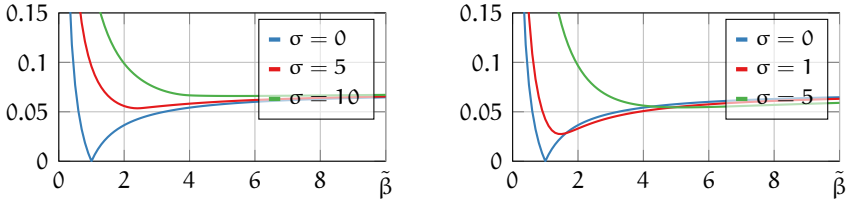

(c) $\eta = 2$

Figure 2.13: Values of the performance criterion $E(\tilde{\beta})$ for the disturbed system. State-independent disturbance in the left plots, and state-dependent disturbance in the right plots.

this positive influence visibly overcomes the decrease of performance observed in Fig. 2.11 and the overall performance of the disturbed system increases with the input gain underestimation. This phenomenon is observed for both considered types of disturbances regardless of the chosen degree of measurability and is valid up to the threshold value of $\tilde{\beta}$ for which the system loses its stability according to the results of Fig. 2.9. Moreover, the scenario employing the disturbance being a function of the plant state shows also its impact on this stability threshold. According to (2.51) one may expect that in the presence of state-dependent disturbance the exact form of $\mathbf{N}$ differs from the one given in (2.94) due to the presence of terms derived from the dynamics of the disturbance. Thus, not only the performance but also the stability region is affected by the presence of the state-dependent disturbance acting upon the plant. Specifically, it can be noticed that the non-dissipative disturbance employed in the second scenario leads to the decrease of this stable region which shrinks with an increase of σ despite unchanged ω_o, ω_c parameters. The proper behavior of the system is thus not always achieved for the values of $\tilde{\beta}$ which stabilized the undisturbed plants in the earlier trials.

The presented numerical results seem to imply that in the presence of significant disturbances affecting the plant the conscious choice of the input gain estimate which is substantially smaller than the nominal value of this parameter in the plant my positively affect the performance of the closed-loop system. This phenomenon may be partially caused by the indirect scaling of l_m by $\tilde{\beta}$ as shown in (2.47), yet is not limited to this reason, as explicitly shown by (2.95) where the impact of the modeling uncertainty on the other elements of the dynamics of the system is highlighted. The following notions can thus be stated.

Conjecture 2.3. *For system* (2.21) *with* $\psi = 0, d = 0$, *observer* (2.26) *and control law* (2.32)–(2.33) *the best quality of reference trajectory tracking in terms of* $E(\tilde{\beta})$ *criterion is achieved for* $\hat{b} = b$.

Conjecture 2.4. *For system* (2.21) *with* $\psi = 0, d = d(t, \mathbf{x})$, *observer* (2.26) *and control law* (2.32)–(2.33) *the quality of the reference trajectory tracking can be improved in terms of* $E(\tilde{\beta})$ *criterion by setting* $\hat{b} < b$ *if the extent of the disturbing term* $d(t, \mathbf{x})$ *is large enough.*

Remark 2.4. *While the aforestated conjectures assume a lack of any known dynamics of the plant (i.e.* $\psi = 0$*), the results can be trivially extended to the systems with some parts of the dynamics known. In such a case, for the purposes of the proposed conjectures, the impact of the drift parameters uncertainty may be lumped with disturbance* d *as shown in Section 2.2. The same holds for subsequent conjectures.*

While the majority of published research focuses on the investigation of the ADRC performance under an assumption that the input gain estimate at least roughly corresponds to its correct value, the first notion that it may be chosen differently to improve the efficiency of the controller was suggested already in 2010 in [341]. The authors noticed that the increase in this estimate enlarges the stability margins of the system and thus the greater values of the observer and controller bandwidths may be applied decreasing produced tracking and estimation errors. A similar approach was later employed in [47] leading to the proposition of the tuning which included the choice of $\hat{b}$ in order to satisfy some predefined required setting time. The conclusions presented in these papers are not contradictory to the finding of this thesis, but no proposition concerning a conscious decrease of the input gain estimate was put forth there and was, according to the best knowledge of the author, for the first time proposed by the author of this dissertation.

The proposed tuning of the input gain estimate is valid only for the system in which, under an assumption of perfect knowledge of input gain value, the disturbances scaled only by $\mathbf{P}b_m$ are not outweighed

by thosed scaled also by $\tilde{\beta} - 1$, as Fig. 2.11 and 2.13 showed that the change of $\tilde{\beta}$ caused no improvement of in the control quality for the undisturbed plant and only moderate improvement in the weakly disturbed plant. For the standard ADRC this implies that the impact of the nonzero external disturbances d should outweigh the derivative $x_r^{(m)}$ of the reference trajectory. Alternatively, the EADRC algorithm designed in the error domain and presented in Section 2.1 always satisfies this condition, regardless of the specific structure of the term d and $\mathbf{x}_r$. It is thus justified to extend the earlier studies to incorporate the EADRC control scheme and separately investigate its performance in the presence of the input gain uncertainties. To this end, consider the plant working under the EARDC control as given by (2.17)–(2.20). In order to follow the procedure employed at the beginning of this section and incorporate the input gain uncertainty and mixing matrix $\mathbf{\Pi}$ into the EADRC design, the extended state is defined in the error domain as $\boldsymbol{z} = \begin{bmatrix} \tilde{\boldsymbol{x}}^T & \delta \end{bmatrix}^T$ with the dynamics rewritten from (2.18) as

$$\dot{\boldsymbol{z}} = \boldsymbol{A}_m \boldsymbol{z} - \mathbf{d}\hat{b}u - \mathbf{b}_m \frac{d}{dt}\left(\left(b - \hat{b}\right)u - x_r^{(n)} + d\right) \tag{2.111}$$

and the observer designed as

$$\dot{\hat{\boldsymbol{z}}} = \boldsymbol{A}_m \hat{\boldsymbol{z}} - \mathbf{d}_m \hat{b}u + \mathbf{l}\left(\mathbf{c}_n^T \tilde{\mathbf{x}} - \mathbf{c}_m^T \hat{\boldsymbol{z}}\right). \tag{2.112}$$

The control law is then rewritten from (2.20) in the form of

$$u = \frac{1}{\hat{b}}\left(v + \mathbf{b}_m^T \hat{\boldsymbol{z}}\right) \tag{2.113}$$

with the internal control law employing possibly measurable states of the plant expressed by

$$v_\eta = \mathbf{k}^T \boldsymbol{\Lambda}_n \boldsymbol{z}_\eta^* \tag{2.114}$$

and auxiliary vector $\boldsymbol{z}^*$ defined in the error domain as

$$\boldsymbol{z}_\eta^* = \left(\mathbf{I}_m - \mathbf{\Pi}_{m,\eta}\right)\boldsymbol{z} + \mathbf{\Pi}_{m,\eta}\hat{\boldsymbol{z}}. \tag{2.115}$$

The error dynamics, analogous to (2.91), of the EADRC control algorithm are then obtained as

$$\begin{aligned} \dot{\tilde{\boldsymbol{z}}} &= \mathbf{H}\tilde{\boldsymbol{z}} - \mathbf{b}_m\left(\left(\frac{b}{\hat{b}} - 1\right)\dot{v} - x_r^{(m)} + \dot{d}\right), \\ \dot{\tilde{\boldsymbol{x}}} &= \mathbf{G}\tilde{\mathbf{x}} + \boldsymbol{W}\mathbf{\Pi}_{m,\eta}\tilde{\boldsymbol{z}}. \end{aligned} \tag{2.116}$$

By substituting $\dot{\nu}$ into these equations, the dynamics of the concatenated errors ξ for the EADRC scheme are expressed by

$$\dot{\xi} = \mathbf{N}\xi + \begin{bmatrix} \mathbf{b}_m^T & \mathbf{0}_{n\times 1}^T \end{bmatrix}^T \left(\dot{d} - x_r^{(m)}\right) \tag{2.117}$$

with

$$\mathbf{N} = \begin{bmatrix} \mathbf{H} + \tilde{b}\mathbf{b}_m\mathbf{k}^T\left(\mathbf{\Lambda}_n\mathbf{\Pi}_{m,\eta}\mathbf{H} - \mathbf{W}\mathbf{\Pi}_{m,\eta}\right) & -\tilde{b}\mathbf{b}_m\mathbf{k}^T\mathbf{G} \\ \mathbf{W}\mathbf{\Pi}_{m,\eta} & \mathbf{G} \end{bmatrix}. \tag{2.118}$$

Due to the embraced error definition, the obtained matrix $\mathbf{N}$ differs from its counterpart associated with ADRC control by the signs of elements on its antidiagonal. Such matrices are bound to have the same eigenvalues and thus the stability properties established earlier for the standard form of the algorithm hold also for the variant designed in the error domain. The major difference between the presented expressions and the forms obtained for standard ADRC in (2.93) and (2.94) can be nonetheless noticed. Namely, the dynamics of ξ errors for the EADRC controller do not contain the term $\left(\tilde{\beta} - 1\right)x_r^{(m)}$ which is replaced by the expression $x_r^{(m)}$ only. Such a change has a twofold impact on the analysis of the system. Firstly, it is clear that even if the input gain parameter is perfectly known, it is not possible to eliminate the influence of the reference trajectory on the performance of the system working under the EADRC controller, which is achievable with the standard form of the algorithm. The lack of this property limits however the undesired sensitivity of the EADRC to the input gain uncertainty, as the growth of $\tilde{\beta}$ factor, does not lead to a surge in the disturbance affecting the closed loop system. Both of these notions may be perceived as reasons to consider the proposed input gain underestimation as a tuning method for the EADRC systems. In order to investigate these properties, the numerical simulations conducted in Sim. 2.4 for the standard ADRC controller are repeated here for the EADRC algorithm synthesized in the error domain.

Simulation 2.5. *Consider the scenario given by Sim. 2.4 with EADRC controller employed. The conditions of the simulation remain unchanged and thus the second order system* ($n = 2$) *is considered with a real value of input gain chosen as* $b = 1$, *tuning gains set to* $\omega_o = 100, \omega_c = 1$ *and with the disturbing terms* d *in the forms of either* $d = \sigma\sin(4t)$ *or* $d = \sigma\left(x_1 + x_2\right)$. *The results of the simulations for various values of parameter* σ *are given in Fig. 2.14.*

The obtained results show that due to the lack of scaling of $x_r^{(m)}$ term in the dynamics of the errors in the EADRC scheme, the performance criterion $E(\tilde{\beta})$ does not reach its minimum value for $\tilde{\beta} = 1$ and,

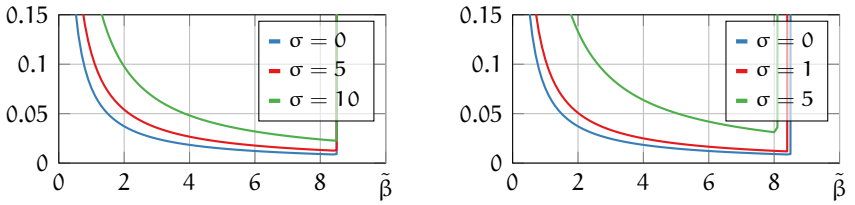

(a) $\eta = 0$

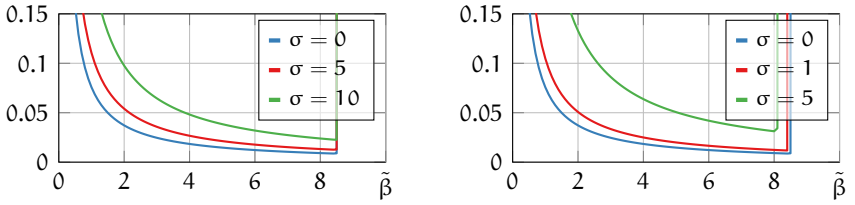

(b) $\eta = 1$

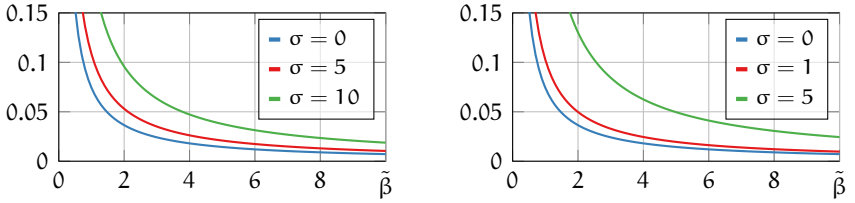

(c) $\eta = 2$

Figure 2.14: Values of the performance criterion $E(\tilde{\beta})$ for the disturbed EADRC system. State-independent disturbance in the left plots, and state-dependent disturbance in the right plots.

in all considered scenarios, monotonically decrease with the growth of input gain underestimation up to the threshold value destabilizing the system. Importantly, the additional simulations performed with the trajectories characterized by significantly smaller values of $x_r^{(m)}$ also confirm this notion which thus arises as a property possibly independent of the chosen trajectory or the type of disturbance. Specifically, if $x_r^{(m)} = 0$ then the asymptotic convergence is achieved for any feasible choice of $\hat{b}$, what corresponds to the special case of Theorem 2.6. The proposed method of input gain tuning thus seems to be well-suited for the application to the plants controlled under the EADRC algorithm. The plots moreover show that the general conclusions concerning the stability of the entire system drawn on the basis of the simulations of the ADRC system hold also for the EADRC algorithm.

Conjecture 2.5. *For system* (2.21) *with* $\psi = 0, d = d(t, x)$, *observer* (2.112) *and control law* (2.113)–(2.114) *the quality of the reference trajectory tracking can be improved in terms of* $E(\tilde{\beta})$ *criterion by setting* $\hat{b} < b$ *for a wide class of disturbances and reference trajectories.*

In order to further verify the obtained results, the experimental trials are performed considering different choices of the input gain estimate value.

Experiment 2.1. *The robotic astronomic telescope device with a mirror of diameter* $0.5\,\mathrm{m}$*, which is described in detail in Section 4.2, is employed. The plant is modeled as a second-order dynamic system* ($n = 2$)*, and the EADRC controller is synthesized and tuned with* $\omega_o = 140, \omega_c = 10$*. The task of trajectory tracking is considered with the reference trajectory expressed by*

$$x_r = 2 \cdot 7.268 \cdot 10^{-r_v} \left(\frac{1}{6}\pi\right)^{-1} \sin(\frac{1}{6}\pi t)\,\mathrm{rad/s}, \tag{2.119}$$

where $r_v \in \{2, 5\}$ *stands for the factor affecting the maximum velocity of the axis of the telescope and varies across performed trials. The choice of higher values of* r_v *corresponds to the slower desired movement of the mount. Although the presented analytical and numerical results imply that the choice of the reference trajectory does not impact the overall performance properties of the system, it has been observed that the character of the disturbance affecting the telescope device varies with the changes in the velocity of the axes of the mount. Namely, for the slow trajectories, the disturbances seem to be characterized mainly by the friction force in the presliding regime that significantly impacts the response of the plant. Conversely, faster movement of the axis allows the friction to enter the sliding regime in which the impact of the friction on the motion of the telescope is strongly limited. The change of the reference trajectory is thus used here to indirectly influence the attributes of the disturbing dynamics. For each choice of velocities of the trajectory, separate trials are performed for different choices of* η *factor. In order to enable choice of* $\eta = 2$*, a separate observer with constant tuning is employed to estimate the velocity of the axis. In line with the outputs of the earlier simulation, the experimental results obtained for* $\eta = 0$ *and* $\eta = 1$ *proved to be visually identical and are thus merged in the presented figures. The modified performance criterion* $E_1(\tilde{\beta})$ *based only on the output of the system and expressed by*

$$E_1(\tilde{\beta}) = \frac{1}{t_1 - t_0} \int_{t_0}^{t_1} \|x_{r1} - x_1\|\,dt \tag{2.120}$$

is then calculated from the results of the experimental trials and presented in Fig. 2.15. The assumed value of $\hat{b}$ *instead of* $\tilde{\beta}$ *is displayed due to the fact that the real value of* b *is not certainly known in the experimental setup.*

The results of the experiments are roughly in line with the outcomes of the earlier simulations. Namely, it is shown that, in some limited range, the decrease of the input gain estimate improves the overall performance of the system in all considered scenarios. For the larger extents of input gain underestimation the errors in the system rapidly

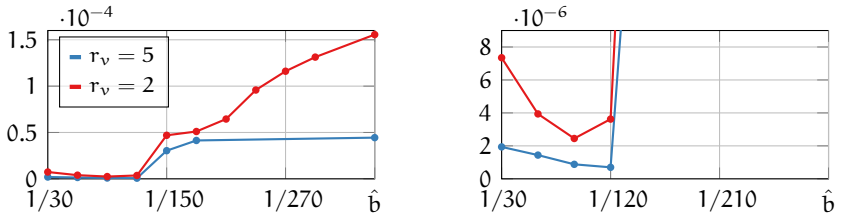

(a) $\eta = 0, 1$

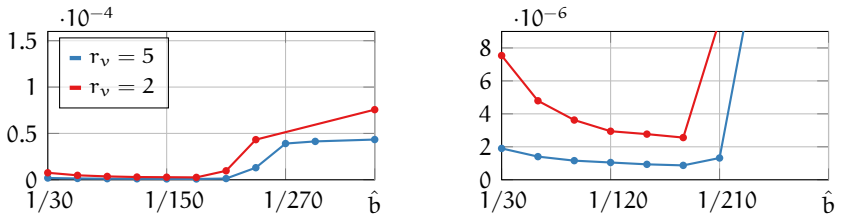

(b) $\eta = 2$

Figure 2.15: Values of the performance criterion $E_1(\tilde{\beta})$ for the experimental EADRC system. Each dot represents the individual experiment. Full range of experiment on the left side, close-up view on the right.

grows (approximately tenfold increase at $\hat{b} \approx 1/150$ for $\eta \in \{0, 1\}$ and at $\hat{b} \approx 1/210$ for $\eta = 2$) what possibly correspond to the theoretical stability limitation as proposed in the Conjecture 2.1. Moreover, the experimental trials confirm that the inclusion of the entire measurable state in the control law design significantly extends the resultant stability region enabling the choice of smaller values of input gain estimate. It has to be nonetheless admitted that the improvement of the performance of the closed-loop system achieved here by the application of the proposed input gain tuning method is comparable with the results achievable with the standard increase of the observer and controller bandwidth. Thus the offered method should be possibly seen rather as a technique of selecting the input gain parameter if its real value is not known in order to avoid deterioration of the performance of the system, than as a way of improving the quality of work of the plant if the true value of the input gain is available.

2.3.3 *Input path dynamics*

Section 2.3 considered so far only the problems of the static uncertainty present in the input path of the system. Specifically, the problem of the unknown value of a single constant input gain parameter and its influence on the stability and performance of the closed-loop system was investigated. In the analysis of some of the practical scenarios, such a simplification is insufficient, and a more detailed study of the input path uncertainty is necessary. Certain plants encountered in

such situations belong to the class of systems with additional stable dynamics present in the input path. If the specific form of these dynamics is unknown, the controller is often designed by assuming a static definition of the input path and synthesizing the algorithm for such a simplified model. The problem of stability of the closed-loop formed by embracing such an approach arises and requires thorough investigation.

Consider once again the system as presented in Section 2.2 with $\psi(t, \boldsymbol{x}) = 0$ and $d(t, \boldsymbol{x}) = d(t)$ expressed by

$$\dot{\boldsymbol{x}} = \boldsymbol{A}_n \boldsymbol{x} + \boldsymbol{b}_n \left(bu + d(t) \right). \tag{2.121}$$

Assume moreover that the value of the input gain b is perfectly known, but the input signal u is not directly available for control purposes and is instead governed by the first order inertial dynamics given by

$$\dot{u} = T_b^{-1} \left(-u + u^* \right), \tag{2.122}$$

where $T_b \in \mathbb{R}_+$ is a positive time constant of the input dynamics. Signal $u^* \in \mathbb{R}$ is a new input of the entire system and can be freely used by the designer to control the plant. Importantly, dynamics (2.122) are inherently stable for any positive value of T_b and thus u always converges toward the value assigned by u^*.

Assuming that both the value of the time constant and the general structure of the input gain dynamics are unknown, the observer and control law may be designed by omitting dynamics (2.122) and treating u^* as the actual input of the plant. Under such an interpretation the state extension can be defined in a standard form of

$$\dot{\boldsymbol{z}} = \boldsymbol{A}_m \boldsymbol{z} + \boldsymbol{d}_m b u + \boldsymbol{b}_m \dot{d} \tag{2.123}$$

with the extended state observer designed as

$$\dot{\hat{\boldsymbol{z}}} = \boldsymbol{A}_m \hat{\boldsymbol{z}} + \boldsymbol{b}_m b u^* + \boldsymbol{l} \boldsymbol{c}_m^T \left(\boldsymbol{z} - \hat{\boldsymbol{z}} \right). \tag{2.124}$$

The control law can be synthesized according to the ADRC paradigm, but applied to the available input, yielding

$$u^* = b^{-1} \left(\boldsymbol{k}^T \left(\boldsymbol{x}_r - \boldsymbol{\Lambda}_n \hat{\boldsymbol{z}} \right) - \boldsymbol{b}_m^T \hat{\boldsymbol{z}} + x_r^{(n)} \right). \tag{2.125}$$

The order of the state observer is thus equal to the order of the entire plant consisting of the nth order nominal system and additional first-order input gain dynamics. Importantly, the interpretations of the appended states are different in both systems. The schematic structure of the considered system is shown in Fig. 2.16.

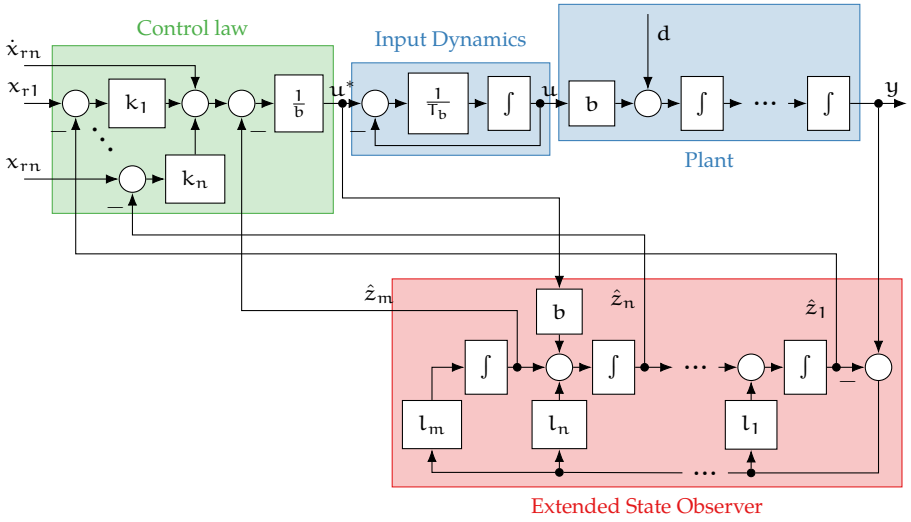

Figure 2.16: The detailed graphical illustration of the system with uncertain input dynamics. Increased order of the plant is visible.

Remark 2.5. *Similarly to the notions of Remark 2.1, the alternative state extension in the form of*

$$\dot{z} = \mathbf{A}_m z + \mathbf{d}_m b u^* + \mathbf{b}_m \left(\dot{d} + b\left(\dot{u} - \dot{u}^*\right)\right)$$

could also be considered in the analysis of the given problem, emphasizing the expectation that the observer may successfully compensate for the unknown dynamics of the input path. The results obtained by the author under this approach are more conservative than the ones presented in the main body of the thesis and are thus not given here in more detail.

In order to investigate the properties of systems with uncertain input dynamics, define the tracking, estimation, and input errors as

$$\tilde{x} = x_r - x, \quad \tilde{z} = z - \hat{z}, \quad \tilde{u} = u^* - u. \tag{2.126}$$

The dynamics of these errors are given by

$$\begin{aligned} \dot{\tilde{x}} &= \mathbf{G}\tilde{x} - \mathbf{W}\tilde{z} + \mathbf{b}_n b\tilde{u}, \\ \dot{\tilde{z}} &= \mathbf{H}\tilde{z} - \mathbf{d}_m b\tilde{u} + \mathbf{b}_m \dot{d}, \\ \dot{\tilde{u}} &= \dot{u}^* - T_b^{-1}\tilde{u} \end{aligned} \tag{2.127}$$

with matrices $\mathbf{G}, \mathbf{H}, \mathbf{W}$ defined as in Section 2.2. The derivative of the nominal control signal is obtained analytically from (2.125) as

$$\dot{u}^* = b^{-1}\left(k^T\mathbf{G}\tilde{x} + \left(\mathbf{b}_n^T\mathbf{W}\mathbf{H} - k^T\mathbf{W}\right)\tilde{z} + x_r^{(m)}\right). \tag{2.128}$$

To further facilitate the study of the closed-loop system the tuning as proposed by (2.41) and state parametrization (2.42) are employed. Thus, the dynamics of the scaled errors are given by

$$\begin{aligned}\dot{\bar{x}} &= \omega_c \bar{\mathbf{G}}\bar{x} - \mathbf{b}_n\left(\bar{k}^T\omega_c\mathbf{\Phi}_c\mathbf{\Lambda}_n\mathbf{\Phi}_o^{-1} + \mathbf{b}_m^T\right)\bar{z} + \mathbf{b}_n b\tilde{u},\\ \dot{\bar{z}} &= \omega_o\bar{\mathbf{H}}\bar{z} - \omega_o\mathbf{d}_m b\tilde{u} + \mathbf{b}_m\dot{d}\end{aligned} \tag{2.129}$$

with $\bar{\mathbf{G}}, \bar{\mathbf{H}}$ being once again defined as in Section 2.2. Moreover, the control law derivative is expressed in terms of scaled errors as

$$\begin{aligned}\dot{u}^* = b^{-1}\Big(&\bar{k}^T\omega_c^2\bar{\mathbf{G}}\bar{x} - \omega_c\bar{k}^T\mathbf{b}_n\left(\bar{k}^T\omega_c\mathbf{\Phi}_c\mathbf{\Lambda}_n\mathbf{\Phi}_o^{-1}\right)\bar{z}\\ &+\left(\bar{k}^T\omega_c\mathbf{\Phi}_c\mathbf{\Lambda}_n\mathbf{\Phi}_o^{-1} + \mathbf{b}_m^T\bar{\mathbf{H}}\right)\bar{z} + x_r^{(m)}\Big).\end{aligned} \tag{2.130}$$

Further analysis of the properties of the system is performed in a twofold manner. Namely, an analytical investigation on the basis of the Lyapunov approach is carried out to obtain some general conclusions valid for a wide class of dynamic systems of arbitrary degree and parameter values. Then, numerical studies are performed to produce more detailed notions applicable to the specific forms of the considered system.

Consider first the following theorem formulated on the basis of analytical investigation.

Theorem 2.10. *For system* (2.21) *with* $\psi = 0, d = d(t)$*, and the input governed by* (2.122)*, observer* (2.124) *and control law* (2.125) *ensure the global convergence of the tracking and estimation errors to some neighborhood of the origin if* ω_o, ω_c *are chosen high enough and time constant* T_b *is simultaneously small enough.*

Proof. *Let the scalar-valued function be given as*

$$V_{2.10}(\bar{x}, \bar{z}, \tilde{u}) = \frac{1}{2}\bar{z}^T\mathbf{P}\bar{z} + \frac{1}{2}\bar{x}^T\mathbf{R}\bar{x} + \frac{1}{2}\tilde{u}^T\tilde{u}. \tag{2.131}$$

The time derivative of function $V_{2.10}(\bar{x}, \bar{z}, \tilde{u})$ *is analytically calculated as*

$$\begin{aligned}\dot{V}_{2.10}(\bar{x}, \bar{z}, \tilde{u}) = & -\omega_o \frac{1}{2}\bar{z}^T\bar{z} - \omega_o \bar{z}^T \mathbf{P}\mathbf{d}_m b\tilde{u} + \bar{z}^T \mathbf{P}\mathbf{b}_m \dot{d} \\ & - \omega_c \frac{1}{2}\bar{x}^T\bar{x} - \bar{x}^T \mathbf{R}\Big(\mathbf{b}_n \bar{k}^T \omega_c \mathbf{\Phi}_c \mathbf{\Lambda}_n \mathbf{\Phi}_o^{-1} \\ & + \mathbf{b}_n \mathbf{b}_m^T\Big)\bar{z} + \bar{x}^T \mathbf{R}\mathbf{b}_n b\tilde{u} - T_b^{-1}\tilde{u}^T\tilde{u} \\ & + \omega_c^2 \tilde{u}^T b^{-1} \bar{k}^T \bar{G}\bar{x} + \tilde{u}^T b^{-1} x_r^{(m)} \\ & + \tilde{u}^T b^{-1}\Big(\Big(\bar{k}^T - \omega_c \bar{k}^T \mathbf{b}_n \bar{k}^T\Big)\omega_c \mathbf{\Phi}_c \mathbf{\Lambda}_n \mathbf{\Phi}_o^{-1} \\ & + \mathbf{b}_m^T \bar{H} - \omega_c \bar{k}^T \mathbf{b}_n \mathbf{b}_m^T\Big)\bar{z}.\end{aligned} \tag{2.132}$$

Under the assumptions of the lipshitzness of the disturbance as given in Section 2.2 the bound on $\dot{V}_{2.10}(\bar{x}, \bar{z}, \tilde{u})$ *may be imposed and is given as*

$$\begin{aligned}\dot{V}_{2.10} \leqslant & -\omega_o \frac{1}{2}\|\bar{z}\|^2 + \omega_o p_M b_M \|\bar{z}\|\|\tilde{u}\| + p_M d_L \|\bar{z}\| \\ & - \omega_c \frac{1}{2}\|\bar{x}\|^2 + r_M\left(k_M\left(\frac{\omega_c}{\omega_o}\right)^{n|1} + 1\right)\|\bar{x}\|\|\bar{z}\| \\ & + r_M b_M \|\bar{x}\|\|\tilde{u}\| - T_b^{-1}\|\tilde{u}\|^2 + \omega_c^2 b_M^{-1} k_M g_M \|\bar{x}\|\|\tilde{u}\| \\ & + b_M^{-1} x_M \|\tilde{u}\| + b_M^{-1}\Big(\left(k_M + \omega_c k_M^2\right)\left(\frac{\omega_c}{\omega_o}\right)^{n|1} \\ & + h_M + \omega_c k_M\Big)\|\bar{z}\|\|\tilde{u}\|,\end{aligned} \tag{2.133}$$

where $b_M = \|b\|$. *By taking advantage of Young's inequality, it can be established that the above satisfies also the following relation.*

$$\begin{aligned}\dot{V}_{2.10} \leqslant & -\frac{1}{2}\Big(\omega_o - r_M\left(k_M\left(\frac{\omega_c}{\omega_o}\right)^{n|1} + 1\right) - p_M b_M \\ & - b_M^{-1}\Big(\left(k_M + \omega_c k_M^2\right)\left(\frac{\omega_c}{\omega_o}\right)^{n|1} + h_M \\ & + \omega_c k_M\Big)\Big)\|\bar{z}\|^2 - \frac{1}{2}\Big(\omega_c - r_M\left(k_M\left(\frac{\omega_c}{\omega_o}\right)^{n|1} + 1\right)\end{aligned}$$

$$
\begin{aligned}
&- r_M b_M - b_M^{-1} k_M g_M \Big) \|\bar{x}\|^2 - \frac{1}{2}\Big(2T_b^{-1} - r_M b_M \\
&- \omega_o^2 p_M b_M - \omega_c^4 b_M^{-1} k_M g_M - b_M^{-1} \Big(h_M + \omega_c k_M \Big) \\
&+ \left(k_M + \omega_c k_M^2 \right) \left(\frac{\omega_c}{\omega_o} \right)^{n|1} \Big) \|\tilde{u}\|^2 + p_M d_L \|\bar{z}\| \\
&+ b_M^{-1} \varkappa_M \|\tilde{u}\| .
\end{aligned}
\tag{2.134}
$$

The negativeness of the two first terms can easily be ensured by choosing ω_c, and then ω_o, high enough. Simultaneously, increasing these parameters disrupts the structure of the term associated with $\|\tilde{u}\|^2$. Thus, once the bandwidths of the controller and observer are set sufficiently high, the time constant of the input gain dynamics is required to be small enough to enable the stabilization of the system. If these conditions are satisfied the convergence of the errors to some neighborhood of the origin, defined by the terms associated with $\|\tilde{u}\|$ and $\|\bar{z}\|$, is ensured.

The results produced by the Lyapunov method apply to the entire class of the systems described by (2.21), but are inherently strongly conservative. In order to gain further insights into the stability properties of the systems with uncertain input gain dynamics, the numerical analysis of a specific form of the plant is considered. To this end, recall the error dynamics as defined by (2.129) and define the vector of concatenated errors in the form of $\xi_u = \begin{bmatrix} \tilde{x}^T & \bar{z}^T & \tilde{u} \end{bmatrix}^T$. The dynamics of these errors are expressed by

$$
\dot{\xi}_u = \mathbf{N}_u \xi_u + \begin{bmatrix} \mathbf{b}_{n+m}^T & 0 \end{bmatrix}^T \dot{d} + \mathbf{b}_{2m} b^{-1} \varkappa_r^{(m)} \tag{2.135}
$$

with matrix $\mathbf{N}_u \in \mathbb{R}^{2m \times 2m}$ having the form of

$$
\mathbf{N}_u = \begin{bmatrix} \mathbf{G} & -\boldsymbol{W} & \mathbf{b}_n b \\ \mathbf{0}_{m \times n} & \mathbf{H} & -\mathbf{d}_m b \\ b^{-1} \mathbf{k}^T \mathbf{G} & b^{-1} \left(\mathbf{b}_n^T \boldsymbol{W} \mathbf{H} - \mathbf{k}^T \boldsymbol{W} \right) & -T_b^{-1} \end{bmatrix} \tag{2.136}
$$

and depending directly on $\mathbf{k}, \mathbf{l}, b$ and T_b parameters. Importantly, it can be shown that the sign of the eigenvalues of this matrix is invariant to the changes of b parameter. The stability of matrix $\mathbf{N}_u$ can be investigated through Hurwitz criterion to establish precise conclusions concerning the convergence of errors ξ_u. To this end consider the second order system ($n = 2$) with the tuning chosen

according to Tab. 2.1 and (2.97). Matrix $\mathbf{N}_u$ for the second-order system is expressed by

$$\mathbf{N}_u\Big|_{n=2} = \begin{bmatrix} 0 & 1 & 0 & 0 & 0 & 0 \\ -k_1 & -k_2 & -k_1 & -k_2 & -1 & b \\ 0 & 0 & -l_1 & 1 & 0 & 0 \\ 0 & 0 & -l_2 & 0 & 1 & -b \\ 0 & 0 & -l_3 & 0 & 0 & 0 \\ \frac{-k_1 k_2}{b} & \frac{k_1 - k_2^2}{b} & n_{6,3} & -\frac{k_2^2 - k_1}{b} & 0 & -\frac{1}{T_b} \end{bmatrix} \tag{2.137}$$

with

$$n_{6,3} = \frac{-l_3 - k_1 k_2 - k_1 l_1 - k_2 l_2}{b}. \tag{2.138}$$

The numerical evaluation of the stability of matrix $\mathbf{N}_u$ in function of ω_o, ω_c, T_b is given in Fig. 2.17.

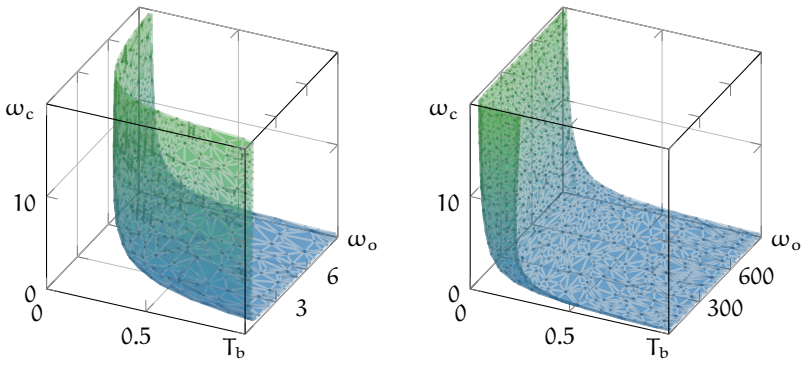

Figure 2.17: Border of stability region of $\mathbf{N}_u$. The stable region is below and to the left of the surface. Plots in different ranges of ω_o parameter are presented.

The numerical results presented in the plots are consistent with the conclusions drawn on the basis of the analytical investigation. It is shown in the figure, that there exists some region in which the system maintains stability despite the presence of some dynamics in the input path. As the time constant T_b approaches zero, this region grows what corresponds to the plant becoming closer to the nominal system without any input path dynamics. Conversely, as the value of T_b grows, the region of stability rapidly shrinks. The graph shows that if the large values of ω_o are chosen, further changes in this bandwidth do not significantly impact the stability of the system. The bandwidth of the observer is commonly chosen significantly greater than that of the controller and its abilities to impact the stability of the system are thus limited according to the presented results. Hence, in the presence of the dynamics in the input path, the tuning limitation is formulated mainly concerninig the choice of the controller bandwidth ω_c. Notably,

the stability conditions of $\mathbf{N}_u$ are more strict than these of the system controlled by the conventional state feedback control with the same tuning. In the system with input dynamics, the ESO itself imposes stability limitations as a tradeoff for the offered disturbance rejection capabilities.

To further investigate the performance of the ADRC controller in the presence of the input gain dynamics, the series of numerical simulations are performed for the system as discussed in this section.

Simulation 2.6. *The second order system with* $d = 0$ *is considered. The task of tracking of time-varying trajectory given by* $x_r(t) = \sin(2t)$ *is investigated. The input gain of the plant is chosen as* $b = 1$ *and the values of* ω_o *and* ω_c *vary in each experiment. The quality factor* $E(T_b)$ *as given by* (2.107) *is calculated for each run and presented in the plots. The results of the simulations are given in Fig. 2.18*

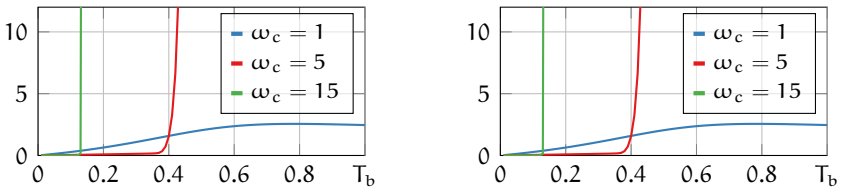

(a) $\omega_o = 10$ (b) $\omega_o = 100$

Figure 2.18: Values of the performance criterion $E(T_b)$ for the system with input dynamics.

The presented simulations are once again in line with the analytical results. Moreover, several properties of the ADRC algorithm working in the presence of input dynamics are unveiled. It can be seen that while the increase of the controller bandwidth ω_c leads to destabilization of the system for higher values of time constant of the input dynamics, it simultaneously weakens the impact of the input dynamics on the performance of the controller enforcing small values of performance criterion in the entire range of stable work. The results of simulations show also, that the changes of ω_o have no significant impact on either the stability or the performance of the controller in the discussed situation. This notion highlights the inability of the ESO to estimate the impact of the input dynamics which leads to the lack of compensation improvement with the increase in the observer bandwidth.

The presented analytical and numerical investigation into the properties of the ADRC scheme in the presence of the input path dynamics answers some questions not previously solved in the literature. The problem of the unknown degree of the plant has been previously studied only for the case of the real degree of the plant being smaller than

the one assumed during the controller synthesis. In works [337–339] it was shown that the ADRC controller can ensure the stability of such a system. According to the best knowledge of the author, no results have been so far published on the applicability of the ADRC to plants with a degree higher than assumed. The presented results are thus the first to show that in the presence of additional stable dynamics in the input path, the ADRC with fixed values of tuning parameters offers the convergence of the errors only for a narrow range of values of input path time constants. It is moreover shown that this range shrinks with the increase of controller bandwidth and the disturbance estimation capabilities of the ESO are insufficient to successfully compensate for the presence of such unknown input dynamics.

2.4 PERFORMANCE IN PRACTICAL SCENARIOS

The increasing interest in the ADRC scheme among practitioners inevitably leads also to an increase in the variety of perturbed and uncertain systems to which the algorithm is applied. Thus, there is a requirement for scientific investigation of the performance of the ADRC approach for various specific types of disturbances. While the results presented in the previous sections highlight numerous aspects of the ADRC approach in the general scenarios satisfying specific predefined conditions, a more detailed study of the chosen systems encountered in engineering practice is necessary. To this end, this chapter presents the results of implementation and application of the ADRC controller to some types of practical problems. Namely, at first, the problem of friction compensation is studied and the results are presented concerning the performance of the ADRC controller in the task of trajectory tracking in the presence of resistive forces. With a view to this, the results presented in [236] are recalled in parts material to the subject of this work. In the second part of this section, the focus is placed on the problem of harmonic disturbance attenuation. The results of the application of the ADRC to a system subject to such a disturbance are given. Moreover, the recently proposed structure of the algorithm more suitable for such tasks is recalled and compared with the standard approach in terms of performance and robustness. These are given on the basis of results shown in [180] where the extensive study of this problem is presented. All of the experiments of this section are carried out using the robotic astronomic telescope mount described in more detail in Section 4.2. The results presented here are strongly focused on the practical aspects of the ADRC algorithm and based on the experimental studies of the author. Analytical considerations are omitted here and only some basic descriptions of the discussed systems are given.

2.4.1 *Friction compensation*

Friction compensation is one of the major concerns in the design of control algorithms for mechanical systems. Several models of the friction effects have been proposed in the literature and tested in practical solutions [33, 113, 215]. Multiple results on the identification of the friction effect have also been presented [23, 96, 294]. Yet, due to the sophisticated character of this phenomenon, obtaining its suitable model with proper parameter values in advance is a difficult and time-consuming process. Significant interest is thus given to the methods of adaptive friction compensation [158, 298, 324]. These allow the designer to omit the demanding identification of the disturbing forces and achieve the satisfying performance of the algorithm due to its ability to online estimate the feasible values of the parameters of the model. An alternative approach to the friction compensation is represented by the solutions employing the ADRC controller to cope with uncertainties in the friction model or complete lack of such a model [27, 50, 283].

The problem of friction compensation is of special importance in the field of astronomic observations [165, 279]. Modern robotic astronomic telescope mounts are subject to high requirements concerning the quality of motion in a wide range of velocities. In order to enable conducting observations of celestial objects, the mounts are required to exhibit high precision of tracking in extremely low velocities. Simultaneously, the devices are expected to be capable of performing fast changes of working point and quick reconfiguration of the mount at high velocities to shorten the delay between the observations. Such working conditions imply the necessity to cope with the presence of friction effect in different operation regimes. The common use of the direct drive schemes further increase the needs for a robust friction compensation. Consider the simple model of a single axis of the robotic telescope mount given by

$$\dot{\mathbf{x}} = \mathbf{A}_n \mathbf{x} + \mathbf{b}_n \left(b u + \psi \right), \tag{2.139}$$

where $n = 2$, $\mathbf{x} = \begin{bmatrix} \varphi & \omega \end{bmatrix}^T \in \mathbb{R}^2$ represents the orientation and rotational velocity of the mount axis, $b = \frac{1}{J}$ stands for the input gain with $J \in \mathbb{R}_+$ being the inertia coefficient of the axis, and $\psi = -b d_f$ with d_f being a disturbing friction force affecting the plant. While the presence of other disturbing effects is expected in the plant, it is here assumed that the friction is a predominant force impacting the system. The control signal u takes the form of the torque exerted by the motor.

Two basic modes of the friction force d_f are distinguished – presliding and sliding regime, exhibited during the slow and fast types

of motion, correspondingly. The behavior of the friction force in the sliding regime may be described by the well-known static model as a function of the velocity of the axis [10]. Such a model takes the form of

$$\begin{aligned} d_f &= \sigma_2 \omega + \operatorname{sgn}(\omega) s(\omega), \\ s(\omega) &= F_c + (F_s - F_c) \exp(-\left|\frac{\omega}{V_s}\right|^{\delta}), \end{aligned} \tag{2.140}$$

where $\sigma_2 \in \mathbb{R}_+$ is a viscous force coefficient, $F_s \in \mathbb{R}_+$ and $F_c \in \mathbb{R}_+$ stand for static and Coloumb friction coefficients, $V_s \in \mathbb{R}_+$ is a Stribeck velocity and $\delta \in \mathbb{R}_+$ is a shape factor. Notably, for very small velocities the exponential term is approximately equal to one and $s(\omega) \approx F_s$ which significantly simplifies the static model and makes it unsuitable for modeling the friction effect in the regime of slow movements. The extension of this static description is given by dynamic Dahl and LuGre models which take into account the characteristics of the friction force in the presliding regime when the external force is too small to break the static friction force [52, 53]. The latter of these is modeled by

$$\begin{aligned} d_f &= \sigma_0 z + \sigma_1 \dot{z} + \sigma_2 \omega, \\ \dot{z} &= \omega - \sigma_0 \frac{|\omega|}{s(\omega)} z, \end{aligned} \tag{2.141}$$

where $s(\omega)$ is given as in (2.140), while $\sigma_0 \in \mathbb{R}_+$ and $\sigma_1 \in \mathbb{R}_+$ are micro-stiffness and micro-damping coefficients responsible for the modeling of small deformations of the contact surfaces. Notably, in a steady state with $\dot{z} = 0$, the dynamic model (2.141) is simplified to the static form expressed by (2.140).

Assuming that the constant parameters of the friction models are roughly known, the controller characterized by inbuild friction compensation can be designed according to the ADRC paradigm and procedures presented in Sections 2.1 and 2.2. To this end, the method and procedure of identification of these parameters given in [236] are employed. As a result of the presented approach, the set of parameters is obtained describing the character of friction force in the vertical axis of the mount bearing an astronomic telescope of diameter 0.5 m. Namely, the micro-stiffness and micro-damping coefficients are found to be equal $\sigma_0 \approx 9.8 \cdot 10^4$ N m/rad and $\sigma_1 \approx 521.4$ N m s/rad. The coefficients of viscous force and both static and Coloumb friction are given as $\sigma_2 \approx 32.8$ N m s/rad and $F_c \approx 2.3$ N m, $F_s \approx 3.3$ N m. Finally, the Stribeck velocity and shape factor are identified as $V_s \approx 4.1 \cdot 10^{-2}$ rad/s and $\delta \approx 2$. Moreover, it is assumed that the moment of inertia of the axis is roughly equal $J \approx 30\,\mathrm{kgm}^2$.

Simulation 2.7. *The simulation study of the behavior of plant* (2.139) *in the presence of the friction modeled by full dynamic system* (2.141) *is carried out. To this end, a problem of slowly varying trajectory tracking is considered, with the reference trajectory chosen according to* (2.34) *with* $x_r(t)$ *given by*

$$x_r(t) = 5 \cdot 7.268 \cdot 10^{-5} \left(\frac{2}{5}\pi\right)^{-1} \sin(\frac{2}{5}\pi t)\,\mathrm{rad/s}. \tag{2.142}$$

In Fig. 2.19 the response of the numerical system is presented for the scenario with the controller without any kind of disturbance compensation (i.e. $\omega_o = 0$, $\hat{z}_m = 0$, *and with state measurements instead of estimates used in the control law), with the controller bandwidth chosen as* $\omega_c = 15$. *Fig. 2.20 presents the results of the simulation with the conventional ADRC controller designed without any knowledge about the model of the disturbance (i.e.* $\psi = 0$ *in the observer design). The controller bandwidth is set to* $\omega_c = 15$ *and the observer is tuned with* $\omega_o = 220$. *In the plot real value of disturbance* d_f *and the trajectory of* $-J\hat{z}_3$, *which corresponds to the estimate of the friction force produced by the obsever, are given.*

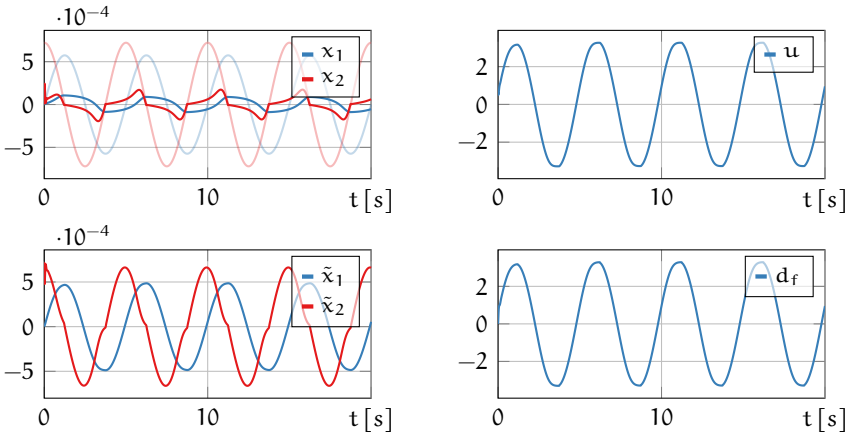

Figure 2.19: Time responses of simulated telescope axis in the presence of LuGre friction model. Results obtained for the controller without any disturbance compensation. Reference state shown in transparent plots.

The results obtained for the controller without disturbance attenuation highlight the significant impact of the friction force on the performance of the plant. It can be seen that the conventional controller exhibits the strongly limited capability to compensate for the resistive force working against the movement of the axis and trajectory tracking is hardly possible. The inclusion of the disturbance rejection according to the ADRC paradigm strongly improves the performance of the system. The tracking errors are reduced and the significant errors are present only in the moments of movement reversals. Simultaneously, the character of the friction force is changed and almost

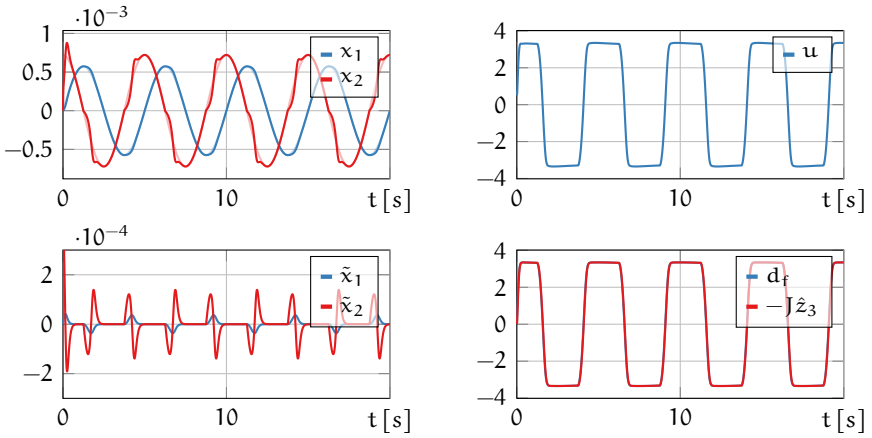

Figure 2.20: Time responses of simulated telescope axis in the presence of LuGre friction model. Results obtained for the ADRC controller without explicit disturbance model.

discontinuous terms become the dominant part of the dynamics of this phenomenon. The final simulations are performed taking into consideration the full control algorithm which includes the explicit model of the friction incorporated in the observer and controller design.

Simulation 2.8. *The settings as in Sim. 2.7 are considered with the controller incorporating a friction model. Both the standard static model of the friction and the dynamic LuGre model corresponding to the actual model used to simulate the plant, are considered. To this end, the models are calculated using the estimate of the state of the plant, and dynamics of z displacement variable in the LuGre model are simulated online without any direct measurement of its value. Importantly, the dynamics given by* (2.141) *are stable ones, and thus the simulation error of z state tends to converge to the origin in the steady state. The results of these simulations are given in Fig. 2.21 and Fig. 2.22, where the results obtained with static and dynamic models are presented.*

The presented plots show the differences in the impact of the incorporation of the discussed friction models in the controller design. Namely, it is shown that the inclusion of the static model, which is a common approach among practitioners, may not lead to an increase in the tracking quality in the simulation environment. Despite the use of identified parameters of the physical phenomenon, the static function is unable to successfully approximate the behavior of the dynamic model. On contrary, the full LuGre model successfully copes with the undesired disturbances. The tracking errors and the disturbance estimate are strongly reduced in the entire time horizon of the simulation, despite employing the state estimates as a basis of the friction model evaluation and lack of direct measurement of z displacement. This property is caused by the character of the displacement dynamics

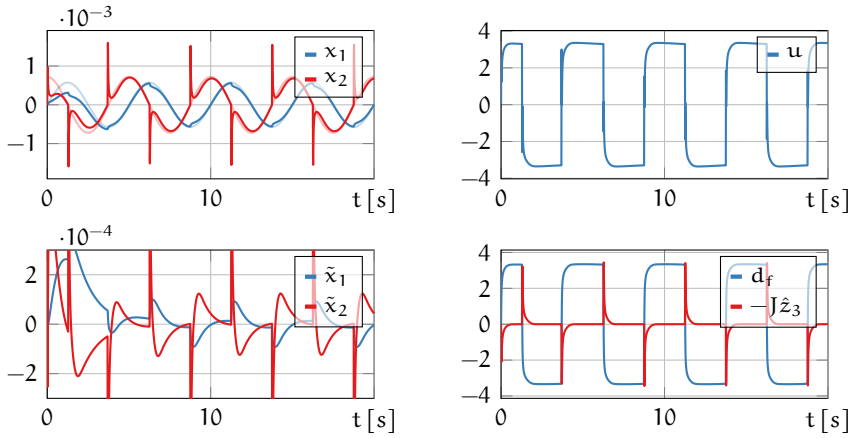

Figure 2.21: Time responses of simulated telescope axis in the presence of LuGre friction model. Results obtained for the ADRC controller with static disturbance model evaluated on the estimated state.

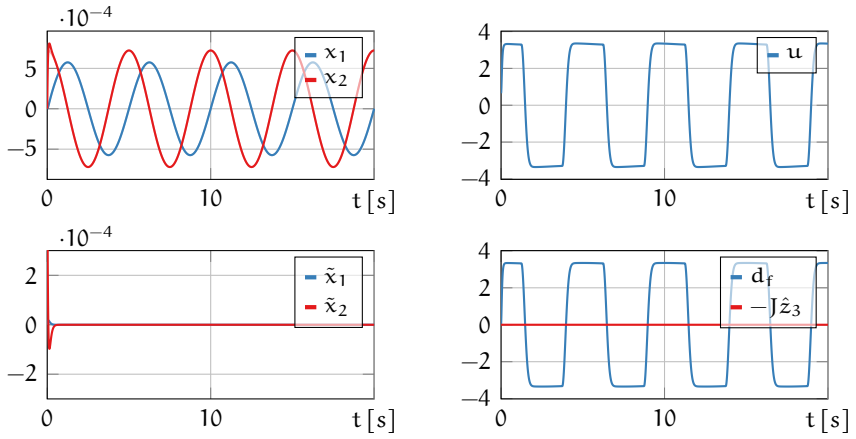

Figure 2.22: Time responses of simulated telescope axis in the presence of LuGre friction model. Results obtained for the ADRC controller with dynamic disturbance model evaluated on the estimated state.

in (2.141) which, for any constant ω, has a form of stable linear dynamics. Thus, for the slowly-varying enough trajectories, both real z and its computed estimate converge to the same configuration despite unknown initial displacement. Vanishing of the estimated signal $-J\hat{z}_3$ shows that the incorporated model succesfully describes the disturbances acting upon the system and thus the observer is not burdened with its estimation. Additional trials unveiled the high robustness of such an approach to the parametric uncertainties of the model – of all the parameters, only the changes of F_s seem to visibly deteriorate the performance of the algorithm. Similarly, the robustness to the decrease of observer bandwidth has been noted with results for $\omega_o = 50$ being visually identical to these obtained with a nominal value of $\omega_o = 220$.

The numerical results imply the usefulness of the ADRC scheme and the dynamic friction model in the task of friction compensation. Experimental trials are performed to further investigate this issue. Additionally, to study the impact of the tracking and estimation errors on the modeling of the friction phenomenon, two versions of the controller are considered. Specifically, unmeasurable ω variable necessary to evaluate (2.140) and (2.141) is substituted with either estimated value produced by the observer or the reference state $x_{r2}(t)$.

Experiment 2.2. *The ADRC controller with static and dynamic friction models is implemented in the main control unit of the telescope mount. The constant parameters are chosen according to the results presented in [236]. The tuning of the observer and controller, as well as the reference trajectory, are chosen as in Sim. 2.8 and remain unchanged. The results of the experiment conducted with the standard ADRC controller without the friction model are presented in Fig. 2.23. The outcomes of employing the static model evaluated using the estimated state and the reference velocity are given in Fig. 2.24 and Fig. 2.25 correspondingly. Finally, Fig. 2.26 and Fig. 2.27 present the products of trials with dynamic LuGre model generated on the basis of the estimated state and the reference velocity, respectively. In all plots, the initial moments of experiments are omitted and only the performance in the steady state is considered for evaluation.*

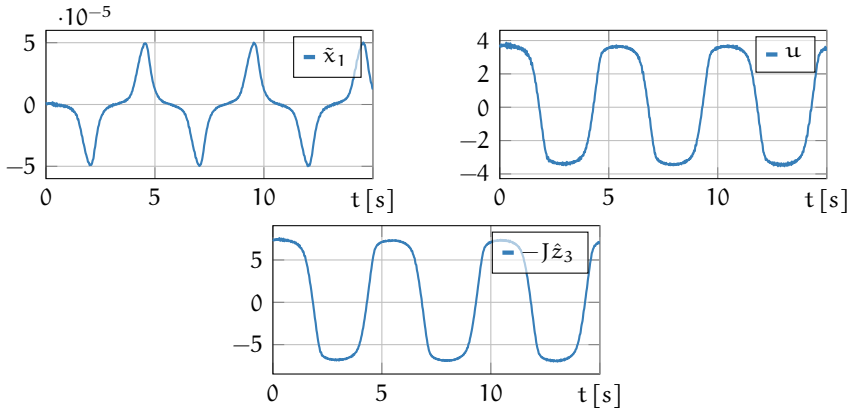

Figure 2.23: Time responses of telescope axis in the experiment. Results obtained for the standard ADRC controller without explicit disturbance model.

The experimental results confirm the effectiveness of the combination of the ADRC algorithm with an explicitly given model of the disturbance in the task of friction compensation in the mechanical system. It is shown that the inclusion of the dynamic model successfully limits the impact of the friction phenomenon in the experimental setting. As the included model is used to compensate for the friction dynamics, the estimate of the total disturbances is also significantly

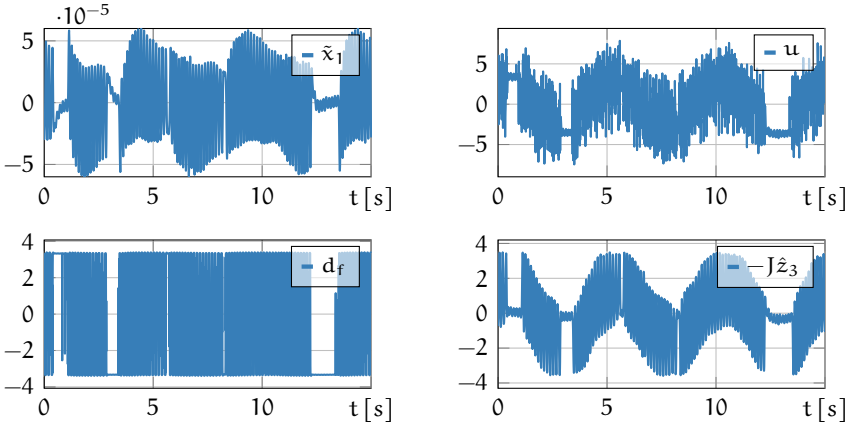

Figure 2.24: Time responses of telescope axis in the experiment. Results obtained for the ADRC controller with static disturbance model evaluated on the estimated state.

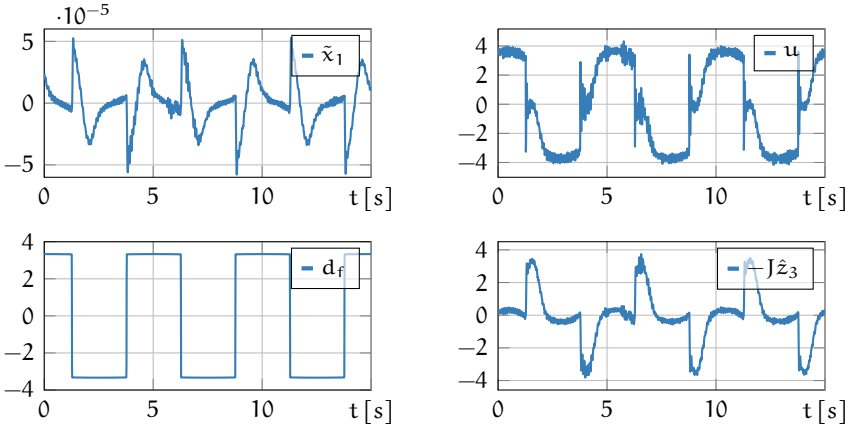

Figure 2.25: Time responses of telescope axis in the experiment. Results obtained for the ADRC controller with static disturbance model evaluated on the reference state.

decreased in the scenarios employing the explicit model. It can also be noted, that the evolution of the disturbance d_f modeled by the LuGre model and shown in Fig. 2.26 and 2.27 strongly resembles the estimate $-J\hat{z}_3$ produced in the first trial. While the trials performed using the dynamic model result in a visible improvement in the tracking quality, the static model does not offer a significant increase in the tracking quality. This notion is in line with the outcomes of the simulations. Notably, the static compensation in the scenario with the model evaluated on the evaluated trajectory offers slight improvement of control, quantified by a decrease of E_1 criterion by approximately 13% in comparison with the standard ADRC approach. On the contrary, the use of a static model calculated using estimated state leads to a significant decrease of tracking quality and an increase of E_1 factor by over 50%. Such an effect is attributed to the high sensitivity of the

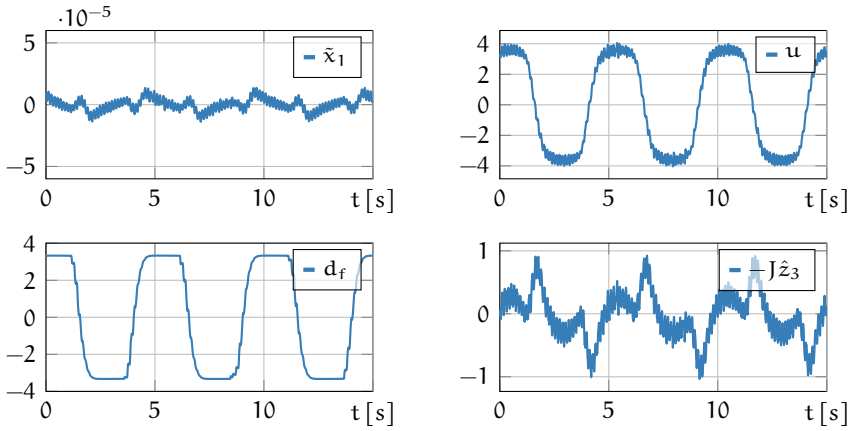

Figure 2.26: Time responses of telescope axis in the experiment. Results obtained for the ADRC controller with dynamic disturbance model evaluated on the estimated state.

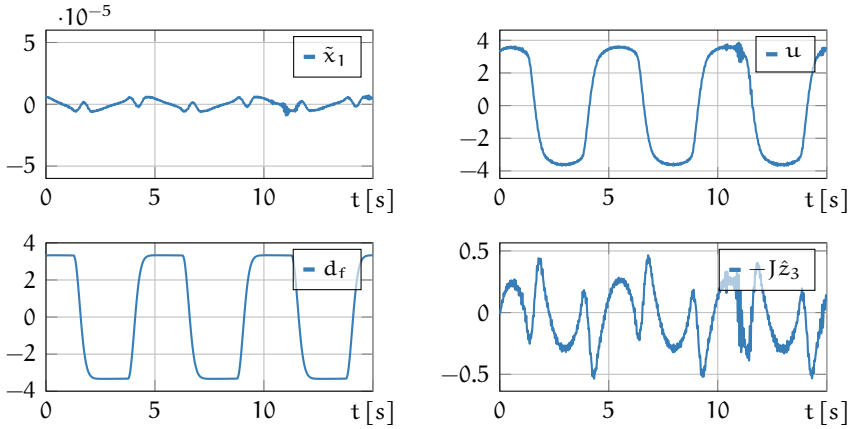

Figure 2.27: Time responses of telescope axis in the experiment. Results obtained for the ADRC controller with dynamic disturbance model evaluated on the reference state.

static discontinuous model to the estimation errors and measurement noises. While the performance of the controller with dynamic model evaluated on the estimated state is also slightly worse than that with the model generated using reference signals, both approaches result in improvement in the control quality, resulting in a decrease of E_1 by 73% and 80% respectively. This notion implies the higher robustness of the dynamic friction model to the measurement noises and estimation errors. Regardless of these differences in performance increase offered by specific friction models, the outcome of the experiment highlights the effectiveness of the inclusion of explicit disturbance dynamics equations in the ADRC controller design and synthesis.

2.4.2 *Harmonic disturbance compensation*

The presence of harmonic and oscillatory disturbances affecting the dynamic systems is a problem commonly encountered in practical scenarios. Different kinds of disturbing vibration forces are encountered in the tasks associated with suspension systems [342, 343], flexible manipulators [135, 199] or elastic gantry cranes [88]. Moreover, similar kinds of uncertainties are commonly observed in other practical dynamic systems due to the manufacturing imperfection or inherent characteristics of the employed components, e. g. possible eccentricity of the rotor of electric motor [36] or ripple torque of brushless motors [24, 78, 169].

In the field of automated astronomic observations, the oscillating disturbances are often caused by vibrations induced in the mechanical structure of the mount and the presence of the torque ripple in the employed motors. The high stiffness of the telescope mount construction and use of a gearless connection between the motors and the telescope, combined with expectations of limited internal clearances, may amplify the impact of the high-frequency oscillations in the structure of the device. Although such phenomenons are often of negligible importance in other engineering tasks, the extremely high precision requirements of the celestial observations enforces the designer to consider the impact of these forces on the performance of the system. To this end, a model of a single axis of the robotic telescope mount is investigated and described as

$$\dot{\mathbf{x}} = \mathbf{A}_n \mathbf{x} + \mathbf{b}_n \left(b u + \psi \right) \tag{2.143}$$

with $n = 2$. The terms $\mathbf{x}$ and b are as discussed in Section 2.4.1. The disturbing term is here denoted as $\psi = -b d_h$ where d_h represents some harmonic disturbance. Once again the assumption is made that d_h is a dominant disturbing force in the plant. This is ensured in the experimental scenario by employing the additional control outer control loop, designed according to the results of Section 2.4.1, for friction compensation. In the paper [180] the comparison of the performance of several methods based on the error-domain ADRC in the task of harmonic disturbance rejection is presented. In order to design an algorithm in the form of the EADRC method, the nominal tracking error is defined as $\tilde{\mathbf{x}} = \mathbf{x}_r - \mathbf{x}$ with dynamics

$$\dot{\tilde{\mathbf{x}}} = \mathbf{A}_n \tilde{\mathbf{x}} - \mathbf{b}_n \left(b u + \psi - x_r^{(n)} \right). \tag{2.144}$$

Regardless of the source of the harmonic disturbance in the considered system, in its most general form, such disturbances may be modeled

as a static sine function or a response of a dynamic oscillating system. The simplest description of such a phenomenon is given by

$$d_h = a_h \sin(2\pi f_h t) \tag{2.145}$$

with $a_h \in \mathbb{R}$ and $f_h \in \mathbb{R}_+$ being the amplitude and frequency of the harmonic function. Following the approach outlined in [275] an internal model is incorporated [73] and function (2.145) is equivalently presented by in the form of an unforced oscillator system without dumping expressed as

$$\ddot{d}_h + (2\pi f_h)^2 d_h = 0. \tag{2.146}$$

Taking derivative of (2.146) the dynamics

$$d_h^{(3)} + (2\pi f_h)^2 \dot{d}_h = 0 \tag{2.147}$$

is obtained. This notion allows one to rewrite the nominal closed-loop system (2.143) including the additional states representing the dynamics of the harmonic disturbance. The dynamics of the plant thus take the form of

$$\dot{\mathbf{q}} = \mathbf{A}_{n+3}\mathbf{q} - \begin{bmatrix} \mathbf{b}_n^T & \mathbf{0}_{3\times 1}^T \end{bmatrix}^T \left(u - x_r^{(n)}\right) - \mathbf{b}_{n+3} (2\pi f_h)^2 \mathbf{d}_{n+3}^T \mathbf{q}, \tag{2.148}$$

where $\mathbf{q} = \begin{bmatrix} \tilde{\mathbf{x}}^T & d_h & \dot{d}_h & \ddot{d}_h \end{bmatrix}^T \in \mathbb{R}^{n+3}$. Due to such a redefinition of the state of the system, the problem of the identification of amplitude a_h is transformed into the problem of state $\mathbf{q}$ estimation.

For such a system three algorithms can be proposed on the basis of the ADRC defined in the error domain. At first, if frequency f_h is known in advance, a standard observer can be designed for a system in the form of (2.148) by taking $\mathbf{z} = \mathbf{q}$. Such an approach has been proposed in the state-domain in [275] under the name of Resonant ESO (RESO, not to be confused with Reduced ESO), and [181] in the domain of the tracking error. The corresponding observer is given by

$$\begin{aligned} \dot{\hat{\mathbf{z}}} = &\left(\mathbf{A}_{n+3} - \mathbf{b}_{n+3} (2\pi f_h)^2 \mathbf{d}_{n+3}^T\right) \hat{\mathbf{z}} \\ &- \begin{bmatrix} \mathbf{b}_n^T & \mathbf{0}_{3\times 1}^T \end{bmatrix}^T u + \mathbf{l}\mathbf{c}_{n+3}^T (\mathbf{z} - \hat{\mathbf{z}}), \end{aligned} \tag{2.149}$$

with the vector of gains $\mathbf{l}$ of suitable order. Alternatively, if the frequency of the harmonic disturbance is unknown, the term $\left(2\pi f_h\right)^2 \mathbf{d}_{n+3}^T \mathbf{q}$ in (2.148) can be considered a part of unmeasurable total disturbance and be omitted in the observer design. A new observer is then designed and expected to estimate the momentary value of the total disturbance corresponding to the state of the oscillatory system gener-

ating the sinusoidal disturbance affecting the plant. Such an alternative observer design takes then the form of the 5th order ESO given by

$$\dot{\hat{z}} = \mathbf{A}_{n+3}\hat{z} - \begin{bmatrix} \mathbf{b}_n^T & \mathbf{0}_{3\times 1}^T \end{bmatrix}^T u + \mathbf{l}\mathbf{c}_{n+3}^T (z - \hat{z}) \tag{2.150}$$

with $z = q$. Finally, the standard 3rd order EADRC algorithm can be designed for the nominal system (2.143) by defining $\delta = d_h$. In such a case, the observer is given by

$$\dot{\hat{z}} = \mathbf{A}_{n+1}\hat{z} - \mathbf{b}_{n+1}u + \mathbf{l}\mathbf{c}_{n+1}^T (z - \hat{z}) \tag{2.151}$$

with the extended state defined in the error-domain in a standard manner as $z = \begin{bmatrix} \tilde{\mathbf{x}}^T & \delta \end{bmatrix}^T \in \mathbb{R}^{n+1}$. For all of the variants, the control law is designed as an ordinary EADRC controller with disturbance compensation on the basis of the disturbance estimate expressed by

$$u = b^{-1}\left(\mathbf{k}^T\hat{\mathbf{x}} + \hat{z}_{n+1}\right). \tag{2.152}$$

The initial studies of the considered approaches are conducted in simulation to investigate the performance of the algorithm in nominal scenarios.

Simulation 2.9. *Model* (2.143) *is implemented with the harmonic disturbances as observed in the real telescope mount during the preliminary experiments and characterized by* $f_h = 7.46\,\mathrm{Hz}$. *The unknown amplidute of this phenomenon is approximated as* $a_h = 0.6\,\mathrm{m/s^2}$ *and* $J = 30\,\mathrm{kgm^2}$. *In all the trials the reference trajectory is chosen according to* (2.142) *and the algorithm is tuned with* $\omega_c = 2, \omega_o = 100$. *For the sake of comparison, the first trial is performed for the controller without any disturbance compensation (i. e.* $\omega_o = 0$, $\hat{z}_{n+1} = 0$, *and with state measurements instead of estimates used in the control law) and its results are presented in Fig. 2.28 where the evolution of the state and control signals, together with the tracking errors and its spectrum, is given.*

It can be seen that the controller missing the disturbance rejection capabilities is unable to correctly compensate for the lack of explicit feedforward signal and the presence of harmonic disturbances. The significant oscillations of the state of the plant are present in the output of the simulation, despite its attempted attenuation signified by the presence of the oscillations also in the control signal. Simultaneously, the tracking errors remain relatively high throughout the entire simulation due to the inability of the algorithm to successfully track the time-varying trajectory.

Simulation 2.10. *Simulations with settings as Sim. 2.9 and different EADRC control schemes are conducted. The results of the simulations employing the 3rd order ESO as given by* (2.151), *5th order ESO given by*

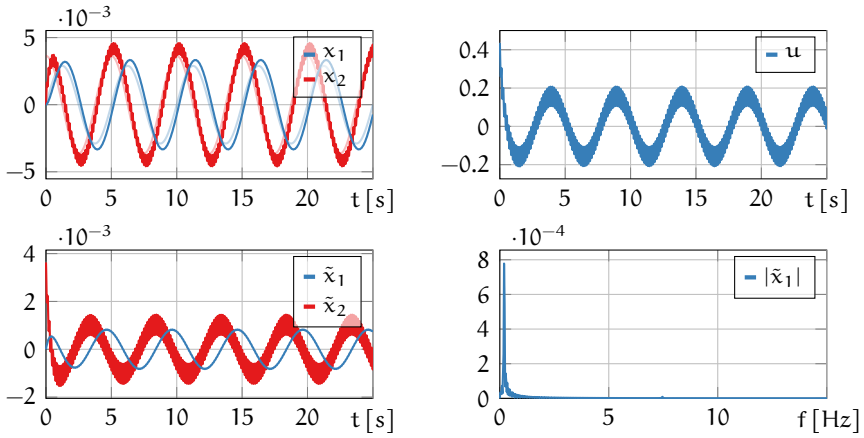

Figure 2.28: Time responses of simulated telescope axis in the presence of harmonic disturbance. The results obtained for the controller without any disturbance compensation. Reference state is shown in transparent plots.

(2.150) *and RESO in the form of* (2.149) *are given in Fig. 2.29, 2.30 and 2.31, correspondingly.*

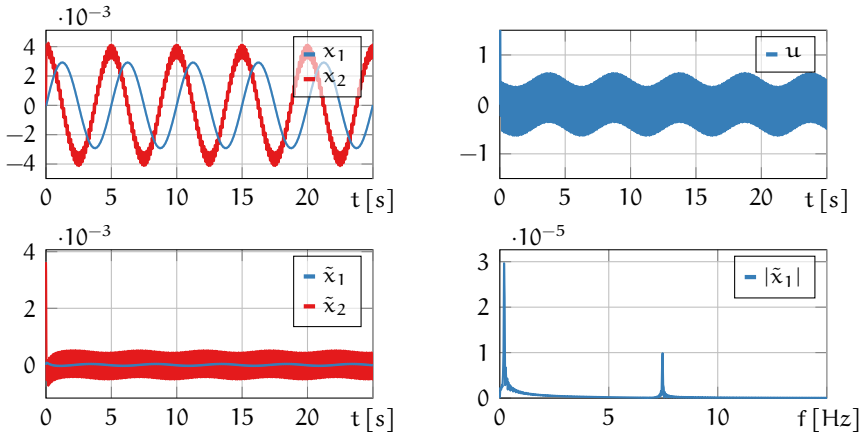

Figure 2.29: Time responses of simulated telescope axis in the presence of harmonic disturbance. Results obtained for the ADRC controller with 3rd order ESO.

Some properties of the three algorithms can be noticed on the basis of the presented plots. The overall quality of the control is significantly improved in every case due to the disturbance rejection capabilities displayed by all of the considered methods. Specifically, the employment of the standard 3rd order ESO resulted in the decrease of E_1 performance factor by over 67% in comparison with results obtained without disturbance compensation. It is shown that an increase in the order of the observer between the 3rd and the 5th order ESO results in the substantial reduction of the impact of the low-frequency disturbance caused by the varying of the reference trajectory. This effect is

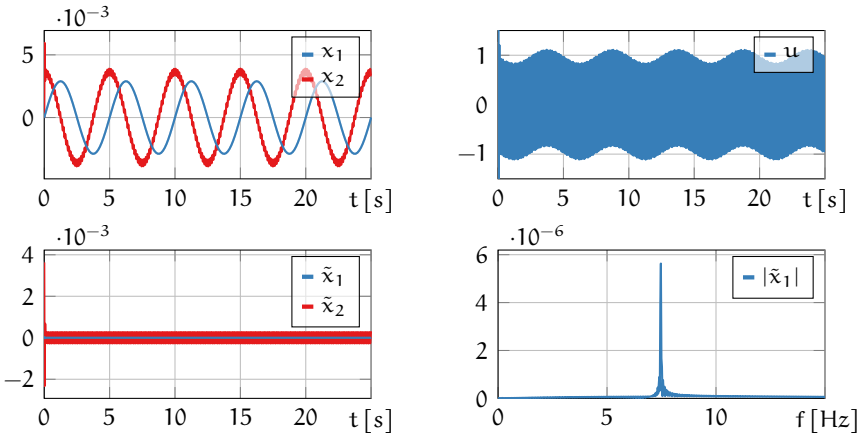

Figure 2.30: Time responses of simulated telescope axis in the presence of harmonic disturbance. Results obtained for the ADRC controller with 5th order ESO.

caused by the fact that the ESO in its standard form is designed on the basis of an assumption that the disturbance is modeled by the function with certain derivatives equal zero. Thus it is inherently better suited for the compensation of low-frequency signals. Simultaneously, the impact of this change on the rejection of the high-frequency harmonic disturbances is limited, and only a twofold decrease in the spectral amplitude is observed. The overall control quality in the scenario employing the 5th order ESO as measured by E_1 criterion is improved by over 81% as compared with the first trial without disturbance compensation. The inclusion of the explicit model of the harmonic dis-

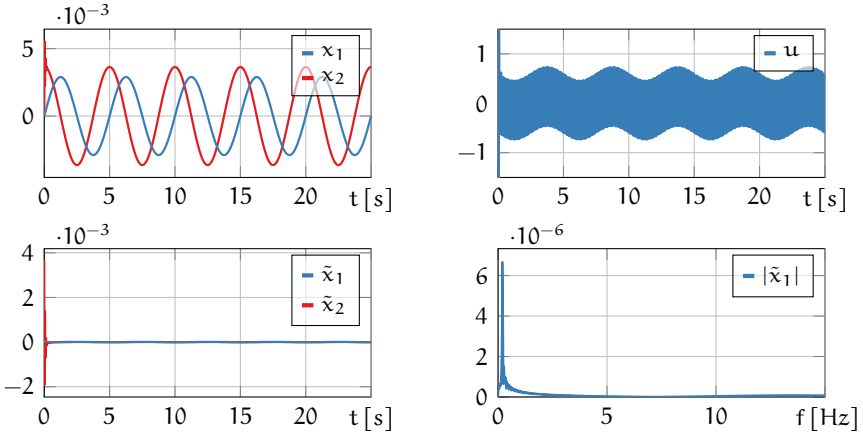

Figure 2.31: Time responses of simulated telescope axis in the presence of harmonic disturbance. Results obtained for the ADRC controller with RESO.

turbance tuned with the proper frequency of the oscillating function significantly changes the properties of the algorithm. The capabilities of the observer to estimate the disturbances of the given frequency

are highly improved at a cost of deterioration in the compensation of other signals. The employment of the RESO allows thus successful compensation of the harmonic disturbance, signified by the almost absolute reduction of its spectral amplitude. As a result, the performance criterion in a steady state is decreased by over 99% in comparison with the nominal scenario. Nonetheless, the compensation of the effect of the varying trajectory is limited in this scenario, and the choice of different $x_r(t)$ function may impact the scale of the achieved performance improvement.

In order to validate the simulational results in the practical scenarios, a series of experimental trials is conducted.

Experiment 2.3. *Three controllers based on the 3rd order ESO, 5th order ESO, and RESO are implemented in the driver of the robotic mount of the telescope and tested in the task of trajectory tracking. To emphasize the presence of the harmonic disturbances in the system, an additional sinusoidal input signal is generated in the control input of the system and an outer loop controller with a friction model is employed to alleviate the impact of the friction phenomenon. The reference trajectory, disturbance model, and controller gains are chosen as in the Sim. 2.9 and 2.10. The observer bandwidth is set to* $\omega_o = 80$ *in the trials employing the 5th order ESO and the RESO algorithms, and to* $\omega_o = 140$ *in the run with standard 3rd order ESO. This tuning method is embraced to ensure a comparable value of* E_1 *in tests with 3rd and 5th order ESO. Due to the dominant character of the harmonic disturbance in the considered system, a similar value of the performance criterion can not be achieved in the scenario employing the RESO controller and the bandwidth in this trial is set equal to the one chosen for a 5th order ESO. The results of the experiments with 3rd order and 5th order ESO, as well as with RESO algorithm, are given in Fig. 2.32, 2.33 and 2.34, respectively.*

The results obtained in the two initial trials bear a strong resemblance due to chosen tuning method aimed at obtaining similar quality of control. The use of the observer of higher order allows a choice of lower tuning gains without a decrease in the resultant tracking precision. Simultaneously, such a choice seems to increase to impact of the high-frequency harmonic disturbance which cannot be effectively reduced due to the limited bandwidth of the observer. This effect is also visible in the plot of the error spectrum, as the amplitude of the high-frequency errors is increased in comparison with the disturbance caused by the low-frequency trajectory. A slight increase in the high-frequency modes in the control signal can also be noticed. Incorporation of the explicit model of the disturbance according to (2.149) in the experimental setting results in a significant attenuation of the high-frequency disturbance. The resultant tracking quality is

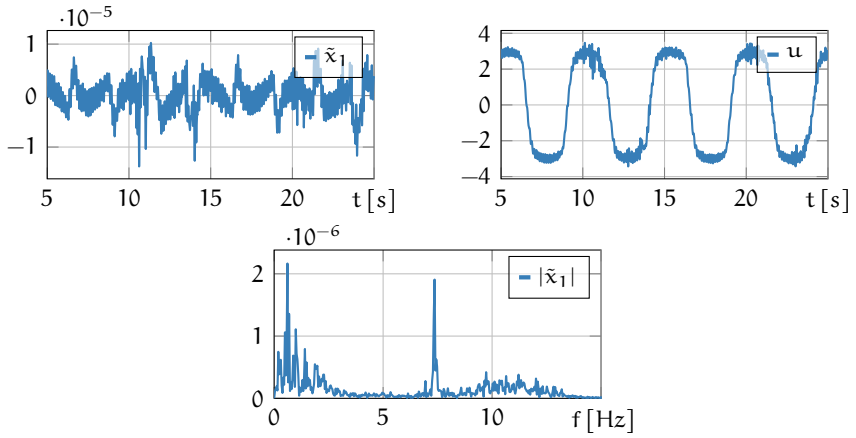

Figure 2.32: Time responses of telescope axis and the error spectrum in the experiment. Results obtained for the ADRC controller with 3rd order ESO.

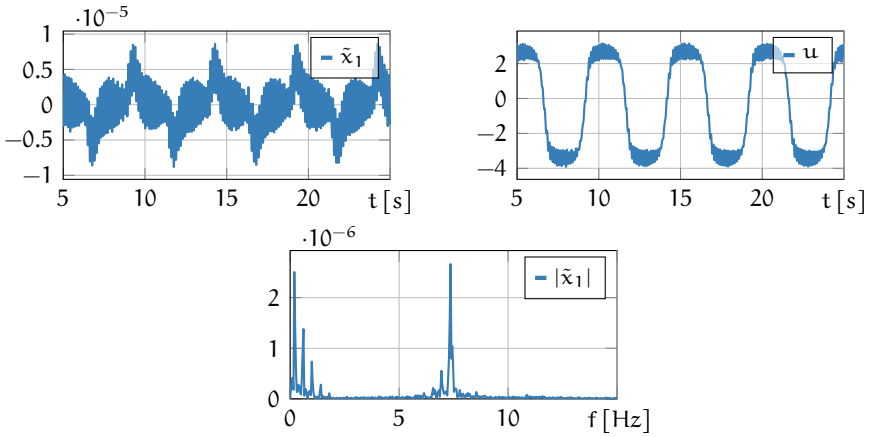

Figure 2.33: Time responses of telescope axis in the experiment. Results obtained for the ADRC controller with 5th order ESO.

thus significantly enhanced, which corresponds to a decrease of E_1 criterion by over 52% in comparison with results obtained for 3rd and 5th order conventional ESOs. The experimental trials do not confirm the superiority of the standard ESO in the task of low-frequency disturbance compensation, as observed in the simulations, in practical situations. As emphasized by the spectrum plots, the RESO employed in the experimental settings of the robotic telescope mount offers not only improved rejection of the disturbance of the prescribed frequency, but also improved attenuation of all disturbances affecting the plant. Such a result is obtained despite the lack of changes in the tuning of the algorithm between the runs employing the 5th order ESO and the RESO method. The exact reason for such a difference between the improvement due to the RESO employment observed in the simulation and experiment is not yet sufficiently explained and investigated.

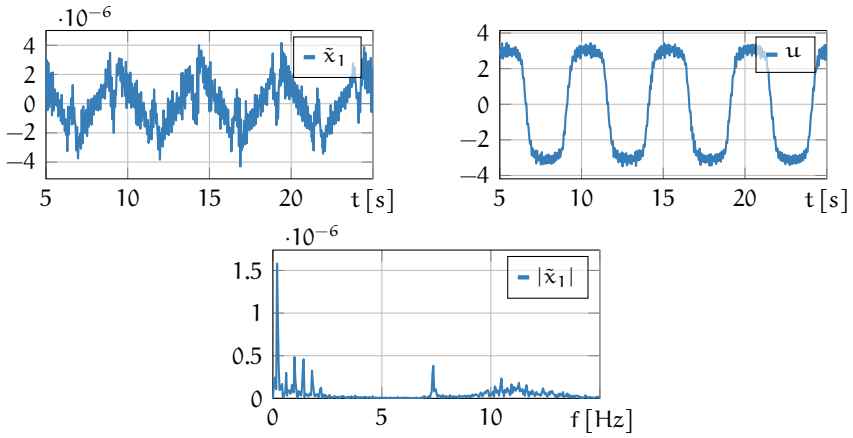

Figure 2.34: Time responses of telescope axis in the experiment. Results obtained for the ADRC controller with RESO.

The presented results of the use of the ADRC controllers in the experimental settings highlight some important properties of the controller. Namely, the algorithms capable of active disturbance rejection show significantly higher performance than standard methods devoid of such possibilities. Both in the task of friction compensation and the harmonic disturbance attenuation, the ADRC algorithm offered a substantial increase in the tracking precision in comparison with preliminary simulations performed using simple state feedback controllers. While the use of a standard ADRC method proved to improve the control quality in the considered scenarios, in both cases it was shown that proper modifications of the controller enabled the further enhancement of the performance of the system. This notion unveils the high customizability of the discussed algorithm, allowing the designer to tailor the method to better suit specific practical problems.

3

PARAMETER IDENTIFYING ADRC

In the ultimate analysis, an adaptive system is merely a complex feedback system.

— K. Narendra, 1991 [203]

In this chapter, the studies of the problem of incorporating adaptive control schemes into the Active Disturbance Rejection framework are presented. To this end, a brief history of adaptive control is recalled and some standard solutions in this field are shortly presented. A survey of results presented in the literature is conducted and discussed. Then, a novel Parameter Identifying Extended State Observer and Parameter Identifying Disturbance Rejection Control algorithms are introduced. The underlying motivation and interpretation are given, and a detailed analytical study of their theoretical properties is conducted. Finally, the performance and applicability of the proposed methods are studied on the basis of simulations and experimental trials.

3.1 ADAPTIVE CONTROL

Adaptive control is intuitively defined as a class of methods that adjust their parameters on the basis of their observed performance [61]. Such a definition, based on the biological concept of the ability of organisms to adjust to changes in their environment, constitutes one of the earliest attempts to draw a clear distinction between adaptive control and other control approaches. Yet, as the idea of an algorithm which is able to respond to unpredicted changes in working conditions is indeed also a cornerstone of the entire field of automatic control, numerous other definitions have been proposed to better describe the essence of adaptive control. An exhausting review of the historically proposed terminologies has been presented in [76], where general notions on the adaptivity in a wide range of scientific problems were discussed. The early definitions by G. Sommerhof and W. Ashby [12, 272] emphasized that the adaptive system evolves toward a specific direction and this evolution is a dynamic process taking place over a period of time. Alternatively, R. Raible stressed in [245] that the operation of the adjustments of the adaptive system should be a result of conscious search for a suitable configuration of the controller. Such a definition collided with a common understanding of an adaptive system, as it excludes a wide class of contollers that incorporate certain

identification schemes. In contrast to this, in the paper [328] L. Zadeh extended the notion of adaptive control to almost all control schemes, by making a claim that any system ensuring a satisfying performance in certain scenarios is adaptive with respect to these scenarios. The ambiguity of the definitions of adaptive control has led J. Truxal to state that the general adaptive system is considered to be adaptive only by those, who are aware of the underlying assumed nominal structure of the plant. The designer unfamiliar with the original system perceives the same controller as merely sophisticated conventional algorithm. The adaptivity of the controller can thus be seen as a subjective matter depending only on the intentions of the designer [288]. Despite the lack of a conclusive definition of adaptive control, the field has attracted growing attention throughout the years. In Fig. 3.1 the number of papers published on the subject in the last decades is given.

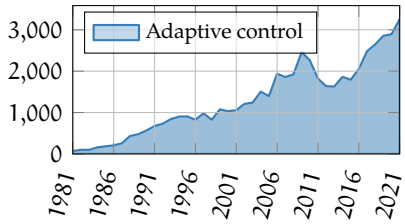

Own work based on [118]

Figure 3.1: Search results of the IEEE Xplore database for papers published each year on *adaptive control*. A temporary decrease of interest in early 2010s, followed by revival of the field, is visible

The difficulty in precisely defining the borders of the field of adaptive control strongly reflects the development of this approach in its early days. The beginnings of the adaptive control approach have been presented in [11, 277] where surveys of the earliest results in this area are given. Notably, as noticed by K. S. Narendra in [203], these first reviews contain also controllers which are no longer considered to be adaptive according to modern standards. Nonetheless, the roots of later solutions can be found in the algorithms recalled in these works. In the papers [203, 204] the later evolution of this field is presented, with the findings up to the 1990s being described. A similar record of the history of adaptive control is given in [120] and recently in [8]. Based on these, the most significant results are recalled here in brief.

The early 1950s can be seen as the beginning of modern adaptive control when the rising interest in the problems of design of autopilot algorithms for airplanes and spacecrafts sparked research on controllers able to adjust their properties to the changing environment. Due to the variations in the working conditions, the dynamics of the considered plants cannot be modeled in advance and some uncertainty

has to be inherently assumed during the synthesis of the controller. To illustrate this problem, consider a simple dynamic system given by

$$\dot{x} = u + \psi(t)\theta, \tag{3.1}$$

where $x \in \mathbb{R}$ is a state of the system, $u \in \mathbb{R}$ in an input variable, $\psi(t) \in \mathbb{R}^{1\times k}$ represent some known structure of the system, and term $\theta \in \mathbb{R}^k$ stands for unknown parameters of the system, possibly depending on the slowly changing working conditions. The general problem of the adaptive control is to ensure that x tracks a desired reference trajectory $x_r(t) \in \mathbb{R}$ despite the presence of unknown parameters θ. The major result of the 1950s was a proposition of the so-called MIT rule introduced in 1958 by a group of H. P. Whitaker in work [303]. The method attempt to identify the parameters of the system according to a simple gradient adaptation law in the form of

$$\frac{d}{dt}\hat{\theta} = -\gamma \frac{d}{d\hat{\theta}}\left(\tilde{x}^2\right), \tag{3.2}$$

where $\gamma \in \mathbb{R}_+$ is an positive adaptation gain, $\hat{\theta} \in \mathbb{R}^k$ is an estimate of unknown parameters θ, and $\tilde{x} = x_r - x \in \mathbb{R}$ is a tracking error achieved by employing a controller in which estimate $\hat{\theta}$ is directly used. As gradient $\frac{d}{d\hat{\theta}}\tilde{x}^2$ cannot be explicitly calculated if the real parameters θ are unknown, the MIT rule proposes to approximate the momentary value of this unknown gradient by some other measurable quantity [188].

The MIT rule belongs to the class of sensitivity methods, which employs the knowledge accumulated during system operation to calculate or estimate the gradient of some performance criterion and use it to appropriately adjust the values of parameter estimates. The sensitivity methods, together with the perturbance methods, for which the adaptation laws are based on the observation of the effects of some variations of the parameter estimates consciously introduced into the control loop, constituted one of the major direction of early research in the field of adaptive control. Within these approaches, two major methods ultimately arose – the Model Reference Adaptive Control (MRAC) and the Self Tuning Regulators (STR). The MRAC method, initially proposed by I. D. Landau in [152], defines the control problem as a task of forcing the considered system to track the output of some predefined reference model. Thus, the control law is proposed and the adaptation laws are defined to identify the set of parameters of the controller ensuring that the behavior of the system is consistent with the desired reference model. Alternatively, R. E. Kalman in [134] proposed the STR method, which employs the adaptive scheme as an extension of the conventional control law. The problem is thus

formed as one of the trajectory tracking or setpoint stabilization, and the adaptation law is formulated to identify the real dynamics of the system and on their basis update the parameters of the controller. The MRAC and STR approaches thus represent two distinct modes of adaptive control – the direct, or implicit, mode in which the adaptation law is employed to find the suitable values of the parameters of the controller, and the indirect, or explicit, mode in which the adaptive scheme is used to identify the dynamics of the controlled plant and the parameters of the controller are separately updated to suit the identified model. The conceptual schemes of the direct and indirect adaptive control modes are given in Fig. 3.2 and Fig. 3.3. Numerous

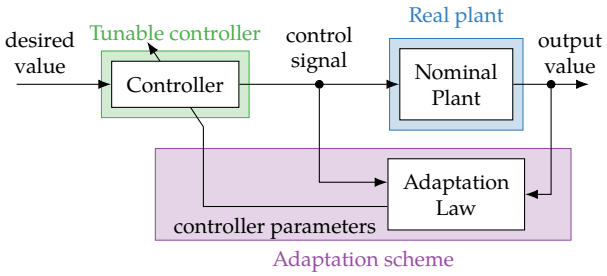

Figure 3.2: The simplified graphical illustration of the general direct adaptive control approach. The adaptation law directly adjusts the parameters of the controller.

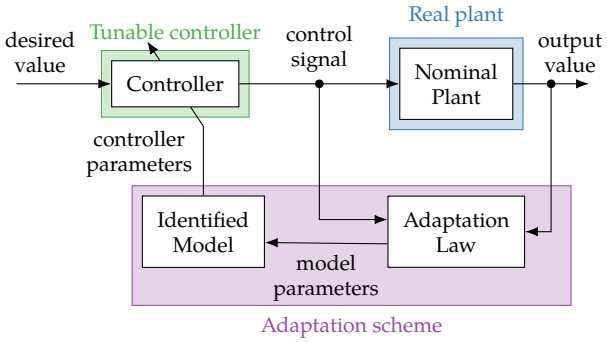

Figure 3.3: The simplified graphical illustration of the general indirect adaptive control approach. The adaptation law identifies the model of the plant used to tune the controller.

propositions of MRAC and STR methods working in both direct and indirect modes have been since proposed in the literature, leading to a blurring of the clean threshold between these two approaches.

The initially proposed adaptive schemes lacked proven stability conditions and attempts have been undertaken to analytically study the behavior of the adaptive systems. In the 1960s the strictly positive real (SPR) condition, as well as the persistency of the excitation (PE) condition, were formulated. The former, proposed by B. Shackloth and

R. L. Butchart in [257] and by P. Parks in [223], employs the properties of the passive systems to state that the adaptive scheme is stable if certain matrices describing the dynamics of the system are strictly positive real. The persistency of excitation condition, introduced by K. Åström and T. Bohlin in [16], tied the stability of the adaptive system and the ability to correctly estimate real parameters of the plant to the requirement that certain signals in the system are rich enough. Namely, the system in the form of (3.1) is said to be persistently excited, and thus the identification of its parameters is possible, if

$$\int_{t}^{t+T_{PE}} \boldsymbol{\psi}^{T}(\tau)\boldsymbol{\psi}(\tau)\,d\tau \geqslant \mu \mathbf{I}_{k} \tag{3.3}$$

for some constant positive values T_{PE} and μ and any time instant t. If regressor $\boldsymbol{\psi}(t)$ depends on the state of the plant then the PE condition can be ensured by the proper choice of the input signal. Yet, it has been soon found that even if these conditions are satisfied, the adaptive systems are prone to instability in the presence of unmodeled dynamics, excessive initial errors, or time-varying parameters of the plant. To cope with these phenomena various modifications of the adaptation laws were proposed in the late 1970s and 1980s. The use of a projection operator to confine the parameter estimates to some predefine set containing also the unknown values of the real parameters was proposed by B. Edgart in [62], as well as by G. Kreisselmeier and K. S. Narendra in [149]. While such an approach requires certain knowledge about the real parameters of the system, it effectively prevents the drift of the parameters in the presence of unmodeled disturbance. Alternatively, in [62] B. Edgart proposed also the use of conditional updating, nowadays known as the dead zone, which disables the adaptation law if the tracking error is sufficiently small. Thus the impact of small modeling uncertainties can be suppressed. The analysis of the stability of a system working in such a regime was presented in [253]. Another method was proposed by P. Ioannou and P. Kokotovic in [121] who incorporated a leakage term into the adaptation law to create the artificial drift of the parameters away from the regions of instability. Both leakage term and dead zone result in improved stability of the system at a cost of the inability to achieve the asymptotic convergence of the errors.

In the later years, the studies of the stability properties of the adaptive control scheme continued and led to the establishment of multiple new results. In the year 1986, in work [35] the persistency of excitation of linear systems was shown to be tied to the spectral measure of the control signal. Numerous attempts to weaken the PE condition have been presented in the literature, including the works defining relaxed conditions for certain classes of dynamic systems or types of

stability [174, 222] or proposing new adaptation algorithms capable of operating with milder persistency assumptions [142, 198, 248]. These methods are commonly designed to take advantage of the presence of persistent excitation only in some specified intervals during the operation of the system. Thanks to the acquisition of the data from the past time instants the convergence of the estimates can be guaranteed in these schemes even if the PE condition is not satisfied in the entire horizon of operation. Yet, such modifications are often sensitive to measurement noise and external disturbance affecting the plant in the moments of data acquisition. A better understanding of the properties of the adaptive controllers led also to more detailed investigations of different types of stability and the extension of these works to nonlinear systems. Specifically, the conditions for both exponential and uniform stability have been studied for nonlinear or linear time-varying adaptive systems with results presented in [86, 172, 173]. Throughout the most of development of adaptive control, the stability of such systems has been studied by employing a combination of converse Lyapunov theorems, conclusions drawn from Barbalăt lemma [19] and the SPR condition, as no unified approach to the design of the Lyapunov functions for adaptive systems have been found to prove the asymptotic convergence of both control and identification errors. A solution to this problem has been presented by the group of F. Mazenc in 2009 in the book [195] on the basis of their results from [194] published in 2003. Recently, this new approach has been used by a group of A. Loria in [171] and strict functions have been proposed to prove the exponential convergence of tracking and estimation errors in the MRAC scheme if the PE condition is satisfied.

Simultaneously to the works on the stability of the adaptive control schemes, the design of adaptive observers able to estimate the state of the system despite the presence of unknown parameters has been investigated. One of the first propositions of such an observer was formulated by R. Carroll and D. Lindorff in 1973 in the paper [38]. Thanks to the proper redefinition of the state matrix of the system and the introduction of additional virtual control signals into the observer design the problem of estimation of both state and unknown parameters of the plant has been solved. The subsequent propositions of adaptive observer algorithms presented in [176, 177] and [148] enhanced this initial design by overcoming the need for the inclusion of custom auxiliary input signals. While the initial study of adaptive observers has been focused on linear systems only, the later research extended their applicability to certain classes of nonlinear plants. In 1988 in work [22] G. Bastin and M. R. Gevers proposed the stable adaptive observer for nonlinear systems which can be represented in a specific observable form. The conditions for the existence of the trans-

formation into such an observable form have been then formulated by R. Marino in [190]. A different structure of the adaptive observer has been also given by the group of G. Besançon in [29] and the group of R. Ortega in [216]. In the work [189] the robustness of the observer to the unmodelled dynamics has been guaranteed by employing the parameter projection to confine them to some predefined set. Some attempts to formulate the unified theory of the adaptive observers for nonlinear systems have been presented in [28, 49].

Over half of a century of development of adaptive control methods resulted in the appearance of multiple approaches outside of the mainstream of this field. Among these, advances in the subjects of pattern recognition [304] and reinforcement learning [281] have been made. In recent years, a growing interest in the methods of adaptive control based on machine learning can be noticed [130, 131, 166]. While these problems are outside of the scope of interest of this dissertation and are not described here in more detail, some insights on the latest advances in these fields can be found in recent papers [26, 85]. In Fig. 3.4 the timeline of selected results in the mainstream development of the adaptive control methods is presented.

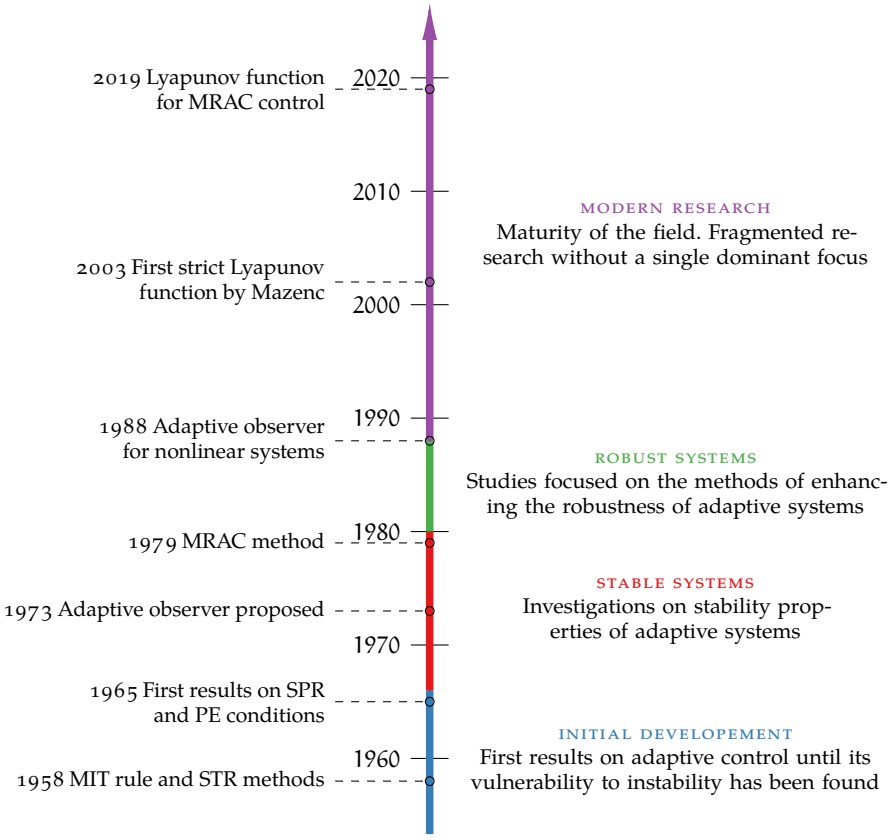

Figure 3.4: The timeline of adaptive control development. Research periods according to divisions presented in the literature.

In order to introduce the cornerstone ideas of adaptive control one can recall some standard algorithms as presented in numerous textbooks on the subject [15, 122, 150, 206, 255]. To this end, consider the dynamic system in the canonical controllable form given by

$$\dot{\mathbf{x}} = \left(\mathbf{A}_n + \mathbf{b}_n \boldsymbol{\theta}^T\right) \mathbf{x} + \mathbf{b}_n b u, \tag{3.4}$$

where $\mathbf{x} \in \mathbb{R}^n$ is a state of the system, $u \in \mathbb{R}$ is an input signal, $b \in \mathbb{R} \setminus \{0\}$ stand for the input gain and $\boldsymbol{\theta} \in \mathbb{R}^n$ is a vector of unknown parameters. Matrices $\mathbf{A}_n$ and $\mathbf{b}_n$ are as denoted in Section 1.5. Notably, such a system is consistent with hitherto discussed (2.21) with $\boldsymbol{\psi}(t, \mathbf{x}) = \mathbf{x}^T$. The standard MRAC algorithm can be employed to solve the problem of closed-loop control of plant (3.4). To simplify the analysis, assume that the general structure of the plant and the input gain b are known. The reference model can be defined as

$$\dot{\mathbf{q}} = \left(\mathbf{A}_n + \mathbf{b}_n \boldsymbol{\theta}_r^T\right) \mathbf{q} + \mathbf{b}_n b \nu, \tag{3.5}$$

where $\mathbf{q} = \begin{bmatrix} q_1 & \dots & q_n \end{bmatrix}^T \in \mathbb{R}^n$ stands for a state of the reference model and $\boldsymbol{\theta}_r \in \mathbb{R}^n$ is a vector of parameters chosen by the designer to guarantee the stability of the reference system and ensure its desired dynamics. Signal ν is some new control input of the reference system which can be chosen to satisfy the needs of the designer. Within the MRAC approach, the controller is designed in such a way, that the state of the nominal plant (3.4) asymptotically converges to the reference state (3.5). Thus, the control law is proposed in the form of

$$u = \boldsymbol{\phi} \mathbf{x} + \nu, \tag{3.6}$$

where $\boldsymbol{\phi} \in \mathbb{R}^{1 \times n}$ is a matrix of adjustable coefficients. Defining the tracking error as $\tilde{\mathbf{q}} = \mathbf{q} - \mathbf{x}$, the adaptation law is designed to ensure that $\tilde{\mathbf{q}}$ converges to the origin for any initial conditions of $\boldsymbol{\phi}$, and is given by

$$\dot{\boldsymbol{\phi}} = \boldsymbol{\Gamma} \mathbf{b}_n^T \mathbf{P} \tilde{\mathbf{q}} \mathbf{x}^T, \tag{3.7}$$

where $\boldsymbol{\Gamma} \in \mathbb{R}^{n \times n}$ is a positive definite matrix of adaptation gains and $\mathbf{P} \in \mathbb{R}^{n \times n}$ is a positive definite matrix satisfying the Lyapunov equation $\left(\mathbf{A}_n^T + \boldsymbol{\theta}_r \mathbf{b}_n^T\right)^T \mathbf{P} + \mathbf{P}\left(\mathbf{A}_n + \mathbf{b}_n \boldsymbol{\theta}_r^T\right) = -\mathbf{Q}$ with $\mathbf{Q} \in \mathbb{R}^{n \times n}$ being some arbitrarily chosen positive definite matrix. The adaptation law thus directly adjusts the parameter of the control law in the explicit adaptation scheme. Estimates $\hat{\boldsymbol{\theta}} \in \mathbb{R}^k$ of the true parameters of the

system can be obtained due to the notion, that in the steady state the nominal plant follows the reference system if

$$\left(\mathbf{A}_n + \mathbf{b}_n \theta^T\right) + \mathbf{b}_n b \boldsymbol{\phi} = \left(\mathbf{A}_n + \mathbf{b}_n \theta_r^T\right). \tag{3.8}$$

By substituting the unknown parameters with their estimated values it follows that the estimate $\hat{\theta} \in \mathbb{R}^n$ of the plant parameters is obtained as

$$\hat{\theta} = \theta_r - b\boldsymbol{\phi}, \tag{3.9}$$

what allows recovery of the parameter estimates from the adjustable elements of $\boldsymbol{\phi}$ and the parameters of the designed reference system. The graphical illustration of the MRAC approach as presented here is given in Fig. 3.5.

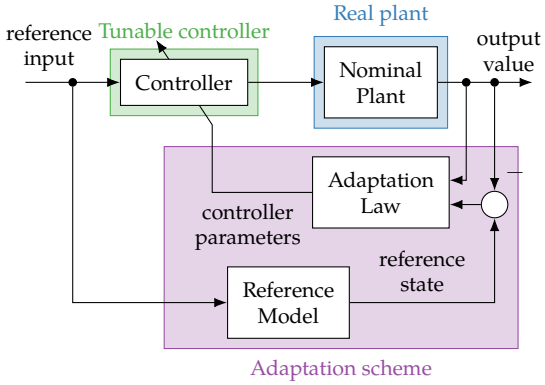

Figure 3.5: The graphical illustration of the MRAC adaptive control method.

Simulation 3.1. *The numerical simulation of the system working within the MRAC approach is conducted to illustrate the performance of the method. To this end, a third-order system ($n = 3$) is considered with $b = 1$. The unknown parameters of the plant are chosen as $\theta = \begin{bmatrix} -1 & 3 & 3 \end{bmatrix}^T$ and the reference model is designed with $\theta_r = \begin{bmatrix} -1 & -3 & -3 \end{bmatrix}^T$ which yields the stable state matrix of (3.5) with eigenvalues located at $\lambda = -1$. The reference input is designed as $v = -\theta_r^T \mathbf{x}_r + x_r^{(n)}$ with reference trajectory $\mathbf{x}_r(t)$ designed as in (2.34) with $x_r(t) = \sin(\frac{2\pi}{10}t) + \frac{1}{2}\sin(\frac{2\pi}{3}t)$. Such a choice of reference input guarantees that the state $\mathbf{q}$ of the reference model follows the desired reference trajectory. The MRAC algorithm is designed according to (3.6) and (3.7) with $\mathbf{Q} = \mathbf{I}_n$ and $\Gamma = 0.8\mathbf{I}_n$. The initial conditions are all set to zero. The results of the simulation are given in Fig. 3.6.*

The plots show that successful identification and control are achieved by the MRAC algorithm. The tracking errors converge to the origin and the estimated parameters evolve toward the values of their real counterparts. Notably, even though the initial value of $\hat{\theta}_1$ is chosen correctly due to the setting $\theta_{r1} = \theta_1$ and $\boldsymbol{\phi}(0) = \mathbf{0}_{1\times n}$, the estimate drifts

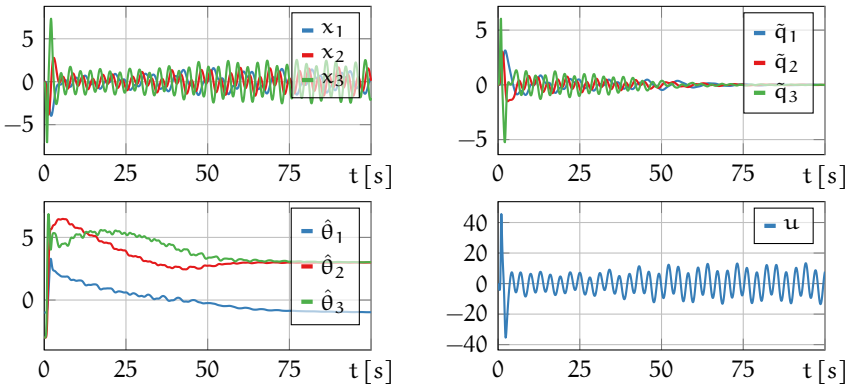

Figure 3.6: Time responses of the third order system under the MRAC controller.

away from this value in the first stage of the simulation. Nonetheless, in the limit the estimate returns to its starting value. The stability analysis of the MRAC method is presented in many textbooks on adaptive control with various approaches employed. The study using a strict Lyapunov function has been recently published in [171].

An alternative approach can be also embraced if only the task of parameter identification is considered. In such a situation a standard gradient algorithm, which is also a basis of the MIT rule, can be considered if the derivative of the state is available for measurement or can be otherwise obtained. Namely, consider the dynamics of the last state variable x_n of system (3.4) which are expressed by

$$\dot{x}_n = \mathbf{x}^T\theta + bu. \tag{3.10}$$

If the entire state of the plant is available, estimate q of $\dot{x}_n$ can be calculated as

$$q = \mathbf{x}^T\hat{\theta} + bu. \tag{3.11}$$

It is clear, that if the plant parameters are known and $\hat{\theta} = \theta$, then $\dot{x}_n = q$ at any time instant. Else, the estimation error $\tilde{q}$ can be defined as

$$\tilde{q} = \dot{x}_n - q = \mathbf{x}^T\left(\theta - \hat{\theta}\right). \tag{3.12}$$

By attempting to minimize the expression $\tilde{q}^2$ the following adaptation law can be proposed to adjust the values of the parameter estimates

$$\dot{\hat{\theta}} = -\frac{1}{2}\Gamma\frac{d}{d\hat{\theta}}\tilde{q}^2 = \Gamma\mathbf{x}\mathbf{x}^T\left(\theta - \hat{\theta}\right) = \Gamma\mathbf{x}\tilde{q} \tag{3.13}$$

in a manner similar to (3.7).

Simulation 3.2. *The third order plant with* $b = 1$ *and* $\theta = \begin{bmatrix} -1 & 3 & 3 \end{bmatrix}^T$ *is considered. A nonadaptive feedback controller is incorporated into the simulation to generate a control law that ensures that the state of the plant follows the reference trajectory* $\mathbf{x}_r(t)$ *as given in Sim. 3.1. The adaptation gain is chosen as* $\Gamma = 0.05\mathbf{I}_n$ *The simulation results of the employment of the presented gradient scheme are given in Fig. 3.7.*

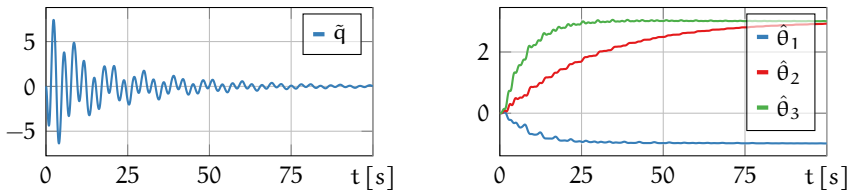

Figure 3.7: Time responses of the third order system under the gradient identification scheme.

The presented results show that the gradient method is capable of successful identification of the parameters of the plant if the derivatives of the state are available for measurement. Several methods enabling the application of the gradient adaptation if this condition is not satisfied have also been presented in the literature, e. g. [255]. Notably, the gradient identification based on the measurable derivative of the state displays a comparable convergence to the MRAC method despite the significantly lower adaptation gains employed.

Similarly to the MRAC method, numerous proofs of the stability of the gradient approach have been published in the literature. Lately, in paper [231] the author of this dissertation has presented a new study based on the Lyapunov approach and the results of the group of A. Loria presented in [171]. This analysis is recalled here as a basis for the investigations presented in the later parts of this work. To this end, consider first the following assumptions imposed on the evolution of the state of the plant.

Assumption 3.1. *Let the evolution of the plant be such, that*

$$\|\mathbf{x}(t)\| \leqslant x_M \tag{3.14}$$

for any time instant $t \in \mathbb{R}$ *and some positive constant* $x_M \in \mathbb{R}_+$.

Assumption 3.2. *Let the evolution of the plant be such, that*

$$\int_t^{t+T_{PE}} \mathbf{x}(\tau)\mathbf{x}^T(\tau)\,d\tau \geqslant \mu\mathbf{I}_n \tag{3.15}$$

for any time instant $t \in \mathbb{R}$ *and some positive constants* $\mu, T_{PE} \in \mathbb{R}_+$.

Assumption 3.2 is essential here and constitutes the necessary conditions for the successful identification of the parameters of the plant. It

requires system (3.10) to satisfy the persistency of excitation condition as formulated by (3.3). On the contrary, Assumption 3.1 is introduced due to the embraced analysis method and could be omitted if different approach is chosen. Consider also the following corollary formulated on the basis of [171, 194] that establishes some properties of the systems satisfying the assumptions given above.

Corollary 3.1. *If Assumptions 3.1 and 3.2 hold, then there exists matrix*

$$\mathbf{M}(t,\mathbf{x}) = \int_t^{\infty} e^{t-\tau}\mathbf{x}(\tau)\mathbf{x}^T(\tau)\,d\tau \in \mathbb{R}^{n\times n} \tag{3.16}$$

satisfying

$$\mu e^{-T_{PE}}\|\boldsymbol{\nu}\|^2 \leqslant \boldsymbol{\nu}^T\mathbf{M}\boldsymbol{\nu} \leqslant x_M^2\|\boldsymbol{\nu}\|^2 \tag{3.17}$$

for any vector $\boldsymbol{\nu} \in \mathbb{R}^n$*. The time derivative of matrix* $\mathbf{M}(t,\mathbf{x})$ *is given as*

$$\frac{d}{dt}\mathbf{M}(t,\mathbf{x}) = \mathbf{M}(t,\mathbf{x}) - \mathbf{x}(t)\mathbf{x}^T(t). \tag{3.18}$$

Corollary 3.1 states that if the system satisfies the PE condition then some persistently excited matrix can be defined in the form of an integral accumulating the temporary effects of the system excitation. Notably, due to the PE condition, this matrix is ensured to be positive definite. Moreover, if the state of the plant is bounded, this integral is also bounded for any time instant. By taking advantage of this notion, the following stability properties of the system can be concluded.

Lemma 3.1. *If Assumptions 3.1 and 3.2 hold, then the identification law* (3.13) *guarantees global exponential convergence of the parameter estimates* $\hat{\theta}$ *to the real parameters* θ *of plant* (3.10) *if the adaptation gains are chosen small enough.*

Proof. *Define the parameter identification error* $\tilde{\theta} = \theta - \hat{\theta}$ *and compute the error dynamics to obtain*

$$\dot{\tilde{\theta}} = -\Gamma\mathbf{x}\mathbf{x}^T\tilde{\theta}. \tag{3.19}$$

Recall Corollary 3.1 and consider a scalar function

$$V_{L3.1}(\tilde{\theta}) = \frac{1}{2}\tilde{\theta}^T\Gamma^{-1}\tilde{\theta} - \tilde{\theta}^T\mathbf{M}(t,\mathbf{x})\tilde{\theta}. \tag{3.20}$$

Under Assumptions 3.1 and 3.2 function $V_{L3.1}(\tilde{\theta})$ *satisfies*

$$V_{L3.1}(\tilde{\theta}) \geqslant \left(\frac{1}{2}\gamma_M^{-1} - x_M^2\right)\|\tilde{\theta}\|^2, \tag{3.21}$$

where $\gamma_M = \|\Gamma\| \in \mathbb{R}_+$. *Function* $V_{L3.1}(\tilde{\theta})$ *is thus positive for any choice of adaptation gains satisfying* $\gamma_M < \frac{1}{2}x_M^2$. *Calculating its time derivative yields*

$$\dot{V}_{L3.1} = -\tilde{\theta}^T \mathbf{x}\mathbf{x}^T\tilde{\theta} + 2\tilde{\theta}^T \mathbf{M}\Gamma\mathbf{x}\mathbf{x}^T\tilde{\theta} - \tilde{\theta}^T \mathbf{M}\tilde{\theta} + \tilde{\theta}^T \mathbf{x}\mathbf{x}^T\tilde{\theta} \tag{3.22}$$

with the arguments of $\mathbf{M}(t, \mathbf{x})$ *omitted for brevity. This is rewritten as*

$$\dot{V}_{L3.1} = \tilde{\theta}^T \left(2\mathbf{M}\Gamma\mathbf{x}\mathbf{x}^T - \mathbf{M}\right)\tilde{\theta}. \tag{3.23}$$

Thus, the following bound of $\dot{V}_{L3.1}$ *is established*

$$\dot{V}_{L3.1} \leqslant \left(2\gamma_M x_M^4 - \mu e^{-T_{PE}}\right)\|\tilde{\theta}\|^2. \tag{3.24}$$

Hence, $\dot{V}_{L3.1}(\tilde{\theta})$ *is negative definite if* $\gamma_M < \frac{1}{2}x_M^{-4}\mu e^{-T_{PE}}$. *Thus* $V_{L3.1}(\tilde{\theta})$ *is strictly positive definite with strictly negative definite derivative which proves a global exponential convergence of* $\tilde{\theta}$ *to the origin.*

While Lemma 3.1 is more restrictive than the theorems given in the literature (as some limitation on the choice of Γ is imposed, which is not necessary according to other theoretical results) and its proof closely follows the path of [171], according to the author's best knowledge, it has not been given in the literature in this form before [231] and is a cornerstone of the analysis conducted in further parts of this paper.

3.2 PARAMETER IDENTIFYING ESO

The methods of adaptive control aim to actively obtain some information on the uncertain dynamics of the plant and incorporate it into the control scheme, leading to improvement in the control quality. Similarly, the ADRC paradigm postulates the control input to be computed based on online estimation of the disturbance affecting the uncertain plant. Thus, a notion of a certain connection between the ADRC approach and adaptive control schemes arises intuitively. In the 2010s this idea gained the interest of the scientific community and sparked the research on methods of combining the merits of ADRC and adaptive schemes. Initially, these efforts have been focused on the methods of direct adaptation able to adjust the controller parameters on the basis of the performance of the closed-loop system. Apparently, one of the first results on this problem was published in 2009 in the work [56] by Q. Dong and Q. Li. The authors employed the fuzzy algorithm to online tune the nonlinear ADRC controller. Other results on this subject include [313] where the adaptive scheme is employed to increase the robustness of the ADRC method to the measurement

noise or [241] with tuning adaptation used to enhance the flexibility of the linear ADRC approach.

Possibly the first notion of employing the combination of the ADRC method and indirect adaptive scheme was made in 2009 by S. Li and Z. Liu in work [162] where an additional disturbance observer is incorporated into the control algorithm to online estimate the input gain of the plant. The method was verified by the experimental control of a permanent-magnet motor, but no analytical study of the stability of the system was given. In the work [325] the switching functions were used in an adaptation law for a specific case of adaptive control of DC motors. The authors proposed the use of a projection operator to ensure the boundedness of the parameter estimates in the presence of the peaking phenomenon. Recently, a similar method has been employed in [54] to solve the control task for electro-hydraulic servomechanisms. In both works, only the convergence of the tracking errors and parameter estimation errors to some boundary of the origin was proved. The use of extremum seeking optimization scheme has been presented in [185, 186] where it was used to seek for the value of input gain estimate minimizing a certain cost function. The algorithm was designed in the discrete domain and only an empirical evaluation of its performance was given. Importantly, in all of these methods, the identification and adaptation schemes have been designed on the basis of the tracking error and the disturbance estimate produced by the ESO has not been directly incorporated into the adaptation procedure. Possibly the first method employing the estimated disturbance in the adaptation scheme was proposed in 2012 by C. Huang and L. Guo in the paper [111]. The authors took advantage of the disturbance estimate in the gradient adaptation scheme, but the ESO itself was not adaptively adjusted and thus only a convergence to some boundary of the origin was established. Additionally, only the input gain of the plant was identified in the proposed solution, which was also a case in the recent [299], where the sign projection of the gradient of some cost function is used to extract the input gain estimate from the total disturbance estimated by the observer. The adaptation procedure was extended to a larger set of parameters in [126], but the structure of the ESO was still not adaptive and asymptotic convergence was not achieved. An alternative approach based on the least squares algorithm has been proposed in [175, 219] which also led to the boundedness of the tracking and identification errors only. In the recent work [183] the results concerning the design of the RESO algorithm as presented in [181, 275] and Section 2.4.2 have been extended and adaptation scheme has been incorporated to identify the frequency of the disturbance in the specific case of a system with harmonic disturbance.

The novel solution to the problem of adaptive control within the ADRC paradigm has been recently proposed by the author of this dissertation in [231] and [232]. In these papers, new Parameter Identifying Extended State Observer (PIESO) and Parameter Identifying Disturbance Rejection Control (PIDRC) methods were proposed to enable the identification of the parameters of the plant and incorporate them into the control scheme, respectively. The proposed approach is based on the notion, that if the nominal model of the plant is represented in a specific form, the total disturbance in the ADRC scheme can be perceived as a measure of the modeling error. Thus, the output of the disturbance observer can be used directly in the gradient adaptation law to online identify the parameters of the plant, which in turn leads to a decrease in the modeling error constituting the only disturbance affecting the plant. As the result, the amplitude of the total disturbance continuously decreases and the performance of the entire closed-loop system is improved. The asymptotic convergence of the tracking, estimation, and identification errors can then be proved under certain conditions and assumptions. The applicability of the methods in the practical scenarios was verified in [229, 230]. A detailed description and study of these methods are given in this and subsequent sections.

Consider first the problem of the state estimation and parameter identification of the dynamic system in the presence of parametric uncertainty of the dynamics of the plant. Specificaly, let the dynamic system in the following form be defined,

$$\begin{aligned} \dot{\mathbf{x}} &= \mathbf{A}_n \mathbf{x} + \mathbf{b}_n \left(b u + \boldsymbol{\psi}(t, \mathbf{x}) \boldsymbol{\theta} \right), \\ y &= \mathbf{c}_n^T \mathbf{x}, \end{aligned} \tag{3.25}$$

where $\mathbf{x} = \begin{bmatrix} x_1 & \dots & x_n \end{bmatrix}^T \in \mathbb{R}^n$ is a state of the plant, $b \in \mathbb{R}$ is an input gain, $u \in \mathbb{R}$ represents a control input, and $y \in \mathbb{R}$ stand for the output. The term $\boldsymbol{\psi}(t, \mathbf{x}) = \begin{bmatrix} \psi_1(t, \mathbf{x}) & \dots & \psi_k(t, \mathbf{x}) \end{bmatrix} \in \mathbb{R}^{1 \times k}$ stands for some dynamics of the plant with a known structure and $\boldsymbol{\theta} = \begin{bmatrix} \theta_1 & \dots & \theta_k \end{bmatrix}^T \in \mathbb{R}^k$ represents unknown constant parameters. Matrices $\mathbf{A}_n, \mathbf{b}_n$ and $\mathbf{c}_n$ are as given in Section 1.5.

Remark 3.1. *Notably, the input gain of the considered plant is defined as* $b \in \mathbb{R}$ *and thus* $b = 0$ *is a feasible choice of this parameter. If the real value of the input gain is unknown, parameter* b *may be assumed equal to zero and the actual input gain may be included in unknown vector* $\boldsymbol{\theta}$ *with control signal* u *incorporated into known regressor* $\boldsymbol{\psi}(t, \mathbf{x})$.

The following assumptions are made concerning the dynamics of the plant.

Assumption 3.3. *Let $\psi(t,x)$ be Lipschitz with respect to its second argument, i.e. let*

$$\|\psi(t,x_a)-\psi(t,x_b)\| \leqslant \psi_L \|x_a - x_b\| \tag{3.26}$$

for some constant $\psi_L \in \mathbb{R}_+$ and any $x_a, x_b \in \mathbb{R}^n$.

Assumption 3.4. *Let the system evolve in such a way that*

$$\max(\|\psi(t,x)\|, \left\|\frac{d}{dt}\psi(t,x)\right\|) \leqslant \psi_M \tag{3.27}$$

for some constant $\psi_M \in \mathbb{R}_+$ and any t.

Assumption 3.5. *Let the system evolve in such a way that regressor $\psi(t,x)$ satisfies*

$$\int_t^{t+T_{PE}} \psi^T(\tau,x(\tau))\psi(\tau,x(\tau))\,d\tau \geqslant \mu I_k \tag{3.28}$$

for some constants $\mu, T_{PE} \in \mathbb{R}_+$ and all $t \geqslant 0$.

Corollary 3.2. *If Assumptions 3.4 and 3.5 hold, then there exists matrix*

$$M(t,x) = \int_t^{\infty} e^{t-\tau}\psi^T(\tau,x(\tau))\psi(\tau,x(\tau))\,d\tau \in \mathbb{R}^{k\times k} \tag{3.29}$$

satisfying

$$\mu e^{-T_{PE}}\|\nu\|^2 \leqslant \nu^T M \nu \leqslant \psi_M^2 \|\nu\|^2 \tag{3.30}$$

for any vector $\nu \in \mathbb{R}^k$. The time derivative of matrix $M(t,x)$ is given as

$$\frac{d}{dt}M(t,x) = M(t,x) - \psi^T(t,x(t))\psi(t,x(t)). \tag{3.31}$$

The presented assumptions come from the combination of the properties of the ADRC and adaptive algorithms. Assumption 3.3 is reminiscent of Assumption 2.1 and requires the regressor of the plant to change slowly enough. This feature ensures that some bound on the system dynamics can be imposed in the presence of the transient estimation errors. Assumptions 3.4 and 3.5 are the generalizations of Assumption 3.1 and 3.2 as used in the analysis of the gradient method identification. Similarly, Corollary 3.2 generalizes the notions of Corollary 3.1 and introduces the definition of the persistently excited matrix for the general linearly parametrized system. Notably, while these assumptions impose some restrictions on the evolution of the state of the plant, they can be easily verified and satisfied by a proper design of the experiment, as only the tasks of identification and estimation, and not of control, are considered here. To facilitate the design of the

proposed PIESO observer two distinct cases are considered. Namely, the separate scenarios of a plant with the regressor dependent on time only, and thus denoted as $\psi(t)$, and of the system with regressor given by $\psi(t, x)$ and explicitly depending on both time and momentary state of the plant, are discussed in detail.

3.2.1 *State independent regressor*

Consider a simplified version of the nominal system (3.25) given by

$$\dot{x} = A_n x + b_n \left(bu + \psi(t)\theta\right) \tag{3.32}$$

with regressor $\psi(t) = \begin{bmatrix} \psi_1(t) & \dots & \psi_k(t) \end{bmatrix} \in \mathbb{R}^{1\times k}$ being a function of time only. Such a definition of the system implies that the exact value of $\psi(t)$ is known at any time instant and can be explicitly used in the design of the controller and identification procedure. In order to estimate the state and the parameters of the system, the following extended dynamics are considered

$$\begin{aligned} \dot{x} &= A_n x + b_n \left(bu + \psi(t)\hat{\theta} + \delta\right), \\ \dot{\delta} &= \frac{d}{dt}\left(\psi(t)\left(\theta - \hat{\theta}\right)\right), \end{aligned} \tag{3.33}$$

where $\hat{\theta} = \begin{bmatrix} \hat{\theta}_1 & \dots & \hat{\theta}_k \end{bmatrix}^T \in \mathbb{R}^k$ stands for some estimate of parameters θ, and $\delta = \psi(t)\left(\theta - \hat{\theta}\right) \in \mathbb{R}$ is the total disturbance corresponding to the modeling error due to the imperfect parameter estimation. Clearly, if $\hat{\theta} = \theta$, then $\delta = 0$ for any time instant. On the contrary, if the value of θ is not known, then δ directly corresponds to the modeling error which can serve as a basis of the adaptation law reminiscent of (3.12). Model (3.33) can be used to synthesize the adaptive PIESO algorithm. By introducing the extended state in the form of $z = \begin{bmatrix} x^T & \delta \end{bmatrix}^T = \begin{bmatrix} z_1 & \dots & z_m \end{bmatrix}^T \in \mathbb{R}^m$ with $m = n + 1$, dynamics (3.33) are expressed as

$$\dot{z} = A_m z + d_m \left(bu + \psi(t)\hat{\theta}\right) + b_m \frac{d}{dt}\left(\psi(t)\left(\theta - \hat{\theta}\right)\right). \tag{3.34}$$

For the system formulated in such a way, the PIESO is proposed as

$$\dot{\hat{z}} = A_m \hat{z} + d_m \left(bu + \psi(t)\hat{\theta}\right) + l\left(z_1 - \hat{z}_1\right) \tag{3.35}$$

with the parameter adaptation law given by

$$\dot{\hat{\theta}} = \Gamma \psi^T(t)\hat{z}_m, \tag{3.36}$$

where $\hat{z} = \begin{bmatrix} \hat{z}_1 & \dots & \hat{z}_m \end{bmatrix}^T \in \mathbb{R}^m$ is the extended state estimate, $l = \begin{bmatrix} l_1 & \dots l_m \end{bmatrix} \in \mathbb{R}^m_+$ are positive observer gains chosen to ensure the stability of the observer and $\Gamma \in \mathbb{R}^{k\times k}$ is a positive definite matrix of adaptation gains. The detailed scheme of the considered system and algorithm is given in Fig. 3.8.

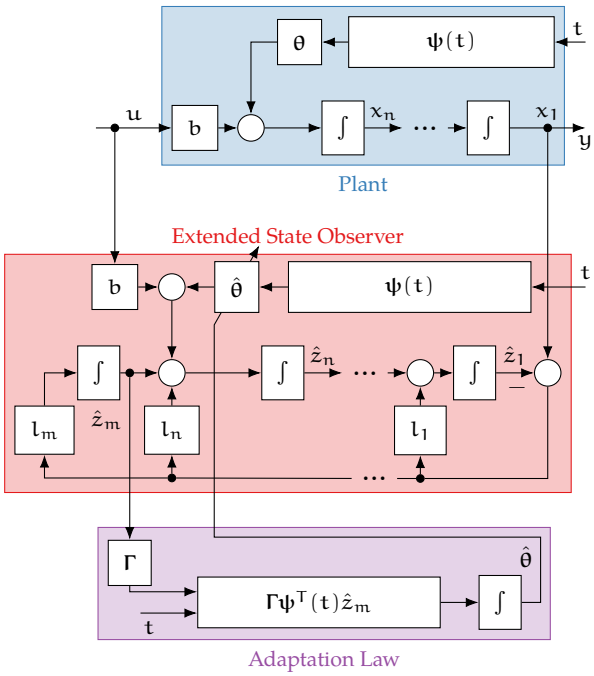

Figure 3.8: The detailed graphical illustration of the considered PIESO observer with regressor independent of state. The adaptation law extending the conventional ESO is visible.

Denote the estimation and identification errors in the forms of $\tilde{z} = z - \hat{z}$ and $\tilde{\theta} = \theta - \hat{\theta}$. Applying the proposed PIESO observer given by (3.35) and (3.36) to the considered dynamic plant expressed by (3.34) yields the error dynamics

$$\begin{aligned} \dot{\tilde{z}} &= H\tilde{z} + b_m\dot{\psi}(t)\tilde{\theta} + b_m\psi(t)\Gamma\left(\psi^T(t)b_m^T\tilde{z} - \psi^T(t)\psi(t)\tilde{\theta}\right), \\ \dot{\tilde{\theta}} &= -\Gamma\psi^T(t)\psi(t)\tilde{\theta} + \Gamma\psi^T(t)b_m^T\tilde{z}, \end{aligned} \tag{3.37}$$

where $H = A_m - lc_m^T$ with c_m as defined in Section 1.5. To facilitate further analysis, consider the tuning parameters of the PIESO observer chosen according to the bandwidth parametrization presented in Section 2.1. Namely, let l gains be taken as

$$l_i = \bar{l}_i\omega_o^i, \quad i \in \{1, m\}, \tag{3.38}$$

where $\omega_o \in \mathbb{R}_+$ is a new positive tuning parameter. Define also scaled estimation errors $\bar{z}$ as in Section 2.2 by denoting

$$\bar{z}_i = \omega_o^{m-i}\tilde{z}_i, \quad i \in \{1, m\}. \tag{3.39}$$

Equivalently, these scalings can be expressed as

$$\mathbf{l} = \omega_o^m \mathbf{\Phi}_o^{-1}\bar{\mathbf{l}}, \quad \bar{z} = \mathbf{\Phi}_o \tilde{z}, \tag{3.40}$$

with $\mathbf{\Phi}_o = \operatorname{diag}(\omega_o^{m-1}, \omega_o^{m-2}, \dots, 1) \in \mathbb{R}^{m\times m}$ being a scaling operator dependent on the chosen bandwidth ω_o. Employing these scaled errors yields the closed-loop system dynamics of the form

$$\begin{aligned}
\dot{\bar{z}} &= \omega_o \bar{\mathbf{H}}\bar{z} + \mathbf{b}_m \dot{\boldsymbol{\psi}}(t)\tilde{\theta} + \mathbf{b}_m \boldsymbol{\psi}(t)\mathbf{\Gamma}\left(\boldsymbol{\psi}^\top(t)\mathbf{b}_m^\top \bar{z} - \boldsymbol{\psi}^\top(t)\boldsymbol{\psi}(t)\tilde{\theta}\right), \\
\dot{\tilde{\theta}} &= -\mathbf{\Gamma}\boldsymbol{\psi}^\top(t)\boldsymbol{\psi}(t)\tilde{\theta} + \mathbf{\Gamma}\boldsymbol{\psi}^\top(t)\mathbf{b}_m^\top \bar{z}
\end{aligned} \tag{3.41}$$

with $\bar{\mathbf{H}} = \mathbf{A}_m - \bar{\mathbf{l}}\mathbf{c}_m^\top$ and explicitly given by

$$\bar{\mathbf{H}} = \begin{bmatrix} -\bar{l}_1 & 1 & 0 & \cdots & 0 \\ -\bar{l}_2 & 0 & 1 & \ddots & 0 \\ \vdots & \vdots & \ddots & \ddots & \vdots \\ -\bar{l}_n & 0 & 0 & \ddots & 1 \\ -\bar{l}_m & 0 & 0 & \cdots & 0 \end{bmatrix}. \tag{3.42}$$

The following assumption is made concerning the choice of tuning parameters of the observer.

Assumption 3.6. *Let the scaled observer gains $\bar{\mathbf{l}}$ be chosen such that matrix $\bar{\mathbf{H}}$ is Hurwitz.*

The satisfaction of Assumption 3.6 implies that there exists a positive definite matrix $\mathbf{P} \in \mathbb{R}^{m\times m}$ such that $\bar{\mathbf{H}}^\top\mathbf{P} + \mathbf{P}\bar{\mathbf{H}} = -\mathbf{I}_m$. The properties of the proposed PIESO observer are summarized by the following theorem.

Theorem 3.1. *For system* (3.32) *satisfying Assumptions 3.3, 3.4 and 3.5, observer* (3.35) *with adaptation law* (3.36) *guarantees a global exponential convergence of errors $\tilde{z}$ and $\tilde{\theta}$ to the origin under the tuning proposed by Assumption 3.6 for ω_o chosen high enough and $\mathbf{\Gamma}$ chosen with a norm small enough.*

Proof. *Recalling Assumptions 3.4 and 3.5 with Corollary 3.2, the following function can be considered for the system with the time-dependent regressor*

$$V_{3.1}(\bar{z}, \tilde{\theta}) = \frac{1}{2}\bar{z}^\top\mathbf{P}\bar{z} + \tilde{\theta}^\top\left(\frac{1}{2}\mathbf{\Gamma}^{-1} - \mathbf{M}(t)\right)\tilde{\theta}. \tag{3.43}$$

Clearly, function $V_{3.1}(\bar{z}, \tilde{\theta})$ *satisfies*

$$V_{3.1}(\bar{z}, \tilde{\theta}) \geqslant \frac{1}{2} p_m \|\bar{z}\|^2 + \left(\frac{1}{2}\gamma_M^{-1} - \psi_M^2\right) \|\tilde{\theta}\|^2 \tag{3.44}$$

with $p_m = \lambda_{\min}(\mathbf{P}) \in \mathbb{R}_+$ *where* $\lambda_{\min}(\cdot)$ *stand for the smallest eigenvalue of a matrix. Function* $V_{3.1}(\bar{z}, \tilde{\theta})$ *is thus positive for any choice of* $\mathbf{\Gamma}$ *satisfying* $\gamma_M < \frac{1}{2}\psi_M^{-2}$. *The time derivative of* $V_{3.1}(\bar{z}, \tilde{\theta})$ *is given by*

$$\begin{aligned}\dot{V}_{3.1} = \bar{z}^T \left(\mathbf{P}\mathbf{b}_m\boldsymbol{\psi}\mathbf{\Gamma}\boldsymbol{\psi}^T\mathbf{b}_m^T - \frac{1}{2}\omega_o\right)\bar{z} + \tilde{\theta}^T\left(2\mathbf{M}\mathbf{\Gamma}\boldsymbol{\psi}^T\boldsymbol{\psi} - \mathbf{M}\right)\tilde{\theta} \\ + \bar{z}\left(\mathbf{P}\mathbf{b}_m\dot{\boldsymbol{\psi}} - \mathbf{P}\mathbf{b}_m\boldsymbol{\psi}\mathbf{\Gamma}\boldsymbol{\psi}^T\boldsymbol{\psi} + \mathbf{b}_m\boldsymbol{\psi} - 2\mathbf{b}_m\boldsymbol{\psi}\mathbf{\Gamma}\mathbf{M}\right)\tilde{\theta}\end{aligned} \tag{3.45}$$

with arguments of $\boldsymbol{\psi}(t)$ *and* $\mathbf{M}(t)$ *omitted for brevity. By taking advantage of the Young's inequality, it is concluded that the following is satisfied,*

$$\begin{aligned}\dot{V}_{3.1} \leqslant \frac{1}{2}\Bigg(-\omega_o + 2p_M\psi_M^2\gamma_M + \frac{1}{\varepsilon}\Big(p_M\psi_M + \psi_M + \gamma_M p_M\psi_M^3 \\ + 2\gamma_M\psi_M^3\Big)^2\Bigg)\|\bar{z}\|^2 + \left(\frac{\varepsilon}{2} + 2\psi_M^4\gamma_M - \mu e^{-T_{PE}}\right)\|\tilde{\theta}\|^2\end{aligned} \tag{3.46}$$

for any $\varepsilon \in \mathbb{R}_+$ *with* $p_M = \|\mathbf{P}\| \in \mathbb{R}_+$. *By choosing* $\mathbf{\Gamma}$ *such that* $\gamma_M < \frac{1}{2}\psi_M^{-4}\mu e^{-T_{PE}}$ *and setting* $\varepsilon > \frac{1}{2}\left(\mu e^{-T_{PE}} - 2\psi_M^4\gamma_M\right)^{-1}$ *the negativity of the second term is guaranteed. Negative definiteness of entire* $\dot{V}_{3.1}(\bar{z}, \tilde{\theta})$ *is then ensured by choosing* ω_o *high enough.*

While Theorem 3.1 states that to ensure the stability of the system the adaptation gains $\mathbf{\Gamma}$ have to be chosen smaller than some specific threshold value dependent on the dynamics of $\boldsymbol{\psi}(t)$, this proof closely follows that of Lemma 3.1 which is known to be overly conservative. Thus, it seems justified to believe that this limitation on $\mathbf{\Gamma}$ may be alleviated with a better-suited proof. If this is the case, it could be expected that only a requirement concerning the value of ω_o would be formulated depending on the characteristics of $\dot{\boldsymbol{\psi}}(t)$. The evaluation of the performance and applicability of the proposed scheme is done in a numerical simulation.

Simulation 3.3. *Consider a third-order plant with dynamics as given by* (3.32) *with* $n = 3$, $b = 1$, $\boldsymbol{\psi} = \begin{bmatrix}\cos(3t) & \sin^3(t) & 1\end{bmatrix}$ *and* $\theta = \begin{bmatrix}-1 & 3 & 3\end{bmatrix}^T$. *The adaptive PIESO observer is designed according to* (3.35) *and* (3.36) *with* $\mathbf{\Gamma} = 0.2\mathbf{I}_3$ *and* $\omega_o = 100$. *Similarily to Sim. 3.7, the control signal is generated using an additional nonadaptive controller. Notably, in the case of a system with a regressor independent of the state, the choice of control signal does not impact the process of parameter identification. Zero*

initial conditions are chosen for the state, estimates, and identified parameters. The results of the simulation are given in Fig. 3.9.

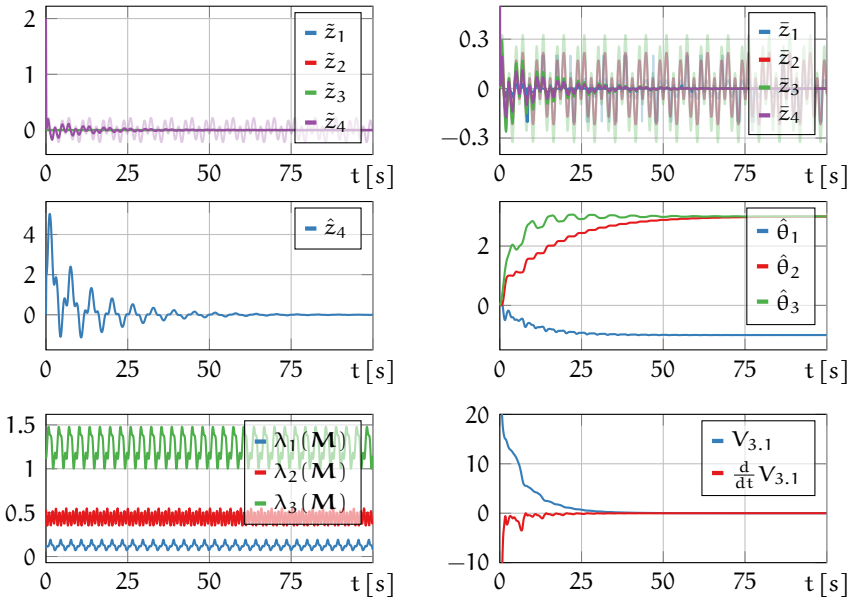

Figure 3.9: Time responses of the third order system with time-dependent regressor under the proposed PIESO observer. Results of conventional ESO with $\Gamma = 0_3$ shown in transparent plots of $\tilde{z}$ and $\bar{z}$.

The conducted trial shows the effectiveness of the proposed approach in the task of state estimation and parameter identification. The parameter estimates converge to the correct values which reduces the total disturbance to zero asyptotically. The resultant asymptotic convergence of the state estimation errors, not achievable in the case of the standard ESO algorithm, is shown. Moreover, the eigenvalues of $\mathbf{M}(t)$ and evolution of function $V_{3.1}(\tilde{z}, \tilde{\theta})$ with its derivative are also given to support the earlier theoretical analysis. It is confirmed that function $V_{3.1}(\tilde{z}, \tilde{\theta})$ satisfies the conditions of the Lyapunov approach in the considered scenario and the properties of $\mathbf{M}(t)$ are consistent with the expected characteristics.

Simulation 3.4. *Consider the settings as in Sim. 3.3. In Fig. 3.10 the results of simulation with different values of Γ are given for comparison.*

The change in the parameter identification speed due to differently chosen adaptation gain is visible. Notably, the relation between the value of adaptation gain and the convergence rate is not a straightforward one, and an increase in the adaptation gain does not always lead to improvement in the identification performance. As discussed in [205], this is a general property of the adaptation schemes with parameter adaptation law in the form reminiscent of (3.19), which is also a case in the PIESO approach. Thus, there exists some Γ with a finite norm guaranteeing the highest convergence speed [217].

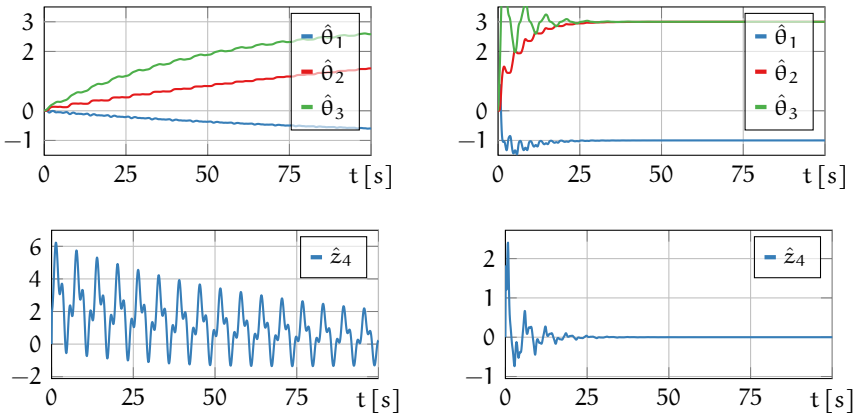

(a) $\Gamma = 0.02\mathbf{I}_3$ (b) $\Gamma = 2\mathbf{I}_3$

Figure 3.10: Time responses of the third order system with time-dependent regressor under the proposed PIESO observer with different adaptation gains.

3.2.2 *State dependent regressor*

The algorithm proposed in Section 3.2.1 offers a simple and intuitive solution to the problem of simultaneous estimation of the state and parameters of the system. Yet, its applicability is limited only to the systems with exactly known regressor which can be evaluated without taking into account the state of the plant. despite lack of measurability of the state of the plant. Such systems are rarely featured in the practical considerations, as the majority of real-life applications are characterized by functions explicitly dependent on the state of the plant. To overcome this limitation, an enhanced algorithm is formulated for a wider class of dynamic systems. To this end, consider once again the system given by (3.25) with regressor explicitly depending on both time and the state of the plant, and expressed by

$$\dot{\mathbf{x}} = \mathbf{A}_n\mathbf{x} + \mathbf{b}_n\left(bu + \boldsymbol{\psi}(t,\mathbf{x})\boldsymbol{\theta}\right). \tag{3.47}$$

Note that (3.47) becomes a standard linear time-invariant system commonly considered in the literature on parameter identification and discussed in Section 3.1 if $\boldsymbol{\psi}(t,\mathbf{x}) = \mathbf{x}^T$. Thus, the proposed observer can be applied to the LTI system if its state $\mathbf{x}$ remains bounded during the evolution to ensure that Assumption 3.4 holds. By denoting the extended state $\boldsymbol{z} = \begin{bmatrix}\mathbf{x}^T & \delta\end{bmatrix}^T \in \mathbb{R}^m$, the dynamics of the system are expressed as

$$\begin{aligned}\dot{\mathbf{x}} &= \mathbf{A}_n\mathbf{x} + \mathbf{b}_n\left(bu + \boldsymbol{\psi}(t,\mathbf{x})\hat{\boldsymbol{\theta}} + \delta\right),\\ \dot{\delta} &= \frac{d}{dt}\left(\boldsymbol{\psi}(t,\mathbf{x})\left(\boldsymbol{\theta} - \hat{\boldsymbol{\theta}}\right)\right),\end{aligned} \tag{3.48}$$

where $\hat{\theta} \in \mathbb{R}^k$ denotes some estimate of the unknown parameters and $\delta = \psi(t, x)\left(\theta - \hat{\theta}\right) \in \mathbb{R}$ is a total disturbance corresponding to the modeling error. Note, that the total disturbance is here defined using plant state x, which is in general unknown and unavailable for measurement. The dynamics of the extended state are given by

$$\begin{aligned} \dot{z} = {} & A_m z + d_m \left(bu + \psi(t, \Lambda_n z)\hat{\theta} \right) \\ & + b_m \frac{d}{dt} \left(\psi(t, \Lambda_n z) \left(\theta - \hat{\theta} \right) \right), \end{aligned} \tag{3.49}$$

where $\Lambda_n z = x$ as defined in Section 1.5. The adaptive PIESO for such a system is proposed as

$$\dot{\hat{z}} = A_m \hat{z} + d_m \left(bu + \psi(t, \Lambda_n \hat{z})\hat{\theta} \right) + l\left(z_1 - \hat{z}_1\right), \tag{3.50}$$

which does not require knowledge of state x to evaluate the momentary value of the regressor. The parameter adaptation law is formulated as

$$\dot{\hat{\theta}} = \mathrm{Proj}(\tau, \hat{\theta}, \Theta), \quad \tau = \Gamma \psi^T(t, \Lambda_n \hat{z}) \hat{z}_m, \tag{3.51}$$

where $\tau \in \mathbb{R}^k$ is an internal adaptation law. The term $\mathrm{Proj}(\tau, \hat{\theta}, \Theta)$ stands for a projection operator [150, 154, 325] which satisfies

$$\tilde{\theta}^T \Gamma^{-1} \left(\mathrm{Proj}(\tau, \hat{\theta}, \Theta) - \tau \right) \geqslant 0 \tag{3.52}$$

and $\hat{\theta} \in \Theta$, with Θ being some predefined convex set chosen to contain the real values of θ. Throughout the rest of this dissertation, the second and third arguments of $\mathrm{Proj}(\tau, \hat{\theta}, \Theta)$ will be omitted for brevity.

Remark 3.2. *Numerous propositions of* $\mathrm{Proj}(\tau, \hat{\theta}, \Theta)$ *operator are given in literature [323], with one of the most common choices being elementwise operator defined as*

$$\mathrm{Proj}_i(\tau, \hat{\theta}, \Theta) = \begin{cases} 0 & \tau_i > 0 \wedge \hat{\theta}_i \geqslant \vartheta_i, \\ 0 & \tau_i < 0 \wedge \hat{\theta}_i \leqslant -\vartheta_i, \\ \tau_i & \textit{otherwise} \end{cases} \tag{3.53}$$

with a convex set defined as $\Theta = \{\theta : \theta_i \in (-\vartheta_i, \vartheta_i), i = 1, \ldots, k\}$, $\vartheta_i \in \mathbb{R}_+$ *for* $i \in \{1, \ldots, k\}$ *being some positive constants and adaptation gains chosen as* $\Gamma = \mathrm{diag}(\gamma_1, \ldots, \gamma_k)$. *Yet, the analysis presented further does not assume any specific choice of* $\mathrm{Proj}(\tau, \hat{\theta}, \Theta)$ *operator.*

Corollary 3.3. *It follows from* (3.52) *and the definition of the projection operator, that there exists a constant* $\theta_M \in \mathbb{R}_+$ *such that*

$$\max(\left\|\theta - \hat{\theta}\right\|, \left\|\hat{\theta}\right\|) \leqslant \theta_M \tag{3.54}$$

for any t. *Thus, it also holds that* $\left\|\theta - \hat{\theta}\right\|^2 \leqslant \left\|\theta - \hat{\theta}\right\|\theta_M$. *Moreover,* $\left\|\mathrm{Proj}(\boldsymbol{\tau}, \hat{\theta}, \boldsymbol{\Theta})\right\| \leqslant \left\|\boldsymbol{\tau}\right\|$ *for any* $\boldsymbol{\tau}$.

Remark 3.3. *Note that bound* θ_M *imposed on the identification error* $\left\|\theta - \hat{\theta}\right\|$ *according to Corollary 3.3 holds even if* $\hat{\theta}(0) \notin \boldsymbol{\Theta}$. *In such a case, bound* θ_M *does not come directly from the definition of set* $\boldsymbol{\Theta}$ *but accomodates also the initial errors of the elements of* $\hat{\theta}$ *outside of the set* $\boldsymbol{\Theta}$ *which are not allowed to grow larger due to the action of the projection operator. Thus, the estimation error remains bounded and further analysis holds in full.*

The incorporation of the projection operator in the proposed scheme is crucial, due to the possible impact of the transient state estimation errors on the dynamics of the parameter estimates. Thus, it is used to disable the adaptation if the temporary estimation errors cause the drift of the parameter estimates. Once the quality of the regressor evaluation is recovered in the steady state, the adaptation is restarted and proper operation of the algorithm is allowed to proceed. The graphical scheme of the proposed algorithm in the case of a system with regressor being a function of the state of the plant is given in Fig. 3.11.

In order to investigate the stability and performance of the considered scheme define the estimation and identification errors $\tilde{z} = z - \hat{z}$, $\tilde{\theta} = \theta - \hat{\theta}$ with the dynamics expressed as

$$\begin{aligned}
\dot{\tilde{z}} &= \mathbf{H}\tilde{z} + \mathbf{d}_m \left(\boldsymbol{\psi}(t, \boldsymbol{\Lambda}_n z) - \boldsymbol{\psi}(t, \boldsymbol{\Lambda}_n \hat{z})\right) \hat{\theta} + \mathbf{b}_m \dot{\boldsymbol{\psi}}(t, \boldsymbol{\Lambda}_n z)\tilde{\theta} \\
&\quad - \mathbf{b}_m \boldsymbol{\psi}(t, \boldsymbol{\Lambda}_n z)\, \mathrm{Proj}(\boldsymbol{\tau}), \\
\dot{\tilde{\theta}} &= -\mathrm{Proj}(\boldsymbol{\tau}), \\
\boldsymbol{\tau} &= \boldsymbol{\Gamma}\Big(\left(\boldsymbol{\psi}^T(t, \boldsymbol{\Lambda}_n \hat{z}) - \boldsymbol{\psi}^T(t, \boldsymbol{\Lambda}_n z)\right) \\
&\quad + \boldsymbol{\psi}^T(t, \boldsymbol{\Lambda}_n z)\Big) \left(\boldsymbol{\psi}(t, \boldsymbol{\Lambda}_n z)\tilde{\theta} - \tilde{z}_m\right),
\end{aligned} \tag{3.55}$$

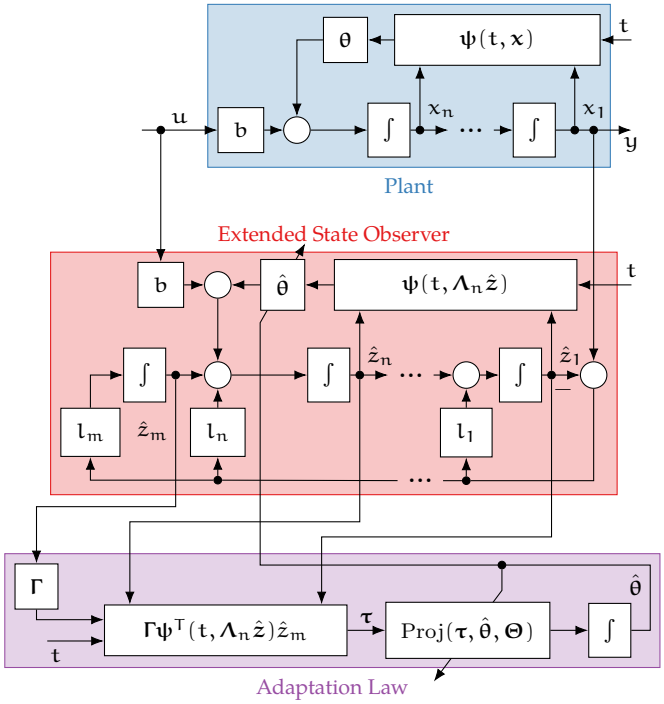

Figure 3.11: The detailed graphical illustration of the considered PIESO observer with regressor dependent on the state. The adaptation law with the projection operator is visible.

where $\mathbf{H} = \mathbf{A}_m - \mathbf{l}\mathbf{c}^T$. Recalling the scaled observer gains $\bar{\mathbf{l}}$, such that $\mathbf{l} = \omega_o^m \mathbf{\Phi}_o^{-1} \bar{\mathbf{l}}$, and the scaled estimation errors $\bar{\mathbf{z}} = \mathbf{\Phi}_o \tilde{\mathbf{z}}$, the dynamics of the closed-loop system take the form of

$$\begin{aligned}
\dot{\bar{\mathbf{z}}} &= \omega_o \bar{\mathbf{H}} \bar{\mathbf{z}} + \omega_o \mathbf{d}_m \left(\boldsymbol{\psi}(t, \mathbf{\Lambda}_n \mathbf{z}) - \boldsymbol{\psi}(t, \mathbf{\Lambda}_n \hat{\mathbf{z}}) \right) \hat{\theta} \\
&\quad + \mathbf{b}_m \dot{\boldsymbol{\psi}}(t, \mathbf{\Lambda}_n \mathbf{z}) \tilde{\theta} - \mathbf{b}_m \boldsymbol{\psi}(t, \mathbf{\Lambda}_n \mathbf{z}) \operatorname{Proj}(\boldsymbol{\tau}), \\
\dot{\tilde{\theta}} &= -\operatorname{Proj}(\boldsymbol{\tau}), \\
\boldsymbol{\tau} &= \mathbf{\Gamma} \Bigg(\left(\boldsymbol{\psi}^T(t, \mathbf{\Lambda}_n \hat{\mathbf{z}}) - \boldsymbol{\psi}^T(t, \mathbf{\Lambda}_n \mathbf{z}) \right) \\
&\quad + \boldsymbol{\psi}^T(t, \mathbf{\Lambda}_n \mathbf{z}) \Bigg) \left(\boldsymbol{\psi}(t, \mathbf{\Lambda}_n \mathbf{z}) \tilde{\theta} - \bar{z}_m \right),
\end{aligned} \tag{3.56}$$

with $\bar{\mathbf{H}} = \mathbf{A}_m - \bar{\mathbf{l}}\mathbf{c}^T$. By taking advantage of Assumption 3.6, the properties of the PIESO observer designed for the plant with regressor being a function of time and state are summarized by the following theorem.

Theorem 3.2. *For system* (3.47) *satisfying Assumptions 3.3, 3.4 and 3.5, observer* (3.50) *with adaptation law* (3.51) *guarantees a global asymptotic convergence of errors* $\tilde{\mathbf{z}}$ *and* $\tilde{\theta}$ *to the origin under the tuning proposed by Assumption 3.6 for* ω_o *chosen high enough and* $\mathbf{\Gamma}$ *chosen with a norm small enough.*

Proof. *The stability of the analysis of the proposed method is conducted in two distinct steps. First, under the notion of the boundedness of identification errors guaranteed by the projection operator, the boundedness of state estimates is established. Next, this notion is used to conclude an asymptotic convergence of both identification and estimation errors to the origin. Consider the auxiliary function* $V_{3.2}^*(\bar{z})$ *given by*

$$V_{3.2}^*(\bar{z}) = \frac{1}{2}\bar{z}^\top \mathbf{P}\bar{z} + \frac{1}{2}\tilde{\theta}^\top \Gamma^{-1}\tilde{\theta} - \bar{z}^\top \mathbf{P}\mathbf{b}_m \psi(t, \mathbf{\Lambda}_n z)\tilde{\theta}, \tag{3.57}$$

which satisfies

$$V_{3.2}^*(\bar{z}) \geqslant \frac{1}{2}\left(p_m - \varepsilon p_M \psi_M\right)\|\bar{z}\|^2 + \frac{1}{2}\left(\gamma_M^{-1} - \frac{1}{\varepsilon}p_M\psi_M\right)\|\tilde{\theta}\|^2 \tag{3.58}$$

for any $\varepsilon \in \mathbb{R}_+$. *Function* $V_{3.2}^*(\bar{z})$ *is positive for the choice of* Γ *satisfying* $\gamma_M < \varepsilon\left(p_M\psi_M^2\right)^{-1}$ *with* $\varepsilon < p_m\left(p_M\psi_M\right)^{-1}$. *The time derivative of this function along the trajectories of the system is given by*

$$\begin{aligned}\dot{V}_{3.2}^* = &-\frac{1}{2}\omega_o \bar{z}^\top \bar{z} + \omega_o \bar{z}^\top \mathbf{P}\mathbf{d}_m\left(\psi - \hat{\psi}\right)\hat{\theta} - \tilde{\theta}^\top \Gamma^{-1}\,\mathrm{Proj}(\tau)\\ &- \omega_o \tilde{\theta}^\top \psi^\top \mathbf{b}_m^\top \mathbf{P}\bar{H}\bar{z} - \omega_o \tilde{\theta}^\top \psi^\top \mathbf{b}_m^\top \mathbf{P}\mathbf{d}_m\left(\psi - \hat{\psi}\right)\hat{\theta}\\ &- \tilde{\theta}^\top \psi^\top \mathbf{b}_m^\top \mathbf{P}\mathbf{b}_m \dot{\psi}\tilde{\theta} + \tilde{\theta}^\top \psi^\top \mathbf{b}_m^\top \mathbf{P}\mathbf{b}_m \psi\,\mathrm{Proj}(\tau),\end{aligned} \tag{3.59}$$

where $\psi = \psi(t, \mathbf{\Lambda}_n z)$, *and* $\hat{\psi} = \psi(t, \mathbf{\Lambda}_n \hat{z})$ *are denoted for brevity. By adding and subtrackting* $\tilde{\theta}^\top \Gamma^{-1}\,\mathrm{Proj}(\tau)$, *recalling Corollary 3.2 and assumptions imposed on the system, the following bound is imposed on this derivative,*

$$\begin{aligned}\dot{V}_{3.2}^* \leqslant &\left(-\frac{1}{2}\omega_o + \omega_c^{-n+1|0} p_M \psi_L \theta_M + \omega_o^{-n|-1}\left(\theta_M \psi_L\right.\right.\\ &\left.\left. + \theta_M \psi_M^2 p_M \gamma_M \psi_L\right)\right)\|\bar{z}\|^2 + \theta_M\left(\psi_M^3 p_M \gamma_M\right.\\ &+ \psi_M + \omega_o \psi_M p_M h_M + \omega_c^{-n+1|0}\theta_M \psi_M p_M \psi_L\\ &\left.+ \omega_o^{-n|-1}\theta_M\left(\psi_M^3 p_M \gamma_M \psi_L + \psi_L \psi_M\right)\right)\|\bar{z}\|\\ &+ \theta_M^2\left(\psi_M^2 p_M + \psi_M^4 p_M \gamma_M\right),\end{aligned} \tag{3.60}$$

where $h_M = \left\|\bar{H}\right\| \in \mathbb{R}_+$ *and* $\omega^{\kappa_1|\kappa_2}$ *is a piecewise exponentiation operator as defined in Section 1.5 and by equation* (2.52). *Terms* $\omega_c^{-n+1|0}$ *and* $\omega_o^{-n|-1}$ *are thus nonincreasing in* ω_o. *Hence, there exists* ω_o *high enough to ensure negativeness of* $\dot{V}_{3.2}^*(\bar{z})$ *for* $\left\|\bar{z}\right\|$ *large enough. As a result, the convergence of* $\bar{z}$ *to some boundary of the origin is achieved and it can be concluded that there exist* $z_M, T_z \in \mathbb{R}_+$ *such, that* $\left\|\bar{z}\right\| \leqslant z_M$ *for any* $t \geqslant T_z$.

Importantly, while the precise value of z_M depends on the chosen value of ω_o, by denoting

$$\begin{aligned}\nu_M = \Big(-\frac{1}{2}\omega_o + \omega_c^{-n+1|0} p_M \psi_L \theta_M + \omega_o^{-n|-1}\Big(\theta_M \psi_L \\ + \theta_M \psi_M^2 p_M \gamma_M \psi_L\Big)\Big) \|\bar{z}\|^2 + \theta_M \Big(\psi_M^3 p_M \gamma_M \\ + \psi_M + \omega_o \psi_M p_M h_M + \omega_c^{-n+1|0} \theta_M \psi_M p_M \psi_L \\ + \omega_o^{-n|-1} \theta_M \Big(\psi_M^3 p_M \gamma_M \psi_L + \psi_L \psi_M\Big)\Big) \|\bar{z}\| \\ + \theta_M^2 \Big(\psi_M^2 p_M + \psi_M^4 p_M \gamma_M\Big),\end{aligned} \tag{3.61}$$

and thus

$$\dot{V}_{3.2}^* \leqslant \nu_M, \tag{3.62}$$

it can be shown that

$$\lim_{\omega_o \to \infty} \nu_M = -\frac{1}{2}\omega_o \|\bar{z}\|^2 + \omega_o \theta_M \psi_M p_M h_M \|\bar{z}\|. \tag{3.63}$$

It follows that

$$\lim_{\omega_o \to \infty} z_M = 2\theta_M \psi_M p_M h_M \tag{3.64}$$

and z_M remains bounded with increase of ω_o. Notably, function (3.57) does not employ matrix $\mathbf{M}(t, \boldsymbol{\Lambda}_n z)$ and thus the formulated conclusions hold also if Assumption 3.5 is not satisfied.

Having established the notion of boundedness of $\bar{z}$, the convergence of the errors for $t \geqslant T_z$ can be investigated. To this end, consider the function

$$V_{3.2}(\bar{z}, \tilde{\theta}) = \frac{1}{2}\bar{z}^T \mathbf{P} \bar{z} + \tilde{\theta}^T \left(\frac{1}{2}\boldsymbol{\Gamma}^{-1} - \mathbf{M}(t, \boldsymbol{\Lambda}_n z)\right) \tilde{\theta}, \tag{3.65}$$

which satisfies the bound expressed as

$$V_{3.2}(\bar{z}, \tilde{\theta}) \geqslant \frac{1}{2} p_m \|\bar{z}\|^2 + \left(\frac{1}{2}\gamma_M^{-1} - \psi_M^2\right) \|\tilde{\theta}\|^2. \tag{3.66}$$

Function $V_{3.2}(\bar{z}, \tilde{\theta})$ is hence positive definite for any choice of $\boldsymbol{\Gamma}$ such that $\gamma_M < \frac{1}{2}\psi_M^{-2}$. The time derivative of this function is given by

$$\begin{aligned}\dot{V}_{3.2} = & -\frac{1}{2}\omega_o \bar{z}^T \bar{z} + \omega_o \bar{z}^T \mathbf{P} \mathbf{d}_m \left(\psi - \hat{\psi}\right) \hat{\theta} + \bar{z}^T \mathbf{P} \mathbf{b}_m \dot{\psi} \tilde{\theta} \\ & - \bar{z}^T \mathbf{P} \mathbf{b}_m \psi \operatorname{Proj}(\boldsymbol{\tau}) - \tilde{\theta}^T \boldsymbol{\Gamma}^{-1} \operatorname{Proj}(\boldsymbol{\tau}) + 2\tilde{\theta}^T \mathbf{M} \operatorname{Proj}(\boldsymbol{\tau}) \\ & - \tilde{\theta}^T \mathbf{M} \tilde{\theta} + \tilde{\theta}^T \psi^T \psi \tilde{\theta}.\end{aligned} \tag{3.67}$$

By adding and subtracting the term $\tilde{\theta}^{\mathsf{T}}\Gamma^{-1}\tau$*, and recalling Corollary 3.3, Assumption 3.4 and* (3.52)*, it is inferred that*

$$\begin{aligned}\dot{V}_{3.2} \leqslant \Bigg(&-\frac{1}{2}\omega_o + p\psi_M^2\gamma_M + \omega_c^{-n+1|0}p_M\psi_L\theta_M \\ &+ \omega_o^{-n|-1}\Big(p_M\psi_M^2\psi_L\gamma_M\theta_M + p_M\psi_M\psi_L\gamma_M z_M \\ &+ \theta_M\psi_L + 2\theta_M\psi_M^2\psi_L\gamma_M\Big) + \frac{1}{2\varepsilon}\Big(p_M\psi_M + p_M\gamma_M\psi_M^3 \\ &+ 2\psi_M^3\gamma + \omega_o^{-n|-1}\theta_M\psi_L\left(2\psi_M^3\gamma_M + \psi_M\right) \\ &+ \psi_M\Big)^2\Bigg)\|\bar{z}\|^2 + \left(-\mu e^{-T_{PE}} + 2\gamma_M\psi_M^4 + \frac{\varepsilon}{2}\right)\|\tilde{\theta}\|^2\end{aligned} \tag{3.68}$$

for any $\varepsilon \in \mathbb{R}_+$*. By setting* Γ *such that* $\gamma_M < \mu e^{-T_{PE}}\psi_M^{-4}$ *and choosing* ε *small enough with* ω_o *high enough the entire expression is made negative definite. The intermediate calculations are presented in more detail in Appendix A.2. On the basis of* $V_{3.2}(\bar{z}, \tilde{\theta})$ *it is concluded that once the estimation errors converge below some arbitrary threshold* z_M*, further exponential convergence of the estimation and identification errors to the origin is guaranteed.*

The stability analysis of the proposed method in the presented form has a straightforward interpretation. As the adaptation law is formulated on the basis of the state and disturbance estimates, in the first stage it is ensured that for any initial values these converge to some neighborhood of their true values if ω_o is chosen high enough. The second part ensures that due to this boundedness property, the adaptation law is able to successfully drive all errors to the origin. Thus, the presented analysis shows that the proposed adaptation scheme does not disrupt the well-known property of boundedness of errors in the ESO observer, and additionally improves the performance of the algorithm. In order to evaluate the practical efficiency of the PIESO observer in the system with the regressor being a function of the state of the plant, a numerical simulation is conducted.

Simulation 3.5. *Consider a linear time-invariant plant of the third order with the dynamics expressed by* (3.47) *with* $b = 1$ *and* $\psi = x^{\mathsf{T}}$ *and* $\theta = \begin{bmatrix}-1 & 3 & 3\end{bmatrix}^{\mathsf{T}}$*. Note that such a system is conforming with the plant employed in the simulations of the MRAC scheme and gradient identification in Section 3.1. The adaptive PIESO observer is designed according to* (3.50) *and* (3.51) *with* $\omega_o = 100$*,* $\Gamma = 0.05\mathbf{I}_3$*. The projection operator in the form given in Remark 3.2 is employed with* $\vartheta_i = 100$ *for* $i \in \{1, 2, 3\}$*. Importantly, the boundary imposed by the projection operator is here chosen significantly greater than the real values of the parameters of the plant, to visualize that only a very limited knowledge about the system dynamics is necessary to*

design the PIESO observer. Once again the additional nonadaptive controller is incorporated into the system to ensure that the state of the plant follows the reference trajectory given by (2.34) *with* $x_r(t) = \sin(\frac{2\pi}{10}t) + \frac{1}{2}\sin(\frac{2\pi}{3}t)$. *The zero initial conditions for all variables are chosen. The results of the simulation are given in Fig. 3.12.*

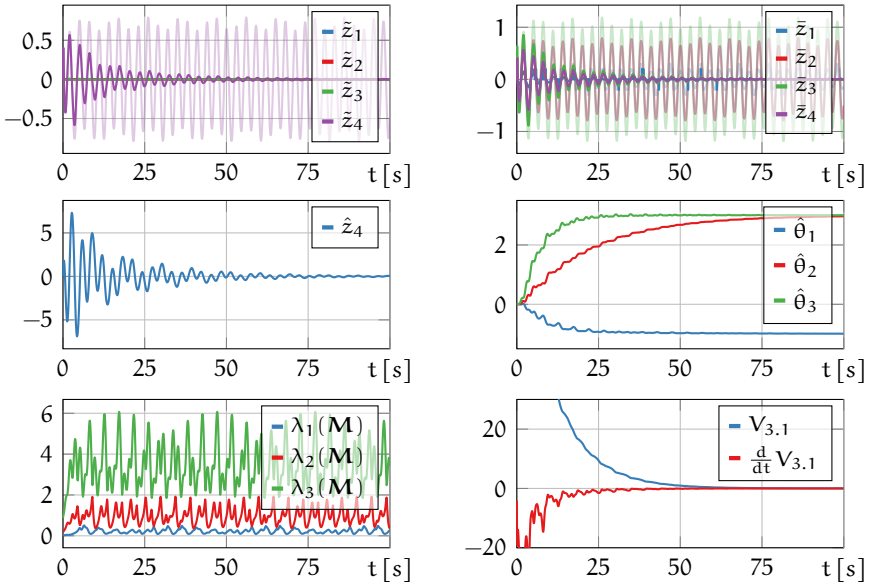

Figure 3.12: Time responses of the third order system with state-dependent regressor under the proposed PIESO observer. Results of conventional ESO with $\Gamma = 0_3$ shown in transparent plots of $\tilde{z}$ and $\bar{z}$.

The obtained results resemble the outcomes of Sim. 3.3 where a case of a system with regressor independent of the state was investigated. The convergence of the estimation errors to the origin, as well as parameter estimates to their nominal values, is visible on the plots. Notably, the evolution of the disturbance estimate and parameter estimates are reminiscent of the results of gradient identification presented in Section 3.1 as the adaptive scheme of PIESO is based on the underlying gradient approach. Thus, the relatively high speed of identification, as compared with the MRAC method, is maintained in the proposed observer. The evolution of function $V_{3.2}(\bar{z}, \tilde{\theta})$ confirms the results of the analytical investigation. The auxiliary function $V^*_{3.2}(\bar{z})$ is omitted in the plots as during the trials it was observed that it serves its purposes only in some extreme cases of very large initial estimation errors. In all other cases, function $V_{3.2}(\bar{z}, \tilde{\theta})$ satisfies the conditions of Lyapunov function on its own throughout the entire simulation horizon.

Notably, the plots given in Fig. 3.12 does not show the impact of the projection operator, as the estimation errors are small enough to avoid the drift of the parameter estimates. To explicitly visualize the

effect of the incorporation of the projection operator, the simulation is repeated with different initial values of the state estimates to trigger the appearance of the peaking phenomenon and generate larger identification errors in the first time instants.

Simulation 3.6. *Consider the settings as in Sim. 3.5 with initial values of state estimates changed. Namely, the initial conditions are set as* $\hat{\mathbf{z}}(0) = \begin{bmatrix} 10 & 10 & 10 & 10 \end{bmatrix}^T$, $\hat{\boldsymbol{\theta}}(0) = \begin{bmatrix} 0 & 0 & 0 \end{bmatrix}^T$ *and the projection limit is changed to* $\vartheta_i = 10$ *for* $i \in (1,2,3)$. *The results of the simulation are presented in Fig. 3.13.*

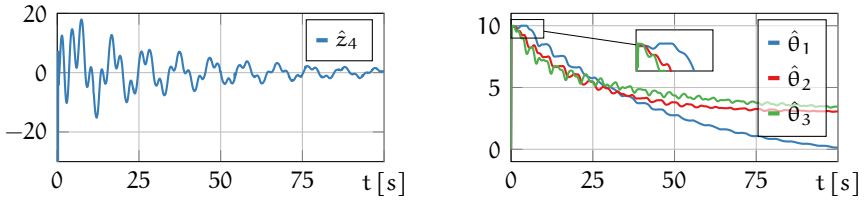

Figure 3.13: Time responses of the third order system with state-dependent regressor and significant initial estimation errors under the proposed PIESO observer.

The initial increase in the disturbance estimate and the momentary growth of the parameter estimates are visible. Due to the action of the projection operator, the boundedness of the parameter estimates is guaranteed what results in the boundedness of the entire total disturbance. This allows the PIESO to efficiently estimate the disturbance despite the presence of the peaking effect and enables it to successfully drive all the errors to the origin.

3.2.3 *Alternative systems*

The adaptive PIESO observer as proposed in Sections 3.2.1 and 3.2.2 is nominally designed for systems expressed by (3.25). Nonetheless, the algorithm is applicable also to several classes of dynamic systems not directly conforming to this model. Specifically, the considered method can be successfully employed to estimate the state and parameters of the disturbed systems with disturbances which can be incorporated into the structure of (3.25) or nonlinear plants transformable into the form of (3.25) by the means of a state transformation. In this section, two specific cases of such systems are discussed and a tutorial on the applicability of the PIESO observer in these scenarios is given. Namely, the plant with harmonic disturbance reminiscent of that considered in Section 2.4.2 and the two–mass–spring flexible mechanical system are presented. In both cases, a significant parametric uncertainty is assumed. For each of the plants, a suitable transformation that brings

the system to the form feasible for PIESO application is given and the observer synthesis is performed. The performance of the algorithm in these scenarios is validated by the means of numerical simulations.

Consider the plant with harmonic disturbance as discussed in Section 2.4.2 with dynamics given by

$$\dot{\mathbf{x}} = \mathbf{A}_n \mathbf{x} + \mathbf{b}_n \left(b u + d \right) \tag{3.69}$$

with the disturbing term $d = -b d_h$ where d_h represents the harmonic disturbance expressed by

$$d_h = a_h \sin(2\pi f_h t), \tag{3.70}$$

with $a_h \in \mathbb{R}$ and $f_h \in \mathbb{R}_+$ being the amplitude and frequency of the harmonic function. Following the approach presented in [275] where internal model principle has been employed, the term d_h is equivalently expressed as a response of the unforced dynamic oscillatory system in the form of

$$\ddot{d}_h + (2\pi f_h)^2 d_h = 0. \tag{3.71}$$

The time derivative of the dynamics of this disturbance is given as

$$d_h^{(3)} + (2\pi f_h)^2 \dot{d}_h = 0. \tag{3.72}$$

By taking advantage of such a reformulation of disturbance d_h, the dynamics of the entire plant are rewritten as

$$\dot{\mathbf{q}} = \mathbf{A}_{n+3} \mathbf{q} + \begin{bmatrix} \mathbf{b}_n^T & 0_{3\times 1}^T \end{bmatrix}^T u - \mathbf{b}_{n+3} (2\pi f_h)^2 \mathbf{d}_{n+3} \mathbf{q} \tag{3.73}$$

with $\mathbf{q} = \begin{bmatrix} \mathbf{x}^T & d_h & \dot{d}_h & \ddot{d}_h \end{bmatrix}^T \in \mathbb{R}^{n+3}$. Notably it can be further expressed as

$$\dot{\mathbf{q}} = \mathbf{A}_{n+3} \mathbf{q} + \begin{bmatrix} \mathbf{b}_n^T & 0_{3\times 1}^T \end{bmatrix}^T u + \mathbf{b}_{n+3} \boldsymbol{\psi}(\mathbf{q}) \theta \tag{3.74}$$

with $\boldsymbol{\psi}(\mathbf{q}) = \mathbf{d}_{n+3} \mathbf{q}$ and $\theta = -\left(2\pi f_h\right)^2$ what closely resembles the nominal system (3.25) and allows application of the PIESO observer to estimate the state and unknown parameter of the system.

The solution to this problem has been initially proposed in [183]. The modification of the Resonant ESO observer formulated in [181, 275] and presented in Section 2.4.2 has been proposed by incorporating an adaptive frequency estimator [108, 255] to online identify the frequency of oscillations on the basis of total disturbance estimate produced by ESO. Here an alternative approach to this task is given by taking advantage of the proposed PIESO observer following the results shown in [231]. Treating $\mathbf{q}$ as a nominal state of the transformed system, the

state extension is defined as $z = \begin{bmatrix} q^T & \delta \end{bmatrix}^T \in \mathbb{R}^m$ with $m = n+4$ and dynamics given by

$$\begin{aligned} \dot{z} = A_m z + \begin{bmatrix} b_n^T & 0_{4\times 1}^T \end{bmatrix}^T u + d_m \psi(\Lambda_{n+3} z)\hat{\theta} \\ + b_m \frac{d}{dt}\left(\psi(\Lambda_{n+3} z)\left(\theta - \hat{\theta}\right)\right). \end{aligned} \tag{3.75}$$

The adaptive observer for the considered system is formulated as

$$\dot{\hat{z}} = A_m \hat{z} + \begin{bmatrix} b_n^T & 0_{4\times 1}^T \end{bmatrix}^T u + d_m \psi(\Lambda_{n+3}\hat{z})\hat{\theta}. \tag{3.76}$$

Due to the explicit dependence of the regressor on the extended state z, the adaptation law is formulated according to (3.51) as

$$\dot{\hat{\theta}} = \mathrm{Proj}(\tau, \hat{\theta}, \Theta), \quad \tau = \Gamma \psi^T(\Lambda_{n+3}\hat{z})\hat{z}_m. \tag{3.77}$$

Since the considered plant is relatively simple, the internal adaptation rule τ can be explicitly expressed as $\tau = -\gamma \hat{z}_m \hat{z}_{m-2}$ where $\gamma \in \mathbb{R}_+$ is a scalar positive adaptation gain.

Simulation 3.7. *The algorithm is implemented according to the presented approach and the performance of the method is validated in simulation. Namely, a second order plant consistent with the one discussed in Section 2.4.2 is considered, with* $n = 2$, $b = \frac{1}{30}$, $f_h = 7.46$ *and* $a_h = 0.6$. *The observer is tuned with* $\omega_o = 50$ *and the adaptation gain is set to* $\gamma = 10$. *For the sake of the experiment, an additional nonadaptive controller is incorporated into the system to generate the control signal* u. *The results of the simulation are given in Fig. 3.14.*

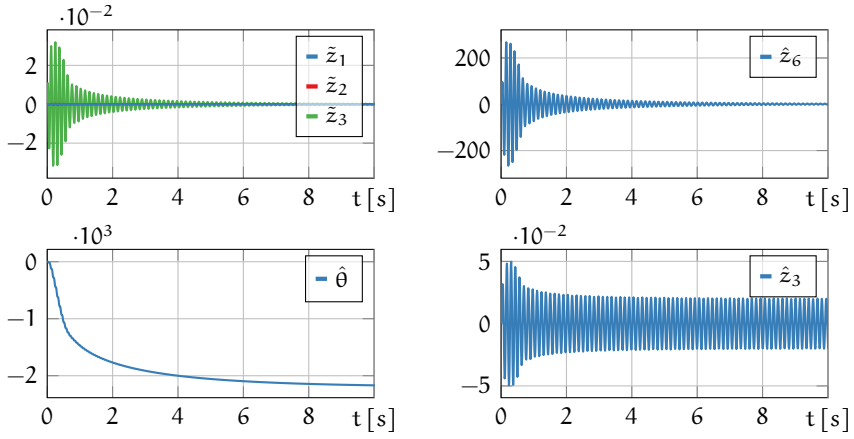

Figure 3.14: Time responses of the second order system with harmonic disturbance under the proposed PIESO observer.

It can be seen that the proposed adaptation method successfully identifies the unknown parameter of the plant, with the parameter estimate converging to the value of $\hat{\theta} \approx -(2\pi f_h)^2 \approx -2199.6$, which

results also in the vanishing of the state estimation errors $\tilde{z}$ and the estimate $\hat{z}_6$ of the total disturbance affecting the plant. Due to the choice of high adaptation gain γ, fast and efficient identification is achieved. Moreover, the estimate $\hat{z}_3$ of the harmonic disturbance converges to the expected form of the sine wave of amplitude equal to $ba_h = 0.02$ as the estimation progresses. The presented results show that under the proposed PIESO observer the state, parameters, and disturbance estimation is achieved despite the unknown amplitude and frequency of the harmonic disturbance affecting the plant.

The application of the proposed PIESO algorithm is also possible for a class of dynamic systems transformable into the nominal structure (3.25) by a static state transformation. As an example, a simple two–mass–spring system can be considered [305]. Such a plant consists of two masses connected by a flexible spring, with the input signals in the form of two forces acting upon the objects. The schematic view of the considered system is given in Fig. 3.15 where forces $F_1, F_2 \in \mathbb{R}$ are the controllable inputs of the system. Taking into account characteristics

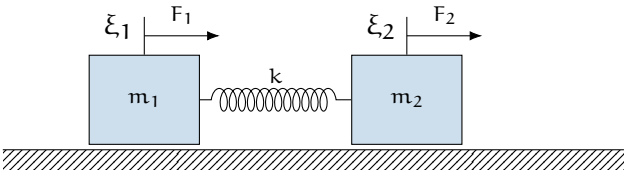

Figure 3.15: The schematic view of the two–mass–spring system.

of some compliant mechanical systems, it is usually assumed that the output of the system is represented by the position of only one of the masses and only one of the input forces is directly available for control. The considered plant is thus an underactuated fourth-order dynamic system with a single input and a single output. In the forthcoming analysis, it is assumed that the position of the first mass, denoted by ξ_1, is a measurable output of the system.

The general dynamics of the two–mass–spring system are expressed by

$$\begin{aligned} m_1\dot{v}_1 &= k(\xi_2 - \xi_1) + F_1, \\ m_1\dot{v}_2 &= k(\xi_1 - \xi_2) + F_2, \\ y &= \xi_1, \end{aligned} \tag{3.78}$$

where $\xi_1, \xi_2 \in \mathbb{R}$ and $v_1, v_2 \in \mathbb{R}$ are positions and velocities of two masses, $m_1, m_2 \in \mathbb{R}_+$ are masses of each of the connected objects and $k \in \mathbb{R}_+$ is a stiffness coefficient of the spring. By defining the state of

the system as $\mathbf{x} = \begin{bmatrix} \xi_1 & \nu_1 & \xi_2 & \nu_2 \end{bmatrix}^T \in \mathbb{R}^n$ with $n = 4$, the following state–space representation is obtained

$$\begin{aligned} \dot{x}_1 &= x_2, \\ \dot{x}_2 &= \frac{k}{m_1}(x_3 - x_1) + \frac{1}{m_1}F_1, \\ \dot{x}_3 &= x_4, \\ \dot{x}_4 &= \frac{k}{m_2}(x_1 - x_3) + \frac{1}{m_2}F_2. \end{aligned} \tag{3.79}$$

The dynamics of the system in such a form are not suitable for a direct application of the PIESO observer. In order to transform the system into a feasible form, the static state transformation $\mathbf{q} = \mathbf{T}(\mathbf{x})$ is proposed on the basis of [274, 282] in the form of

$$\begin{aligned} q_1 &= x_1,\ q_2 = x_2, \\ q_3 &= \frac{k}{m_1}(x_3 - x_1), \\ q_4 &= \frac{k}{m_2}(x_4 - x_2), \end{aligned} \tag{3.80}$$

with the inverse transformation given by

$$\begin{aligned} x_1 &= q_1,\ x_2 = q_2, \\ x_3 &= q_1 + \frac{m_1}{k}q_3, \\ x_4 &= q_2 + \frac{m_1}{k}q_4. \end{aligned} \tag{3.81}$$

Application of the considered transformation to the dynamics of the nominal system (3.79) yields

$$\begin{aligned} \dot{q}_1 &= q_2, \\ \dot{q}_2 &= q_3 + \frac{1}{m_1}F_1, \\ \dot{q}_3 &= q_4, \\ \dot{q}_4 &= -k\left(\frac{1}{m_1} + \frac{1}{m_2}\right)q_3 - \frac{k}{m_1^2}F_1 + \frac{k}{m_1 m_2}F_2. \end{aligned} \tag{3.82}$$

The transformed dynamics are rewritten in the compact form resembling (3.25) as

$$\dot{\mathbf{q}} = \mathbf{A}_n \mathbf{q} + \frac{1}{m_1}\begin{bmatrix} \mathbf{b}_2^T & \mathbf{0}_{2\times 1}^T \end{bmatrix}^T F_1 + \mathbf{b}_n \boldsymbol{\psi}(t, \mathbf{q})\boldsymbol{\theta} \tag{3.83}$$

with $\boldsymbol{\psi}(t, \mathbf{q}) = \begin{bmatrix} q_3 & F_1 & F_2 \end{bmatrix}$ and the new vector of transformed parameters given by $\boldsymbol{\theta} = \begin{bmatrix} -k\left(\frac{1}{m_1} + \frac{1}{m_2}\right) & -\frac{k}{m_1^2} & \frac{k}{m_1 m_2} \end{bmatrix}^T$.

The specific properties of the algorithm depends directly on the availability of the system inputs. It can be noted that the inverse transformation $\mathbf{x} = \mathbf{T}^{-1}(\mathbf{q})$ given by (3.81), which enables the recovery of the original state coordinates $\mathbf{x}$ from the transformed state $\mathbf{q}$, requires knowledge of the term $\frac{m_1}{k}$ only. It also follows from (3.83) that if the control input F_1 is used, then the knowledge of m_1 parameter is necessary to synthesize the observer and recover the estimates of the original state of the system. Alternatively, if F_2 is considered as an input of the plant, then the observer can be synthesized without any known parameter, but the structure of $\boldsymbol{\psi}(t, \mathbf{x})$ enables the identification of only two lumped parameters of the system and at least one of the nominal parameters of the plant has to be nonetheless known in advance in order to recover the state estimates of the original plant. Finally, if both control inputs are available and measurable, the regressor makes it possible to successfully identify of all three lumped parameters. However, the synthesis of the observer itself still requires the knowledge of m_1 parameter present in the input path of F_1 force, and thus the redundancy in the design of the system appears. The design of the observer and the adaptation law is here given in its most general form, assuming that both F_1 and F_2 are available for control. The synthesis of the algorithm for chosen simplified scenarios with only one input signal avaiable follows trivially and is omitted here.

On the basis of (3.83) the extended state can be designed as $\mathbf{z} = \begin{bmatrix} \mathbf{q}^T & \delta \end{bmatrix}^T \in \mathbb{R}^m$, with $m = n + 1$. The dynamics of the extended state are given as

$$\begin{aligned} \dot{\mathbf{z}} = \mathbf{A}_m \mathbf{z} + \frac{1}{m_1} \begin{bmatrix} \mathbf{b}_2^T & \mathbf{0}_{3\times 1}^T \end{bmatrix} F_1 + \mathbf{d}_m \boldsymbol{\psi}(t, \boldsymbol{\Lambda}_n \mathbf{z}) \hat{\theta} \\ + \mathbf{b}_m \frac{d}{dt} \left(\boldsymbol{\psi}(t, \boldsymbol{\Lambda}_n \mathbf{z}) \left(\theta - \hat{\theta} \right) \right), \end{aligned} \tag{3.84}$$

what is reminiscent of (3.49). According to the established approach to the PIESO design, an adaptive observer is proposed in the form of

$$\dot{\hat{\mathbf{z}}} = \mathbf{A}_m \hat{\mathbf{z}} + \frac{1}{m_1} \begin{bmatrix} \mathbf{b}_2^T & \mathbf{0}_{3\times 1}^T \end{bmatrix} F_1 + \mathbf{d}_m \boldsymbol{\psi}(t, \boldsymbol{\Lambda}_n \hat{\mathbf{z}}) \hat{\theta} + \mathbf{l} (z_1 - \hat{z}_1) \tag{3.85}$$

with adaptation law designed as

$$\dot{\hat{\theta}} = \mathrm{Proj}(\boldsymbol{\tau}, \hat{\theta}, \boldsymbol{\Theta}), \quad \boldsymbol{\tau} = \boldsymbol{\Gamma} \boldsymbol{\psi}^T(t, \boldsymbol{\Lambda}_n \hat{\mathbf{z}}) \hat{z}_m. \tag{3.86}$$

The requirement of knowledge of m_1 parameter is clearly visible in equation (3.85), where it is required to properly synthesize the observer. Forces F_1 and F_2 are here treated as a part of regressor $\boldsymbol{\psi}(t, \boldsymbol{\Lambda}_n \mathbf{z})$ and are used in the identification procedure.

Simulation 3.8. *The simulation results of the application of the discussed scheme to two–mass–spring system in three different scenarios are obtained.*

1. *Only* F_1 *is available for control and chosen as* $F_1 = \frac{1}{2}\sin(\frac{1}{2}t)$. *The observer is tuned with* $\mathbf{\Gamma} = 1.5\mathbf{I}$.

2. *Only* F_2 *is available for control and chosen as* $F_2 = \frac{1}{2}\sin(\frac{1}{2}t)$. *The observer is tuned with* $\mathbf{\Gamma} = 1.5\mathbf{I}$.

3. *Both* F_1 *and* F_2 *available for control and chosen as* $F_1 = \frac{1}{2}\sin(\frac{1}{2}t)$, $F_2 = \frac{1}{2}\sin^2(\frac{1}{2}t)$ *to ensure satisfaction of PE condition. The observer is tuned with* $\mathbf{\Gamma} = 3\mathbf{I}$.

In all cases the observer bandwidth is set to $\omega_o = 50$, *nominal parameters of the plant are chosen as* $m_1 = 1\,\mathrm{kg}$, $m_2 = 1.5\,\mathrm{kg}$, $k = 0.1\,\mathrm{N/m}$, *and parameter* m_1 *is assumed to be known. In the first and second scenarios, only parameters* m_2 *and* k *are identified. The third scenario enables the identification of three parameters of the linearized system and thus all three coefficients of the nominal system are also estimated. The produced results are given in Fig. 3.16–3.18. In each trial the observer is designed according to* (3.85)–(3.86), *the estimates of transformed state* $\mathbf{q}$ *and lumped parameters* θ *are obtained, and then the values of the nominal parameters* k, m_1, m_2 *and the original state* $\mathbf{x}$ *of the plant are recovered according to* (3.81) *and* (3.83).

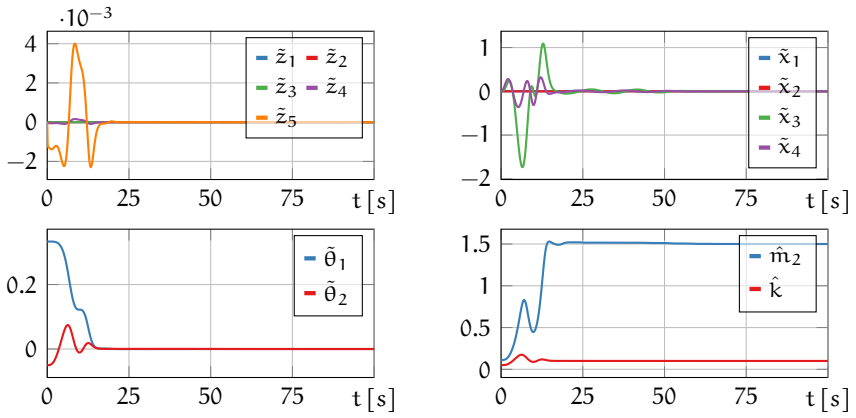

Figure 3.16: Time responses of the two-mass-system with only F_1 available.

In the plots the error of the transformed state estimation $\tilde{\mathbf{z}} = \mathbf{z} - \hat{\mathbf{z}}$, the nominal state estimation $\tilde{\mathbf{x}} = \mathbf{x} - \mathbf{T}(\mathbf{\Lambda}_n\hat{\mathbf{z}})$, the parameter identification $\tilde{\theta} = \theta - \hat{\theta}$, and the estimates of the physical coefficients of the nominal system $\hat{m}_1, \hat{m}_2, \hat{k}$ are given. It can be seen, that in all cases the estimation and identification errors converge to the origin, and the estimates of the physical parameters converge toward their real values. Notably, if only one control input is available the number of identified parameters is limited and only two of them can be successfully estimated. Moreover, from the definition of parameter vector θ

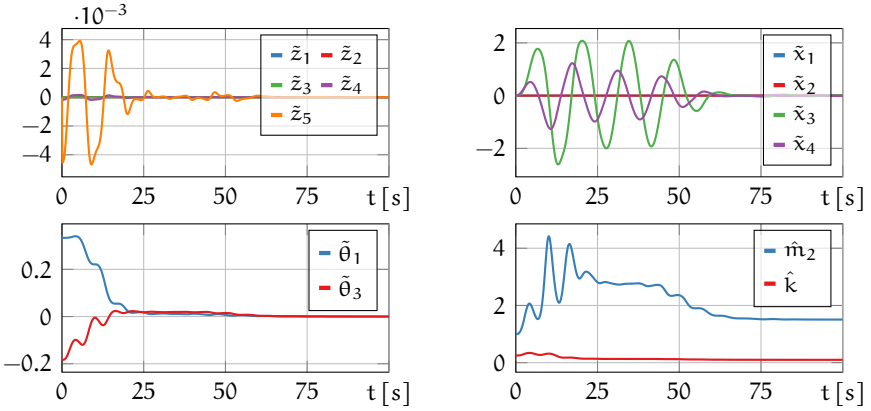

Figure 3.17: Time responses of the two-mass-system with only F_2 available.

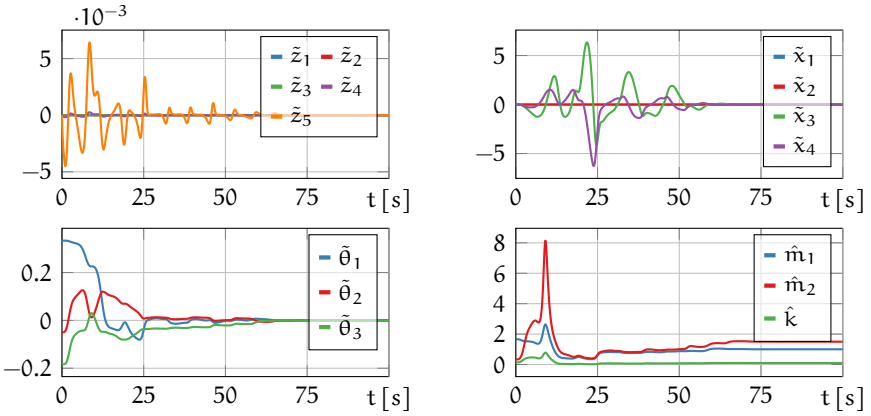

Figure 3.18: Time responses of the two-mass-system with both F_1 and F_2 available.

in (3.83) it may be noted that

$$\begin{aligned} m_1 &= -\frac{\theta_1}{\theta_3 - \theta_2}, \\ m_2 &= \frac{\theta_1 \theta_2}{\theta_3^2 - \theta_2 \theta_3}, \\ k &= -\frac{\theta_1^2 \theta_2}{(\theta_3 - \theta_2)^2}. \end{aligned} \tag{3.87}$$

The values of physical parameters of the nominal system thus cannot be recovered for some combinations of the momentary values of the identified parameters $\hat{\theta}$ for which denominators of expressions in (3.87) approaches zero. While the employed approach ensures that the parameter estimates converge to their correct values, these unfeasible values of the parameters may be reached in the transient states and the recovery of the nominal parameters and state of the nominal system may be impossible in such time instants. Due to this phenomenon, the presented scheme may not be suitable for use in

real-time tasks. To mitigate this effect the use of a differently defined projection operator may be considered to disable adaptation if the parameters approach some of the unfeasible values. The numerical trials presented in Fig. 3.16–3.18 are given here as a proof of concept and thus such modifications are not incorporated into the observation method. The initial conditions of the parameter estimates were instead carefully chosen to ensure the flawless recovery of the physical parameters of the plant.

3.3 PARAMETER IDENTIFYING DRC

The PIESO observer proposed in the preceding section constituted a tailored solution to the problem of state estimation and parameter identification of the systems with unknown parameters. Nonetheless, in the practical scenarios, the problem of adaptive control in the presence of parametric uncertainty is often considered and the means of application of the proposed methods to the task of closed-loop control are thus required. To this end, a new adaptive ADRC scheme named Parameter Identifying Disturbance Rejection Control (PIDRC) is designed by combining the PIESO observer with a conventional ADRC control law enhanced by the disturbance model evaluated using the identified parameters of the plant. Due to the proven capability of the algorithm to asymplotically estimate the disturbance impacting the plant, the performance of such a controller is ultimately improved and the asymptotic convergence of the estimation, identification, and tracking errors is achieved.

In order to facilitate the controller design, consider the nominal system as given by (3.25) and expressed by

$$\begin{aligned} \dot{\mathbf{x}} &= \mathbf{A}_n \mathbf{x} + \mathbf{b}_n \left(b u + \boldsymbol{\psi}(t, \mathbf{x}) \boldsymbol{\theta} \right), \\ y &= \mathbf{c}_n^T \mathbf{x}, \end{aligned} \tag{3.88}$$

where $\mathbf{x} = \begin{bmatrix} x_1 & \dots & x_n \end{bmatrix}^T \in \mathbb{R}^n$ represents a state of the plant, $b \in \mathbb{R} \setminus \{0\}$ is a known input gain, $u \in \mathbb{R}$ stands for a control input, and $y \in \mathbb{R}$ represent the output of the plant. The term $\boldsymbol{\psi}(t, \mathbf{x}) = \begin{bmatrix} \psi_1(t, \mathbf{x}) & \dots & \psi_k(t, \mathbf{x}) \end{bmatrix} \in \mathbb{R}^{1 \times k}$ represents some dynamics of the plant with a known structure and $\boldsymbol{\theta} = \begin{bmatrix} \theta_1 & \dots & \theta_k \end{bmatrix}^T \in \mathbb{R}^k$ are unknown constant parameters of the system. Matrices $\mathbf{A}_n$, $\mathbf{b}_n$ and $\mathbf{c}_n$ are as given in Section 1.5. Reminiscent of the procedure of Section 2.2, the problem of simultaneous state estimation, parameter identification

and tracking reference trajectory $\mathbf{x}_r(t)$ by state $\mathbf{x}$ of the plant is defined, with

$$\mathbf{x}_r = \begin{bmatrix} x_{r1} & \dots & x_{rn} \end{bmatrix}^T = \begin{bmatrix} x_r^{(0)}(t) & \dots & x_r^{(n-1)}(t) \end{bmatrix}^T \in \mathbb{R}^n, \tag{3.89}$$

where $x_r(t) \in \mathbb{R}$ is some function of time chosen freely by the designer. The application of PIESO observer requires the nominal plant to satisfy some assumptions, defined on the basis of the character of the regressor and state of the plant as Assumption 3.3–3.5. If the problem of closed-loop control is considered, the satisfaction of some of them cannot be verified in advance, as the evolution of the state of the system is initially unknown. Thus, following the approach of Section 2.2, the set of similar assumptions is defined on the basis of the reference trajectory. Namely, assume that the nominal plant is such that Assumption 3.3 holds and the reference trajectory satisfies what follows.

Assumption 3.7. *Let reference trajectory $\mathbf{x}_r(t)$ be such that*

$$\max(\|\boldsymbol{\psi}(t, \mathbf{x}_r)\|, \left\| \frac{d}{dt}\boldsymbol{\psi}(t, \mathbf{x}_r) \right\|) \leqslant \psi_M \tag{3.90}$$

for some constant $\psi_M \in \mathbb{R}_+$ and any $t \geqslant 0$.

Assumption 3.8. *Let the reference trajectory $\mathbf{x}_r(t)$ be such that regressor $\boldsymbol{\psi}(t, \mathbf{x}_r)$ evaluated on the reference trajectory satisfies*

$$\int_t^{t+T_{PE}} \boldsymbol{\psi}^T(\tau, \mathbf{x}_r(\tau))\boldsymbol{\psi}(\tau, \mathbf{x}_r(\tau))\, d\tau \geqslant \mu \mathbf{I}_k \tag{3.91}$$

for some constants $\mu, T_{PE} \in \mathbb{R}_+$ and all $t \geqslant 0$.

Corollary 3.4. *If Assumptions 3.7 and 3.8 hold, then there exists matrix*

$$\mathbf{M}(t, \mathbf{x}_r) = \int_t^{\infty} e^{t-\tau}\boldsymbol{\psi}^T(\tau, \mathbf{x}_r(\tau))\boldsymbol{\psi}(\tau, \mathbf{x}_r(\tau))\, d\tau \in \mathbb{R}^{k\times k} \tag{3.92}$$

satisfying

$$\mu e^{-T_{PE}} \|\boldsymbol{\nu}\|^2 \leqslant \boldsymbol{\nu}^T \mathbf{M} \boldsymbol{\nu} \leqslant \psi_M^2 \|\boldsymbol{\nu}\|^2 \tag{3.93}$$

for any vector $\boldsymbol{\nu} \in \mathbb{R}^k$. The time derivative of matrix $\mathbf{M}(t, \mathbf{x}_r)$ is given as

$$\frac{d}{dt}\mathbf{M}(t, \mathbf{x}_r) = \mathbf{M}(t, \mathbf{x}_r) - \boldsymbol{\psi}^T(t, \mathbf{x}_r(t))\boldsymbol{\psi}(t, \mathbf{x}_r(t)). \tag{3.94}$$

Reminiscent of the approach embraced in the PIESO design, multiple variants of the controller are proposed depending on the specific characteristics of the plant or properties of the system. Namely, the

simple solution similar to that of Section 3.2.1 is presented for the systems with regressor being a known function of time only. For the more sophisticated systems with disturbance directly depending on the state of the system, two distinct methods are proposed, with the regressor evaluated either on the estimated state or reference trajectory. For each of the proposed approaches, a suitable stability analysis is presented and validation is conducted through simulation trials.

3.3.1 *State independent regressor*

In order to introduce the fundamental principles of the PIDRC design, the simplified system with regressor independent of the state of the plant is first considered. The dynamics of such a system are expressed by

$$\dot{\mathbf{x}} = \mathbf{A}_n \mathbf{x} + \mathbf{b}_n \left(bu + \boldsymbol{\psi}(t)\boldsymbol{\theta} \right), \tag{3.95}$$

where $\boldsymbol{\psi}(t) = \begin{bmatrix} \psi_1(t) & \dots & \psi_k(t) \end{bmatrix} \in \mathbb{R}^{1\times k}$ is a function of time only. By treating the modeling uncertainty as a separate state variable, the dynamics of the plant are rewritten as

$$\begin{aligned} \dot{\mathbf{x}} &= \mathbf{A}_n \mathbf{x} + \mathbf{b}_n \left(bu + \boldsymbol{\psi}(t)\hat{\boldsymbol{\theta}} + \delta \right), \\ \dot{\delta} &= \frac{d}{dt}\left(\boldsymbol{\psi}(t) \left(\boldsymbol{\theta} - \hat{\boldsymbol{\theta}} \right) \right), \end{aligned} \tag{3.96}$$

where $\delta = \boldsymbol{\psi}(t)\left(\boldsymbol{\theta} - \hat{\boldsymbol{\theta}}\right) \in \mathbb{R}$ is a total disturbance in the system and $\hat{\boldsymbol{\theta}} \in \mathbb{R}^k$ stands for an estimate of the unknown parameters $\boldsymbol{\theta}$ of the nominal plant. The state extension of such a system is intuitively achieved by defining $\mathbf{z} = \begin{bmatrix} \mathbf{x}^T & \delta \end{bmatrix}^T = \begin{bmatrix} z_1 & \dots & z_m \end{bmatrix}^T \in \mathbb{R}^m$, where $m = n + 1$, with the dynamics given by

$$\dot{\mathbf{z}} = \mathbf{A}_m \mathbf{z} + \mathbf{d}_m \left(bu + \boldsymbol{\psi}(t)\hat{\boldsymbol{\theta}} \right) + \mathbf{b}_m \frac{d}{dt}\left(\boldsymbol{\psi}(t) \left(\boldsymbol{\theta} - \hat{\boldsymbol{\theta}} \right) \right). \tag{3.97}$$

Following the procedure presented in the previous sections, the PIESO observer for this system is designed as

$$\dot{\hat{\mathbf{z}}} = \mathbf{A}_m \hat{\mathbf{z}} + \mathbf{d}_m \left(bu + \boldsymbol{\psi}(t)\hat{\boldsymbol{\theta}} \right) + \mathbf{l}\left(z_1 - \hat{z}_1 \right) \tag{3.98}$$

with the parameter adaptation law given by

$$\dot{\hat{\boldsymbol{\theta}}} = \boldsymbol{\Gamma}\boldsymbol{\psi}^T(t)\hat{z}_m, \tag{3.99}$$

where $\hat{\mathbf{z}} = \begin{bmatrix} \hat{z}_1 & \dots & \hat{z}_m \end{bmatrix}^T \in \mathbb{R}^m$ stands for the estimates of the extended state $\mathbf{z}$, $\mathbf{l} = \begin{bmatrix} l_1 & \dots & l_k \end{bmatrix}^T \in \mathbb{R}^k_+$ defines the observer gains and $\boldsymbol{\Gamma} \in \mathbb{R}^{k\times k}$ is a positive definite matrix of adaptation gains. To

enable the algorithm to drive the state of the plant along the desired reference trajectory, the estimated model of the plant is incorporated into the standard ADRC controller given by (2.32). Namely, the control law is proposed as

$$u = b^{-1}\left(\nu - \psi(t)\hat{\theta} - \hat{z}_m\right) \tag{3.100}$$

with the internal control law ν designed as

$$\nu = \mathbf{k}^T\left(\mathbf{x}_r - \mathbf{\Lambda}_n\hat{\mathbf{z}}\right) + x_r^{(n)}. \tag{3.101}$$

The controller is here designed in accordance with the general principle of the proposed adaptive ADRC scheme. In the initial time instants, the estimate of the total disturbance is a major factor of the control law, as the quality of the estimated model of the plant may be insufficient to ensure the proper operation of the plant. As the adaptation progresses, the total disturbance is expected to vanish and the dynamics of the plant evaluated using the identified parameters are instead used to compensate for the impact of the nominal modeling uncertainty. The control law (3.100) thus ultimately converges to the form suitable for a conventional non-adaptive feedback controller. The graphical visualization if the proposed control scheme is presented in Fig. 3.19.

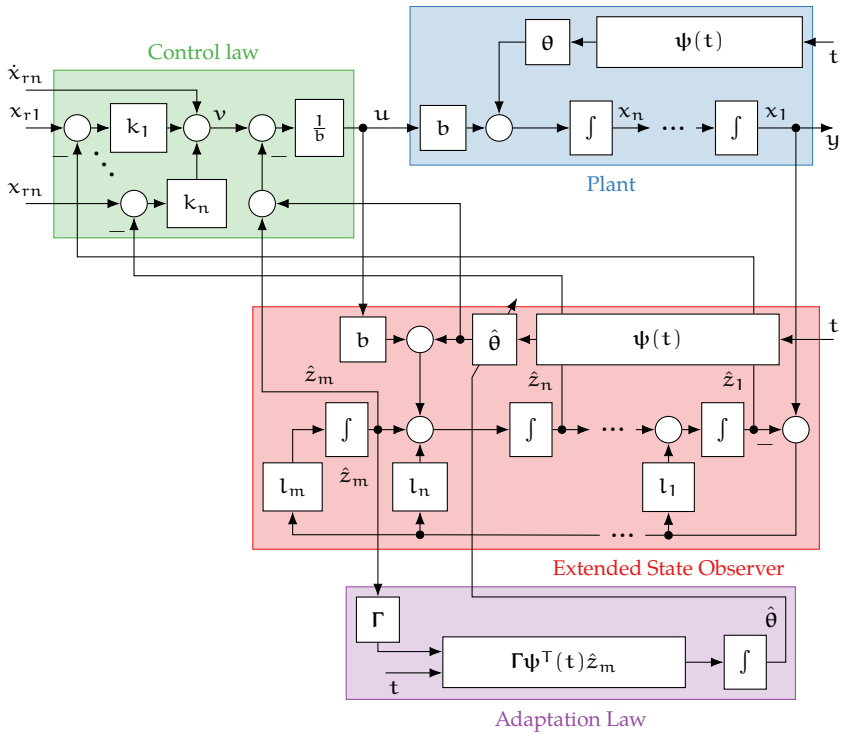

Figure 3.19: The detailed graphical illustration of the considered PIDRC controller with regressor dependent on the state.

Following the analysis approach presented in the previous sections, denote the tracking, estimation, and identification errors as $\tilde{x} = x_r - x$, $\tilde{z} = z - \hat{z}$, and $\tilde{\theta} = \theta - \hat{\theta}$, respectively. The dynamics of these errors under the proposed control scheme are given by

$$\begin{aligned}
\dot{\tilde{x}} &= G\tilde{x} - W\tilde{z}, \\
\dot{\tilde{z}} &= H\tilde{z} + b_m\dot{\psi}(t)\tilde{\theta} + b_m\psi(t)\Gamma\left(\psi^T(t)b_m^T\tilde{z} - \psi^T(t)\psi(t)\tilde{\theta}\right), \\
\dot{\tilde{\theta}} &= -\Gamma\psi^T(t)\psi(t)\tilde{\theta} + \Gamma\psi^T(t)b_m^T\tilde{z},
\end{aligned} \tag{3.102}$$

where $G = A_n - b_n k^T$, $H = A_m - l c_m^T$ and $W = b_n k^T \Lambda_n + b_n b_m^T$. By applying the standard bandwidth parametrization of the controller and observer gains, as given in Section 2.1, the algorithm is tuned with

$$\begin{aligned}
l_i &= \bar{l}_i \omega_o^i, && i \in \{1, m\}, \\
k_j &= \bar{k}_j \omega_c^{n+1-j}, && j \in \{1, n\}
\end{aligned} \tag{3.103}$$

with $\omega_c, \omega_o \in \mathbb{R}_+$ being the bandwidths of the controller and observer. The scaled tracking and estimation errors are then formulated as

$$\begin{aligned}
\bar{z}_i &= \omega_o^{m-i}\tilde{z}_i, \quad i \in \{1, m\}, \\
\bar{x}_j &= \omega_c^{n-j}\tilde{x}_j, \quad j \in \{1, n\},
\end{aligned} \tag{3.104}$$

which is equivalent to

$$\begin{aligned}
l &= \omega_o^m \Phi_o^{-1}\bar{l}, \quad k = \omega_c \Phi_c \bar{k}, \\
\bar{z} &= \Phi_o \tilde{z}, \qquad \bar{x} = \Phi_c \tilde{x}
\end{aligned} \tag{3.105}$$

with the scaling matrices $\Phi_o = \mathrm{diag}(\omega_o^{m-1}, \omega_o^{m-2}, \ldots, 1) \in \mathbb{R}^{m\times m}$ and $\Phi_c = \mathrm{diag}(\omega_c^{n-1}, \omega_c^{n-2}, \ldots, 1) \in \mathbb{R}^{n\times n}$ being expressed in terms of the chosen bandwidths ω_o, ω_c. Substituting (3.102) to (3.105) yields the dynamics of the scaled errors given by

$$\begin{aligned}
\dot{\bar{x}} &= \omega_c \bar{G}\bar{x} - b_n\left(\bar{k}^T\omega_c\Phi_c\Lambda_n\Phi_o^{-1} + b_m^T\right)\bar{z}, \\
\dot{\bar{z}} &= \omega_o \bar{H}\bar{z} + b_m\dot{\psi}(t)\tilde{\theta} + b_m\psi(t)\Gamma\left(\psi^T(t)b_m^T\bar{z} - \psi^T(t)\psi(t)\tilde{\theta}\right), \\
\dot{\tilde{\theta}} &= -\Gamma\psi^T(t)\psi(t)\tilde{\theta} + \Gamma\psi^T(t)b_m^T\bar{z}
\end{aligned} \tag{3.106}$$

with $\bar{\mathbf{G}} = \mathbf{A}_n - \mathbf{b}_n\bar{\mathbf{k}}^\top$, $\bar{\mathbf{H}} = \mathbf{A}_m - \bar{\mathbf{l}}\mathbf{c}_m^\top$, and explicitly given by

$$\bar{\mathbf{H}} = \begin{bmatrix} -\bar{l}_1 & 1 & 0 & \cdots & 0 \\ -\bar{l}_2 & 0 & 1 & \ddots & 0 \\ \vdots & \vdots & \ddots & \ddots & \vdots \\ -\bar{l}_n & 0 & 0 & \ddots & 1 \\ -\bar{l}_m & 0 & 0 & \cdots & 0 \end{bmatrix}, \; \bar{\mathbf{G}} = \begin{bmatrix} 0 & 1 & \cdots & 0 \\ \vdots & \vdots & \ddots & \vdots \\ 0 & 0 & \ddots & 1 \\ -\bar{k}_1 & -\bar{k}_2 & \cdots & -\bar{k}_n \end{bmatrix}. \tag{3.107}$$

Assumption 3.9. *Let the scaled control and observer gains $\bar{\mathbf{k}}, \bar{\mathbf{l}}$ be chosen such that matrices $\bar{\mathbf{G}}, \bar{\mathbf{H}}$ are Hurwitz.*

If Assumption 3.9 is satisfied then there exist positive definite matrices $\mathbf{R} \in \mathbb{R}^{n\times n}$ and $\mathbf{P} \in \mathbb{R}^{m\times m}$ such that $\bar{\mathbf{G}}^\top\mathbf{R} + \mathbf{R}\bar{\mathbf{G}} = -\mathbf{I}_n$ and $\bar{\mathbf{H}}^\top\mathbf{P} + \mathbf{P}\bar{\mathbf{H}} = -\mathbf{I}_m$. By taking advantage of this notion, the properties of the presented PIDRC controller are expressed by the following theorem.

Theorem 3.3. *For system* (3.95) *satisfying Assumptions 3.3, 3.7 and 3.8, the control law* (3.100) *with observer* (3.98) *and adaptation law* (3.99) *guarantees a global exponential convergence of errors $\tilde{\mathbf{x}}$, $\tilde{\mathbf{z}}$ and $\tilde{\theta}$ to the origin under the tuning proposed by Assumption 3.9 for ω_o and ω_c chosen high enough and Γ chosen with a norm small enough.*

Proof. *Following the footsteps of the PIESO analysis, recall Assumptions 3.7 and 3.8 with Corollary 3.4 and consider the following function*

$$V_{3.3}(\bar{\mathbf{x}}, \bar{\mathbf{z}}, \tilde{\theta}) = \frac{1}{2}\bar{\mathbf{x}}^\top\mathbf{R}\bar{\mathbf{x}} + \frac{1}{2}\bar{\mathbf{z}}^\top\mathbf{P}\bar{\mathbf{z}} + \tilde{\theta}^\top\left(\frac{1}{2}\Gamma^{-1} - \mathbf{M}(t)\right)\tilde{\theta}, \tag{3.108}$$

which satisfies the inequality

$$V_{3.3}(\bar{\mathbf{x}}, \bar{\mathbf{z}}, \tilde{\theta}) \geqslant \frac{1}{2}r_m\left\|\bar{\mathbf{x}}\right\|^2 + \frac{1}{2}p_m\left\|\bar{\mathbf{z}}\right\|^2 + \left(\frac{1}{2}\gamma_M^{-1} - \psi_M^2\right)\left\|\tilde{\theta}\right\|^2 \tag{3.109}$$

with $r_m = \lambda_{\min}(\mathbf{R}) \in \mathbb{R}_+$ and $\gamma_M = \left\|\Gamma\right\| \in \mathbb{R}_+$. The considered function is thus positive definite for any adaptation gains Γ satisfying $\gamma_M < \frac{1}{2}\psi_M^{-2}$.

The time derivative of function $V_{3.3}$ along the trajectories of the system is given by

$$\begin{aligned}\dot{V}_{3.3} = &-\frac{1}{2}\omega_c\bar{x}^T\bar{x} - \bar{x}^T\mathbf{R}\mathbf{b}_n\left(\bar{k}^T\omega_c\mathbf{\Phi}_c\mathbf{\Lambda}_n\mathbf{\Phi}_o^{-1} + \mathbf{b}_m^T\right)\bar{z} \\ &+ \bar{z}^T\left(-\frac{1}{2}\omega_o + \mathbf{P}\mathbf{b}_m\psi\mathbf{\Gamma}\psi^T\mathbf{b}_m^T\right)\bar{z} + \tilde{\theta}^T\Big(2\mathbf{M}\mathbf{\Gamma}\psi^T\psi \\ &- \mathbf{M}\Big)\tilde{\theta} + \bar{z}^T\Big(\mathbf{b}_m\psi - 2\mathbf{b}_m\psi\mathbf{\Gamma}\mathbf{M} - \mathbf{P}\mathbf{b}_m\psi\mathbf{\Gamma}\psi^T\psi \\ &+ \mathbf{P}\mathbf{b}_m\dot{\psi}\Big)\tilde{\theta}\end{aligned} \tag{3.110}$$

with arguments of $\boldsymbol{\psi}(t)$ and $\mathbf{M}(t)$ omitted for brevity. By taking advantage of properties of $\mathbf{M}(t)$ matrix and invoking the Young's inequality, the following bound of $\dot{V}_{3.3}(\bar{x},\bar{z},\tilde{\theta})$ can be defined,

$$\begin{aligned}\dot{V}_{3.3} \leqslant &\frac{1}{2}\left(-\omega_c + r_M\left(k_M\left(\frac{\omega_c}{\omega_o}\right)^{n|1} + 1\right)\right)\|\bar{x}\|^2 + \Big(-\mu e^{-T_{PE}} \\ &+ 2\psi_M^4\gamma_M + \frac{1}{2}\varepsilon\Big)\|\tilde{\theta}\|^2 + \frac{1}{2}\Big(-\omega_o + 2p_M\psi_M^2\gamma_M \\ &+ r_M\left(k_M\left(\frac{\omega_c}{\omega_o}\right)^{n|1} + 1\right) + \frac{1}{\varepsilon}\Big(\psi_M + 2\psi_M^3\gamma_M \\ &+ p_M\psi_M^3\gamma_M + p_M\psi_M\Big)^2\Big)\|\bar{z}\|^2\end{aligned} \tag{3.111}$$

for any $\varepsilon \in \mathbb{R}_+$ with $r_M = \|\mathbf{R}\| \in \mathbb{R}_+$, $k_M = \|\bar{k}\| \in \mathbb{R}_+$ and $p_M = \|\mathbf{P}\| \in \mathbb{R}_+$. By choosing $\omega_c > r_M\big(k_M\big(\frac{\omega_c}{\omega_o}\big)^{n|1} + 1\big)$, $\gamma_M < \frac{1}{2}\mu e^{-T_{PE}}\psi_M^{-4}$ and $\varepsilon < \frac{1}{2}\big(\mu e^{-T_{PE}} - 2\psi_M^4\gamma_M\big)$, the entire expression is made negative definite for ω_o chosen high enough. Function $V_{3.3}(\bar{x},\bar{z},\tilde{\theta})$ thus satisfies the conditions of Lyapunov theorem and its existence implies the asymptotic convergence of the tracking, estimation and identification errors to the origin.

The stability analysis presented here relies strongly on the earlier results obtained for the PIESO observer, yielding similar conclusions concerning the proper tuning of the controller. It is shown that if the bandwidths of the controller and observer are set high enough, preferably with ω_o significantly larger than ω_c to suppress the impact of transient state estimation errors on the control law, and the adaptation gain is chosen small enough, the stability of the closed-loop system is ensured and all errors converge to the origin despite initial modeling uncertainty present in the system. To better evaluate the performance of the proposed solution a numerical simulation is conducted.

Simulation 3.9. *The third order system with dynamics conforming to* (3.95) *and $n = 3, b = 1, \psi = \begin{bmatrix}\cos(3t) & \sin^3(t) & 1\end{bmatrix}$, as well as $\theta =$*

$\begin{bmatrix} -1 & 3 & 3 \end{bmatrix}^T$, *is considered. The PIDRC control scheme is designed for such a system following* (3.98)–(3.100) *with* $\Gamma = 0.2\mathbf{I}_3$, $\omega_o = 100$ *and* $\omega_c = 1$. *The reference trajectory is chosen as* (3.89) *with* $x_r(t) = \sin(\frac{2}{10}\pi t) + \frac{1}{2}\sin(\frac{2}{3}\pi t)$. *While the choice of a reference trajectory does not impact the ability of the observer to estimate the parameters of the plant, in the closed-loop control scheme it directly impacts the tracking procedure and state estimation. The results of the conducted simulation are given in Fig. 3.20. The choice of* $\omega_c = 1$ *implies that scaled tracking errors* $\bar{\mathbf{x}} = \tilde{\mathbf{x}}$ *and are thus omitted in the plots.*

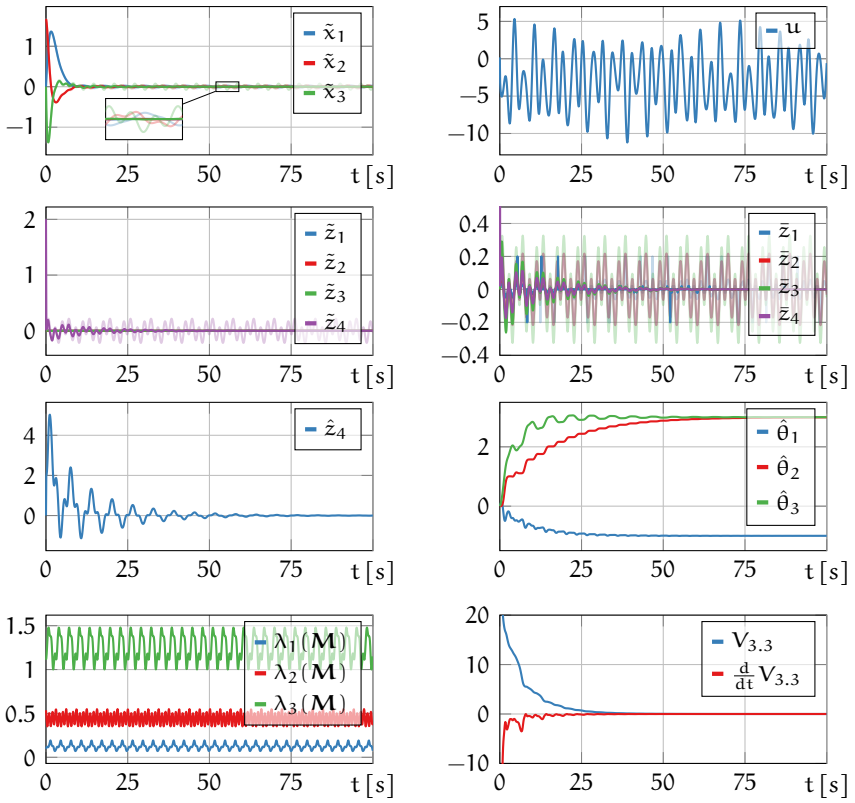

Figure 3.20: Time responses of the third order system with time-dependent regressor under the proposed PIDRC controller. Results of conventional ADRC with $\Gamma = 0_3$ shown in transparent plots of $\tilde{\mathbf{x}}$, $\tilde{\mathbf{z}}$ and $\bar{\mathbf{z}}$.

The presented results confirm the findings of the theoretical analysis. Convergence of the tracking, estimation, and identification errors to the origin is visible. Similarily, the vanishing of the total disturbance can be observed, which indicates the correct progress of the identification procedure. Eigenvalues of $\mathbf{M}(t)$ and the evolution of $V_{3.3}(\bar{\mathbf{x}}, \bar{\mathbf{z}}, \tilde{\theta})$ are also shown to further reinforce the analytical results. Notably, due to the character of the regressor, the identification of the parameters is here independent of the tracking of the reference trajectory, and the evolution of the parameters is the same as in shown in Fig. 3.9. It

follows that the speed of the adaptation of the PIDRC controller can also be adjusted by a proper choice of Γ matrix, as demonstrated in Fig. 3.10.

3.3.2 *Adaptation based on the reference state*

As is the case with the task of parameter identification using PIESO observer, in the problem of closed-loop trajectory tracking, the PIDRC controller in the proposed form utilizing the regressor expressed as a function of time only is not suitable for application in the majority of practical scenarios. The need for a controller in a more universal form, applicable to a general system given by (3.88), thus arises. Recall the considered nominal system given by (3.88) as

$$\dot{x} = \mathbf{A}_n x + \mathbf{b}_n \left(bu + \psi(t, x)\theta \right). \tag{3.112}$$

Following the approach embraced in the analysis of Section 2.2, the dynamics of the systems are reformulated to incorporate the reference trajectory and isolate the impacts of the tracking and estimation error as

$$\begin{aligned} \dot{x} &= \mathbf{A}_n x + \mathbf{b}_n \Big(bu + \left(\psi(t, \Lambda_n z) - \psi(t, x_r)\right) \left(\theta - \hat{\theta}\right) \\ &\quad + \psi(t, \Lambda_n z)\hat{\theta} + \delta \Big), \\ \dot{\delta} &= \frac{d}{dt} \left(\psi(t, x_r) \left(\theta - \hat{\theta}\right) \right), \end{aligned} \tag{3.113}$$

where $\delta = \psi(t, x_r)\left(\theta - \hat{\theta}\right)$ is the total disturbance of the system with ψ being a function of state. The dynamics of the extended state $z = \begin{bmatrix} x^T & \delta \end{bmatrix}^T \in \mathbb{R}^m$ take the form of

$$\begin{aligned} \dot{z} &= \mathbf{A}_m z + \mathbf{d}_m \Big(bu + \left(\psi(t, \Lambda_n z) - \psi(t, x_r)\right) \left(\theta - \hat{\theta}\right) \\ &\quad + \psi(t, \Lambda_n z)\hat{\theta} \Big) + \mathbf{b}_m \frac{d}{dt} \left(\psi(t, x_r) \left(\theta - \hat{\theta}\right) \right). \end{aligned} \tag{3.114}$$

In order to synthesize the observer and the controller for such a system some evaluation of the unknown state of the plant is necessary to calculate the momentary value of the regressor. The proposed standalone PIESO designed for the identification task utilizes the state estimate produced by the observer to solve this issue. Alternatively, as the task of closed-loop control is considered here, the reference trajectory may be employed by taking advantage of the expectation that state of the plant indeed converges to this reference signal. Thus,

two distinct solutions to the problem of PIDRC design in the presence of regressor being a function of state arise.

Consider first the approach employing the reference trajectory to synthesize the observer and controller. Incorporation of the reference signal into the PIESO observer designed for a system with state-dependent regressor yields

$$\dot{\hat{\mathbf{z}}} = \mathbf{A}_m \hat{\mathbf{z}} + \mathbf{d}_m \left(bu + \boldsymbol{\psi}(t, \mathbf{x}_r)\hat{\boldsymbol{\theta}} \right) + \mathbf{l}\,(z_1 - \hat{z}_1) \tag{3.115}$$

with $\hat{\mathbf{z}} = \begin{bmatrix} \hat{z}_1 & \dots & \hat{z}_m \end{bmatrix}^T \in \mathbb{R}^m$ being the state estimate produced by the observer. Notably, the observer in the proposed form can be synthesized and implemented on the basis of available and known signals. The parameter adaptation law is then proposed as

$$\dot{\hat{\boldsymbol{\theta}}} = \mathrm{Proj}(\boldsymbol{\tau}, \hat{\boldsymbol{\theta}}, \boldsymbol{\Theta}), \quad \boldsymbol{\tau} = \boldsymbol{\Gamma}\boldsymbol{\psi}^T(t, \mathbf{x}_r)\hat{z}_m, \tag{3.116}$$

where $\mathrm{Proj}(\cdot)$ satisfies (3.52) and thus Remarks 3.2 and 3.3, as well as Corollary 3.3, still hold. Finally, the control law is synthesized by taking advantage of the regressor evaluated on the reference trajectory and takes the form of

$$u = b^{-1} \left(\nu - \boldsymbol{\psi}(t, \mathbf{x}_r)\hat{\boldsymbol{\theta}} - \hat{z}_m \right) \tag{3.117}$$

with

$$\nu = \mathbf{k}^T (\mathbf{x}_r - \boldsymbol{\Lambda}_n \hat{\mathbf{z}}) + x_r^{(n)}. \tag{3.118}$$

The graphical illustration of the considered method is presented in Fig. 3.21.

The application of the PIDRC method in the presented form to the system with the regressor being a function of the state of the plant leads to the dynamics of tracking, estimation, and identification errors in the form of

$$\begin{aligned}
\dot{\tilde{\mathbf{x}}} &= \mathbf{G}\tilde{\mathbf{x}} - \boldsymbol{W}\tilde{\mathbf{z}} - \mathbf{b}_n \left(\boldsymbol{\psi}(t, \boldsymbol{\Lambda}_n \mathbf{z}) - \boldsymbol{\psi}(t, \mathbf{x}_r) \right) \boldsymbol{\theta}, \\
\dot{\tilde{\mathbf{z}}} &= \mathbf{H}\tilde{\mathbf{z}} + \mathbf{d}_m \left(\boldsymbol{\psi}(t, \boldsymbol{\Lambda}_n \mathbf{z}) - \boldsymbol{\psi}(t, \mathbf{x}_r) \right) \boldsymbol{\theta} + \mathbf{b}_m \Big(\dot{\boldsymbol{\psi}}(t, \mathbf{x}_r)\tilde{\boldsymbol{\theta}} \\
&\qquad - \boldsymbol{\psi}(t, \mathbf{x}_r)\,\mathrm{Proj}(\boldsymbol{\tau}) \Big), \\
\dot{\tilde{\boldsymbol{\theta}}} &= -\mathrm{Proj}(\boldsymbol{\tau}), \\
\boldsymbol{\tau} &= \boldsymbol{\Gamma}\boldsymbol{\psi}^T(t, \mathbf{x}_r)\boldsymbol{\psi}(t, \mathbf{x}_r)\tilde{\boldsymbol{\theta}} - \boldsymbol{\Gamma}\boldsymbol{\psi}^T(t, \mathbf{x}_r)\mathbf{b}_m^T \tilde{\mathbf{z}}.
\end{aligned} \tag{3.119}$$

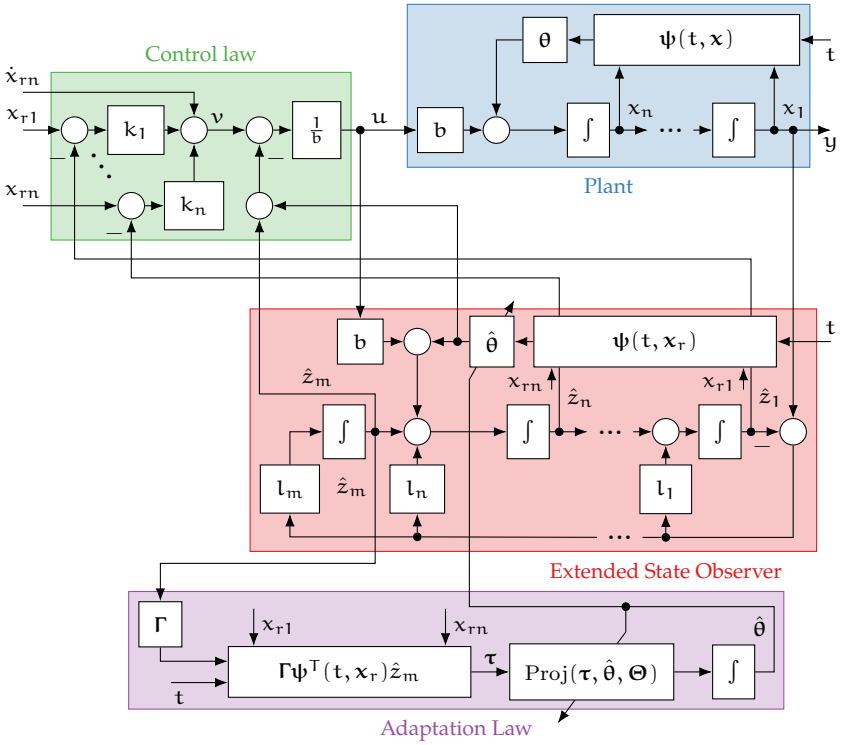

Figure 3.21: The detailed graphical illustration of the considered PIDRC controller with regressor dependent on the state and algorithm synthesized on the basis of the reference trajectory.

Embracing the tuning method of bandwidth parametrization given by (3.103) and recalling the definition of the scaled tracking and estimation errors in the form of (3.104) yields

$$\begin{aligned}
\dot{\bar{x}} &= \omega_c \bar{G}\bar{x} - b_n\left(\bar{k}^T \omega_c \Phi_c \Lambda_n \Phi_o^{-1} + b_m^T\right)\bar{z} - b_n\Big(\psi(t,\Lambda_n z) \\
&\quad - \psi(t,x_r)\Big)\theta, \\
\dot{\bar{z}} &= \omega_o \bar{H}\bar{z} + \omega_o d_m\left(\psi(t,\Lambda_n z) - \psi(t,x_r)\right)\theta + b_m\Big(\dot{\psi}(t,x_r)\tilde{\theta} \\
&\quad - \psi(t,x_r)\,\mathrm{Proj}(\tau)\Big), \\
\dot{\tilde{\theta}} &= -\mathrm{Proj}(\tau), \\
\tau &= \Gamma\psi^T(t,x_r)\psi(t,x_r)\tilde{\theta} - \Gamma\psi^T(t,x_r)b_m^T\bar{z}.
\end{aligned} \tag{3.120}$$

with $\bar{G}$ and $\bar{H}$ as given by (3.107). The following theorem summarizes the properties of the proposed solution.

Theorem 3.4. *For system* (3.112) *satisfying Assumptions 3.3, 3.7 and 3.8, the control law* (3.117) *with observer* (3.115) *and adaptation law* (3.116) *guarantees a global exponential convergence of errors* $\tilde{x}$, $\tilde{z}$ *and* $\tilde{\theta}$ *to the origin under the tuning proposed by Assumption 3.9 for* ω_o *and* ω_c *chosen high enough and* Γ *chosen with a norm small enough.*

Proof. *Consider the function given by*

$$V_{3.4}(\bar{x},\bar{z},\tilde{\theta}) = \frac{1}{2}\omega_o \bar{x}^T \mathbf{R}\bar{x} + \frac{1}{2}\bar{z}^T \mathbf{P}\bar{z} + \tilde{\theta}^T \left(\frac{1}{2}\mathbf{\Gamma}^{-1} - \mathbf{M}(t,\mathbf{x}_r)\right)\tilde{\theta}. \tag{3.121}$$

Function in such a form satisfies

$$V_{3.4}(\bar{x},\bar{z},\tilde{\theta}) \geqslant \frac{1}{2}\omega_o r_m \|\bar{x}\|^2 + \frac{1}{2}p_m \|\bar{z}\|^2 + \left(\frac{1}{2}\gamma_M^{-1} - \psi_M^2\right)\|\tilde{\theta}\|^2 \tag{3.122}$$

and is thus positive definite for any $\mathbf{\Gamma}$ *satisfying* $\gamma_M < \frac{1}{2}\psi_M^{-2}$. *By taking advantage of the dynamics of the scaled errors* (3.120), *the time derivative of* $V_{3.4}(\bar{x},\bar{z},\tilde{\theta})$ *is obtained as*

$$\begin{aligned}
\dot{V}_{3.4} = & -\frac{1}{2}\omega_c\omega_o \bar{x}^T\bar{x} - \omega_o \bar{x}^T \mathbf{R}\mathbf{b}_n \left(\bar{k}^T \omega_c \mathbf{\Phi}_c \mathbf{\Lambda}_n \mathbf{\Phi}_o^{-1} + \mathbf{b}_m^T\right)\bar{z} \\
& - \omega_o \bar{x}^T \mathbf{R}\mathbf{b}_n (\psi - \psi_r)\theta - \frac{1}{2}\omega_o \bar{z}^T\bar{z} \\
& + \omega_o \bar{z}^T \mathbf{P}\mathbf{d}_m (\psi - \psi_r)\theta + \bar{z}^T \mathbf{P}\mathbf{b}_m \left(\dot{\psi}_r\tilde{\theta} - \psi_r \operatorname{Proj}(\tau)\right) \\
& - \tilde{\theta}^T \mathbf{\Gamma}^{-1} \operatorname{Proj}(\tau) + 2\tilde{\theta}^T \mathbf{M} \operatorname{Proj}(\tau) - \tilde{\theta}^T \mathbf{M}\tilde{\theta} + \tilde{\theta}^T \psi_r^T \psi_r \tilde{\theta}
\end{aligned} \tag{3.123}$$

with $\psi = \psi(t, \mathbf{\Lambda}_n z)$ *and* $\psi_r = \psi(t,\mathbf{x}_r)$ *denoted for brevity. By adding and subtracting the term* $\tilde{\theta}\mathbf{\Gamma}^{-1}\tau$ *and recalling* (3.52) *the following inequality is established,*

$$\begin{aligned}
\dot{V}_{3.4} \leqslant & \left(-\frac{1}{2}\omega_o \left(1 - \varepsilon_1 \left(r_M k_M \left(\frac{\omega_c}{\omega_o}\right)^{n|1} + r_M \right.\right.\right. \\
& \left.\left.\left. + \omega_c^{-n+1|0} p_M \psi_L \theta_M\right)\right) + p_M \gamma_M \psi_M^2 + \frac{1}{2\varepsilon_2}\left(p_M \psi_M \right.\right. \\
& \left.\left. + p_M \gamma_M \psi_M^3 + 2\psi_M^3 \gamma_M + \psi_M\right)^2\right)\|\bar{z}\|^2 + \omega_o \left(-\frac{1}{2}\omega_c \right. \\
& \left. + \omega_c^{-n+1|0} r_M \psi_L \theta_M + \frac{1}{2\varepsilon_1}\left(r_M \left(k_M \left(\frac{\omega_c}{\omega_o}\right)^{n|1} + 1\right)\right.\right. \\
& \left.\left. + \omega_c^{-n+1|0} p_M \psi_L \theta_M\right)\right)\|\bar{x}\|^2 + \left(-\mu e^{-T_{PE}} + 2\psi_M^4 \gamma_M \right. \\
& \left. + \frac{1}{2}\varepsilon_2\right)\|\tilde{\theta}\|^2
\end{aligned} \tag{3.124}$$

for any $\varepsilon_1, \varepsilon_2 \in \mathbb{R}_+$. *More details of the presented calculations are given in Appendix A.2. Derivative* $\dot{V}_{3.4}(\bar{x},\bar{z},\tilde{\theta})$ *is negative definite if* $\mathbf{\Gamma}$ *is chosen to satisfy* $\gamma_M < \frac{1}{2}\mu e^{-T_{PE}}\psi_M^{-4}$, *setting* $\varepsilon_2 < \frac{1}{2}\left(\mu e^{-T_{PE}} - 2\psi_M^4\gamma_M\right)$ *and* ε_1 *small enough, and finally tuning* ω_c *and* ω_o *high enough. Thus positive*

definite $V_{3.4}(\bar{x}, \bar{z}, \tilde{\theta})$ *with negative definite derivative implies the convergence of all errors to the origin.*

The presented analysis consists of a single Lyapunov function used as a basis for the proof of the error convergence in the closed-loop system. Despite the presence of the regressor in the form of function of the state of the plant, the use of two separate functions, as in Theorem 3.2, is not necessary. The proposition of the PIDRC controller based on the reference trajectory is thus of significant importance from the theoretical perspective, as the complete proof of stability is obtained using the standard Lyapunov approach and the exponential converge of the errors is established. This notion justifies a separate proposition of two distinct synthesis methods of the PIESO controller for the plants with a state-dependent regressor. The performance of the considered approach is validated in simulation.

Simulation 3.10. *Consider a third-order system in the form of* (3.112). *The investigated plant is characterized by* $b = 1, \psi = x^T$ *and* $\theta = \begin{bmatrix} -1 & 3 & 3 \end{bmatrix}^T$. *The PIDRC controller is designed with according to* (3.115)–(3.117) *with* $\Gamma = 0.05 I_3$, $\omega_o = 100$ *and* $\omega_c = 1$. *The projection operator is designed as in Remark 3.2 with* $\vartheta_i = 100$ *for* $i \in \{1, 2, 3\}$. *The reference trajectory is chosen as* (3.89) *with* $x_r(t) = \sin(\frac{2\pi}{10}t) + \frac{1}{2}\sin(\frac{2}{3}\pi t)$. *The results of the simulation are given in Fig. 3.22.*

The presented results are in line with the conclusions of Theorem 3.4. The convergence of all errors to the origin is visible and proper identification of the unknown parameters is performed. Evolution of $V_{3.4}(\bar{x}, \bar{z}, \tilde{\theta})$ and its derivative also conform to the expectations formed on the basis of the results of analytical investigations. Similarily, as in Fig. 3.12, the choice of projection operator does not impact the results of the simulation, as the transient values of $\hat{\theta}$ are within bounds imposed by the projection operator throughout the entire simulation. Had the initial errors or character of the system been different, the projection operator would suppress the exceeding growth of the parameters estimates as shown for the case of PIESO observer in Fig. 3.13.

3.3.3 *Adaptation based on the estimated state*

The controller in the form proposed in the previous section is designed with the adaptation procedure based on the reference trajectory. Thus, its operation is dependent on the capability of the conventional ADRC incorporated into the controller to drive the state of the system close enough to the reference trajectory where the adaptation law becomes suitable for a real system. Alternatively, the focus may be given only

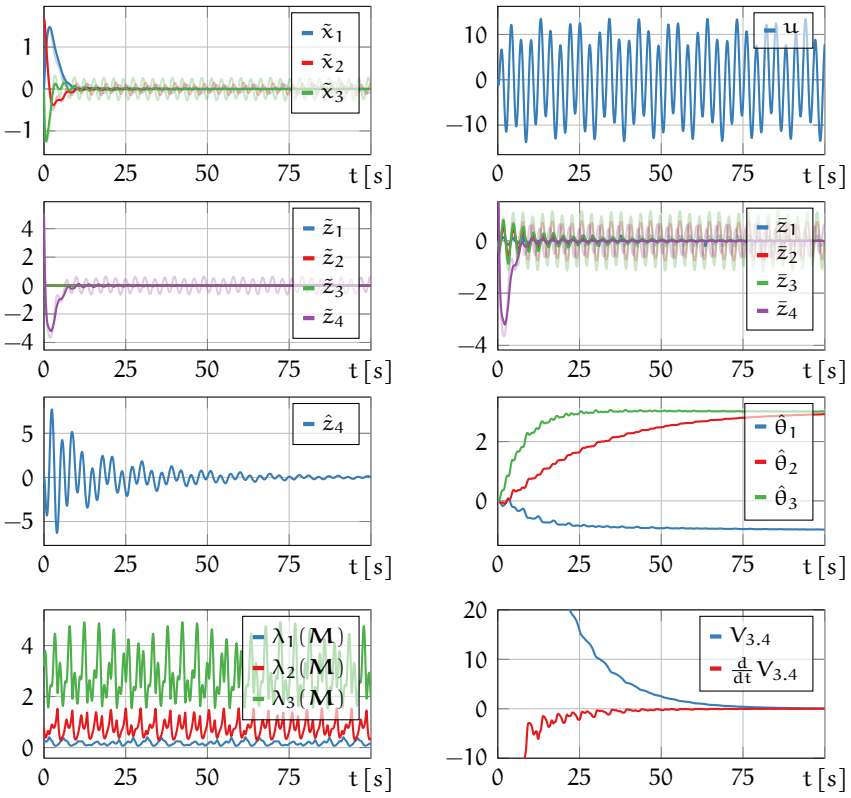

Figure 3.22: Time responses of the third order system with state-dependent regressor under the proposed PIDRC controller designed on the basis of the reference trajectory. Results of conventional ADRC with $\Gamma = 0_3$ shown in transparent plots of $\tilde{x}$, $\tilde{z}$ and $\bar{z}$.

to the abilities of the ESO observer and the adaptation law can be designed employing the estimates of the system. Thus, the performance of ESO in producing the estimates close enough to the real state of the plant becomes crucial in the operation of the algorithm. To this end, by taking into consideration the nominal system (3.112) with an extended state (3.114), the observer is designed incorporating the state estimates as a basis of the regressor evaluation as

$$\dot{\hat{z}} = \mathbf{A}_m \hat{z} + \mathbf{d}_m \left(bu + \psi(t, \Lambda_n \hat{z})\hat{\theta} \right) + l\,(z_1 - \hat{z}_1) \tag{3.125}$$

with $\hat{z} = \begin{bmatrix} \hat{z}_1 & \dots & \hat{z}_m \end{bmatrix}^T \in \mathbb{R}^m$ being the state estimate produced by the observer. By taking advantage of this approach, the parameter adaptation law is synthesized as

$$\dot{\hat{\theta}} = \mathrm{Proj}(\tau, \hat{\theta}, \Theta), \quad \tau = \Gamma \psi^T(t, \Lambda_n \hat{z})\hat{z}_m \tag{3.126}$$

with $\mathrm{Proj}(\cdot)$ satisfying (3.52) and Remarks 3.2 and 3.3. The control law is formulated in the same manner, as

$$u = b^{-1}\left(v - \psi(t, \Lambda_n \hat{z})\hat{\theta} - \hat{z}_m\right) \tag{3.127}$$

with

$$v = k^T\left(x_r - \Lambda_n \hat{z}\right) + x_r^{(n)}. \tag{3.128}$$

The graphical illustration of the considered method is presented in Fig. 3.23.

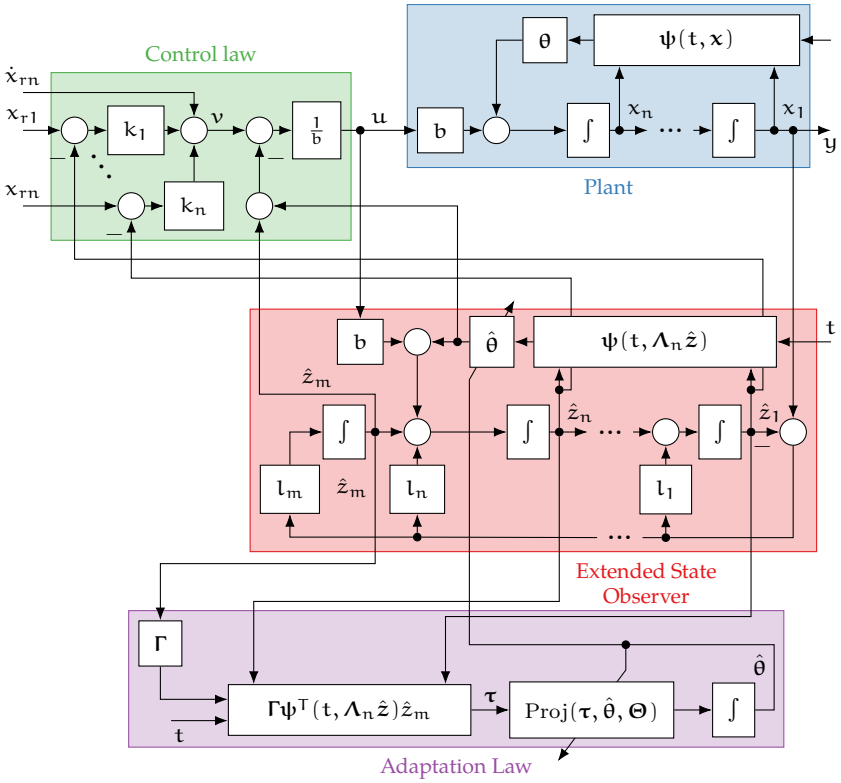

Figure 3.23: The detailed graphical illustration of the considered PIDRC controller with regressor dependent on the state.

The closed-loop system with the proposed PIDRC controller designed on the basis of the state estimates is characterized by the track-

ing, estimation, and adaptation errors with the dynamics expressed by

$$\begin{aligned}
\dot{\tilde{x}} &= G\tilde{x} - W\tilde{z} - b_n\Big((\psi(t, \Lambda_n z) - \psi(t, x_r))\,\tilde{\theta} \\
&\quad + (\psi(t, \Lambda_n z) - \psi(t, \Lambda_n \hat{z}))\,\hat{\theta}\Big), \\
\dot{\tilde{z}} &= H\tilde{z} + d_m\Big((\psi(t, \Lambda_n z) - \psi(t, x_r))\,\tilde{\theta} + \Big(\psi(t, \Lambda_n z) \\
&\quad - \psi(t, \Lambda_n \hat{z})\Big)\hat{\theta}\Big) + b_m\left(\dot{\psi}(t, x_r)\tilde{\theta} - \psi(t, x_r)\,\mathrm{Proj}(\tau)\right), \\
\dot{\tilde{\theta}} &= -\mathrm{Proj}(\tau), \\
\tau &= \Gamma\Big(\left(\psi^T(t, \Lambda_n \hat{z}) - \psi^T(t, \Lambda_n z)\right) + \left(\psi^T(t, \Lambda_n z) - \psi^T(t, x_r)\right) \\
&\quad + \psi^T(t, x_r)\Big)\left(\psi(t, x_r)\tilde{\theta} - b_m^T \tilde{z}\right).
\end{aligned} \tag{3.129}$$

Embracing the tuning method of bandwidth parametrization given by (3.103) and recalling the definition of the scaled tracking and estimation errors in the form of (3.104) yields

$$\begin{aligned}
\dot{\tilde{x}} &= \omega_c \bar{G}\tilde{x} - b_n\left(\bar{k}^T \omega_c \Phi_c \Lambda_n \Phi_o^{-1} + b_m^T\right)\bar{z} - b_n\Big(\Big(\psi(t, \Lambda_n z) \\
&\quad - \psi(t, x_r)\Big)\tilde{\theta} + (\psi(t, \Lambda_n z) - \psi(t, \Lambda_n \hat{z}))\,\hat{\theta}\Big), \\
\dot{\bar{z}} &= \omega_o \bar{H}\bar{z} + \omega_o d_m\Big((\psi(t, \Lambda_n z) - \psi(t, x_r))\,\tilde{\theta} + \Big(\psi(t, \Lambda_n z) \\
&\quad - \psi(t, \Lambda_n \hat{z})\Big)\hat{\theta}\Big) + b_m\left(\dot{\psi}(t, x_r)\tilde{\theta} - \psi(t, x_r)\,\mathrm{Proj}(\tau)\right), \\
\dot{\tilde{\theta}} &= -\mathrm{Proj}(\tau), \\
\tau &= \Gamma\Big(\left(\psi^T(t, \Lambda_n \hat{z}) - \psi^T(t, \Lambda_n z)\right) + \left(\psi^T(t, \Lambda_n z) - \psi^T(t, x_r)\right) \\
&\quad + \psi^T(t, x_r)\Big)\left(\psi(t, x_r)\tilde{\theta} - b_m^T \tilde{z}\right)
\end{aligned} \tag{3.130}$$

with $\bar{G}$ and $\bar{H}$ as given by (3.107). The following theorem summarizes the properties of the proposed solution.

Theorem 3.5. *For system* (3.112) *satisfying Assumptions 3.3, 3.7 and 3.8, the control law* (3.127) *with observer* (3.125) *and adaptation law* (3.126) *guarantees a global asymptotic convergence of errors* $\tilde{x}$, $\tilde{z}$ *and* $\tilde{\theta}$ *to the origin under the tuning proposed by Assumption 3.9 for* ω_o *and* ω_c *chosen high enough and* Γ *chosen with a norm small enough.*

Proof. *Similarily to the approach employed in the analysis of Theorem 3.2 on the PIESO observer synthesized on the basis of the state estimate, proof of the considered theorem is carried in two distinct steps. Initially, taking*

advantage of the properties of the projection operator, the boundedness of the tracking and estimation errors is established. Then, this notion is embraced to proof the convergence of all errors to the origin. Consider first the auxiliary function

$$\begin{aligned} V_{3.5}^{*}(\bar{\mathbf{x}},\bar{\mathbf{z}}) = \frac{1}{2}\omega_o \bar{\mathbf{x}}^{\mathsf{T}}\mathbf{R}\bar{\mathbf{x}} + \frac{1}{2}\bar{\mathbf{z}}^{\mathsf{T}}\mathbf{P}\bar{\mathbf{z}} + \frac{1}{2}\tilde{\boldsymbol{\theta}}^{\mathsf{T}}\boldsymbol{\Gamma}^{-1}\tilde{\boldsymbol{\theta}} \\ - \bar{\mathbf{z}}^{\mathsf{T}}\mathbf{P}\mathbf{b}_m\boldsymbol{\psi}(t,\mathbf{x}_r)\tilde{\boldsymbol{\theta}}, \end{aligned} \tag{3.131}$$

which satisfies

$$\begin{aligned} V_{3.5}^{*}(\bar{\mathbf{x}},\bar{\mathbf{z}}) \geqslant \frac{1}{2}\omega_o r_m \|\bar{\mathbf{x}}\|^2 + \frac{1}{2}\left(p_m - \varepsilon\left(p_M\psi_M\right)\right)\|\bar{\mathbf{z}}\|^2 \\ + \frac{1}{2}\left(\gamma_M^{-1} - \frac{1}{\varepsilon}p_M\psi_M\right)\left\|\tilde{\boldsymbol{\theta}}\right\|^2 \end{aligned} \tag{3.132}$$

for any $\varepsilon \in \mathbb{R}_+$. Thus, $V_{3.5}^{*}(\bar{\mathbf{x}},\bar{\mathbf{z}})$ is positive for any choice of $\boldsymbol{\Gamma}$ satisfying $\gamma_M < \varepsilon\left(p_M\psi_M^2\right)^{-1}$ with $\varepsilon < p_m\left(p_M\psi_M\right)^{-1}$. The time derivative of $V_{3.5}^{*}(\bar{\mathbf{x}},\bar{\mathbf{z}})$ takes the form of

$$\begin{aligned} \dot{V}_{3.5}^{*} = &-\frac{1}{2}\omega_c\omega_o\bar{\mathbf{x}}^{\mathsf{T}}\bar{\mathbf{x}} - \omega_o\bar{\mathbf{x}}^{\mathsf{T}}\mathbf{R}\mathbf{b}_n\left(\bar{\mathbf{k}}^{\mathsf{T}}\omega_c\boldsymbol{\Phi}_c\boldsymbol{\Lambda}_n\boldsymbol{\Phi}_o^{-1} + \mathbf{b}_m^{\mathsf{T}}\right)\bar{\mathbf{z}} \\ &- \omega_o\bar{\mathbf{x}}^{\mathsf{T}}\mathbf{R}\mathbf{b}_n\left(\left(\boldsymbol{\psi}-\boldsymbol{\psi}_r\right)\tilde{\boldsymbol{\theta}} + \left(\boldsymbol{\psi}-\hat{\boldsymbol{\psi}}\right)\hat{\boldsymbol{\theta}}\right) - \frac{1}{2}\omega_o\bar{\mathbf{z}}^{\mathsf{T}}\bar{\mathbf{z}} \\ &+ \omega_o\bar{\mathbf{z}}^{\mathsf{T}}\mathbf{P}\mathbf{d}_m\left(\left(\boldsymbol{\psi}-\boldsymbol{\psi}_r\right)\tilde{\boldsymbol{\theta}} + \left(\boldsymbol{\psi}-\hat{\boldsymbol{\psi}}\right)\hat{\boldsymbol{\theta}}\right) \\ &- \tilde{\boldsymbol{\theta}}^{\mathsf{T}}\boldsymbol{\Gamma}^{-1}\operatorname{Proj}(\boldsymbol{\tau}) - \omega_o\tilde{\boldsymbol{\theta}}^{\mathsf{T}}\boldsymbol{\psi}_r^{\mathsf{T}}\mathbf{b}_m^{\mathsf{T}}\mathbf{P}\bar{\mathbf{H}}\bar{\mathbf{z}} \\ &- \omega_o\tilde{\boldsymbol{\theta}}^{\mathsf{T}}\boldsymbol{\psi}_r^{\mathsf{T}}\mathbf{b}_m^{\mathsf{T}}\mathbf{P}\mathbf{d}_m\left(\left(\boldsymbol{\psi}-\boldsymbol{\psi}_r\right)\tilde{\boldsymbol{\theta}} + \left(\boldsymbol{\psi}-\hat{\boldsymbol{\psi}}\right)\hat{\boldsymbol{\theta}}\right) \\ &- \tilde{\boldsymbol{\theta}}^{\mathsf{T}}\boldsymbol{\psi}_r^{\mathsf{T}}\mathbf{b}_m^{\mathsf{T}}\mathbf{P}\mathbf{b}_m\left(\dot{\boldsymbol{\psi}}_r\tilde{\boldsymbol{\theta}} - \boldsymbol{\psi}_r\operatorname{Proj}(\boldsymbol{\tau})\right) \end{aligned} \tag{3.133}$$

and satisfies

$$\begin{aligned} \dot{V}_{3.5}^{*} \leqslant \omega_o\Bigg(&-\frac{1}{2}\omega_c + r_M\psi_L\theta_M\omega_c^{-n+1|0} + \frac{1}{2\varepsilon}\Bigg(r_M k_M\left(\frac{\omega_c}{\omega_o}\right)^{n|1} \\ &+ r_M + p_M\psi_L\theta_M\omega_c^{-n+1|0}\Bigg)\Bigg)\|\bar{\mathbf{x}}\|^2 \\ &+ \Bigg(-\frac{1}{2}\omega_o\Bigg(1 - \varepsilon\Bigg(r_M k_M\left(\frac{\omega_c}{\omega_o}\right)^{n|1} + r_M \\ &+ p_M\psi_L\theta_M\omega_c^{-n+1|0}\Bigg)\Bigg) + \omega_c^{-n+1|0}p_M\psi_L\theta_M \\ &+ \omega_o^{-n|-1}\left(\theta_M\psi_L + \theta_M p_M\gamma_M\psi_M^2\psi_L\right)\Bigg)\|\bar{\mathbf{z}}\|^2 \end{aligned}$$

$$+\left(\omega_c^{-n+1|0} r_M \psi_L \theta_M + \omega_c^{-n+1|0}\left(\theta_M p_M \gamma_M \psi_L \psi_M^2 + \theta_M \psi_L\right)\right)\|\bar{x}\|\,\|\bar{z}\| + \left(\omega_o \theta_M \psi_M p_M h_M + \theta_M p_M \gamma_M \psi_M^3 + \theta_M \psi_M + \omega_o^{-n+1|0}\theta_M^2 \psi_M p_M \psi_L + \omega_o^{-n|-1}\left(\theta_M^2 \psi_L \psi_M + p_M \gamma_M \psi_L \psi_M^3 \theta_M^2\right)\right)\|\bar{z}\| + \omega_c^{-n+1|0}\left(\omega_o \theta_M^2 \psi_M p_M \psi_L + \theta_M^2 \psi_L \psi_M + p_M \gamma_M \psi_L \psi_M^3 \theta_M^2\right)\|\bar{x}\| + p_M \gamma_M \psi_M^4 \theta_M^2 \tag{3.134}$$

for any $\varepsilon \in \mathbb{R}_+$ *with* $h_M = \|\bar{H}\| \in \mathbb{R}_+$. *By setting* ε, ω_c *and finally* ω_o *high enough, this expression is made negative definite for* $\|\bar{x}\|$ *and* $\|\bar{z}\|$ *large enough. It is inferred, that* $\bar{x}$ *and* $\bar{z}$ *converge to some neighborhood of the origin, and there exist some constants* $x_M, z_M, T_{xz} \in \mathbb{R}_+$, *such that* $\|\bar{x}\| \leqslant x_M$ *and* $\|\bar{z}\| \leqslant z_M$ *for any* $t \geqslant T_{xz}$. *Similarily as in the proof of Theorem 3.2, it can be shown that* x_M *and* z_M *remain bounded with the growth of* ω_o *and* ω_c *and thus the proper tuning of the algorithm is not hindered.*

By taking advantage of the established notion of the boundedness of the tracking and estimation errors, the convergence of all errors in the considered system can be proved. To this end, consider the function in the form of

$$V_{3.5}(\bar{x}, \bar{z}, \tilde{\theta}) = \frac{1}{2}\omega_o \bar{x}^T \mathbf{R} \bar{x} + \frac{1}{2}\bar{z}^T \mathbf{P} \bar{z} + \tilde{\theta}^T \left(\frac{1}{2}\Gamma^{-1} - \mathbf{M}(t, x_r)\right)\tilde{\theta}. \tag{3.135}$$

The proposed function satisfies

$$V_{3.5}(\bar{x}, \bar{z}, \tilde{\theta}) \geqslant \frac{1}{2}\omega_o r_m \|\bar{x}\|^2 + \frac{1}{2} p_m \|\bar{z}\|^2 + \left(\frac{1}{2}\gamma_M^{-1} - \psi_M^2\right)\|\tilde{\theta}\|^2 \tag{3.136}$$

and is positive definite for any Γ *satisfying* $\gamma_M < \frac{1}{2}\psi_M^{-2}$. *Calculation of the time derivative of this function yields*

$$\begin{aligned}\dot{V}_{3.5} = &-\frac{1}{2}\omega_c \omega_o \bar{x}^T \bar{x} - \omega_o \bar{x}^T \mathbf{R} \mathbf{b}_n \left(\bar{k}^T \omega_c \mathbf{\Phi}_c \mathbf{\Lambda}_n \mathbf{\Phi}_o^{-1} + \mathbf{b}_m^T\right)\bar{z} \\ &- \omega_o \bar{x}^T \mathbf{R} \mathbf{b}_n \left((\psi - \psi_r)\tilde{\theta} + \left(\psi - \hat{\psi}\right)\hat{\theta}\right) - \frac{1}{2}\omega_o \bar{z}^T \bar{z} \\ &+ \omega_o \bar{z}^T \mathbf{P} \mathbf{d}_m \left((\psi - \psi_r)\tilde{\theta} + \left(\psi - \hat{\psi}\right)\hat{\theta}\right) + \bar{z}^T \mathbf{P} \mathbf{b}_m \Big(\dot{\psi}_r \tilde{\theta} \\ &- \psi_r \operatorname{Proj}(\tau)\Big) - \tilde{\theta}^T \Gamma^{-1} \operatorname{Proj}(\tau) - \tilde{\theta}^T \mathbf{M} \tilde{\theta} \\ &- 2\tilde{\theta}^T \mathbf{M} \operatorname{Proj}(\tau) + \tilde{\theta}^T \psi_r^T \psi_r \tilde{\theta}.\end{aligned} \tag{3.137}$$

This can be further transformed by adding and subtracting the term $\tilde{\theta}\Gamma^{-1}\tau$ *and recalling the property given by* (3.52) *to obtain*

$$\begin{aligned}
\dot{V}_{3.5} \leqslant & \Bigg(\omega_o\Bigg(-\frac{1}{2}\omega_c + \omega_c^{-n+1|0}\theta_M r_M \psi_L + \frac{1}{2\varepsilon_1}\Bigg(r_M \\
& + r_M k_M \left(\frac{\omega_c}{\omega_o}\right)^{n|1} + \omega_c^{-n+1|0} p_M \theta_M \psi_L\Bigg)\Bigg) \\
& + \frac{1}{2}\theta_M\Big(\omega_c^{-n+1|0} r_M \psi_L + \omega_c^{-n+1|0}\Big(p_M \gamma_M \psi_L \psi_M^2 \\
& + \psi_L + 2\psi_M^2 \gamma_M \psi_L\Big)\Big) + \frac{1}{2\varepsilon_2}\Big(\omega_c^{-n+1|0}\Big(\theta_M \psi_L \psi_M \\
& + 2\theta_M \gamma_M \psi_M^3 \psi_L\Big)\Big)^2\Bigg)\|\bar{x}\|^2 + \Bigg(\frac{1}{2}\omega_o\Bigg(-1 + \varepsilon_1\Big(r_M \\
& + r_M k_M \left(\frac{\omega_c}{\omega_o}\right)^{n|1} + \omega_c^{-n+1|0} p_M \theta_M \psi_L\Big)\Bigg) \\
& + \omega_c^{-n+1|0} p_M \theta_M \psi_L + \omega_c^{-n+1|0} x_M p_M \gamma_M \psi_M \psi_L \\
& + \omega_o^{-n|-1}\Big(p_M \gamma_M \psi_L \psi_M^2 \theta_M + z_M p_M \gamma_M \psi_M \psi_L \\
& + \theta_M \psi_L + 2\theta_M \psi_M^2 \gamma_M \psi_L\Big) + p_M \gamma_M \psi_M^2 \\
& + \frac{1}{2}\Big(\omega_c^{-n+1|0}\theta_M r_M \psi_L + \omega_c^{-n+1|0}\Big(p_M \gamma_M \psi_L \psi_M^2 \theta_M \\
& + \theta_M \psi_L + 2\theta_M \psi_M^2 \gamma_M \psi_L\Big)\Big) + \frac{1}{2\varepsilon_3}\Big(p_M \gamma_M \psi_M^3 \\
& + p_M \psi_M + \psi_M + 2\gamma_M \psi_M^3 + \omega_o^{-n|-1}\Big(\theta_M \psi_M \psi_L \\
& + 2\theta_M \gamma_M \psi_M^3 \psi_L\Big)\Big)^2\Bigg)\|\bar{z}\|^2 + \Bigg(-\mu e^{-T_{PE}} + 2\gamma_M \psi_M^4 \\
& + \frac{1}{2}\varepsilon_2 + \frac{1}{2}\varepsilon_3\Bigg)\|\tilde{\theta}\|^2
\end{aligned} \tag{3.138}$$

for any $\varepsilon_1, \varepsilon_2, \varepsilon_3 \in \mathbb{R}_+$. *More detailed calculations are shown in Appendix A.2. The first terms of the expressions associated with squares of* $\|\bar{x}\|$ *and* $\|\bar{z}\|$ *are negative for* ε_1 *and ratio of* ω_c *and* ω_o *small enough with* ω_c *high enough. The coefficient of the square of* $\|\tilde{\theta}\|$ *is negative for* $\varepsilon_2, \varepsilon_3$ *and* Γ *small enough. Finally, the negative definiteness of the entire function is guaranteed by choosing* ω_o *high enough. Thus, the errors in the system exponentially converge to the origin once the tracking and estimation errors reach the neighborhood of the origin which is ensured by the earlier analysis.*

In order to verify the characteristics of the proposed PIDRC controller designed on the basis of the state estimates, the numerical simulation is conducted.

Simulation 3.11. *The third order system is considered with the dynamics given by* (3.112) *and* $b = 1, \psi = x^T, \theta = \begin{bmatrix} -1 & 3 & 3 \end{bmatrix}^T$. *The controller is*

synthesized according to (3.125)–(3.127) *and tuned with* $\Gamma = 0.05\mathbf{I}_3, \omega_o = 100, \omega_c = 1$. *The projection operator is incorporated according to Remark 3.2 with* $\vartheta_i = 100$ *for* $i \in \{1, 2, 3\}$. *The reference trajectory to be tracked is chosen as* (3.89) *with* $x_r(t) = \sin(\frac{2\pi}{10}t) + \frac{1}{2}\sin(\frac{2\pi}{3}t)$. *The obtained results are given in Fig. 3.24.*

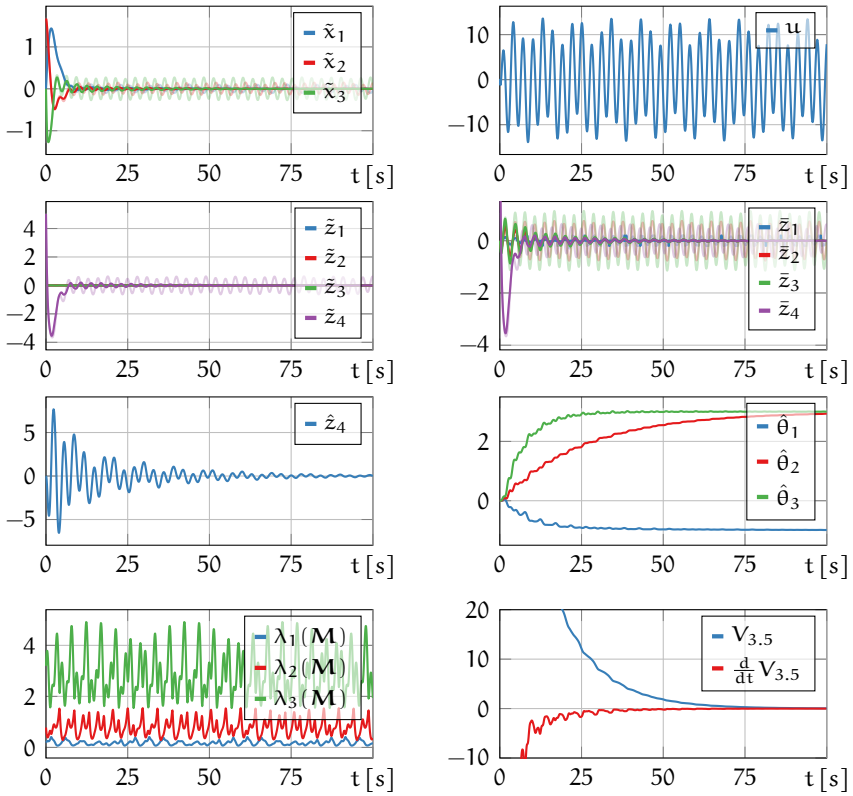

Figure 3.24: Time responses of the third order system with state-dependent regressor under the proposed PIDRC controller designed on the basis of state estimates. Results of conventional ADRC with $\Gamma = 0_3$ shown in transparent plots of $\tilde{x}$, $\tilde{z}$ and $\bar{z}$.

The results of the simulation show the effectiveness of the proposed control scheme in the task of reference trajectory tracking in the presence of parametric uncertainty of the plant. The convergence of the tracking, estimation, and identification errors to the origin is achieved, with the evolution of the signals resembling that presented in Fig. 3.22. Importantly, this similarity is not guaranteed in all cases and the advised choice of the controller based either on the reference trajectory or estimated state depends on the properties of the considered system. In the plots only the evolution of $V_{3.2}(\bar{x}, \bar{z}, \tilde{\theta})$ is given, as the analysis of the auxiliary function $V^*_{3.2}(\bar{x}, \bar{z})$ appears to be required only in some specific cases of exceedingly large transient estimation and tracking error, which is not a case in the considered scenario.

3.4 EXPERIMENTAL VALIDATION

The PIESO and PIDRC algorithms proposed in the proceeding section constitute a novel solution to the problem of adaptive control and state estimation in the presence of parametric uncertainty of the plant. Thanks to their straightforward interpretation and intuitive design they may be easily applied to a wide variety of practical problems. Yet, presented analysis and numerical trials on simplified systems unveiled only the theoretical properties of these methods and rigorous experimental verification of their performance in real-life scenarios is necessary. To this end, the application of the considered algorithms to two distinct mobile robotic systems is studied. At first, the results of the identification of the dynamic model of the hovercraft platform are presented on the basis of findings reported in [229]. It is shown that the proposed PIESO observer is capable of successful identification of the entire set of parameters of the strongly underactuated dynamic system. In the second part of this section, the series of experiments on both identification and adaptive control of the two-wheeled mobile robot is presented following the results of [230]. Notably, both examples discussed in this section do not strictly conform to the nominal structure of the system considered in Section 3.2 and 3.3, and thus the presented results unveil some flexibility of the proposed algorithms as highlighted already in Section 3.2.3.

3.4.1 *Identification of the hovercraft system*

The hovercraft is a type of mobile vehicle utilizing an air cushion to reduce the friction between the vehicle and the ground, and the propeller providing the thrusting force. Such systems are inherently characterized by high inertia of movement and are highly underactuated as the direction and magnitude of the thrust generated by the propeller are usually the only control signals of the device. Some of the earliest results on the automated control of hovercraft vehicles have been reported in [66, 235] and considered the problem of position stabilization only. These solutions either required full knowledge of the dynamics of the system or assumed a simplified model without any parameters, thus limiting the performance of the controller. In the papers [267–269] the advantage has been taken of the property of the differential flatness to solve the problem of the trajectory tracking of the discussed plant. Solutions employing the traversal functions were also reported in [25, 94, 202]. Many of these methods refer to the simplified model of the hovercraft which may hinder their application in real-life scenarios. Recently, attempts to lift this limitation by incorporating parameter identification schemes into the control

algorithms have been made. The solution employing the Kalman filter used to online estimate the parameters of the plant and combined with the input-output decoupling algorithm was presented in [37]. The assumption was made that the velocities of the platform are measurable and the hovercraft was modeled as a first-order system with parametric uncertainty. The control schemes with incorporated adaptation algorithms have also been reported in [125, 311] with the focus given mainly to the identification of the friction effect. Following the ADRC paradigm, the controllers utilizing the extended state observer to estimate the impact of the unmodeled dynamics without explicit identification of the model of the vehicle have been proposed in [201, 301].

An alternative solution to the problem of the control of the hovercraft can be proposed by utilizing the PIESO observer to estimate the parameters of the system and subsequently employ them in one of the nonadaptive model-based controllers suitable for the dynamics of the hovercraft system. Such an application of the adaptive observer in the task of parameter identification is covered in this section. To this end, consider the experimental testbed consisting of the remotely controlled hovercraft model. The discussed vehicle employs two separate propellers to generate lift and thrust forces, with the latter coupled with a simple rudder used to control the direction of the vehicle movement. The detailed description of the considered plant is given in Section 4.1 and the schematic view of the system is shown in Fig. 3.25. Consider

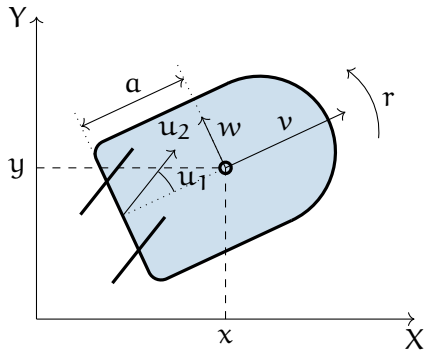

Figure 3.25: Scheme of the kinematics of the hovercraft robot

the dynamics of the hovercraft system expressed by the following non-affine system,

$$\begin{aligned} \dot{\mathbf{q}} &= \mathbf{R}(\varphi)\mathbf{x}, \\ \dot{\mathbf{x}} &= -\mathbf{D}\mathbf{x} + \mathbf{b}(u_1)u_2 + \mathbf{c}(\mathbf{x}) \end{aligned} \tag{3.139}$$

with the rotation matrix $\mathbf{R}(\varphi) \in \mathbb{R}^{3\times3}$ is given by

$$\mathbf{R}(\varphi) = \begin{bmatrix} \cos(\varphi) & -\sin(\varphi) & 0 \\ \sin(\varphi) & -\cos(\varphi) & 0 \\ 0 & 0 & 1 \end{bmatrix} \tag{3.140}$$

and used to transform the velocities of the hovercraft between the body frame and the inertial frame. The term $\mathbf{q} = \begin{bmatrix} x & y & \varphi \end{bmatrix}^T \in \mathbb{R}^3$ corresponds to the position and orientation of the hovercraft in the inertial frame, $\mathbf{x} = \begin{bmatrix} v & w & r \end{bmatrix}^T \in \mathbb{R}^3$ stands for the linear and angular velocity of the platform in the local coordinate system, and $\mathbf{u} = \begin{bmatrix} u_1 & u_2 \end{bmatrix}^T \in \mathbb{R}^2$ are input signals representing the orientation of the rudder and the control signal of the propeller correspondingly. Damping matrix $\mathbf{D} = \text{diag}(\frac{\sigma_v}{m}, \frac{\sigma_w}{m}, \frac{\sigma_r}{J}) \in \mathbb{R}^{3\times3}$ represents the friction forces and aerodynamic drag impacting the moving hovercraft with $\sigma_v, \sigma_w, \sigma_r \in \mathbb{R}_+$ being the damping coefficients in each direction of the local coordinate system and $m, J \in \mathbb{R}_+$ standing for the mass and inertia of the robot. The term $\mathbf{b} = \begin{bmatrix} \frac{b}{m}\cos(u_1) & \frac{b}{m}\sin(u_1) & -\frac{b}{J}a\sin(u_1) \end{bmatrix}^T \in \mathbb{R}^3$ describes the input gains in each of degrees of freedom with respect to the orientation of the rudder and $b \in \mathbb{R}_+$ representing the scaling between the input signal u_2 and the thrusting force generated by the propeller. Constant $a \in \mathbb{R}_+$ is a distance between the propeller and the center of the mass of the hovercraft. Moreover, $\mathbf{c}(\mathbf{x}) = \begin{bmatrix} wr & -vr & 0 \end{bmatrix}^T \in \mathbb{R}^3$ stands for the nonlinear couplings due to the centifugal effects.

The problem of the parameter identification of system (3.139) is considered under an assumption that all of the physical parameters, namely $\sigma_v, \sigma_w, \sigma_r, m, J, a$ and b, are unknown, but the local velocities $\mathbf{x}$ of the system are available for direct measurement. In order to design the adaptive PIESO observer, the dynamics of the system are rewritten following the footsteps of [37] to obtain

$$\dot{\mathbf{x}} = \boldsymbol{\Psi}(\mathbf{u}, \mathbf{x})\boldsymbol{\theta} + \mathbf{c}(\mathbf{x}) \tag{3.141}$$

with $\boldsymbol{\Psi}(\mathbf{u}, \mathbf{x}) \in \mathbb{R}^{3\times5}$ being new regressor of the system and $\boldsymbol{\theta} \in \mathbb{R}^5$ standing for the lumped parameters of the plant. Specifically, taking advantage of dynamics (3.139), expressions $\boldsymbol{\Psi}(\mathbf{u}, \mathbf{x})$ and $\boldsymbol{\theta}$ are given as

$$\boldsymbol{\Psi}(\mathbf{u}, \mathbf{x}) = \begin{bmatrix} -v & 0 & 0 & \cos(u_1)u_2 & 0 \\ 0 & -w & 0 & \sin(u_1)u_2 & 0 \\ 0 & 0 & -r & 0 & -\sin(u_1)u_2 \end{bmatrix} \tag{3.142}$$

and

$$\boldsymbol{\theta} = \begin{bmatrix} \frac{\sigma_v}{m} & \frac{\sigma_w}{m} & \frac{\sigma_r}{J} & \frac{b}{m} & \frac{ab}{J} \end{bmatrix}^T. \tag{3.143}$$

The system expressed by (3.141) can be interpreted as the composition of three distinct first-order systems governing movement in each degree of freedom coupled by the impact of $\mathbf{c}(\mathbf{x})$ matrix. Notably, the dimension of θ is lower than the number of unknown physical parameters and thus only the estimation of the accumulated parameters is considered and the recovery of the full set of coefficients of the nominal system is not possible. Parameters m and a are nonetheless relatively easy to measure in practical scenarios and an advantage may be taken of this notion to calculate the values of physical parameters on the basis of produced estimates.

In order to design a suitable PIESO observer, the dynamics of the system are further transformed into

$$\begin{aligned} \dot{\mathbf{x}} &= \boldsymbol{\Psi}(\mathbf{u},\mathbf{x})\hat{\theta} + \mathbf{c}(\mathbf{x}) + \boldsymbol{\delta}, \\ \dot{\boldsymbol{\delta}} &= \frac{d}{dt}\left(\boldsymbol{\Psi}(\mathbf{u},\mathbf{x})\left(\theta - \hat{\theta}\right)\right), \end{aligned} \tag{3.144}$$

where $\hat{\theta} \in \mathbb{R}^5$ is the estimate of the unknown parameters and $\boldsymbol{\delta} = \boldsymbol{\Psi}(\mathbf{u})\big(\theta - \hat{\theta}\big) \in \mathbb{R}^3$ is the total disturbance in each degree of freedom. Importantly, as the velocities of the platform and the control signals are assumed to be known or measurable, the terms $\boldsymbol{\Psi}(\mathbf{u})$ and $\mathbf{c}(\mathbf{x})$ are known and can be evaluated at any time instant. The design procedure for the system with the regressor being the function of time is thus followed. Namely, extended state is defined as $\mathbf{z} = \begin{bmatrix} \mathbf{x}^T & \boldsymbol{\delta}^T \end{bmatrix}^T \in \mathbb{R}^6$ and the adaptive observer is designed in the form of

$$\begin{aligned} \dot{\hat{\mathbf{x}}} &= \boldsymbol{\Psi}(\mathbf{u})\hat{\theta} + \mathbf{c}(\mathbf{x}) + \hat{\boldsymbol{\delta}} + l_1\left(\mathbf{x} - \hat{\mathbf{x}}\right), \\ \dot{\hat{\boldsymbol{\delta}}} &= l_2\left(\mathbf{x} - \hat{\mathbf{x}}\right) \end{aligned} \tag{3.145}$$

with $\hat{\mathbf{z}} = \begin{bmatrix} \hat{\mathbf{x}}^T & \hat{\boldsymbol{\delta}}^T \end{bmatrix}^T \in \mathbb{R}^6$ being an estimate of the extended state of the system and $\mathbf{l} = \begin{bmatrix} l_1 & l_2 \end{bmatrix}^T \in \mathbb{R}^2_+$ representing gains of the observer. The dependence of $\boldsymbol{\Psi}(\mathbf{u},\mathbf{x})$ on $\mathbf{x}$ is ommited in the observer definition and subsequent analysis, as the hovercraft velocities are assumed to be measurable and thus do not impact the identification procedure. The structure of the observer may also be viewed as a combination of three separate observers designed for each degree of freedom. The adaptation law for the parameter estimation is synthesized as

$$\dot{\hat{\theta}} = \boldsymbol{\Gamma}\boldsymbol{\Psi}^T(\mathbf{u})\hat{\boldsymbol{\delta}} \tag{3.146}$$

with adaptation gains chosed for simplicity as $\boldsymbol{\Gamma} = \gamma \mathbf{I}_5 \in \mathbb{R}^{5\times 5}_+$, where $\gamma \in \mathbb{R}_+$ is some positive gain coefficient.

Remark 3.4. *Notably, the structure of regressor $\boldsymbol{\Psi}(\mathbf{u})$ leads to inherent redundancy of the identifier, as parameter θ_4 is identified through both the first and the second element of the total disturbance $\boldsymbol{\delta}$. In some practical*

scenarios, it may be advised to modify the adaptation law and employ only one of these signals. Such a procedure may improve the performance of the algorithm, e. g. when the velocity measurement of one of the axes is expected to be of lower quality. Nonetheless, in the experiments presented here, the conventional form of the PIESO as given by (3.145) *and* (3.146) *is employed.*

To verify the feasibility of the proposed PIESO observer for the hovercraft system with three degrees of freedom, a numerical simulation is first conducted.

Simulation 3.12. *Consider the system with dynamics given by* (3.139) *with the physical parameters chosen as* $\sigma_v = 0.5\,\mathrm{kg/s}$, $\sigma_w = 0.6\,\mathrm{kg\,m^2/s}$, $\sigma_r = 0.7\,\mathrm{kg/s}$, $m = 1\,\mathrm{kg}$, $J = 2\,\mathrm{kg\,m^2}$, $a = 0.5\,\mathrm{m}$ *and* $b = 1$ *to yield*

$$\theta = \begin{bmatrix} 0.5 & 0.6 & 0.35 & 1 & 0.25 \end{bmatrix}^T. \tag{3.147}$$

The PIESO observer is implemented according to the presented approach and is tuned with $l = \begin{bmatrix} 20 & 100 \end{bmatrix}^T$ *and* $\gamma = 10$. *The control signals of the robot are chosen as* $u = \begin{bmatrix} \sin(0.01\pi t) & 0.6\sin(0.03\pi t) \end{bmatrix}^T$. *The results of the simulation are given in Fig. 3.26.*

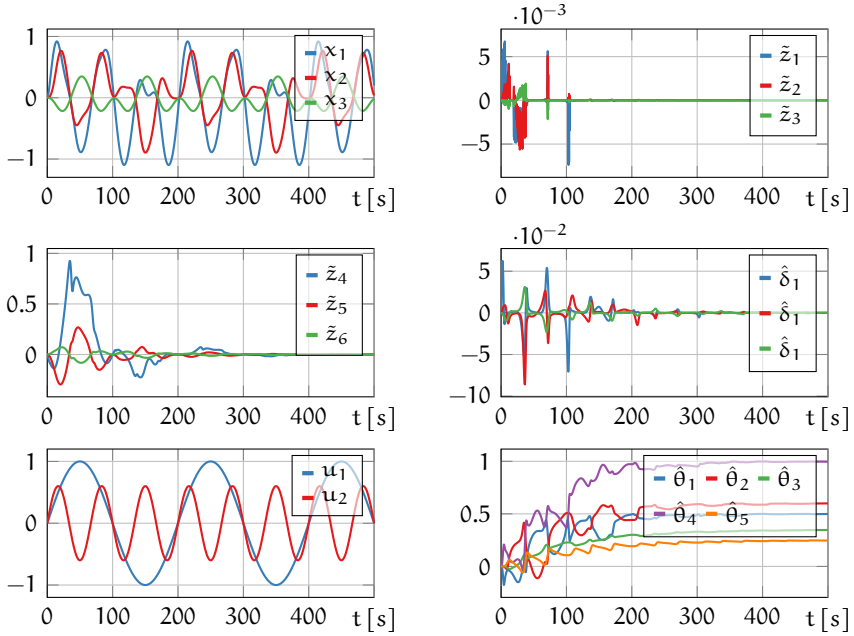

Figure 3.26: Time responses of simulation of the hovercraft identification using PIESO observer.

The trajectories of the extended state estimation errors, the disturbance estimates, the control signals, and the parameter estimates are presented. It is shown that both the estimation errors and the disturbance estimates itself converge to the origin as the simulation progresses. The convergence of the parameter estimates to their nominal values, as given by (3.147), is also visible. Notably, despite the

simplicity of the chosen control signals all of the parameters are correctly identified and their real values are recovered. Due to the low frequency of the employed control inputs only moderate level of system excitation is achieved and the adaptation procedure is relatively slow in spite of the high values of the chosen adaptation gains. The higher speed of the adaptation can be obtained by choosing the control signals of the higher frequencies. Moreover, the use of control signals with a greater number of distinct frequencies, e. g. in the form of a sum of multiple sine waves, tends to lead to smoother trajectories of the parameter and disturbance estimates, which may have significant importance in some of the practical scenarios.

Following the presented numerical trials, the experimental evaluation of the proposed algorithm is conducted.

Experiment 3.1. *The experiment with a laboratory-scale hovercraft model is conducted and the identification procedure is carried out. Due to the character of the robot, the control signals are generated live during the experiment by the operator through the keyboard input. It is thus ensured that the movement of the robot is rich enough to satisfy the PE condition while simultaneously collisions with any external obstacles are avoided in the limited space of the laboratory. Throughout the trial, the velocities of the robot are measured according to the method outlined in Section 4.1 making it possible to implement the identification algorithm in the form given by* (3.145) *and* (3.146)*. The results of the experiment are illustrated in Fig. 3.27.*

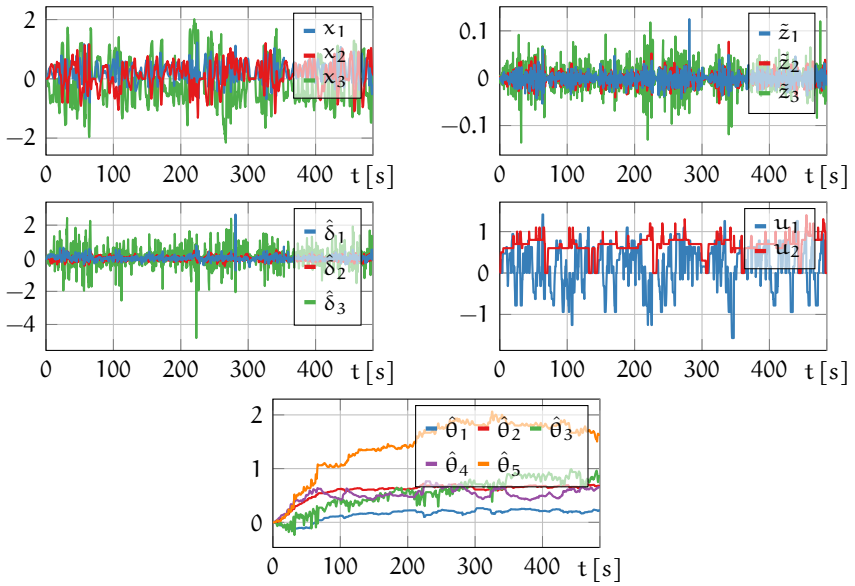

Figure 3.27: Time responses of the experiment of the hovercraft identification using PIESO observer.

The presented plots show that the parameter estimates of the system converge to the neighborhood of some constant values in the real-life

scenario. Namely, the parameters in the final time instant take the values of

$$\hat{\theta} \approx \begin{bmatrix} 0.2289 & 0.6751 & 0.8333 & 0.6543 & 1.6287 \end{bmatrix}^{T}. \tag{3.148}$$

Notably, the presented plots unveil the presence of significant noise in the measured velocities of the robot which were obtained numerically from the position measurements of the motion capture system. In the result, the estimates of the total disturbance do not converge to the origin in the considered trial but are characterized by the presence of some nonzero noise disturbing the estimated values. The successful identification of the parameters is nonetheless achieved. Although the true parameters of the system are unknown, some preliminary investigations imply that $\frac{b}{m} = \theta_4 \approx 0.7$ and $\frac{\sigma_v}{m} = \theta_1 \approx 0.48$. It can be noted that the PIESO observer produced a very similar value of the parameter associated with the input gain. The quality of the friction force estimation is significantly lower, which may be explained by the differences between the effects of the real friction phenomenon impacting the vehicle and the strongly simplified model of the damping forces assumed in the observer synthesis. Moreover, the real hovercraft robot is subject to numerous external disturbances affecting the quality of obtained parameter estimates.

In order to verify the correctness of the obtained results, an additional trial is performed and its results are compared with the simulations of dynamics (3.139) with parameters (3.148).

Simulation 3.13. *Several time instants are chosen from the experimental data and the measured configurations of the robot are employed as the initial conditions in the simulations of the hovercraft model. The input signals in the simulation are also consistent with those from the experimental trial. In Fig. 3.28 the comparison of trajectories on* (X, Y) *plane obtained from the experiment and simulation is given.*

The similarity of the overall character of the movement in simulation and experiment is shown. Although the trajectories of the experimental hovercraft and its numerical counterpart tend to diverge in all cases due to the open loop integration in the simulated model, the quality of identification may be deemed good enough in the short time horizon. Specifically, the distance traversed in both cases is roughly the same in all trials which signifies the correctness of the input gain of the propeller estimation. More significant differences are observed in the rotational movement of the platform, as the simulated hovercraft tend to display higher rotational inertia. This effect may be associated with a lower quality of the identification of damping forces which limit the free rotations of the real vehicle.

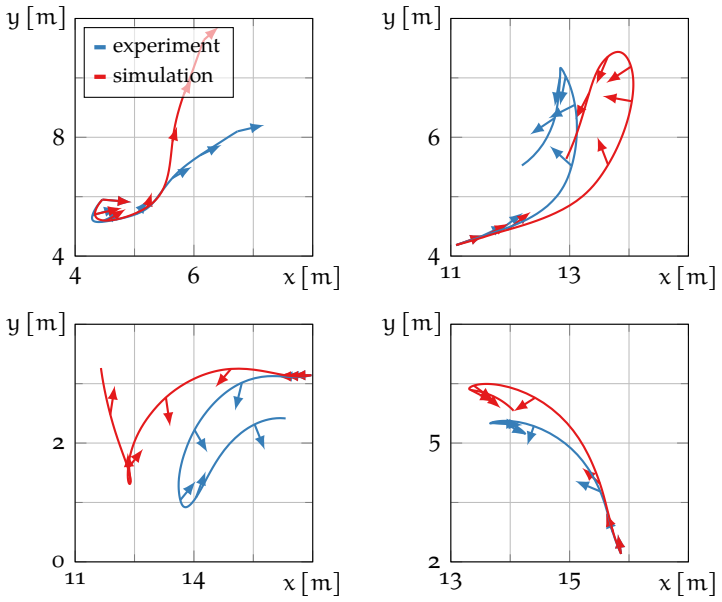

Figure 3.28: Comparison of simulation and experiment with the hovercraft robot. The arrows show the momentary orientation of the robot. Each plot covers 10 s of experiment and simulation.

Further verification of the obtained results is performed by repeating the identification procedure with a different approach embraced. To this end, an alternative identification scheme designed on the basis of the Kalman filter and presented initially in [37] is employed. The same data as used in PIESO identification is used and new parameter estimates are generated. The Kalman filter is tuned empirically with covariance matrices chosen as $\mathbf{R} = \mathbf{I}_3 \cdot 10^{-2}$ and $\mathbf{Q} = \mathrm{diag}(\mathbf{I}_3 \cdot 10^{-2}, \mathbf{I}_5 \cdot 10^{-4})$. The evolution of the state and parameter estimates is given in Fig. 3.29. The similarity of the character of

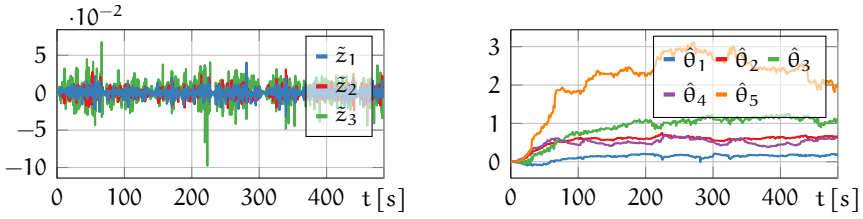

Figure 3.29: Time responses of the experiment of the hovercraft identification using Kalman filter.

the evolution of the parameter estimates in the results of the PIESO observer and Kalman filter approaches is visible. Specifically, the identification performed with a Kalman filter results in the final estimates given by

$$\hat{\theta}_{\text{Kalman}} \approx \begin{bmatrix} 0.2002 & 0.6536 & 1.0657 & 0.6268 & 1.9845 \end{bmatrix}^{\mathrm{T}}. \quad (3.149)$$

Both methods thus result in similar values of the parameter estimates and the efficiency of the proposed method is confirmed. The difference between the methods is more clearly visible in the parameters associated with the rotational movement of the hovercraft. This is a result of the fact that the hovercraft is an underactuated system and thus it is inherently characterized by higher difficulty in the identification of parameters associated with certain degrees of freedom.

3.4.2 *Identification of the wheeled mobile robot*

The exhaustive experimental validation of the proposed scheme is conducted employing a two-wheeled mobile MTracker 3 robot. The considered vehicle is equipped with a low-level TI TMS 320F28335 microcontroller and wireless CC2500 radio module. The control algorithms are implemented in the onboard controller which is responsible for the generation of control signals to track the desired reference velocities defined using the remote PC computer. The PWM signals produced by the microcontroller are fed into H-bridges driving two DC motors, coupled with 14 : 1 planetary gearheads and pulse encoders with 512 pulses per turn, enabling measurement of the momentary velocities of the wheels of the robot. Additionally, a 12-bit A/C converter is installed to measure the currents of each motor [145, 332]. The photo of the employed robot is given in Fig. 3.30

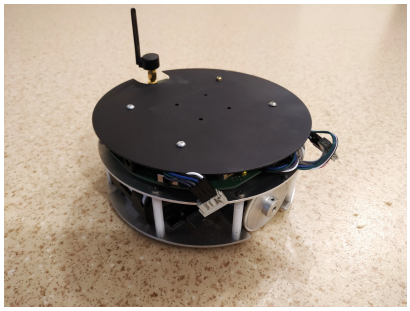

Figure 3.30: Photo of the MTracker 3 robot used in the experiments.

The kinematics of the considered robot are consistent with the unicycle kinematics given by

$$\dot{\mathbf{q}} = \mathbf{R}(\varphi)\mathbf{x} \tag{3.150}$$

with $\mathbf{q} = \begin{bmatrix} x & y & \varphi \end{bmatrix}^T \in \mathbb{R}^3$ being the coordinates of the robot in the inertial frame and $\mathbf{x} = \begin{bmatrix} v & r \end{bmatrix}^T \in \mathbb{R}^2$ representing the linear and

rotation velocities of the robot in a local coordinate system. Matrix $\mathbf{R}(\varphi) \in \mathbb{R}^{3\times 2}$ is given by

$$\mathbf{R}(\varphi) = \begin{bmatrix} \cos(\varphi) & 0 \\ \sin(\varphi) & 0 \\ 0 & 1 \end{bmatrix}. \tag{3.151}$$

The schematic view of the robot with such kinematics is presented in Fig. 3.31.

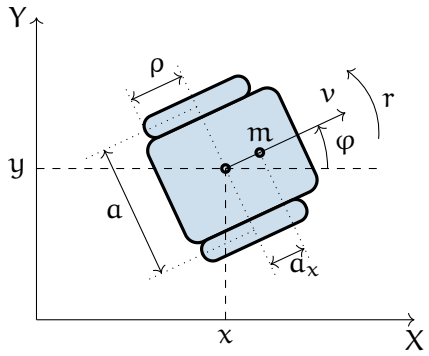

Figure 3.31: Scheme of the kinematics of the unicycle robot

Velocities $\mathbf{x}$ are directly dependent on the velocities of each wheel of the mobile robot and, under an assumption of lack of wheel slip during the motion of the robot, are expressed as

$$\mathbf{x} = \mathbf{T}^{-1}\rho\boldsymbol{\omega}, \tag{3.152}$$

where $\boldsymbol{\omega} = \begin{bmatrix} \omega_R & \omega_L \end{bmatrix}^T \in \mathbb{R}^2$ are velocities of the right and left wheel of the robot, $\rho \in \mathbb{R}_+$ is the wheel radius, and matrix $\mathbf{T} \in \mathbb{R}^{2\times 2}$ is given by

$$\mathbf{T} = \begin{bmatrix} 1 & \frac{1}{2}a \\ 1 & -\frac{1}{2}a \end{bmatrix}, \tag{3.153}$$

where $a \in \mathbb{R}_+$ is the distance between the two wheels. The dynamics of the platform are considered taking into account movements on the 2D plane only. It is assumed that the center of the mass of the robot is placed on its axis of symmetry but does not lie on the axis of the wheels of the robot. Such an offset of the center of mass is caused by the position of the onboard battery which is installed behind the axis of the wheels in the MTracker 3 robot. The dynamics of the platform are thus expressed by

$$\mathbf{M}\dot{\mathbf{x}} + \mathbf{C}(\mathbf{x})\mathbf{x} = \mathbf{F} \tag{3.154}$$

with mass matrix $\mathbf{M} \in \mathbb{R}^{2\times 2}$ and Coriollis matrix $\mathbf{C}(\mathbf{x}) \in \mathbb{R}^{2\times 2}$ given by

$$\mathbf{M} = \begin{bmatrix} m & 0 \\ 0 & J + ma_x^2 \end{bmatrix}, \quad \mathbf{C}(\mathbf{x}) = \begin{bmatrix} 0 & -ma_x r \\ ma_x r & 0 \end{bmatrix}, \tag{3.155}$$

where $a_x \in \mathbb{R}$ is an offset of the center of mass from the axis of the wheels. Moreover, $\mathbf{F} = \begin{bmatrix} F_v & F_r \end{bmatrix}^T \in \mathbb{R}^2$ are the driving forces acting upon the robot in the linear and rotational degrees of freedom. These are generated by the motors coupled with the wheels of the robot and derived as

$$\mathbf{F} = \mathbf{T}^T \mathbf{F}_\omega \tag{3.156}$$

with $\mathbf{F}_\omega = \begin{bmatrix} F_R & F_L \end{bmatrix}^T \in \mathbb{R}^2$ being forces produced by the motors in the point of contact of the wheels with the ground. Finally, forces $\mathbf{F}_\omega$ are given by

$$\mathbf{F}_\omega = \rho^{-1} \left(b\mathbf{u}_\omega - \sigma\boldsymbol{\omega} - \sigma_f \mathbf{sgn}(\boldsymbol{\omega}) - J_\omega \dot{\boldsymbol{\omega}} \right), \tag{3.157}$$

where $\sigma \in \mathbb{R}_+$ is a coefficient of lumped viscous friction and electromagnetic induction, $\sigma_f \in \mathbb{R}_+$ stand for a coefficient of Coloumb friction, and $J_\omega \in \mathbb{R}_+$ represent the inertia of the wheel, gearhead and the motor with respect to the axis of rotation. The term $\mathbf{sgn}(\cdot)$ stand for the element-wise signum operator. The terms $b \in \mathbb{R}_+$ and $\mathbf{u}_\omega = \begin{bmatrix} u_R & u_L \end{bmatrix}^T \in \mathbb{R}^2$ are the input gain coefficient and control signals of the motors driving the right and left wheel correspondingly. By considering the geometrical properties of the robot, the control inputs of the system are transformed as

$$\mathbf{u} = \rho^{-1} \mathbf{T}^T \mathbf{u}_\omega \tag{3.158}$$

with $\mathbf{u} = \begin{bmatrix} u_v & u_r \end{bmatrix}^T \in \mathbb{R}^2$ standing for the new virtual control signals in each of degrees of freedom. While only $\mathbf{u}_\omega$ are realizable at the level of the actuators, the transformed inputs $\mathbf{u}$ enable formulation of the dynamics of the robot in a more refined form.

Taking advantage of the presented properties of the considered robot, the substitution of (3.157) and (3.152) into (3.156) yields

$$\mathbf{F} = \mathbf{T}^T \rho^{-1} \left(b\mathbf{u}_\omega - \sigma \mathbf{T} \rho^{-1} \mathbf{x} - \sigma_f \mathbf{sgn}(\mathbf{T}\mathbf{x}) - J_\omega \mathbf{T} \rho^{-1} \dot{\mathbf{x}} \right). \tag{3.159}$$

Further substitution of this expression into (3.154), together with recalling of (3.158), produces

$$\dot{\mathbf{x}} = \bar{\mathbf{M}}^{-1} \left(b\mathbf{u} - \frac{\sigma}{\rho^2} \mathbf{T}^T \mathbf{T} \mathbf{x} - \frac{\sigma_f}{\rho} \mathbf{T}^T \mathbf{sgn}(\mathbf{T}\mathbf{x}) - \mathbf{C}(\mathbf{x})\mathbf{x} \right) \tag{3.160}$$

with $\bar{\mathbf{M}} = \mathbf{M} + J_\omega \mathbf{T}^T \mathbf{T} \rho^{-2} = \text{diag}(\bar{m}, \bar{J}) \in \mathbb{R}^{2\times 2}$ and $\bar{m} = m + \frac{2}{\rho^2} J_\omega, \bar{J} = J + m a_x^2 + \frac{a^2}{\rho^2} J_\omega$. As parameters ρ and a correspond to the easily measurable physical dimensions of the robot, it can be assumed that they are known, and dynamics (3.160) are thus linear in all unknown parameters. The proposed PIESO and PIDRC algorithms are applicable as viable solution to the problems of parameter identification and adaptive control of such a system.

In order to employ the PIESO observer in the parameter identification scheme, dynamics (3.160) are rewritten by taking advantage of the diagonal structure of matrix $\bar{\mathbf{M}}$ as

$$\dot{\mathbf{x}} = \boldsymbol{\Psi}(\mathbf{x}, \mathbf{u})\boldsymbol{\theta} \tag{3.161}$$

with

$$\boldsymbol{\theta} = \begin{bmatrix} \frac{b}{\bar{m}} & \frac{\sigma}{\bar{m}} & \frac{\sigma_f}{\bar{m}} & \frac{m a_x}{\bar{m}} & \frac{b}{\bar{J}} & \frac{\sigma}{\bar{J}} & \frac{\sigma_f}{\bar{J}} & \frac{m a_x}{\bar{J}} \end{bmatrix}^T \in \mathbb{R}^8 \tag{3.162}$$

and regressor $\boldsymbol{\psi}(\mathbf{x}, \mathbf{u}) \in \mathbb{R}^{2\times 8}$ given by

$$\boldsymbol{\Psi}(\mathbf{x}, \mathbf{u}) = \begin{bmatrix} u_1 & -\frac{2}{\rho^2} v & \psi_{1,3}(\mathbf{x}) & r^2 & 0 & 0 & 0 & 0 \\ 0 & 0 & 0 & 0 & u_2 & -\frac{a^2}{2\rho^2} r & \psi_{2,7}(\mathbf{x}) & -rv \end{bmatrix} \tag{3.163}$$

with elements $\psi_{1,3}(\mathbf{x})$ and $\psi_{2,7}(\mathbf{x})$ given by $\psi_{1,3}(\mathbf{x}) = -\frac{1}{\rho}\Big(\text{sgn}(v + \frac{a}{2} r) + \text{sgn}(v - \frac{a}{2} r) \Big)$ and $\psi_{2,7}(\mathbf{x}) = -\frac{a}{2\rho}\Big(\text{sgn}(v + \frac{a}{2} r) - \text{sgn}(v - \frac{a}{2} r) \Big)$. Notably, the obtained formula of parametrized dynamics of the plant may be interpreted as a combination of two dynamic systems resembling (3.25) and (3.141). To facilitate the design of the adaptive observer, the dynamics are further rewritten as

$$\begin{aligned} \dot{\mathbf{x}} &= \boldsymbol{\Psi}(\mathbf{x}, \mathbf{u})\hat{\boldsymbol{\theta}} + \boldsymbol{\delta}, \\ \dot{\boldsymbol{\delta}} &= \frac{d}{dt}\Big(\boldsymbol{\Psi}(\mathbf{x}, \mathbf{u}) \Big(\boldsymbol{\theta} - \hat{\boldsymbol{\theta}} \Big) \Big) \end{aligned} \tag{3.164}$$

with $\hat{\boldsymbol{\theta}} \in \mathbb{R}^8$ standing for the estimate of the parameters of the robot and $\boldsymbol{\delta} = \boldsymbol{\Psi}(\mathbf{x}, \mathbf{u})\big(\boldsymbol{\theta} - \hat{\boldsymbol{\theta}}\big) \in \mathbb{R}^2$ representing the total disturbance affecting the linear and rotational movements of the robot. Although both $\mathbf{x}$ and $\mathbf{u}$ are measurable in the considered scenario, the more general scheme for regressor dependent on unmeasurable state is employed here to better investigate the properties of the discussed

methods. The adaptive observer is thus synthesized on the basis state extension $z = \begin{bmatrix} x^T & \delta^T \end{bmatrix}^T \in \mathbb{R}^6$ as

$$\begin{aligned} \dot{\hat{x}} &= \Psi(\hat{x}, u)\hat{\theta} + \hat{\delta} + l_1 (x - \hat{x}), \\ \dot{\hat{\delta}} &= l_2 (x - \hat{x}), \end{aligned} \tag{3.165}$$

where $\hat{z} = \begin{bmatrix} \hat{x}^T & \hat{\delta}^T \end{bmatrix}^T \in \mathbb{R}^6$ is the estimate of the extended state of the system and $l = \begin{bmatrix} l_1 & l_2 \end{bmatrix}^T \in \mathbb{R}^2_+$ are the positive observer gains. The parameter adaptation is conducted through

$$\dot{\hat{\theta}} = \mathrm{Proj}(\Gamma \Psi^T(\hat{x}, u)\hat{\delta}) \tag{3.166}$$

with adaptation gains chosen as $\Gamma = \mathrm{diag}(\gamma_1, \ldots, \gamma_8) \in \mathbb{R}^{8\times 8}$ and the projection operator defined as in Remark 3.2.

The preliminary verification of the considered scheme is conducted through simulational studies of the system.

Simulation 3.14. *The kinematics and dynamics of the mobile robot are implemented according to* (3.150), (3.160), (3.156) *and* (3.157). *The parameters corresponding to the dimensions of the robot are chosen as* $a = 0.148\,\mathrm{m}$, $\rho = 0.025\,\mathrm{m}$, $m = 1.25\,\mathrm{kg}$ *according to the roughly known properties of the real robot. Remaining parameters are chosen as* $b = 0.097\,\mathrm{N\,m/A}$, $J = 0.03\,\mathrm{kg\,m^2}$, $J_\omega = 10^{-4}\,\mathrm{kg\,m^2}$, $a_x = -0.1\,\mathrm{m}$, $\sigma = 4 \cdot 10^{-4}\,\mathrm{N\,m^2\,s/rad}$, *and* $\sigma_f = 0.01\,\mathrm{N\,m}$. *The accumulated parameters* θ *take thus a form of*

$$\begin{aligned} \theta \approx \Big[& 0.0618 \quad 2.5478 \cdot 10^{-4} \quad 0.0064 \quad -0.0796 \\ & 2.1085 \quad 0.0087 \quad 0.2174 \quad -2.7171 \Big]^T. \end{aligned} \tag{3.167}$$

An additional non-adaptive controller is designed for the velocities of the wheels with the reference signal given as $\omega_r = \begin{bmatrix} \omega_r(t, 0) & \omega_r(t, 0.05t) \end{bmatrix}^T$ *with*

$$\begin{aligned} \omega_r(t, \phi) = {} & 12 \sin(0.6t + \phi) + 3 \sin(1.2t + \phi) \\ & + 2.4 \sin(3t + \phi) + 2.4 \sin(4.2t + \phi). \end{aligned} \tag{3.168}$$

For such a system the adaptive PIESO is implemented according to (3.165) *and* (3.166) *with observer and adaptation gains tuned empirically as* $l = \begin{bmatrix} 40 & 400 \end{bmatrix}^T$ *and* $\Gamma = \mathrm{diag}(5 \cdot 10^{-2}, 5 \cdot 10^{-6}, 5 \cdot 10^{-4}, 5 \cdot 10^{-2}, 2.5 \cdot 10^{-2}, 5 \cdot 10^{-4}, 5 \cdot 10^{-3}, 1)$. *The boundary imposed by the projection parameter is chosen as* $\vartheta_i = 100$ *for* $i \in \{1, \ldots, 8\}$. *The results of the simulation are given in Fig. 3.32.*

The obtained results are consistent with the earlier conclusions. Namely, the convergence of the disturbance estimates to the origin, as well as the evolution of the parameters of the system toward their

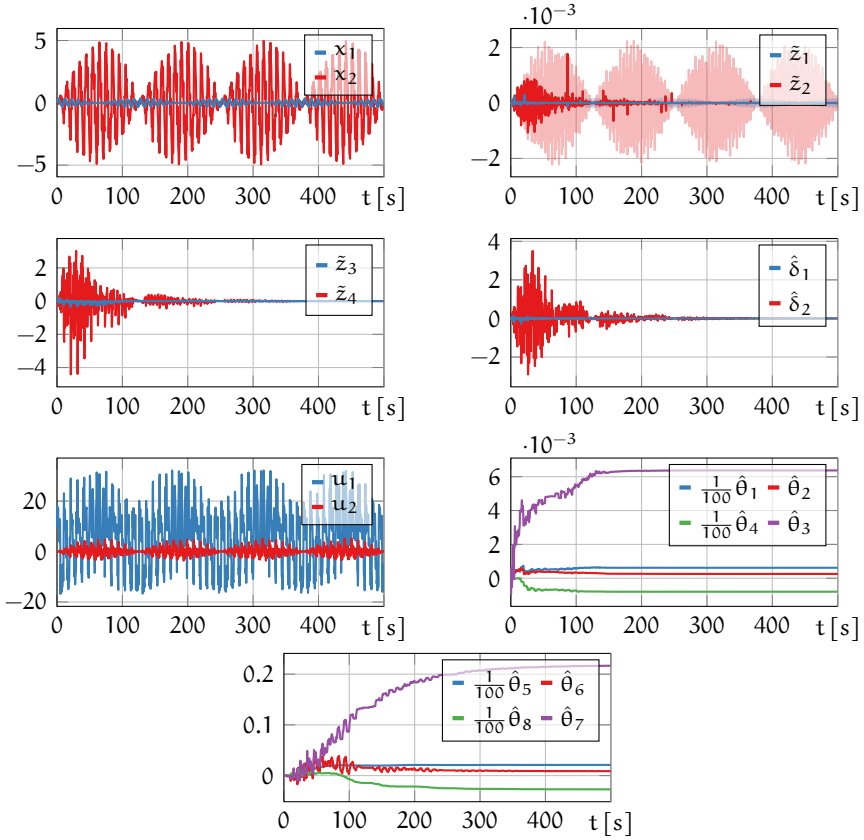

Figure 3.32: Time responses of the simulation of the unicycle robot identification using PIESO observer.

correct values, is seen. A significant improvement in the quality of the state estimation is also observed despite the presence of coupling between the dynamics of the systems representing linear and rotational movements of the vehicle. The correct estimation of the parameters of the system is achieved and their final values correspond to the parameters derived from the physical properties of the modeled plant. The existence of a constant ratio between the parameters of both subsystems is also visible here. Specifically, according to the parametrization given in (3.161) it holds that

$$\frac{\bar{J}}{\bar{m}} = \frac{\theta_1}{\theta_5} = \frac{\theta_2}{\theta_6} = \frac{\theta_3}{\theta_7} = \frac{\theta_4}{\theta_8}. \tag{3.169}$$

The presented relation can be later used to verify the results of the experimental trials.

Following the numerical trial, the experimental verification of the considered algorithm is conducted.

Experiment 3.2. *The experiment with mobile MTracker 3 robot is conducted. All settings of the experiments are the same as in Sim. 3.14, including the control signals, structure of the observer, and employed estimates of*

dimensions α *and* ρ *of the robot. Only the tuning of the adaptation law is chosen differently and is given by* $\Gamma = \mathrm{diag}(5 \cdot 10^{-4}, 1 \cdot 10^{-6}, 2.5 \cdot 10^{-4}, 5 \cdot 10^{-4}, 2.5 \cdot 10^{-1}, 1 \cdot 10^{-4}, 4 \cdot 10^{-2}, 1)$. *The results of the experimental run are given in Fig. 3.32.*

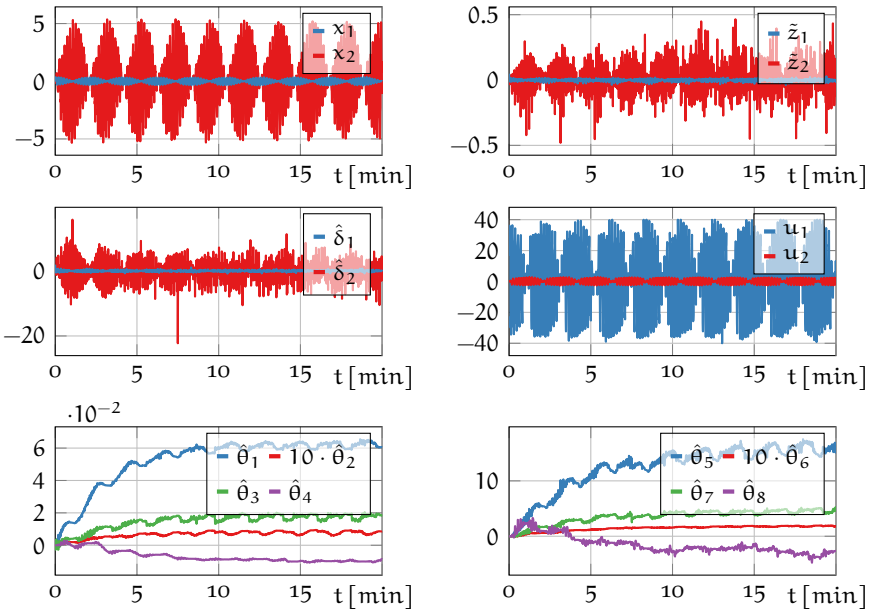

Figure 3.33: Time responses of the experiment of the unicycle robot identification using PIESO observer.

The presented plots confirm the usefulness of the considered scheme in the practical scenario of identification of dynamic parameters of the wheeled robot. Specifically, all of the parameter estimates converge toward some constant values with roughly the same ratios between the corresponding parameters in both dynamic subsystems. The final values of the obtained parameter estimates are given by

$$\hat{\theta} \approx \begin{bmatrix} 0.0606 & 8.59 \cdot 10^{-4} & 0.0184 & -0.0087 \\ 16.1363 & 0.1759 & 4.8587 & -2.7931 \end{bmatrix}^{\mathsf{T}}. \tag{3.170}$$

The ratio of $\frac{\bar{I}}{\bar{m}}$ is approximately calculated as $\frac{\hat{\theta}_1}{\hat{\theta}_5} \approx 0.0038$, $\frac{\hat{\theta}_2}{\hat{\theta}_6} \approx 0.0049$, $\frac{\hat{\theta}_3}{\hat{\theta}_7} \approx 0.0038$, $\frac{\hat{\theta}_4}{\hat{\theta}_8} \approx 0.0031$. The similarity of the values calculated on the basis of each pair of corresponding parameters implies the effectiveness of the conducted identification procedure. Resembling the results of the experimental identification of the hovercraft system, the state and disturbance estimates are heavily noised due to the character of the experimental setup, but a diminishing of the disturbance estimate with identification progress is observed. Notably, the state of the system constitutes a measurable output of the plant, and thus the

resultant quality of the state estimation is not of crucial importance in the conducted experiment.

Further verification of the obtained parameters is conducted by a method similar to one employed in Section 3.4.1.

Simulation 3.15. *The experimental measurements of the robot are compared with the trajectories produced by the simulation of the system modeled with the parameters equal* (3.170). *The initial conditions in each simulation are set equal to configuration of the real robot at chosen time instants and control signals recorded during the experiments are used to calculate the movements of the modeled robot. The results of such a comparison, in the form of trajectories on* (X, Y) *plane, are given in Fig. 3.34.*

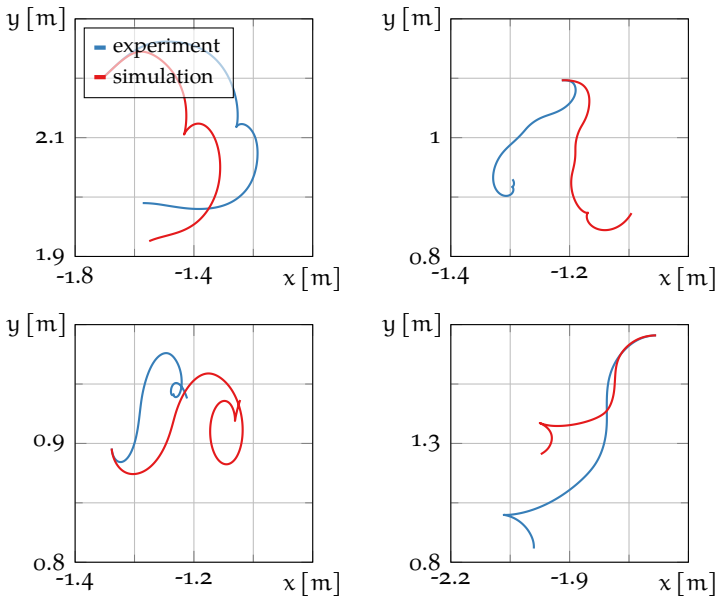

Figure 3.34: Comparison of simulation and experiment with MTracker 3 robot. Each plot covers 5 s of experiment and simulation.

The presented plots show a similarity between the trajectories of the real and simulated robot modeled on the basis of the identified parameters. Despite the presence of some errors in the recovery of the movements of the robot, the general character of the movements is correctly maintained implying that the obtained parameters roughly correspond to the real properties of the robot.

3.4.3 *Adaptive control of the wheeled mobile robot*

The adaptive PIDRC controller for the considered wheeled mobile robot can be designed by taking advantage of the transformed dynamics of the system as derived in the previous section. The discussed control scheme is thus applied to the problem of wheels velocity

control in the presence of dynamic uncertainties. Various structures of such controllers are commonly employed in the design of mobile robots to separate the low-level task of drive control from the higher-level problems of trajectory tracking, path planning, or obstacle avoidance.

In order to design the PIDRC controller for the MTracker 3 robot, dynamics (3.161) are further transformed into the form reminiscent of (3.88) by removing the control signals from the regressor of the plant and assuming that the input gains are known in advance. Thus, the dynamics of the robot are rewritten as

$$\dot{\mathbf{x}} = \mathbf{B}\mathbf{u} + \boldsymbol{\Psi}(\mathbf{x})\theta, \tag{3.171}$$

where $\mathbf{B} = \operatorname{diag}(\frac{b}{\bar{m}}, \frac{b}{\bar{J}}) \in \mathbb{R}^{2\times 2}$ and $\boldsymbol{\Psi}(\mathbf{x}) \in \mathbb{R}^{2\times 6}$ are the input gain matrix and the reduced regressor of the system. Matrix $\boldsymbol{\Psi}(\mathbf{x})$ is expressed by

$$\boldsymbol{\Psi}(\mathbf{x}) = \begin{bmatrix} -\frac{2}{\rho^2}v & \psi_{1,2}(\mathbf{x}) & r^2 & 0 & 0 & 0 \\ 0 & 0 & 0 & -\frac{a^2}{2\rho^2}r & \psi_{2,5}(\mathbf{x}) & -rv \end{bmatrix} \tag{3.172}$$

with elements $\psi_{1,2}(\mathbf{x})$ and $\psi_{2,5}(\mathbf{x})$ given by $\psi_{1,2}(\mathbf{x}) = -\frac{1}{\rho}\Big(\operatorname{sgn}(v + \frac{a}{2}r) + \operatorname{sgn}(v - \frac{a}{2}r)\Big)$ and $\psi_{2,5}(\mathbf{x}) = -\frac{a}{2\rho}\Big(\operatorname{sgn}(v + \frac{a}{2}r) - \operatorname{sgn}(v - \frac{a}{2}r)\Big)$ analogously to (3.161). The reduced parameter vector takes the form of

$$\theta = \begin{bmatrix} \frac{\sigma}{\bar{m}} & \frac{\sigma_f}{\bar{m}} & \frac{m a_x}{\bar{m}} & \frac{\sigma}{\bar{J}} & \frac{\sigma_f}{\bar{J}} & \frac{m a_x}{\bar{J}} \end{bmatrix}^T \in \mathbb{R}^6. \tag{3.173}$$

Once again, the parametrized system is interpretable as two interconnected dynamic systems corresponding to each degree of freedom of the robot. The PIDRC controller is then independently designed for each subsystem. Following the method presented in Section 3.3, the parametrized system is extended to incorporate the modeling error as a disturbance variable, yielding

$$\begin{aligned} \dot{\mathbf{x}} &= \mathbf{B}\mathbf{u} + \boldsymbol{\Psi}(\mathbf{x}) - \boldsymbol{\Psi}(\mathbf{x}_r)\left(\theta - \hat{\theta}\right) + \boldsymbol{\Psi}(\mathbf{x})\hat{\theta} + \delta, \\ \dot{\delta} &= \frac{d}{dt}\left(\boldsymbol{\Psi}(\mathbf{x}_r)\left(\theta - \hat{\theta}\right)\right) \end{aligned} \tag{3.174}$$

with $\mathbf{z} = \begin{bmatrix} \mathbf{x}^T & \delta^T \end{bmatrix}^T \in \mathbb{R}^4$ being the extended state of the system and $\hat{\theta} \in \mathbb{R}^6$ standing for the estimate of the parameters of the plant. The term $\mathbf{x}_r$ stand for the reference trajectories of the linear and rotational velocities of the robot. The control algorithm is synthesized in two versions, employing both the reference trajectory and the estimated state of the plant as the basis of the regressor evaluation.

In order to design the PIDRC algorithm on the basis of the reference trajectory, the adaptive observer is synthesized for the extended system (3.174) as

$$\begin{aligned} \dot{\hat{\mathbf{x}}} &= \mathbf{B}\mathbf{u} + \boldsymbol{\Psi}(\mathbf{x}_r)\hat{\boldsymbol{\theta}} + \hat{\boldsymbol{\delta}} + l_1 (\mathbf{x} - \hat{\mathbf{x}}), \\ \dot{\hat{\boldsymbol{\delta}}} &= l_2 (\mathbf{x} - \hat{\mathbf{x}}) \end{aligned} \tag{3.175}$$

with $\hat{\mathbf{z}} = \begin{bmatrix} \hat{\mathbf{x}}^T & \hat{\boldsymbol{\delta}}^T \end{bmatrix}^T \in \mathbb{R}^4$ being the estimate of the extended state and $\mathbf{l} = \begin{bmatrix} l_1 & l_2 \end{bmatrix}^T \in \mathbb{R}^2_+$ standing for the gains of the adaptive observer. The adaptation law is synthesized as

$$\dot{\hat{\boldsymbol{\theta}}} = \mathrm{Proj}(\boldsymbol{\tau}, \hat{\boldsymbol{\theta}}, \boldsymbol{\Theta}), \quad \boldsymbol{\tau} = \boldsymbol{\Gamma}\boldsymbol{\Psi}^T(\mathbf{x}_r)\hat{\boldsymbol{\delta}} \tag{3.176}$$

with the projection operator as given in Remark 3.2 and adaptation gains $\boldsymbol{\Gamma} = \mathrm{diag}(\gamma_1, \ldots, \gamma_6) \in \mathbb{R}^{6\times 6}$. The control laws for each degree of freedom of the robot are given by

$$\mathbf{u} = \mathbf{B}^{-1} \left(k (\mathbf{x}_r - \hat{\mathbf{x}}) + \dot{\mathbf{x}}_r - \boldsymbol{\Psi}(\mathbf{x}_r)\hat{\boldsymbol{\theta}} - \hat{\boldsymbol{\delta}} \right), \tag{3.177}$$

where $k \in \mathbb{R}_+$ is a positive controller gain.

Alternatively, the PIDRC controller employing the state estimates to evaluate the regressor is also designed. To this end, the observer is defined on the basis of (3.174) as

$$\begin{aligned} \dot{\hat{\mathbf{x}}} &= \mathbf{B}\mathbf{u} + \boldsymbol{\Psi}(\hat{\mathbf{x}})\hat{\boldsymbol{\theta}} + \hat{\boldsymbol{\delta}} + l_1 (\mathbf{x} - \hat{\mathbf{x}}), \\ \dot{\hat{\boldsymbol{\delta}}} &= l_2 (\mathbf{x} - \hat{\mathbf{x}}) \end{aligned} \tag{3.178}$$

with the adaptation law taking the form of

$$\dot{\hat{\boldsymbol{\theta}}} = \mathrm{Proj}(\boldsymbol{\tau}, \hat{\boldsymbol{\theta}}, \boldsymbol{\Theta}), \quad \boldsymbol{\tau} = \boldsymbol{\Gamma}\boldsymbol{\Psi}^T(\hat{\mathbf{x}})\hat{\boldsymbol{\delta}}. \tag{3.179}$$

Finally, the control law is synthesized as

$$\mathbf{u} = \mathbf{B}^{-1} \left(k (\mathbf{x}_r - \hat{\mathbf{x}}) + \dot{\mathbf{x}}_r - \boldsymbol{\Psi}(\hat{\mathbf{x}})\hat{\boldsymbol{\theta}} - \hat{\boldsymbol{\delta}} \right). \tag{3.180}$$

Both algorithms are thus designed under the assumption of measurability of the state of the system, but this measurable state is not directly used in the regressor evaluation or the control law design.

The initial verification of the designed controller is conducted by making use of the numerical simulation of the system with parameters given by (3.167).

Simulation 3.16. *Two controllers are implemented according to* (3.175)–(3.177) *and* (3.178)–(3.180)*. In both cases the reference signals are chosen by making use of property* (3.152) *as* $\mathbf{x}_r = \mathbf{T}^{-1}\rho\boldsymbol{\omega}_r$ *with the reference wheels velocity given by* $\boldsymbol{\omega}_r = \begin{bmatrix} \omega_r(t, 0) & \omega_r(t, 0.05t) \end{bmatrix}^T$ *with* $\omega_r(t, \phi)$

as expressed by (3.168). *Both controllers are tuned with* $k = 1$ *and the parameters of the observer are the same as in the test of the PIESO observer and are given by* $l = \begin{bmatrix} 40 & 400 \end{bmatrix}^T$ *and* $\Gamma = \operatorname{diag}(5 \cdot 10^{-6}, 5 \cdot 10^{-4}, 5 \cdot 10^{-2}, 5 \cdot 10^{-4}, 5 \cdot 10^{-3}, 1)$. *The projection operator is implemented with* $\vartheta_i = 100$ *for* $i \in \{1, \ldots, 6\}$. *The results of the simulations are given in Fig. 3.35 for the reference-based controller and in Fig. 3.36 for the controller synthesized using the state estimates.*

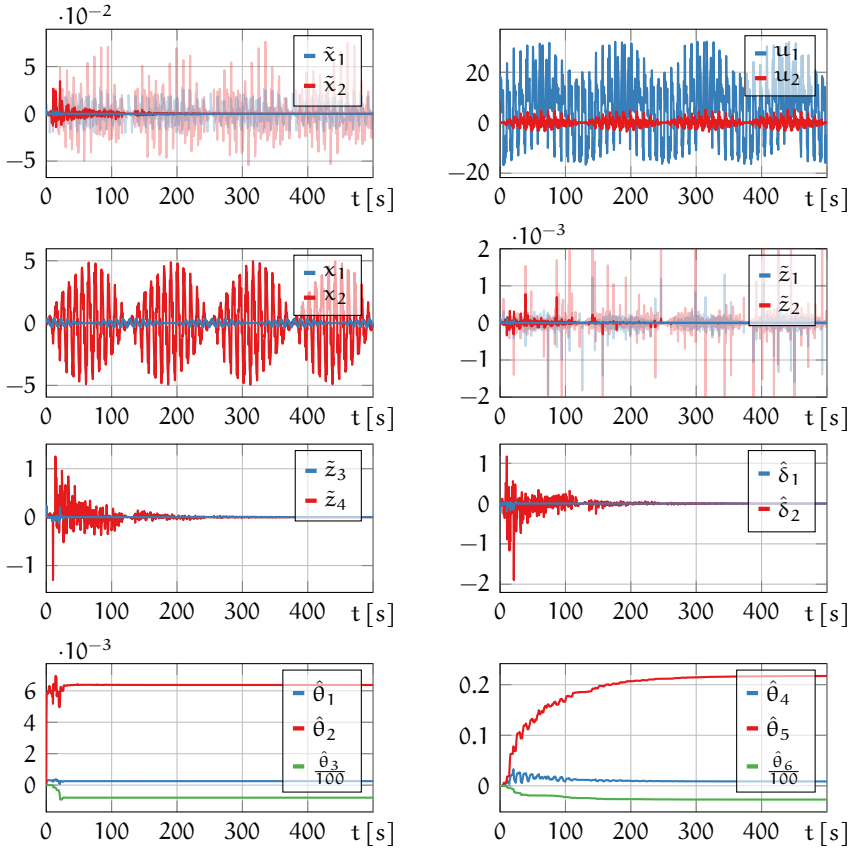

Figure 3.35: Time responses of the simulation of the unicycle robot adaptive control using PIDRC controller synthesized on the basis of reference state. The results obtained for conventional ADRC controller are given in transparent plots of $\tilde{x}$ and $\tilde{z}$.

The strong similarity between results produced with both methods is visible. In both cases, a significant improvement of the tracking quality in comparison with conventional nonadaptive ADRC is achieved and the convergence of the parameter estimates toward their correct values is shown. The tracking performance is increased and a significant improvement in the state estimation is achieved. In the plots, the vanishing of the total disturbance and its estimate due to the progress of the adaptation procedure is also visible. Notably, the character of the evolution of the signals in both cases is strongly similar, implying that they can be used interchangeably in many practical scenarios.

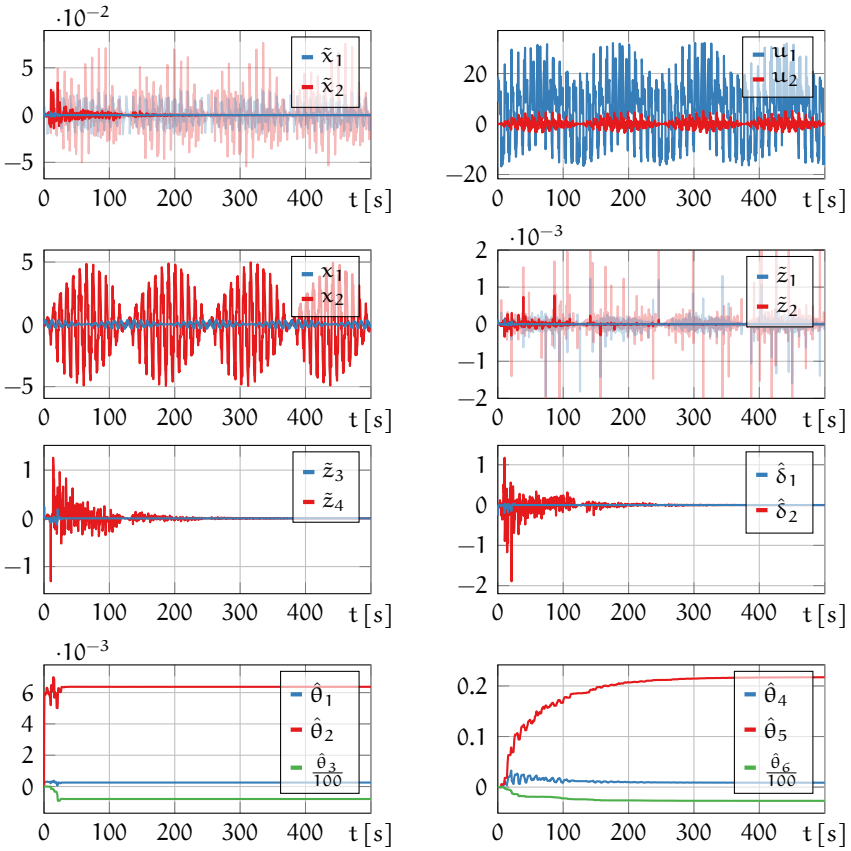

Figure 3.36: Time responses of the simulation of the unicycle robot adaptive control using PIDRC controller synthesized on the basis of estimated state. The results obtained for conventional ADRC controller given in transparent plots of $\tilde{\mathbf{x}}$ and $\tilde{\mathbf{z}}$.

Moreover, as the same tuning is employed in the task of the closed-loop adaptive control and the open-loop parameter identification, the considered method is shown to be easily tuned and deployed.

Further validation of the PIDRC approach to the task of adaptive control is carried out by the practical experiment.

Experiment 3.3. *The algorithms are implemented in the low-level controller unit of the MTracker 3 robot. The controller thus generates the input signals for the motors of the wheels and takes advantage of the measured velocities of the robot. The control signals for each motor are calculated from the linear and rotational controls produced by the controller according to* (3.158)*. In the experiments the controller gain is chosen as* $k = 7.5$ *and the observer is tuned with* $\mathbf{l} = \begin{bmatrix} 5 & 6.25 \end{bmatrix}^T$*. The adaptation gains are chosen as* $\gamma = \mathrm{diag}(4 \cdot 10^{-8}, 1 \cdot 10^{-6}, 2 \cdot 10^{-4}, 2 \cdot 10^{-5}, 2 \cdot 10^{-4}, 1)$ *in the scenario with the estimate-based approach, and* $\gamma = \mathrm{diag}(4 \cdot 10^{-8}, 2 \cdot 10^{-6}, 2 \cdot 10^{-4}, 2 \cdot 10^{-5}, 4 \cdot 10^{-4}, 2)$*. Some of the parameters are thus finely tuned to ensure satisfactory performance in both scenarios. In the synthesis of the controller, the input gains of the system are chosen as* $\mathbf{B} = \mathrm{diag}(0.06, 13.85)$ *according*

to the best known estimates of these parameters at the time of experiment. The results of the experiment are given in Fig. 3.37 and Fig. 3.38 for the algorithm synthesized using the reference and estimated trajectory, correspondingly.

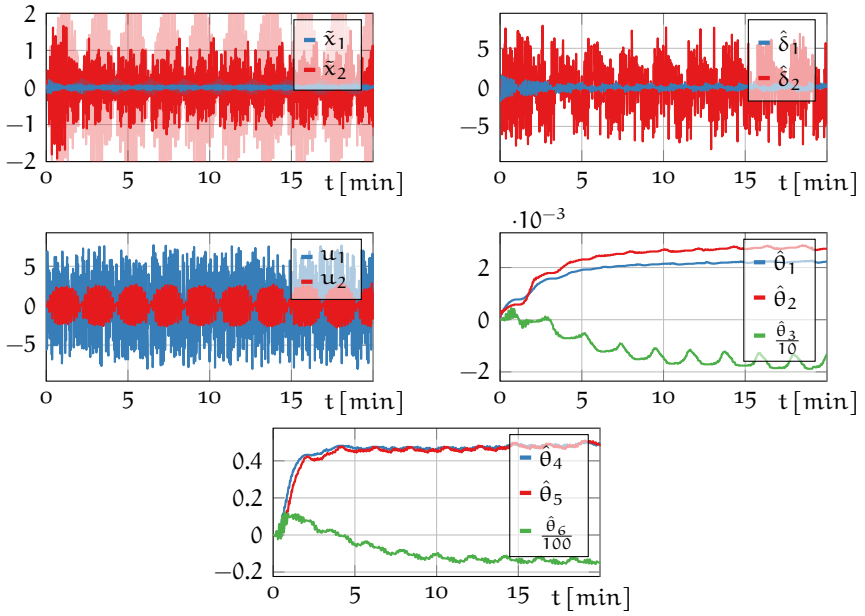

Figure 3.37: Time responses of the experiment of the unicycle robot adaptive control using PIDRC algorithm synthesized on the basis of the reference state.

The results of the experiments are in line with the output of the numerical simulations. The estimates of the unknown parameters converge to some constant values and the tracking error decrease due to the adaptive action. The final values of the obtained parameter estimates are given by

$$\hat{\theta} = \begin{bmatrix} 0.0022 & 0.0027 & -0.0134 & 0.4910 & 0.4880 & -15.1318 \end{bmatrix}^T \tag{3.181}$$

in the experiment employing the controller based on the reference trajectory and

$$\hat{\theta} = \begin{bmatrix} 0.0023 & 0.0048 & -0.0144 & 0.4863 & 0.6304 & -25.1758 \end{bmatrix}^T \tag{3.182}$$

in the experiment with the controller utilizing the estimated state. The obtained parameter estimates thus differ from (3.170) – not only due to the different definition of θ which does not include the input gains, but also due to different values obtained of the corresponding parameters. Noticeably, the control signals generated by the adaptive PIDRC controller differ from these produced by the nonadaptive control law used in the experiments shown in Fig. 3.33 despite the

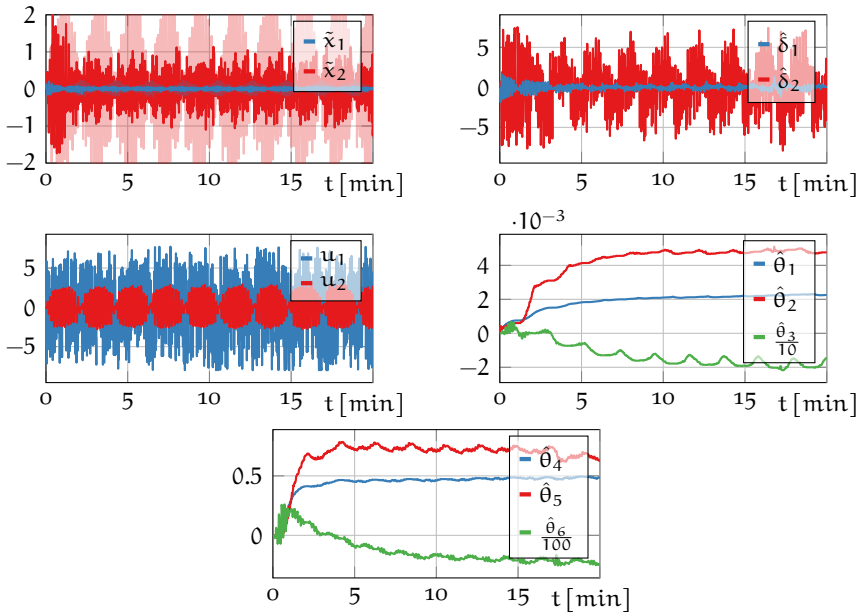

Figure 3.38: Time responses of the experiment of the unicycle robot adaptive control using PIDRC algorithm synthesized on the basis of the estimated state.

same reference trajectory employed in all trials. Thus, the degree of excitation differs between the trials and the quality of identification may not be maintained. Moreover, the values of the input gains assumed in the controller synthesis are not consistent with these obtained through the PIESO experimental trial, as these were not yet known at the time of the PIDRC experiment. In order to evaluate the quality of the identified parameters, the ratio of $\frac{\bar{I}}{\bar{m}}$ is calculated as $\frac{\hat{\theta}_1}{\hat{\theta}_4} \approx 0.0045$, $\frac{\hat{\theta}_2}{\hat{\theta}_5} \approx 0.0056$, $\frac{\hat{\theta}_3}{\hat{\theta}_6} \approx 0.0009$ for the results produced by the reference-based PIDRC and $\frac{\hat{\theta}_1}{\hat{\theta}_4} \approx 0.0047$, $\frac{\hat{\theta}_2}{\hat{\theta}_5} \approx 0.0076$, $\frac{\hat{\theta}_3}{\hat{\theta}_6} \approx 0.0006$ for the algorithm based on the estimated state. It can be concluded that the overall quality of parameters estimation is decreased, especially in terms of the identification of θ_3 and θ_6, in the considered experiments in comparison with the results obtained during experimental validation of the PIESO algorithm. Nonetheless, the identified parameters enable successful improvement of the tracking quality in comparison with the nonadaptive ADRC algorithm.

The results of the experimental validations of the PIESO and PIDRC algorithms presented in this section confirm that the proposed methods can be successfully applied to the problems of parameter identification and adaptive control in practical scenarios. Application of the proposed schemes to two distinct systems, corresponding to the dynamics of the underactuated hovercraft and the wheeled mobile robot, is presented. In both cases, the procedure of the parameter identification is conducted by taking advantage of the PIESO observer and

the problem of adaptive control of the wheeled robot is solved through the PIDRC controller. It is shown that the identification of the plant parameters is achieved with a satisfactory quality despite the presence of the measurement noised and unmodeled dynamics inherent to the real systems. The experiments with the wheeled robot shown also that the tracking quality achieved with the PIDRC controller is significantly improved in comparison with the nonadaptive ADRC method.

4

TESTBED SYSTEMS

Perhaps the facts, or data, are more convincing than mere articulation of ideas.

— J. Han, 2009 [102]

Throughout the research concluded by this dissertation, multiple testbed systems have been used to investigate the considered problems and verify proposed solutions and theorems. Specifically, the astronomic telescope mount has been used to investigate the impact of the input gain uncertainty on the performance of the ADRC schemes, and the hovercraft and wheeled mobile robot have been employed to verify the applicability of the proposed PIESO and PIDRC methods in practical scenarios. The author of this dissertation has been directly involved in the development of the two formers of these. In this chapter, some details on the structure and construction of these systems are given.

4.1 HOVERCRAFT SYSTEM

The custom hovercraft system has been employed to investigate the properties of PIESO and PIDRC algorithms in experimental settings. The considered device is based on the remote Mk. 1 Sirius 600 hovercraft model produced by Palaform Ltd [218] modified to better fit the needs of scientific research. The standard model consists of the vacuum-formed hull made of 1 mm thick high-impact polystyrene and a rubber skirt used to form an air cushion beneath the vehicle. The model has the dimensions of 60 cm length by 30 cm width and 20 cm height. The vehicle is equipped with a two-bladed propeller made of resin polymer with a diameter of 17.8 cm providing thrusting force and a smaller propeller of diameter 10.2 cm generating a lifting force. The propellers of the hovercraft are mounted on two brushless motors delivered with electronic speed controllers (ESC). A motor with a single-direction controller is employed to drive the lift propeller and bi-directional motor is used as a source of thrust force. The use of a controller able to drive the thrust motor in both directions, together with a properly shaped propeller, enables the hovercraft to move both forward and backward. The direction of movement is moreover controlled by the incorporated rudder placed behind the thrusting fan and consisting of two polystyrene plates rotating around the vertical pivots mounted parallelly to the plane of the propeller and perpendicularly

to the ground. The orientation of the rudder is controlled by a single modeling micro servo with 180° range of motion. In order to power all of the motors, a three-cell lithium-ion polymer battery with the output voltage of 11.1 V is recommended. The standard assembly of the Sirius 600 hovercraft employs a modeling four-channel radio receiver coupled with a manual remote controller to generate the control signals for the rudder servo and speed controllers of the lift and thrust motors. The assembled model with motors, radio receiver, and battery pack has a total weight of approximately 1 kg and achieves maximum velocities of 4 m/s on water and up to 5.5 m/s on flat solid surfaces.

For the purposes of the experimental research, the hovercraft has been modified to enable the implementation of the control and identification algorithms and acquiring of the experimental data. Specifically, the control of the hovercraft was adjusted to enable the generation of the control signals on the remote PC computer using the Matlab software [192]. Wireless communication through the Wi-Fi protocol was thus incorporated. To this end, the suggested radio receiver is replaced with ESP32-DEVKITC-32D module based on the ESP32-WROOM-32D microcontroller unit (MCU) capable of Wi-Fi networking [63] and compatible with Arduino core [9]. The module is powered directly from the speed controller of one of the motors by taking advantage of the battery eliminator circuit (BEC) providing a constant voltage of 5 V and thanks to the voltage stabilizer incorporated into ESP32 module allowing input voltage up to 12 V. The direct control of the motors of the hovercraft is carried out through the PWM outputs of the MCU by taking advantage of the ESP32Servo library [104]. Three independent PWM channels are used to produce the control signals for the rudder servo and speed controllers of the lift and thrust propeller motors. The wiring diagram of the onboard electronics is given in Fig. 4.1.

Dedicated custom software is deployed on the ESP32 microcontroller. At the startup of the system, the arming procedure of the ESC is performed by issuing a series of specific PWM signals to each of the controllers to ensure their proper initialization. The rudder servo is restored to the default position. In order to enable the wireless control of the robot, the Wi-Fi protocol is enabled. The MCU works as a Wi-Fi access point (AP) hosting its own network with a predefined SSID identifier and hardcoded password. Alternatively, the controller can be switched into non-AP mode and automatically connect to the given network on the launch of the system. Usage of the robot in the laboratory environment is thus strongly simplified and the device can be made available for experiments immediately after startup. The onboard button is configured to allow emergency stop of the motors. Once the configuration procedure is completed, the hovercraft enters the operation mode and awaits control commands from the exter-

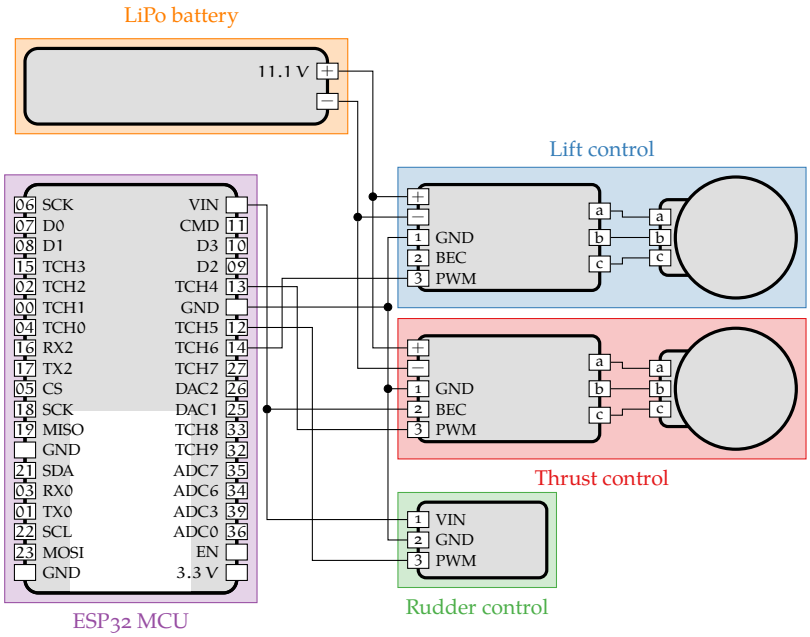

Figure 4.1: Scheme of the wiring of the onboard electronics of the hovercraft

nal source. The input signals of the system are defined as messages containing three 32-bit floating point numbers corresponding to the desired settings of the ESC of the motors and the servo of the rudder. The ESC control signals are initially scaled in the range from -1 to 1 to confine the most used controls within this set. Nonetheless, inputs of other values are accepted by lift and thrust motors resulting in higher speeds of the propellers. The control input of the rudder servo is scaled to correspond to the position of the rudder in the range of $-\frac{1}{2}\pi$ to $\frac{1}{2}\pi$.

The control software is developed in the Matlab environment to enable easy prototyping and testing of control solutions. The custom class is implemented to facilitate the operation of the system. Distinct member functions are incorporated to establish the connection between the PC computer and the hovercraft MCU unit. Moreover, a separate class is proposed enabling direct reading of the measurement data of the hovercraft from the OptiTrack vision system [209]. To this end, a set of markers is mounted on the body of the hovercraft, and the geometric properties of the vehicle are defined in the OptiTrack environment. The combination of wireless communication with the robot and data acquisition based on the vision system results in a robust system suitable for experimental research. The entire system is capable of operating with the frequency of the main control and measurement loop equal to approximately 50 Hz. The photo of the modified hovercraft with the custom control unit and motion capture markers is given in Fig. 4.2.

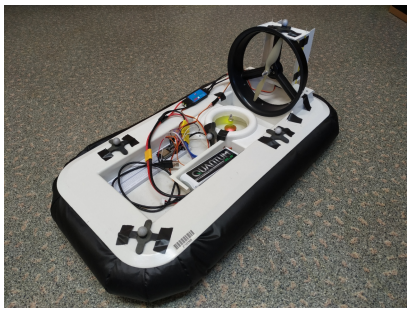

Customized Sirius hovercraft, own photo

Figure 4.2: Photo of the customized Mk. 1 Sirius 600 hovercraft.

The dynamics and kinematics of the hovercraft system can be modeled according to [37] in the form presented in Section 3.4.1 as

$$\begin{aligned} \dot{\mathbf{q}} &= \mathbf{R}(\varphi)\mathbf{x}, \\ \dot{\mathbf{x}} &= \boldsymbol{\Psi}(\mathbf{u})\boldsymbol{\theta} + \mathbf{c}(\mathbf{x}), \end{aligned} \tag{4.1}$$

where $\mathbf{q} = \begin{bmatrix} x & y & \varphi \end{bmatrix}^T \in \mathbb{R}^3$ is the position and orientation of the system in the global coordinate system, and $\mathbf{x} = \begin{bmatrix} v & w & r \end{bmatrix}^T \in \mathbb{R}^3$ stands for the linear and angular velocity of the platform in the local frame. The terms $\mathbf{R}(\varphi) \in \mathbb{R}^{3\times3}$, $\boldsymbol{\Psi}(\mathbf{u}) \in \mathbb{R}^{3\times5}$ and $\mathbf{c}(\mathbf{x}) \in \mathbb{R}^3$ are given by

$$\begin{aligned} \mathbf{R}(\varphi) &= \begin{bmatrix} \cos(\varphi) & -\sin(\varphi) & 0 \\ \sin(\varphi) & -\cos(\varphi) & 0 \\ 0 & 0 & 1 \end{bmatrix}, \quad \mathbf{c}(\mathbf{x}) = \begin{bmatrix} wr \\ -vr \\ 0 \end{bmatrix}, \\ \boldsymbol{\Psi}(\mathbf{u},\mathbf{x}) &= \begin{bmatrix} -v & 0 & 0 & \cos(u_1)u_2 & 0 \\ 0 & -w & 0 & \sin(u_1)u_2 & 0 \\ 0 & 0 & -r & 0 & -\sin(u_1)u_2 \end{bmatrix}, \end{aligned} \tag{4.2}$$

and

$$\boldsymbol{\theta} = \begin{bmatrix} \frac{\sigma_v}{m} & \frac{\sigma_w}{m} & \frac{\sigma_r}{J} & \frac{b}{m} & \frac{ab}{J} \end{bmatrix}^T \tag{4.3}$$

with $m \in \mathbb{R}_+$ standing for the mass of the hovercraft, $J \in \mathbb{R}_+$ representing the inertia of the vehicle, $\sigma_v, \sigma_w, \sigma_r \in \mathbb{R}_+$ being coefficients of friction forces and aerodynamic drag in each degree of freedom. The term $a \in \mathbb{R}$ stand for the offset of the propeller from the center of mass and b stand for some ratio between the input of the ESC of the thrust motor and the force generated by the rotating propeller. Signals $u_1 \in (-\frac{1}{2}\pi, \frac{1}{2}\pi)$ and $u_2 \in \mathbb{R}$ represent the orientation of the rudder and the control signal of the thrust propeller. The input of the lift motor is omitted in this representation and is assumed to be constant. The dynamic parameters are thus indirectly dependent on the chosen

speed of the lift propeller. Throughout all of the experiments presented within this work, the lift motor is set to the constant input of $u_{\text{lift}} = 1.5$ corresponding to the PWM signal of pulses with the width of $1.75\,\text{ms}$. According to the identification procedure and results presented in Section 3.4.1, the remaining parameters of the robot are given by

$$\hat{\theta} \approx \begin{bmatrix} 0.2289 & 0.6751 & 0.8333 & 0.6543 & 1.6287 \end{bmatrix}^{\mathsf{T}} \tag{4.4}$$

under the assumption of the constant lift motor speed.

In order to visualize some of the basic dynamics properties of the robot, a series of short experiments are conducted and the measured data is acquired.

Experiment 4.1. *The hovercraft mobile robot is employed in the series of basic illustratory experiments. Firstly, short positive and negative pulses are issued to the thrusting propeller with the rudded fixed in the default position. Then, forward pulses are issued to the thrusting propeller with varying orientation of the rudder. The results are given in Fig. 4.3.*

The presented trajectories of the robot unveil certain dynamic characteristics of the system. The high inertia of the vehicle in linear movement is visible with the nonzero velocity of the robot lasting significantly long after the vanishing of the thrust input signal. The presence of some disturbing force generating sideway and rotational movements is also visible. This force is caused by the imperfect assembly of the skirt of the hovercraft and can be mitigated by the choice of a smaller lift input signal. The lack of symmetry of the thrusting propeller is also shown by the plots, as linear velocities of similar magnitudes are achieved by strongly differing positive and negative input signals. Simultaneously, the efficiency of the rudder as the mean of changing the orientation and direction of movement of the robot is visible and changes in the orientation of the hovercraft corresponding to the momentary position of the rudder are achieved.

4.2 ASTRONOMIC TELESCOPE MOUNT

The research summarized in the first part of this dissertation has been mainly conducted using the robotic astronomic telescope mounts developed by a research team at Poznan University of Technology. The advances in the development of this equipment have been reported in [143, 151] and recently in [21, 147]. The device consists of an altazimuth robotic mount capable of carrying the astronomic telescopes with diameters of $0.5\,\text{m}$ or a collection of smaller observation tools. The exemplary configuration of the considered system is given in Fig. 4.4. Two axes of the mount are directly driven by independent

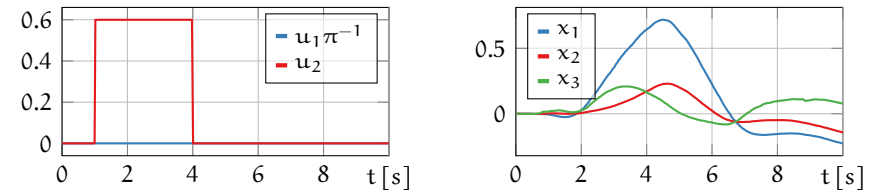

(a) Thrust forward pulse

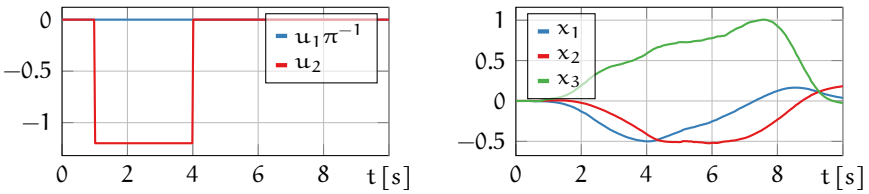

(b) Thrust backward pulse

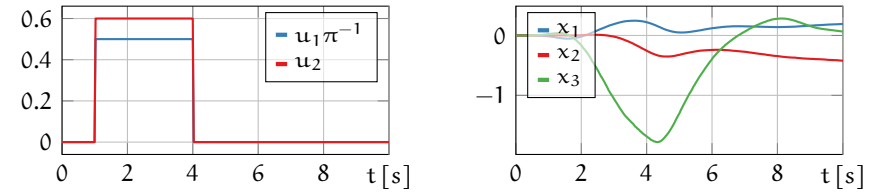

(c) Forward and turn

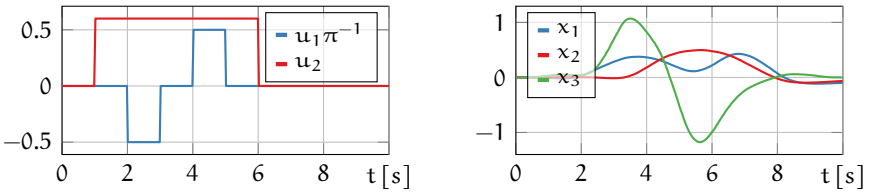

(d) Forward and two turns

Figure 4.3: Results of the basic hovercraft experiments

permanent magnet synchronous motors (PMSM) coupled with high-precision encoders enabling measurement of the momentary position of the telescope. The control signals for the motors are generated by a microcontroller implementing the main control loop and basic safety procedures. The dynamics of a single mechanical axis are vaguely modeled as

$$\dot{\mathbf{x}} = \mathbf{A}_2\mathbf{x} + \mathbf{b}_2\left(\frac{1}{J}u + d(t,\mathbf{x})\right), \tag{4.5}$$

where $\mathbf{x} = \begin{bmatrix}\varphi & \omega\end{bmatrix}^T \in \mathbb{R}^2$ is a state with $\varphi, \omega \in \mathbb{R}$ being the momentary orientation and rotational velocity of the axis. The term $d(t,\mathbf{x})$ accumulates all disturbing phenomenons including friction forces, coupling between the axes, or the force of the gravitation in the case of the horizontal axis. Review of some effects represented by $d(t,\mathbf{x})$ is given in Section 2.4. The term $u \in \mathbb{R}$ is the control variable of the plant

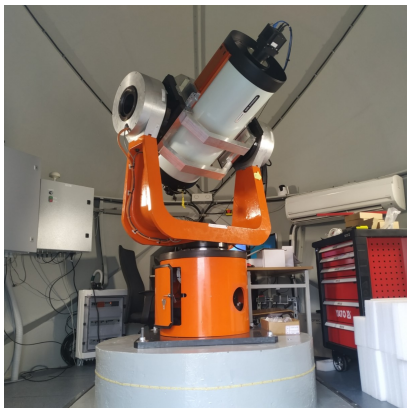

Robotic telescope mount, own photo

Figure 4.4: Photo of the exemplary configuration of the developed telescope mount.

corresponding to the desired torque to be produced by the motor of the axis.

The control of the developed system is based on the modular composition of computing units with varying tasks and capabilities. Namely, the low-level control of the system is realized using a STM32H743ZI2 microcontroller unit (MCU) [276], while the high-level communication with the user is made available by Raspberry Pi 4 microcomputer hosting Linux operating system and capable of Ethernet communication [72] which serves as a mediator between the user and the controller of the telescope. The algorithm implemented in the MCU incorporates separated current and position control loops, designed using PI and ADRC methods correspondingly, both working with a frequency of 10 kHz. Thanks to the cascade approach of the control of the system the current loop ensures that the motors provide desired torque to each axis. The position loop is designed under such an assumption in the form of the ADRC controller. A combination of the measurements conducted by taking advantage of high-resolution encoders with disturbance rejection capabilities of the ADRC scheme ensures high precision of operation despite significant friction forces affecting the axes in slow movements necessary during the astronomic observations. Extension of the employed controllers by various compensation modules has been considered, including a friction compensation module or ripple torque compensation, as well as the inclusion of fractional feedback exponents into the controller and observer schemes.

In order to provide the reference trajectory for the control algorithms, the trajectory generator module is implemented. Specifically, the sampled trajectory supplied by the user of the system is interpolated to obtain the desired signal with sufficient frequency. The interpolation algorithm is designed on the basis of 6th order polynomials used to

recover the sampled signal of frequency 1 Hz. Thus, the generated trajectory is guaranteed to be at least twice differentiable with values of position and velocity conforming to the samples defined by the user and the acceleration calculated to ensure its continuity at any time instant. Each segment of the recovered trajectory is calculated using information about the reference position in four consecutive samples and velocity in two samples, as well as the acceleration of the previously generated segment. Additionally, to ensure a smooth transition of the telescope from its initial configuration to the desired trajectory, a transient path is generated at the beginning of each observation.

To facilitate the delivery of sampled trajectory from the client-side PC computer and other data exchange with the controller of the plant, a custom communication protocol has been devised. In the early versions of the system, a prototype scheme resembling the Modbus protocol has been employed. This approach enabled the exchange of predefined commands to read or write data to the controller or trigger the execution of certain functions implemented locally on the MCU. The communication scheme has been later replaced by a more sophisticated proposition named AST Communication Module (ASTCom) implemented in the form of a programming library [224]. The considered package provides an interface for fast serialization and data exchange between multiple devices taking advantage of the WebSocket protocol. The serialization itself is performed using a custom format similar to the well-known MessagePack standard enhanced with several extensions to accommodate features of the proposed scheme. Mainly, the possibility to dynamically configure the set of exchanged data at run-time is introduced.

The basis of the ASTCom library design is the system of variable and class registration, which allows the library to discover each and every desired variable declared in the code of the telescope controller. To this end, a conceptual ASTVariable is defined as any variable or class that can be serialized by the ASTCom library. Serialization procedures for multiple basic types (e. g. integer, float, string, array, etc.) are predefined by the library itself. Moreover, ASTVariable can also represent a function with an arbitrary signature. In order to enable serialization of custom-defined classes, the special macro is declared which, when included in the class definition, declares a set of functions used to serialize and deserialize all variables of the chosen class. The types of variables and the proper way of their processing are discovered automatically by the library. Thus, once a class is defined, a call to a single function automatically serializes the entire content of its object, including any member objects that were implemented taking advantage of the aforementioned macro. A globally accessible Collection class is then defined, which can be called to recursively scan

and register any object of the ASTVariable type. During this process, information about the name, type, and address of data in physical memory and addresses of serializing and deserializing functions of the object is stored in the memory of the Collection singleton. Thanks to the recursiveness of this operation, it is sufficient to register only the top-level object, provided that all member objects are also of the ASTVariable type. Thus, if any change in the structure of the software is made, there is no requirement for any additional modifications outside the affected classes, as their proper registration is automatically ensured by the top-level class. It is of major significance that all of these operations are performed either at compile time or on the device startup and do not slow down its further operations. Once the initial registration of objects is performed, the current state of any signal in the telescope can be easily obtained by invoking the Collection object with the name and type of the required variable.

In order to make use of the proposed approach, two separate modules are implemented – the Endpoint module, to be employed on the board of the telescope, and the Client module, run in each of the client applications. Both modules are derived from the single Interface class. These two are then used to establish communication between various devices in the ASTCom network. To this end, a series of hard-coded ASTCommands is defined and used to exchange basic commands between devices. These are in nature similar to functions of the Modbus protocol and are first used to establish a formal connection between the nodes, during which version compatibility is verified and access rights are granted through password verification. Each connection is represented by both parties by a separate Connection class object, which stores all information necessary to carry on the communication. Notably, multiple Client devices can be simultaneously connected to a single Endpoint and their number can be limited by the Endpoint to reduce the performance impact. Once the connection is defined, the Client uses proper ASTCommands to query the Endpoint device and request it to define new ASTMessages – virtual structures consisting of several ASTVariables with a unique ID number assigned. Once the Endpoint receives such a request, it queries the Collection for desired entries and copies pointers to serialization functions. Hence, once the ASTMessage is defined in the Endpoint, it is directly available for use, and no additional overhead is created beside a brief configuration of the messages, which can be done before the proper start of operation of the telescope system. On the Client side, the newly defined ASTMessage is also bound to a chosen locally defined variable of the same type. It is noteworthy that as the serialization procedures of the basic types are hard-coded into the library, the Client device is not required to have counterparts of the defined data in its source code, as

they can always be built in the runtime from objects of basic types. On both sides, defined ASTMessages are stored in the MessageRegister class object, with a notion that the Endpoint defines a single register used by all connections, while the Clients assign separate storage for each connection. The process of ASTMessage definition can be seen as the creation of a bond between the local and remote variables on two devices. In the case of an ASTMessage containing ASTVariables representing the function, the bond is made between the function on one device and variables used as its arguments on the other. Such messages containing references to a function can be transferred only in one direction, as arguments can only be written to functions. A graphical scheme showing an example of this binding is given in Fig. 4.5.

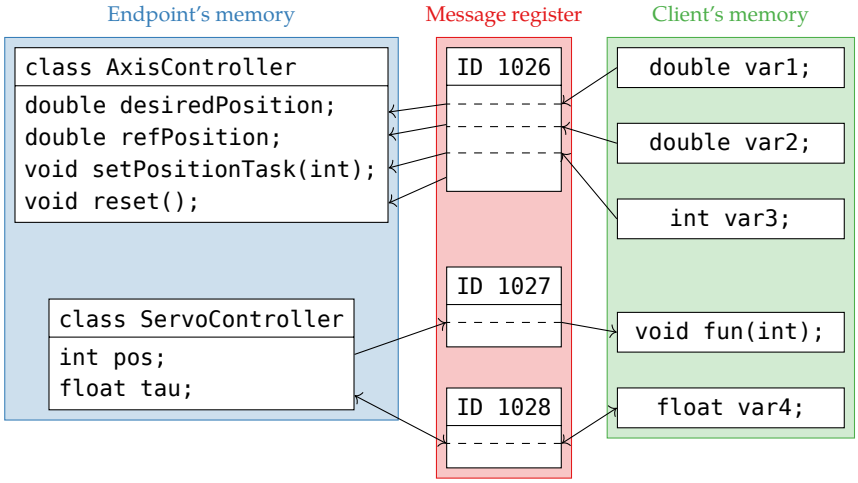

Figure 4.5: Example of variable binding in ASTCom. Function `reset()` is called without any argument and the remote variable `int pos` is used to invoke a local callback function. Variables `float tau` and `float var4` can be transferred in both directions.

Two modes of data exchange are supported by the ASTCom library – the private channel communication used to transfer data between two devices and the stream channel used by the Endpoint to broadcast large amounts of data to all connected clients. All of the aforementioned ASTCommands are also sent through the private channel. Importantly, the ASTCom library does not define the precise transport layer of the channels, and thus the communication can be carried out using several media, including Websocket, TCP/IP, or SPI communication with both channels supported by a single connection or separated between two independent routes, e.g. two separate Websocket connections. The Client can request to exchange the data through one of these communication channels. In the case of the private channel, the Client requests a single exchange of data of a chosen ASTMessage in the desired direction – the data can be both read from or written to the telescope. Once the command is carried

out, the values of the bound variables are identical on both devices. If the considered ASTMessage contains ASTVariables representing the function, it is remotely invoked, which can be used to control the behavior of the telescope controller.

While the private channel is designed mainly to control the telescope by the user or the supervisor, the stream channel is intended for the constant acquisition of information about the state of the device. To this end, the Client may request the Endpoint to start recording chosen ASTMessages with a desired frequency. Currently, on the considered setup of the telescope controller, the recording with a frequency up to 10 kHz is possible. The Endpoint executes such a command, by cyclically serializing the value of requested variables into a local predefined buffer. Once a certain volume of data is acquired, the data is flushed and sent to all connected Clients, which receive the packets containing the amassed record of the state of the telescope in the previous time instants. Importantly, Clients may bind the received data to some custom callback functions and this way process each sample of data separately upon arrival. Thus, a significant amount of data can be exchanged between devices to allow constant monitoring of the telescope performance. The proposed approach was first implemented in C++ code, as this is the language of the main controller of the telescope. To enable support of various client applications, the Client class with all necessary dependencies was later ported into JavaScript (using LLVM/Clang-based Emscripten compiler [329, 330]), pure C and C# (using p/invoke feature).

The practical performance of the developed robotic telescope mount is illustrated by the following experiments.

Experiment 4.2. *The automatic robotic telescope mount is employed in the series of experimental trials. At first, the problem of tracking an object in geostationary orbit, corresponding to the set-point stabilization of the telescope, is considered. Then, the task of sidereal object tracking, representing the problem of tracking the slowly varying trajectory, is investigated. Finally, tracking of a fast artificial satellite in the low Earth orbit is studied. The results of all trials are given in Fig. 4.6.*

The results of the experiments show some basic properties of the considered system. Specifically, the high precision of the controller in the tasks of set-point stabilization and trajectory tracking is visible. It can be noted, that the horizontal axis is characterized by higher tracking precision in comparison with the vertical axis of the mount. This difference is caused by significantly greater mass and inertia of the vertical axis, as well as the presence of noticeably stronger friction effects affecting rotations of the vertical axis. While the quality of tracking slightly decreases with an increase in the reference velocity,

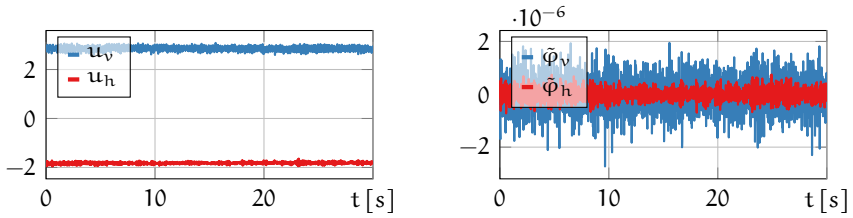

(a) Geostationary object tracking

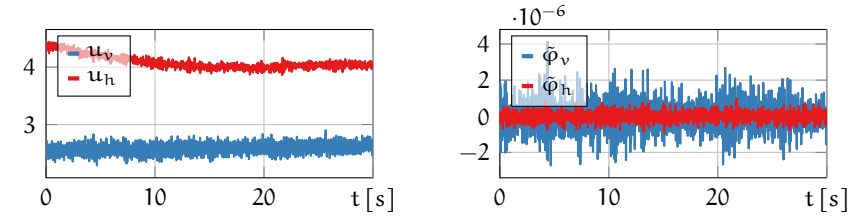

(b) Sidereal tracking

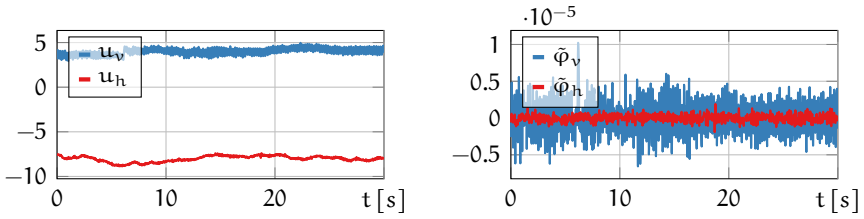

(c) Satellite tracking

Figure 4.6: Results of the telescope experiments. Input torques and tracking errors in vertical and horizontal axes of the mount are given.

errors smaller than a single arcsecond are nonetheless achieved in every scenario. Simultaneously, the high efficiency of the measurement and data acquisition system is shown by the presented plots with a high density and precision of the acquired data.

5

SUMMARY

We strongly believe that non-trivial theory supported by good experimental work may add a new value to robot control.

— K. Kozłowski, 2017 [144]

In the hereby submitted dissertation, the results of research on the problem of modeling uncertainties in the control schemes designed within the Active Disturbance Rejection Paradigm have been conferred. The presented considerations have been divided into two distinct research directions.

In the first part of the work, covered mainly by Chapter 2, the properties of the existing ADRC control schemes have been reported. Specifically, in Section 2.2 a detailed analytical investigation into the impact of the presence of the parametric uncertainties has been presented. Through a novel reformulation of the dynamics of the plant, a uniform analysis for different types of modeling errors has been achieved. On the basis of obtained results, a series of theorems outlining the stability properties of the closed-loop systems under the ADRC control have been formulated highlighting a gradual growth of the stability requirements with an increase in the complexity of the system and extent of present uncertainty. In Section 2.3, by taking advantage of the numerical calculations, the presented results have been extended to cover the problem of input gain uncertainty in more detail. It has been shown that the modeling error of the constant input gain may in some cases violate the theoretical boundaries defined in the literature without loss of stability. Especially, it has been found, that the theoretical stability conditions of the uncertain systems under the ADRC control are imposed mainly by the requirement of the state estimation and not of the disturbance rejection. Thus, it has been shown that if the state of the system is known, the ADRC can be successfully applied to the systems subject to relatively significant uncertainty of the input gain. It has also been shown that the ADRC is not capable of compensating for the disturbances caused by the presence of certain cascade dynamics due to which the order of the system is higher than assumed during the synthesis of the algorithm. As a summary of these considerations, in Section 2.4 results of the application of the ADRC control to some practical problems have been presented and discussed.

In Chapter 3, which constitutes the second part of this work, the solution to some of the issues associated with the presence of model-

ing uncertainties has been proposed. Namely, in Section 3.2 the new PIESO identification scheme for the dynamic systems with unknown constant parameters has been formulated on the basis of the ADRC method. It has been shown that the proper redefinition of the dynamics of the plant enables online estimation of the modeling error which can be subsequently employed in the adaptation method. By taking advantage of this new approach, the adaptive controller called PIDRC has been proposed in Section 3.3. Through a detailed analysis, it has been proved that under certain assumptions these novel tools guarantee asymptotic convergence of the estimation, identification, and tracking errors in the systems for which only a convergence to the neighborhood of the origin is ensured by the conventional ADRC control. The numerical simulations employing both of the proposed schemes have been reported as a verification of the theoretical results. In Section 3.4, the results of experimental trials taking advantage of the considered methods have been reported. Specifically, the solutions to the problems of identification of the hovercraft system and adaptive control of the wheeled mobile robot, have been presented. The obtained results confirmed the effectiveness and usefulness of the devised methods in practical applications.

The studies reported in this dissertation constitute a starting point for further research. New results may be obtained in both directions discussed in Chapters 2 and 3. Concerning the stability properties of the established ADRC methods, the analytical confirmation of the conjectures stated on the basis of numerical or experimental trials awaits to be formulated. Specifically, analytical studies of the feasible range of the input gain uncertainty can be conducted. New methods of performance improvement or model-free control may also be considered following the notion, that an increase in input gain modeling error in the EADRC does not necessarily imply a decrease in the effectiveness of the controller. The methods of PIESO and PIDRC presented in this work are formulated only in their basic and standard forms. Thus, numerous improvements in their structures can be considered in future research. Most notably, the means of ensuring the stability of the adaptive systems without the use of the projection operator may be investigated. The problem of input gain identification in the closed-loop scheme is also to be studied. Finally, various approaches to improvement of the overall performance of the presented methods can be considered. The proposed algorithms are at their core based on the well-known and standard methods of adaptive control and thus new extensions of these methods may possibly be easily transferable also to more general problems.

APPENDIX

A.1 DRIFT TERMS AND CONTROL SIGNAL DERIVATIVES

Recall the error dynamics (2.37) featuring the terms $\dot{\psi}(t, \Lambda_n \hat{z}), \dot{d}(t, x)$ and $\dot{v}$. By embracing the notation $\hat{\psi} = \psi(t, \Lambda_n \hat{z}), d = d(t, \Lambda_n z)$, and taking advantage of the chain rule, the terms $\dot{\psi}(t, \Lambda_n \hat{z}), \dot{d}(t, x)$ are rewritten as

$$\begin{aligned} \dot{\hat{\psi}} &= \frac{\partial \hat{\psi}}{\partial (\Lambda_n \hat{z})} \Lambda_n \dot{\hat{z}} + \frac{\partial \hat{\psi}}{\partial t}, \\ \dot{d} &= \frac{\partial d}{\partial (\Lambda_n z)} \Lambda_n \dot{z} + \frac{\partial d}{\partial t}. \end{aligned} \tag{A.1}$$

By recalling explicit formula of $\dot{\hat{z}}$ as given by (2.27), the first expression of (A.1) is expressed by

$$\begin{aligned} \dot{\hat{\psi}} = \frac{\partial \hat{\psi}}{\partial (\Lambda_n \hat{z})} \Lambda_n \Big(& A_m \hat{z} + d_m \left(\hat{b} u + \psi(t, \Lambda_n \hat{z}) \hat{\theta} \right) \\ & + l c_m^\top (z - \hat{z}) \Big) + \frac{\partial \hat{\psi}}{\partial t}. \end{aligned} \tag{A.2}$$

Substituting the control signal from (2.32) yields

$$\dot{\hat{\psi}} = \frac{\partial \hat{\psi}}{\partial (\Lambda_n \hat{z})} \Lambda_n \left(A_m \hat{z} + d_m \nu - d_m \hat{\delta} + l c_m^\top (z - \hat{z}) \right) + \frac{\partial \hat{\psi}}{\partial t}. \tag{A.3}$$

Further substituting ν from (2.33) yields

$$\begin{aligned} \dot{\hat{\psi}} = \frac{\partial \hat{\psi}}{\partial (\Lambda_n \hat{z})} \Lambda_n \Big(& A_m \hat{z} + d_m k^\top (x_r - \Lambda_n \hat{z}) + d_m x_r^{(n)} \\ & - d_m \hat{\delta} + l c_m^\top (z - \hat{z}) \Big) + \frac{\partial \hat{\psi}}{\partial t}. \end{aligned} \tag{A.4}$$

By rewriting $\hat{\delta} = b_m^\top \hat{z}$ and $\hat{z} = z - \tilde{z}$ the following is obtained,

$$\begin{aligned} \dot{\hat{\psi}} = \frac{\partial \hat{\psi}}{\partial (\Lambda_n \hat{z})} \Lambda_n \Big(& A_m z + d_m k^\top (x_r - x + \Lambda_n \tilde{z}) + d_m x_r^{(n)} \\ & - d_m b_m^\top z + \left(d_m b_m^\top - A_m + l c_m^\top \right) \tilde{z} \Big) + \frac{\partial \hat{\psi}}{\partial t}. \end{aligned} \tag{A.5}$$

By noticing that $\boldsymbol{\Lambda}_n\boldsymbol{A}_m = \boldsymbol{A}_n\boldsymbol{\Lambda}_n + \boldsymbol{b}_n\boldsymbol{b}_m^T$ and $\boldsymbol{\Lambda}_n\boldsymbol{d}_m = \boldsymbol{b}_n$ the expression given in (A.5) is rewritten as

$$\dot{\hat{\psi}} = \frac{\partial\hat{\psi}}{\partial\left(\boldsymbol{\Lambda}_n\hat{\boldsymbol{z}}\right)}\Bigg(\boldsymbol{A}_n\boldsymbol{\Lambda}_n\boldsymbol{z} + \boldsymbol{b}_n\boldsymbol{k}^T\left(\tilde{\boldsymbol{x}} + \boldsymbol{\Lambda}_n\tilde{\boldsymbol{z}}\right) + \boldsymbol{b}_n x_r^{(n)} + \left(-\boldsymbol{A}_n\boldsymbol{\Lambda}_n + \boldsymbol{\Lambda}_n\boldsymbol{l}\boldsymbol{c}_m^T\right)\tilde{\boldsymbol{z}}\Bigg) + \frac{\partial\hat{\psi}}{\partial t}. \tag{A.6}$$

Adding and subtrackting expression $\boldsymbol{A}_n\boldsymbol{x}_r$ and recalling on the basis of (2.34) that $\dot{\boldsymbol{x}}_r = \boldsymbol{A}_n\boldsymbol{x}_r + \boldsymbol{b}_n x_r^{(n)}$ yields

$$\dot{\hat{\psi}} = \frac{\partial\hat{\psi}}{\partial\left(\boldsymbol{\Lambda}_n\hat{\boldsymbol{z}}\right)}\Bigg(\left(-\boldsymbol{A}_n + \boldsymbol{b}_n\boldsymbol{k}^T\right)\tilde{\boldsymbol{x}} + \dot{\boldsymbol{x}}_r + \left(\boldsymbol{b}_n\boldsymbol{k}^T\boldsymbol{\Lambda}_n - \boldsymbol{A}_n\boldsymbol{\Lambda}_n + \boldsymbol{\Lambda}_n\boldsymbol{l}\boldsymbol{c}_m^T\right)\tilde{\boldsymbol{z}}\Bigg) + \frac{\partial\hat{\psi}}{\partial t}. \tag{A.7}$$

At last, recalling $\boldsymbol{G} = \boldsymbol{A}_n - \boldsymbol{b}_n\boldsymbol{k}^T$ the final form of

$$\dot{\hat{\psi}} = \frac{\partial\hat{\psi}}{\partial\left(\boldsymbol{\Lambda}_n\hat{\boldsymbol{z}}\right)}\Bigg(\left(\boldsymbol{\Lambda}_n\boldsymbol{l}\boldsymbol{c}_m^T - \boldsymbol{G}\boldsymbol{\Lambda}_n\right)\tilde{\boldsymbol{z}} - \boldsymbol{G}\tilde{\boldsymbol{x}} + \dot{\boldsymbol{x}}_r\Bigg) + \frac{\partial\hat{\psi}}{\partial t}. \tag{A.8}$$

is obtained, which is consistent with the expression given in (2.39).

The explicit form of $d(t, \boldsymbol{\Lambda}_n\boldsymbol{z})$ is obtained by substituting $\dot{\boldsymbol{z}}$ from (2.27) into (A.1). Such a substitution yields

$$\dot{d} = \frac{\partial d}{\partial\left(\boldsymbol{\Lambda}_n\boldsymbol{z}\right)}\boldsymbol{\Lambda}_n\Bigg(\boldsymbol{A}_m\boldsymbol{z} + \boldsymbol{d}_m\Bigg(\hat{b}u + \boldsymbol{\psi}(t, \boldsymbol{\Lambda}_n\boldsymbol{z})\theta - \boldsymbol{\psi}(t, \boldsymbol{x}_r)\left(\theta - \hat{\theta}\right)\Bigg) + \boldsymbol{b}_m\frac{d}{dt}\delta\Bigg) + \frac{\partial d}{\partial t}. \tag{A.9}$$

Substituting u from (2.32) leads to

$$\dot{d} = \frac{\partial d}{\partial\left(\boldsymbol{\Lambda}_n\boldsymbol{z}\right)}\boldsymbol{\Lambda}_n\Bigg(\boldsymbol{A}_m\boldsymbol{z} + \boldsymbol{d}_m\Bigg(\nu - \hat{\delta} - \boldsymbol{\psi}(t, \boldsymbol{\Lambda}_n\hat{\boldsymbol{z}})\hat{\theta} + \boldsymbol{\psi}(t, \boldsymbol{\Lambda}_n\boldsymbol{z})\theta - \boldsymbol{\psi}(t, \boldsymbol{x}_r)\left(\theta - \hat{\theta}\right)\Bigg) + \boldsymbol{b}_m\frac{d}{dt}\delta\Bigg) + \frac{\partial d}{\partial t}. \tag{A.10}$$

Substituting ν as given by (2.33) yields

$$\dot{d} = \frac{\partial d}{\partial\left(\boldsymbol{\Lambda}_n\boldsymbol{z}\right)}\boldsymbol{\Lambda}_n\Bigg(\boldsymbol{A}_m\boldsymbol{z} + \boldsymbol{d}_m\Bigg(\boldsymbol{k}^T\left(\boldsymbol{x}_r - \boldsymbol{\Lambda}_n\hat{\boldsymbol{z}}\right) + x_r^{(n)} - \hat{\delta} - \boldsymbol{\psi}(t, \boldsymbol{\Lambda}_n\hat{\boldsymbol{z}})\hat{\theta} + \boldsymbol{\psi}(t, \boldsymbol{\Lambda}_n\boldsymbol{z})\theta - \boldsymbol{\psi}(t, \boldsymbol{x}_r)\left(\theta - \hat{\theta}\right)\Bigg) + \boldsymbol{b}_m\frac{d}{dt}\delta\Bigg) + \frac{\partial d}{\partial t}. \tag{A.11}$$

Further rewriting $\hat{\delta} = \mathbf{b}_m^T \hat{z}$ and $\hat{z} = z - \tilde{z}$ gives

$$\begin{aligned}\dot{d} = \frac{\partial d}{\partial (\Lambda_n z)} \Lambda_n \Bigg(A_m z + \mathbf{d}_m \Bigg(\mathbf{k}^T (x_r - \Lambda_n z + \Lambda_n \tilde{z}) + x_r^{(n)} \\ - \mathbf{b}_m^T z + \mathbf{b}_m^T \tilde{z} - \psi(t, \Lambda_n \hat{z}) \hat{\theta} + \psi(t, \Lambda_n z) \theta \\ - \psi(t, x_r) \left(\theta - \hat{\theta} \right) \Bigg) + \mathbf{b}_m \frac{d}{dt} \delta \Bigg) + \frac{\partial d}{\partial t}.\end{aligned} \tag{A.12}$$

Recalling that $\Lambda_n A_m = A_n \Lambda_n + \mathbf{b}_n \mathbf{b}_m^T$, $\Lambda_n \mathbf{d}_m = \mathbf{b}_n$, and moreover $\Lambda_n \mathbf{b}_m = 0_n$, yields

$$\begin{aligned}\dot{d} = \frac{\partial d}{\partial (\Lambda_n z)} \Bigg(A_n \Lambda_n z + \mathbf{b}_n \mathbf{k}^T (x_r - x + \Lambda_n \tilde{z}) + \mathbf{b}_n x_r^{(n)} \\ + \mathbf{b}_n \mathbf{b}_m^T \tilde{z} + \mathbf{b}_n \Bigg(- \psi(t, \Lambda_n \hat{z}) \hat{\theta} + \psi(t, \Lambda_n z) \theta \\ - \psi(t, x_r) \left(\theta - \hat{\theta} \right) \Bigg) \Bigg) + \frac{\partial d}{\partial t}.\end{aligned} \tag{A.13}$$

Once again adding and subtrackting $A_n x_r$ and noticing that $\dot{x}_r = A_n x_r + \mathbf{b}_n x_r^{(n)}$ enables to express (A.13) as

$$\begin{aligned}\dot{d} = \frac{\partial d}{\partial (\Lambda_n z)} \Bigg(\left(-A_n + \mathbf{b}_n \mathbf{k}^T \right) \tilde{x} + \dot{x}_r + \left(\mathbf{b}_n \mathbf{k}^T \Lambda_n + \mathbf{b}_n \mathbf{b}_m^T \right) \tilde{z} \\ \mathbf{b}_n \left(\psi(t, \Lambda_n z) \theta - \psi(t, x_r) \left(\theta - \hat{\theta} \right) - \psi(t, \Lambda_n \hat{z}) \hat{\theta} \right) \Bigg) + \frac{\partial d}{\partial t}.\end{aligned} \tag{A.14}$$

Finally, recalling $G = A_n - \mathbf{b}_n \mathbf{k}^T$ and $W = \mathbf{b}_n \mathbf{k}^T \Lambda_n + \mathbf{b}_n \mathbf{b}_m^T$ yields

$$\begin{aligned}\dot{d} = \frac{\partial d}{\partial (\Lambda_n z)} \Bigg(W \tilde{z} - G \tilde{x} + \dot{x}_r + \mathbf{b}_n \Bigg(\psi(t, \Lambda_n z) \theta \\ - \psi(t, x_r) \left(\theta - \hat{\theta} \right) - \psi(t, \Lambda_n \hat{z}) \hat{\theta} \Bigg) \Bigg) + \frac{\partial d}{\partial t}\end{aligned} \tag{A.15}$$

what corresponds to the expression in (2.39).

In order to obtain an explicit formula of $\dot{\nu}$ consider first the term ν and, by recalling that $\hat{z} = z - \tilde{z}$ rewrite it on the basis of (2.33) as

$$\nu = \mathbf{k}^T (\tilde{x} + \Lambda_n \tilde{z}) + x_r^{(n)}. \tag{A.16}$$

The derivative of this expression is thus given by

$$\dot{\nu} = \mathbf{k}^T \dot{\tilde{x}} + \mathbf{k}^T \Lambda_n \dot{\tilde{z}} + x_r^{(m)}. \tag{A.17}$$

Substituting $\dot{\tilde{\mathbf{x}}}$ and $\dot{\tilde{\mathbf{z}}}$ from (2.37) yields

$$\begin{aligned}\dot{v} = \mathbf{k}^{\mathsf{T}}\Big(\mathbf{G}\tilde{\mathbf{x}} - \boldsymbol{W}\tilde{\mathbf{z}} + \mathbf{b}_n\Big(\boldsymbol{\psi}(t,\mathbf{x}_r)\left(\theta - \hat{\theta}\right) + \boldsymbol{\psi}(t,\boldsymbol{\Lambda}_n\hat{\mathbf{z}})\hat{\theta} \\ - \boldsymbol{\psi}(t,\boldsymbol{\Lambda}_n\mathbf{z})\theta\Big)\Big) + \mathbf{k}^{\mathsf{T}}\boldsymbol{\Lambda}_n\Big(\mathbf{H}\tilde{\mathbf{z}} + \mathbf{d}_m\Big(\boldsymbol{\psi}(t,\boldsymbol{\Lambda}_n\mathbf{z})\theta \\ - \boldsymbol{\psi}(t,\mathbf{x}_r)\left(\theta - \hat{\theta}\right) - \boldsymbol{\psi}(t,\boldsymbol{\Lambda}_n\hat{\mathbf{z}})\hat{\theta}\Big) + \mathbf{b}_m\Big(\dot{\boldsymbol{\psi}}(t,\mathbf{x}_r)\left(\theta - \hat{\theta}\right) \\ - \left(\frac{b}{\hat{b}} - 1\right)\left(\dot{\boldsymbol{\psi}}(t,\boldsymbol{\Lambda}_n\hat{\mathbf{z}})\hat{\theta} - \dot{v}\right) + \dot{d}(t,\boldsymbol{\Lambda}_n\mathbf{z})\Big)\Big) + x_r^{(m)}.\end{aligned} \tag{A.18}$$

By taking advantage of the notion that $\boldsymbol{\Lambda}_n\mathbf{d}_m = \mathbf{b}_n$ and $\boldsymbol{\Lambda}_n\mathbf{b}_m = \mathbf{0}_n$, this is simplified to

$$\begin{aligned}\dot{v} = \mathbf{k}^{\mathsf{T}}\Big(\mathbf{G}\tilde{\mathbf{x}} - \boldsymbol{W}\tilde{\mathbf{z}} + \mathbf{b}_n\Big(\boldsymbol{\psi}(t,\mathbf{x}_r)\left(\theta - \hat{\theta}\right) + \boldsymbol{\psi}(t,\boldsymbol{\Lambda}_n\hat{\mathbf{z}})\hat{\theta} \\ - \boldsymbol{\psi}(t,\boldsymbol{\Lambda}_n\mathbf{z})\theta\Big)\Big) + \mathbf{k}^{\mathsf{T}}\Big(\boldsymbol{\Lambda}_n\mathbf{H}\tilde{\mathbf{z}} + \mathbf{b}_n\Big(\boldsymbol{\psi}(t,\boldsymbol{\Lambda}_n\mathbf{z})\theta \\ - \boldsymbol{\psi}(t,\mathbf{x}_r)\left(\theta - \hat{\theta}\right) - \boldsymbol{\psi}(t,\boldsymbol{\Lambda}_n\hat{\mathbf{z}})\hat{\theta}\Big)\Big) + x_r^{(m)}.\end{aligned} \tag{A.19}$$

The terms multiplied by $\mathbf{k}^{\mathsf{T}}\mathbf{b}_n$ reduce themselves and thus the expression

$$\dot{v} = \mathbf{k}^{\mathsf{T}}\mathbf{G}\tilde{\mathbf{x}} + \mathbf{k}^{\mathsf{T}}\left(\boldsymbol{\Lambda}_n\mathbf{H} - \boldsymbol{W}\right)\tilde{\mathbf{z}} + x_r^{(m)} \tag{A.20}$$

is obtained and corresponds to (2.38).

A.2 LYAPUNOV FUNCTION DERIVATIVES FOR PIESO AND PIDRC

Consider stability analysis of the PIESO scheme designed for the system with the regressor being a function of time and state of the system and presented in Section 3.2.2. Recall the auxiliary function (3.57) given by

$$V_{3.2}^*(\bar{\mathbf{z}}) = \frac{1}{2}\bar{\mathbf{z}}^{\mathsf{T}}\mathbf{P}\bar{\mathbf{z}} + \frac{1}{2}\tilde{\theta}^{\mathsf{T}}\boldsymbol{\Gamma}^{-1}\tilde{\theta} - \bar{\mathbf{z}}^{\mathsf{T}}\mathbf{P}\mathbf{b}_m\boldsymbol{\psi}(t,\boldsymbol{\Lambda}_n\mathbf{z})\tilde{\theta}. \tag{A.21}$$

The derivative of this function is analytically calculated as

$$\begin{aligned}\dot{V}_{3.2}^*(\bar{\mathbf{z}}) = \bar{\mathbf{z}}^{\mathsf{T}}\mathbf{P}\dot{\bar{\mathbf{z}}} + \tilde{\theta}^{\mathsf{T}}\boldsymbol{\Gamma}^{-1}\dot{\tilde{\theta}} - \tilde{\theta}^{\mathsf{T}}\boldsymbol{\psi}^{\mathsf{T}}\mathbf{b}_m^{\mathsf{T}}\mathbf{P}\dot{\bar{\mathbf{z}}} - \bar{\mathbf{z}}^{\mathsf{T}}\mathbf{P}\mathbf{b}_m\dot{\boldsymbol{\psi}}\tilde{\theta} \\ - \bar{\mathbf{z}}^{\mathsf{T}}\mathbf{P}\mathbf{b}_m\boldsymbol{\psi}(\dot{})\tilde{\theta}\end{aligned} \tag{A.22}$$

with $\boldsymbol{\psi} = \boldsymbol{\psi}(t, \boldsymbol{\Lambda}_n z)$ denoted for brevity. Substituting $\dot{\bar{z}}$ and $\dot{\tilde{\theta}}$ from (3.56) yields

$$\begin{aligned}\dot{V}^*_{3.2} = {} & \omega_o \bar{z}^T \mathbf{P} \bar{\mathbf{H}} \bar{z} + \omega_o \bar{z}^T \mathbf{P} \mathbf{d}_m \left(\boldsymbol{\psi} - \hat{\boldsymbol{\psi}}\right) \hat{\theta} + \bar{z}^T \mathbf{P} \mathbf{b}_m \dot{\boldsymbol{\psi}} \tilde{\theta} \\ & - \bar{z}^T \mathbf{P} \mathbf{b}_m \boldsymbol{\psi} \operatorname{Proj}(\boldsymbol{\tau}) - \tilde{\theta}^T \boldsymbol{\Gamma}^{-1} \operatorname{Proj}(\boldsymbol{\tau}) - \omega_o \tilde{\theta}^T \boldsymbol{\psi}^T \mathbf{b}_m^T \mathbf{P} \bar{\mathbf{H}} \bar{z} \\ & - \omega_o \tilde{\theta}^T \boldsymbol{\psi}^T \mathbf{b}_m^T \mathbf{P} \mathbf{d}_m \left(\boldsymbol{\psi} - \hat{\boldsymbol{\psi}}\right) \hat{\theta} - \tilde{\theta}^T \boldsymbol{\psi}^T \mathbf{b}_m^T \mathbf{P} \mathbf{b}_m \dot{\boldsymbol{\psi}} \tilde{\theta} \\ & + \tilde{\theta}^T \boldsymbol{\psi}^T \mathbf{b}_m^T \mathbf{P} \mathbf{b}_m \boldsymbol{\psi} \operatorname{Proj}(\boldsymbol{\tau}) - \bar{z}^T \mathbf{P} \mathbf{b}_m \dot{\boldsymbol{\psi}} \tilde{\theta} \\ & + \bar{z}^T \mathbf{P} \mathbf{b}_m \boldsymbol{\psi} \operatorname{Proj}(\boldsymbol{\tau})\end{aligned} \tag{A.23}$$

with $\hat{\boldsymbol{\psi}} = \boldsymbol{\psi}(t, \boldsymbol{\Lambda}_n \hat{z})$. The terms $\bar{z}^T \mathbf{P} \mathbf{b}_m \dot{\boldsymbol{\psi}} \tilde{\theta}$ and $\bar{z}^T \mathbf{P} \mathbf{b}_m \boldsymbol{\psi} \operatorname{Proj}(\boldsymbol{\tau})$ are reduced in the obtained expression. This is a crucial observation, as the latter of these do not yield the quadratic upper bound and thus its reduction is necessary to ensure the negativeness of the entire expression. By adding and subtracting $\tilde{\theta}^T \boldsymbol{\Gamma}^{-1} \boldsymbol{\tau}$, and substituting $\boldsymbol{\tau}$ from (3.56) the following is obtained,

$$\begin{aligned}\dot{V}^*_{3.2} = {} & -\frac{1}{2} \omega_o \bar{z}^T \bar{z} + \omega_o \bar{z}^T \mathbf{P} \mathbf{d}_m \left(\boldsymbol{\psi} - \hat{\boldsymbol{\psi}}\right) \hat{\theta} - \tilde{\theta}^T \boldsymbol{\Gamma}^{-1} \Big(\operatorname{Proj}(\boldsymbol{\tau}) \\ & - \boldsymbol{\tau} \Big) - \tilde{\theta}^T \left(\hat{\boldsymbol{\psi}}^T - \boldsymbol{\psi}^T\right) \boldsymbol{\psi} \tilde{\theta} - \tilde{\theta}^T \boldsymbol{\psi}^T \boldsymbol{\psi} \tilde{\theta} + \tilde{\theta}^T \Big(\hat{\boldsymbol{\psi}}^T \\ & - \boldsymbol{\psi}^T \Big) \mathbf{b}_m^T \bar{z} + \tilde{\theta}^T \boldsymbol{\psi}^T \mathbf{b}_m^T \bar{z} - \omega_o \tilde{\theta}^T \boldsymbol{\psi}^T \mathbf{b}_m^T \mathbf{P} \bar{\mathbf{H}} \bar{z} \\ & - \omega_o \tilde{\theta}^T \boldsymbol{\psi}^T \mathbf{b}_m^T \mathbf{P} \mathbf{d}_m \left(\boldsymbol{\psi} - \hat{\boldsymbol{\psi}}\right) \hat{\theta} - \tilde{\theta}^T \boldsymbol{\psi}^T \mathbf{b}_m^T \mathbf{P} \mathbf{b}_m \dot{\boldsymbol{\psi}} \tilde{\theta} \\ & + \tilde{\theta}^T \boldsymbol{\psi}^T \mathbf{b}_m^T \mathbf{P} \mathbf{b}_m \boldsymbol{\psi} \operatorname{Proj}(\boldsymbol{\tau}).\end{aligned} \tag{A.24}$$

Recalling the properties of the projection operator given by (3.52) and Corollary 3.3 enables to establish the upper bound of (A.24) as

$$\begin{aligned}\dot{V}^*_{3.2} \leqslant {} & -\frac{1}{2} \omega_o \|\bar{z}\|^2 + \omega_o \|\bar{z}\| p_M \left\|\boldsymbol{\psi} - \hat{\boldsymbol{\psi}}\right\| \theta_M \\ & + \left\|\hat{\boldsymbol{\psi}} - \boldsymbol{\psi}\right\| \psi_M \theta_M^2 + \theta_M \left\|\hat{\boldsymbol{\psi}} - \boldsymbol{\psi}\right\| \|\bar{z}\| + \theta_M \psi_M \|\bar{z}\| \\ & + \omega_o \theta_M \psi_M p_M h_M \|\bar{z}\| + \omega_o \theta_M \psi_M p_M \left\|\boldsymbol{\psi} - \hat{\boldsymbol{\psi}}\right\| \theta_M \\ & + \theta_M^2 \psi_M^2 p_M + \theta_M \psi_M p_M \psi_M \|\operatorname{Proj}(\boldsymbol{\tau})\| .\end{aligned} \tag{A.25}$$

The Lipschitz property of the regressor established by Assumption 3.3 implies that

$$\begin{aligned}\left\|\hat{\boldsymbol{\psi}} - \boldsymbol{\psi}\right\| &\leqslant \|\hat{\mathbf{x}} - \mathbf{x}\| \psi_L = \|\boldsymbol{\Lambda}_n \tilde{z}\| \psi_L = \left\|\boldsymbol{\Lambda}_n \boldsymbol{\Phi}_o^{-1} \bar{z}\right\| \psi_L \\ &\leqslant \left\|\boldsymbol{\Lambda}_n \boldsymbol{\Phi}_o^{-1}\right\| \|\bar{z}\| \psi_L.\end{aligned} \tag{A.26}$$

Moreover, recalling $\boldsymbol{\tau}$ from (3.56),

$$\begin{aligned}\|\mathrm{Proj}(\boldsymbol{\tau})\| \leqslant \gamma_M \left\|\hat{\boldsymbol{\psi}} - \boldsymbol{\psi}\right\| \psi_M \left\|\tilde{\boldsymbol{\theta}}\right\| + \gamma_M \psi_M^2 \left\|\tilde{\boldsymbol{\theta}}\right\| \\ + \gamma_M \left\|\hat{\boldsymbol{\psi}} - \boldsymbol{\psi}\right\| \|\bar{z}\| + \gamma_M \psi_M \|\bar{z}\|.\end{aligned} \tag{A.27}$$

By taking advantage of these properties, the bound of $\dot{V}_{3.2}^*$ is expressed as

$$\begin{aligned}\dot{V}_{3.2}^* \leqslant & -\frac{1}{2}\omega_o \|\bar{z}\|^2 + \omega_o p_M \left\|\boldsymbol{\Lambda}_n \boldsymbol{\Phi}_o^{-1}\right\| \|\bar{z}\|^2 \psi_L \theta_M \\ & + \left\|\boldsymbol{\Lambda}_n \boldsymbol{\Phi}_o^{-1}\right\| \|\bar{z}\| \psi_L \psi_M \theta_M^2 + \theta_M \left\|\boldsymbol{\Lambda}_n \boldsymbol{\Phi}_o^{-1}\right\| \psi_L \|\bar{z}\|^2 \\ & + \theta_M \psi_M \|\bar{z}\| + \omega_o \theta_M \psi_M p_M h_M \|\bar{z}\| \\ & + \omega_o \theta_M^2 \psi_M p_M \left\|\boldsymbol{\Lambda}_n \boldsymbol{\Phi}_o^{-1}\right\| \|\bar{z}\| \psi_L + \theta_M^2 \psi_M^2 p_M \\ & + \theta_M^2 \psi_M^3 p_M \gamma_M \left\|\boldsymbol{\Lambda}_n \boldsymbol{\Phi}_o^{-1}\right\| \|\bar{z}\| \psi_L + \theta_M^2 \psi_M^4 p_M \gamma_M \\ & + \theta_M \psi_M^2 p_M \gamma_M \left\|\boldsymbol{\Lambda}_n \boldsymbol{\Phi}_o^{-1}\right\| \psi_L \|\bar{z}\|^2 \\ & + \theta_M \psi_M^3 p_M \gamma_M \|\bar{z}\|.\end{aligned} \tag{A.28}$$

Importantly, $\left\|\boldsymbol{\Lambda}_n \boldsymbol{\Phi}_o^{-1}\right\| = \omega_o^{-n|-1}$ and $\omega_o \left\|\boldsymbol{\Lambda}_n \boldsymbol{\Phi}_o^{-1}\right\| = \omega_o^{-n+1|0}$, and are thus nonincreasing in ω_o. Grouping the terms yields

$$\begin{aligned}\dot{V}_{3.2}^* \leqslant & \left(-\frac{1}{2}\omega_o + \omega_c^{-n+1|0} p_M \psi_L \theta_M + \omega_o^{-n|-1} \left(\theta_M \psi_L \right.\right. \\ & \left.\left. + \theta_M \psi_M^2 p_M \gamma_M \psi_L\right)\right) \|\bar{z}\|^2 + \theta_M \left(\psi_M^3 p_M \gamma_M \right. \\ & + \psi_M + \omega_o \psi_M p_M h_M + \omega_c^{-n+1|0} \theta_M \psi_M p_M \psi_L \\ & \left. + \omega_o^{-n|-1} \theta_M \left(\psi_M^3 p_M \gamma_M \psi_L + \psi_L \psi_M\right)\right) \|\bar{z}\| \\ & + \theta_M^2 \left(\psi_M^2 p_M + \psi_M^4 p_M \gamma_M\right),\end{aligned} \tag{A.29}$$

what is consistent with the results presented in (3.60).

Consider the function established in (3.65) and given by

$$V_{3.2}(\bar{z}, \tilde{\theta}) = \frac{1}{2}\bar{z}^\top \mathbf{P} \bar{z} + \tilde{\theta}^\top \left(\frac{1}{2}\boldsymbol{\Gamma}^{-1} - \mathbf{M}(t, \boldsymbol{\Lambda}_n z)\right) \tilde{\theta}. \tag{A.30}$$

Its time derivative along the trajectories of the system takes the form of

$$\dot{V}_{3.2}(\bar{z}, \tilde{\theta}) = \bar{z}^\top \mathbf{P} \dot{\bar{z}} + \tilde{\theta}^\top \boldsymbol{\Gamma}^{-1} \dot{\tilde{\theta}} - \tilde{\theta}^\top \dot{\mathbf{M}} \tilde{\theta} - 2\tilde{\theta}^\top \mathbf{M} \dot{\tilde{\theta}}. \tag{A.31}$$

Substituting $\dot{\bar{z}}, \dot{\tilde{\theta}}$ from (3.56) and $\dot{\mathbf{M}}$ given by Corollary 3.2 yields

$$\begin{aligned}\dot{V}_{3.2} = {} & \omega_o \bar{z}^T \mathbf{P} \bar{\mathbf{H}} \bar{z} + \omega_o \bar{z}^T \mathbf{P} \mathbf{d}_m \left(\psi - \hat{\psi}\right) \hat{\theta} + \bar{z}^T \mathbf{P} \mathbf{b}_m \dot{\psi} \tilde{\theta} \\ & - \bar{z}^T \mathbf{P} \mathbf{b}_m \psi \operatorname{Proj}(\boldsymbol{\tau}) - \tilde{\theta}^T \boldsymbol{\Gamma}^{-1} \operatorname{Proj}(\boldsymbol{\tau}) - \tilde{\theta}^T \mathbf{M} \tilde{\theta} \\ & - \tilde{\theta}^T \psi^T \psi \tilde{\theta} + 2 \tilde{\theta}^T \mathbf{M} \operatorname{Proj}(\boldsymbol{\tau}).\end{aligned} \tag{A.32}$$

Adding and subtracting $\tilde{\theta}^T \boldsymbol{\Gamma}^{-1} \boldsymbol{\tau}$, and substituting $\boldsymbol{\tau}$ from (3.56) gives

$$\begin{aligned}\dot{V}_{3.2} = {} & -\frac{1}{2} \omega_o \bar{z}^T \bar{z} + \omega_o \bar{z}^T \mathbf{P} \mathbf{d}_m \left(\psi - \hat{\psi}\right) \hat{\theta} + \bar{z}^T \mathbf{P} \mathbf{b}_m \dot{\psi} \tilde{\theta} \\ & - \bar{z}^T \mathbf{P} \mathbf{b}_m \psi \operatorname{Proj}(\boldsymbol{\tau}) - \tilde{\theta}^T \boldsymbol{\Gamma}^{-1} \left(\operatorname{Proj}(\boldsymbol{\tau}) - \boldsymbol{\tau}\right) \\ & - \tilde{\theta}^T \left(\hat{\psi}^T - \psi^T\right) \psi \tilde{\theta} - \tilde{\theta}^T \psi^T \psi \tilde{\theta} + \tilde{\theta}^T \left(\hat{\psi}^T - \psi^T\right) \mathbf{b}_m^T \bar{z} \\ & + \tilde{\theta}^T \psi^T \mathbf{b}_m^T \bar{z} - \tilde{\theta}^T \mathbf{M} \tilde{\theta} - \tilde{\theta}^T \psi^T \psi \tilde{\theta} + 2 \tilde{\theta}^T \mathbf{M} \operatorname{Proj}(\boldsymbol{\tau}).\end{aligned} \tag{A.33}$$

The terms $\tilde{\theta}^T \psi^T \psi \tilde{\theta}$ reduce each other and by recalling Corollary 3.3 it follows that

$$\begin{aligned}\dot{V}_{3.2} \leqslant {} & -\frac{1}{2} \omega_o \|\bar{z}\|^2 + \omega_o \|\bar{z}\| p_M \left\|\psi - \hat{\psi}\right\| \theta_M + \|\bar{z}\| p_M \psi_M \left\|\tilde{\theta}\right\| \\ & + \|\bar{z}\| p_M \psi_M \|\operatorname{Proj}(\boldsymbol{\tau})\| + \left\|\tilde{\theta}\right\| \left\|\hat{\psi} - \psi\right\| \psi_M \theta_M \\ & + \theta_M \left\|\hat{\psi} - \psi\right\| \|\bar{z}\| + \left\|\tilde{\theta}\right\| \psi_M \|\bar{z}\| - \mu e^{-T_{PE}} \left\|\tilde{\theta}\right\|^2 \\ & + 2 \left\|\tilde{\theta}\right\| \psi_M^2 \|\operatorname{Proj}(\boldsymbol{\tau})\|.\end{aligned} \tag{A.34}$$

By recalling the norm of the projected adaptation law and the Lipschitz property of the regressor, it follows that

$$\begin{aligned}\dot{V}_{3.2} \leqslant {} & -\frac{1}{2} \omega_o \|\bar{z}\|^2 + \omega_o p_M \left\|\boldsymbol{\Lambda}_n \boldsymbol{\Phi}_o^{-1}\right\| \|\bar{z}\|^2 \psi_L \theta_M \\ & + \|\bar{z}\| p_M \psi_M \left\|\tilde{\theta}\right\| + p_M \psi_M^2 \gamma_M \left\|\boldsymbol{\Lambda}_n \boldsymbol{\Phi}_o^{-1}\right\| \|\bar{z}\|^2 \psi_L \theta_M \\ & + \|\bar{z}\| p_M \gamma_M \psi_M^3 \left\|\tilde{\theta}\right\| + \gamma_M p_M \psi_M \left\|\boldsymbol{\Lambda}_n \boldsymbol{\Phi}_o^{-1}\right\| \|\bar{z}\|^3 \psi_L \\ & + p_M \psi_M^2 \gamma_M \|\bar{z}\|^2 + \left\|\tilde{\theta}\right\| \left\|\boldsymbol{\Lambda}_n \boldsymbol{\Phi}_o^{-1}\right\| \|\bar{z}\| \psi_L \psi_M \theta_M \\ & + \theta_M \left\|\boldsymbol{\Lambda}_n \boldsymbol{\Phi}_o^{-1}\right\| \|\bar{z}\|^2 \psi_L + \left\|\tilde{\theta}\right\| \psi_M \|\bar{z}\| - \mu e^{-T_{PE}} \left\|\tilde{\theta}\right\|^2 \\ & + 2\theta_M \psi_M^3 \gamma_M \left\|\boldsymbol{\Lambda}_n \boldsymbol{\Phi}_o^{-1}\right\| \|\bar{z}\| \psi_L \left\|\tilde{\theta}\right\| + 2\psi_M^4 \gamma_M \left\|\tilde{\theta}\right\|^2 \\ & + 2\gamma_M \theta_M \psi_M^2 \left\|\boldsymbol{\Lambda}_n \boldsymbol{\Phi}_o^{-1}\right\| \psi_L \|\bar{z}\|^2 + 2 \left\|\tilde{\theta}\right\| \psi_M^3 \gamma_M \|\bar{z}\|.\end{aligned} \tag{A.35}$$

Recall $\left\|\boldsymbol{\Lambda}_n \boldsymbol{\Phi}_o^{-1}\right\| = \omega_o^{-n|-1}$ and $\omega_o \left\|\boldsymbol{\Lambda}_n \boldsymbol{\Phi}_o^{-1}\right\| = \omega_o^{-n+1|0}$. Consider also that $\left\|\bar{z}\right\| \leqslant z_M$, as implied by the analysis of the auxiliary func-

tion, enables the establishment of the quadratic bound of the term $\gamma_M p_M \psi_M \left\| \boldsymbol{\Lambda}_n \boldsymbol{\Phi}_o^{-1} \right\| \left\| \bar{z} \right\|^3 \psi_L$. Grouping the expressions then yields

$$\begin{aligned}\dot{V}_{3.2} \leqslant & \left(-\frac{1}{2}\omega_o + p_M \psi_M^2 \gamma_M + p_M \omega_o^{-n+1|0} \psi_L \theta_M \right. \\ & + \omega_o^{-n|-1} \left(p_M \psi_M^2 \gamma_M \psi_L \theta_M + \gamma_M p_M \psi_M z_M \psi_L \right. \\ & \left. \left. + \theta_M \psi_L + 2\gamma_M \theta_M \psi_M^2 \psi_L \right) \right) \left\| \bar{z} \right\|^2 + \left(p_M \gamma_M \psi_M^3 \right. \\ & + p_M \psi_M + \psi_M + 2\psi_M^3 \gamma_M + \omega_o^{-n|-1} \left(2\theta_M \psi_M^3 \gamma_M \psi_L \right. \\ & \left. \left. + \psi_L \psi_M \theta_M \right) \right) \left\| \tilde{\theta} \right\| \left\| \bar{z} \right\| + \left(-\mu e^{-T_{PE}} + 2\psi_M^4 \gamma_M \right) \left\| \tilde{\theta} \right\|^2 .\end{aligned} \tag{A.36}$$

Invoking the Young's inequality gives

$$\begin{aligned}\dot{V}_{3.2} \leqslant & \left(-\frac{1}{2}\omega_o + p\psi_M^2 \gamma_M + \omega_c^{-n+1|0} p_M \psi_L \theta_M \right. \\ & + \omega_o^{-n|-1} \left(p_M \psi_M^2 \psi_L \gamma_M \theta_M + p_M \psi_M \psi_L \gamma_M z_M \right. \\ & + \theta_M \psi_L + 2\theta_M \psi_M^2 \psi_L \gamma_M \Big) + \frac{1}{2\varepsilon} \Big(p_M \psi_M + p_M \gamma_M \psi_M^3 \\ & + 2\psi_M^3 \gamma + \omega_o^{-n|-1} \theta_M \psi_L \left(2\psi_M^3 \gamma_M + \psi_M \right) \\ & \left. \left. + \psi_M \Big)^2 \right) \left\| \bar{z} \right\|^2 + \left(-\mu e^{-T_{PE}} + 2\gamma_M \psi_M^4 + \frac{\varepsilon}{2} \right) \left\| \tilde{\theta} \right\|^2 \right.\end{aligned} \tag{A.37}$$

for any $\varepsilon \in \mathbb{R}_+$, what is consistent with (3.68).

In order to investigate the derivation of the Lyapunov function for the reference-based PIDRC scheme as presented in Section 3.3.2, recall function (3.121) expressed by

$$V_{3.4}(\bar{x}, \bar{z}, \tilde{\theta}) = \frac{1}{2}\omega_o \bar{x}^T \mathbf{R} \bar{x} + \frac{1}{2} \bar{z}^T \mathbf{P} \bar{z} + \tilde{\theta}^T \left(\frac{1}{2} \boldsymbol{\Gamma}^{-1} - \mathbf{M}(t, x_r) \right) \tilde{\theta}. \tag{A.38}$$

The derivative of the function is given by

$$\dot{V}_{3.4}(\bar{x}, \bar{z}, \tilde{\theta}) = \omega_o \bar{x}^T \mathbf{R} \dot{\bar{x}} + \bar{z}^T \mathbf{P} \dot{\bar{z}} + \tilde{\theta}^T \boldsymbol{\Gamma}^{-1} \dot{\tilde{\theta}} - \tilde{\theta}^T \dot{\mathbf{M}} \tilde{\theta} - 2\tilde{\theta}^T \mathbf{M} \dot{\tilde{\theta}}. \tag{A.39}$$

Substituting $\dot{\bar{x}}, \dot{\bar{z}}$ and $\dot{\tilde{\theta}}$ from (3.120), as well as $\dot{M}$ from Corollary 3.4 yields

$$\begin{aligned}\dot{V}_{3.4} = {} & \omega_c \omega_o \bar{x}^T \mathbf{R} \bar{G} \bar{x} - \omega_o \bar{x}^T \mathbf{R} \mathbf{b}_n \left(\bar{k}^T \mathbf{\Phi}_c \omega_c \mathbf{\Lambda}_n \mathbf{\Phi}_o^{-1} + \mathbf{b}_m^T \right) \bar{z} \\ & - \omega_o \bar{x}^T \mathbf{R} \mathbf{b}_n \left(\psi - \psi_r \right) \theta + \omega_o \bar{z}^T \mathbf{P} \bar{H} \bar{z} + \omega_o \bar{z}^T \mathbf{P} \mathbf{d}_m \Big(\psi \\ & - \psi_r \Big) \theta + \bar{z}^T \mathbf{P} \mathbf{b}_m \dot{\psi}_r \tilde{\theta} - \bar{z}^T \mathbf{P} \mathbf{b}_m \psi_r \operatorname{Proj}(\tau) \\ & - \tilde{\theta}^T \mathbf{\Gamma}^{-1} \operatorname{Proj}(\tau) - \tilde{\theta}^T \mathbf{M} \tilde{\theta} + \tilde{\theta}^T \psi_r^T \psi_r \tilde{\theta} + 2 \tilde{\theta}^T \mathbf{M} \operatorname{Proj}(\tau)\end{aligned} \tag{A.40}$$

with $\psi_r = \psi(t, x_r)$ denoted for brevity. By adding and subtracting $\tilde{\theta}^T \mathbf{\Gamma}^{-1} \tau$, and substituting τ from (3.120), it follows that

$$\begin{aligned}\dot{V}_{3.4} = {} & -\frac{1}{2} \omega_c \omega_o \bar{x}^T \bar{x} - \omega_o \bar{x}^T \mathbf{R} \mathbf{b}_n \left(\bar{k}^T \mathbf{\Phi}_c \omega_c \mathbf{\Lambda}_n \mathbf{\Phi}_o^{-1} + \mathbf{b}_m^T \right) \bar{z} \\ & - \omega_o \bar{x}^T \mathbf{R} \mathbf{b}_n \left(\psi - \psi_r \right) \theta - \frac{1}{2} \omega_o \bar{z}^T \bar{z} + \omega_o \bar{z}^T \mathbf{P} \mathbf{d}_m \Big(\psi \\ & - \psi_r \Big) \theta + \bar{z}^T \mathbf{P} \mathbf{b}_m \dot{\psi}_r \tilde{\theta} - \bar{z}^T \mathbf{P} \mathbf{b}_m \psi_r \operatorname{Proj}(\tau) \\ & - \tilde{\theta}^T \mathbf{\Gamma}^{-1} \left(\operatorname{Proj}(\tau) - \tau \right) - \tilde{\theta}^T \psi_r^T \psi_r \tilde{\theta} + \tilde{\theta}^T \psi_r^T \mathbf{b}_m^T \bar{z} \\ & - \tilde{\theta}^T \mathbf{M} \tilde{\theta} + \tilde{\theta}^T \psi_r^T \psi_r \tilde{\theta} + 2 \tilde{\theta}^T \mathbf{M} \operatorname{Proj}(\tau).\end{aligned} \tag{A.41}$$

The terms $\tilde{\theta}^T \psi_r^T \psi_r \tilde{\theta}$ reduce each other. By recalling the properties of the projection operator given by (3.52) and Corollary 3.3 yields

$$\begin{aligned}\dot{V}_{3.4} \leqslant {} & -\frac{1}{2} \omega_c \omega_o \left\| \bar{x} \right\|^2 + \omega_o \left\| \bar{x} \right\| \Big(r_M k_M \left\| \mathbf{\Phi}_c \omega_c \mathbf{\Lambda}_n \mathbf{\Phi}_o^{-1} \right\| \\ & + r_M \Big) \left\| \bar{z} \right\| + \omega_o \left\| \bar{x} \right\| r_M \left\| \psi - \psi_r \right\| \theta_M - \frac{1}{2} \omega_o \left\| \bar{z} \right\|^2 \\ & + \omega_o \left\| \bar{z} \right\| p_M \left\| \psi - \psi_r \right\| \theta_M + \left\| \bar{z} \right\| p_M \psi_M \left\| \tilde{\theta} \right\| \\ & + \left\| \bar{z} \right\| p_M \psi_M \operatorname{Proj}(\tau) + \left\| \tilde{\theta} \right\| \psi_M \left\| \bar{z} \right\| - \mu e^{-T_{PE}} \left\| \tilde{\theta} \right\|^2 \\ & + 2 \left\| \tilde{\theta} \right\| \psi_M^2 \left\| \operatorname{Proj}(\tau) \right\|.\end{aligned} \tag{A.42}$$

Once again recalling τ from (3.120) implies

$$\left\| \operatorname{Proj}(\tau) \right\| \leqslant \gamma_M \psi_M^2 \left\| \tilde{\theta} \right\| + \gamma_M \psi_M \left\| \bar{z} \right\|. \tag{A.43}$$

Moreover, due to the Lipschitz property of the regressor

$$\left\| \psi - \psi_r \right\| \leqslant \left\| x - x_r \right\| \psi_L = \left\| \bar{x} \right\| \psi_L \leqslant \left\| \mathbf{\Phi}_c^{-1} \right\| \left\| \bar{x} \right\| \psi_L. \tag{A.44}$$

It follows that

$$\begin{aligned}\dot{V}_{3.4} \leqslant & -\frac{1}{2}\omega_c\omega_o \left\|\bar{x}\right\|^2 + \omega_o \left\|\bar{x}\right\| \Big(r_M k_M \left\|\boldsymbol{\Phi}_c \omega_c \boldsymbol{\Lambda}_n \boldsymbol{\Phi}_o^{-1}\right\| \\ & + r_M\Big) \left\|\bar{z}\right\| + \omega_o \left\|\bar{x}\right\|^2 r_M \left\|\boldsymbol{\Phi}_c^{-1}\right\| \psi_L \theta_M - \frac{1}{2}\omega_o \left\|\bar{z}\right\|^2 \\ & + \omega_o \left\|\bar{z}\right\| p_M \left\|\boldsymbol{\Phi}_c^{-1}\right\| \left\|\bar{x}\right\| \psi_L \theta_M + \left\|\bar{z}\right\| p_M \psi_M \left\|\tilde{\theta}\right\| \\ & + \left\|\bar{z}\right\| p_M \psi_M \gamma_M \psi_M^2 \left\|\tilde{\theta}\right\| + p_M \psi_M^2 \gamma_M \left\|\bar{z}\right\|^2 \\ & + \left\|\tilde{\theta}\right\| \psi_M \left\|\bar{z}\right\| - \mu e^{-T_{PE}} \left\|\tilde{\theta}\right\|^2 + 2\psi_M^4 \gamma_M \left\|\tilde{\theta}\right\|^2 \\ & + 2\left\|\tilde{\theta}\right\| \psi_M^2 \gamma_M \psi_M \left\|\bar{z}\right\|. \end{aligned} \tag{A.45}$$

Notably, $\left\|\boldsymbol{\Phi}_c^{-1}\right\| = \omega_c^{-n+1|0}$ and $\left\|\boldsymbol{\Phi}_c \omega_c \boldsymbol{\Lambda}_n \boldsymbol{\Phi}_o^{-1}\right\| = \left(\frac{\omega_c}{\omega_o}\right)^{n|1}$. These terms are thus nonincreasing in ω_c and in the ratio $\frac{\omega_c}{\omega_o}$ correspondingly. Grouping of the terms yields

$$\begin{aligned}\dot{V}_{3.4} \leqslant & \left(-\frac{1}{2}\omega_o + p_M \psi_M^2 \gamma_M\right) \left\|\bar{z}\right\|^2 + \omega_o \Big(-\frac{1}{2}\omega_c \\ & + r_M \omega_c^{-n+1|0} \psi_L \theta_M\Big) \left\|\bar{x}\right\|^2 + \omega_o \left(r_M k_M \left(\frac{\omega_c}{\omega_o}\right)^{n|1}\right. \\ & \left. + r_M + p_M \omega_c^{-n+1|0} \psi_L \theta_M\right) \left\|\bar{z}\right\| \left\|\bar{x}\right\| + \Big(+ p_M \psi_M \\ & + p_M \gamma_M \psi_M^3 + \psi_M + 2\psi_M^3 \gamma_M\Big) \left\|\bar{z}\right\| \left\|\tilde{\theta}\right\| \\ & + \left(-\mu e^{-T_{PE}} + 2\psi_M^4 \gamma_M\right) \left\|\tilde{\theta}\right\|^2. \end{aligned} \tag{A.46}$$

The following expression corresponding to (3.124) is obtained for any $\varepsilon_1, \varepsilon_2 \in \mathbb{R}_+$ by invoking the Young's inequality,

$$\begin{aligned}\dot{V}_{3.4} \leqslant & \Big(-\frac{1}{2}\omega_o \Big(1 - \varepsilon_1 \Big(r_M k_M \left(\frac{\omega_c}{\omega_o}\right)^{n|1} + r_M \\ & + \omega_c^{-n+1|0} p_M \psi_L \theta_M\Big)\Big) + p_M \gamma_M \psi_M^2 + \frac{1}{2\varepsilon_2}\Big(p_M \psi_M \\ & + p_M \gamma_M \psi_M^3 + 2\psi_M^3 \gamma_M + \psi_M\Big)^2\Big) \left\|\bar{z}\right\|^2 + \omega_o \Big(-\frac{1}{2}\omega_c \\ & + \omega_c^{-n+1|0} r_M \psi_L \theta_M + \frac{1}{2\varepsilon_1}\Big(r_M \left(k_M \left(\frac{\omega_c}{\omega_o}\right)^{n|1} + 1\right) \\ & + \omega_c^{-n+1|0} p_M \psi_L \theta_M\Big)\Big) \left\|\bar{x}\right\|^2 + \Big(-\mu e^{-T_{PE}} + 2\psi_M^4 \gamma_M \\ & + \frac{1}{2}\varepsilon_2\Big) \left\|\tilde{\theta}\right\|^2. \end{aligned} \tag{A.47}$$

At last, consider the analysis presented in Section 3.3.3 to investigate the properties of PIDRC controller designed on the basis of the estimated state. Recall the auxiliary function (3.131) and given by

$$\begin{aligned} V^*_{3.5}(\bar{x},\bar{z}) = \frac{1}{2}\omega_o \bar{x}^T \mathbf{R}\bar{x} + \frac{1}{2}\bar{z}^T \mathbf{P}\bar{z} + \frac{1}{2}\tilde{\theta}^T \Gamma^{-1}\tilde{\theta} \\ - \bar{z}^T \mathbf{P}\mathbf{b}_m \psi(t,x_r)\tilde{\theta}. \end{aligned} \tag{A.48}$$

The time derivative of this function takes the form of

$$\begin{aligned} \dot{V}^*_{3.5}(\bar{x},\bar{z}) = \omega_o \bar{x}^T \mathbf{R}\dot{\bar{x}} + \bar{z}^T \mathbf{P}\dot{\bar{z}} + \tilde{\theta}^T \Gamma^{-1}\dot{\tilde{\theta}} - \bar{z}^T \mathbf{P}\mathbf{b}_m \psi(t,x_r)\dot{\tilde{\theta}} \\ - \bar{z}^T \mathbf{P}\mathbf{b}_m \dot{\psi}(t,x_r)\tilde{\theta} - \tilde{\theta}^T \psi_r^T \mathbf{b}_m^T \mathbf{P}\dot{\bar{z}}. \end{aligned} \tag{A.49}$$

Substituting $\dot{\bar{z}}, \dot{\bar{x}}$ and $\dot{\tilde{\theta}}$ from (3.130) yields

$$\begin{aligned} \dot{V}^*_{3.5} = \omega_c \omega_o \bar{x}^T \mathbf{R}\bar{\mathbf{G}}\bar{x} - \omega_o \bar{x}^T \mathbf{R}\mathbf{b}_n \left(\bar{k}^T \omega_c \mathbf{\Phi}_c \mathbf{\Lambda}_n \mathbf{\Phi}_o^{-1} + \mathbf{b}_m^T\right)\bar{z} \\ - \omega_o \bar{x}^T \mathbf{R}\mathbf{b}_n (\psi - \psi_r)\tilde{\theta} - \omega_o \bar{x}^T \mathbf{R}\mathbf{b}_n \left(\psi - \hat{\psi}\right)\hat{\theta} \\ + \omega_o \bar{z}^T \mathbf{P}\bar{\mathbf{H}}\bar{z} + \omega_o \bar{z}^T \mathbf{P}\mathbf{d}_m (\psi - \psi_r)\tilde{\theta} + \omega_o \bar{z}^T \mathbf{P}\mathbf{d}_m \Big(\psi \\ - \hat{\psi}\Big)\hat{\theta} + \bar{z}^T \mathbf{P}\mathbf{b}_m \dot{\psi}_r \tilde{\theta} - \bar{z}^T \mathbf{P}\mathbf{b}_m \psi_r \operatorname{Proj}(\boldsymbol{\tau}) \\ - \tilde{\theta}^T \Gamma^{-1} \operatorname{Proj}(\boldsymbol{\tau}) + \bar{z}^T \mathbf{P}\mathbf{b}_m \psi_r \operatorname{Proj}(\boldsymbol{\tau}) - \bar{z}^T \mathbf{P}\mathbf{b}_m \dot{\psi}_r \tilde{\theta} \\ - \omega_o \tilde{\theta}^T \psi_r^T \mathbf{b}_m^T \mathbf{P}\bar{\mathbf{H}}\bar{z} - \omega_o \tilde{\theta}^T \psi_r^T \mathbf{b}_m^T \mathbf{P}\mathbf{d}_m (\psi - \psi_r)\tilde{\theta} \\ - \omega_o \tilde{\theta}^T \psi_r^T \mathbf{b}_m^T \mathbf{P}\mathbf{d}_m \left(\psi - \hat{\psi}\right)\hat{\theta} - \tilde{\theta}^T \psi_r^T \mathbf{b}_m \mathbf{P}\mathbf{b}_m^T \dot{\psi}_r \tilde{\theta} \\ + \tilde{\theta}^T \psi_r^T \mathbf{b}_m \mathbf{P}\mathbf{b}_m^T \psi_r \operatorname{Proj}(\boldsymbol{\tau}). \end{aligned} \tag{A.50}$$

The terms $\bar{z}^T \mathbf{P} \mathbf{b}_m \boldsymbol{\psi}_r \operatorname{Proj}(\boldsymbol{\tau})$ and $\bar{z}^T \mathbf{P} \mathbf{b}_m \dot{\boldsymbol{\psi}}_r \tilde{\theta}$ are reduced in the obtained formula. Adding and subtracting term $\tilde{\theta}^T \boldsymbol{\Gamma}^{-1} \boldsymbol{\tau}$, and substituting $\boldsymbol{\tau}$ from (3.130) yields

$$\begin{aligned}
\dot{V}^*_{3.5} = & -\frac{1}{2}\omega_c \omega_o \bar{x}^T \bar{x} - \omega_o \bar{x}^T \mathbf{R} \mathbf{b}_n \left(\bar{k}^T \omega_c \boldsymbol{\Phi}_c \boldsymbol{\Lambda}_n \boldsymbol{\Phi}_o^{-1} + \mathbf{b}_m^T \right) \bar{z} \\
& - \omega_o \bar{x}^T \mathbf{R} \mathbf{b}_n \left(\boldsymbol{\psi} - \boldsymbol{\psi}_r \right) \tilde{\theta} - \omega_o \bar{x}^T \mathbf{R} \mathbf{b}_n \left(\boldsymbol{\psi} - \hat{\boldsymbol{\psi}} \right) \hat{\theta} \\
& - \frac{1}{2}\omega_o \bar{z}^T \bar{z} + \omega_o \bar{z}^T \mathbf{P} \mathbf{d}_m \left(\boldsymbol{\psi} - \boldsymbol{\psi}_r \right) \tilde{\theta} + \omega_o \bar{z}^T \mathbf{P} \mathbf{d}_m \Big(\boldsymbol{\psi} \\
& - \hat{\boldsymbol{\psi}} \Big) \hat{\theta} - \tilde{\theta}^T \boldsymbol{\Gamma}^{-1} \left(\operatorname{Proj}(\boldsymbol{\tau}) - \boldsymbol{\tau} \right) - \tilde{\theta}^T \left(\hat{\boldsymbol{\psi}}^T - \boldsymbol{\psi}^T \right) \boldsymbol{\psi}_r \tilde{\theta} \\
& + \tilde{\theta}^T \left(\hat{\boldsymbol{\psi}}^T - \boldsymbol{\psi}^T \right) \mathbf{b}_m^T \bar{z} - \tilde{\theta}^T \left(\boldsymbol{\psi}^T - \boldsymbol{\psi}_r^T \right) \boldsymbol{\psi}_r \tilde{\theta} \\
& + \tilde{\theta}^T \left(\boldsymbol{\psi}^T - \boldsymbol{\psi}_r^T \right) \mathbf{b}_m^T \bar{z} - \tilde{\theta}^T \boldsymbol{\psi}_r^T \boldsymbol{\psi}_r \tilde{\theta} + \tilde{\theta}^T \boldsymbol{\psi}_r^T \mathbf{b}_m^T \bar{z} \\
& - \omega_o \tilde{\theta}^T \boldsymbol{\psi}_r^T \mathbf{b}_m^T \mathbf{P} \bar{\mathbf{H}} \bar{z} - \omega_o \tilde{\theta}^T \boldsymbol{\psi}_r^T \mathbf{b}_m^T \mathbf{P} \mathbf{d}_m \left(\boldsymbol{\psi} - \boldsymbol{\psi}_r \right) \tilde{\theta} \\
& - \omega_o \tilde{\theta}^T \boldsymbol{\psi}_r^T \mathbf{b}_m^T \mathbf{P} \mathbf{d}_m \left(\boldsymbol{\psi} - \hat{\boldsymbol{\psi}} \right) \hat{\theta} - \tilde{\theta}^T \boldsymbol{\psi}_r^T \mathbf{b}_m \mathbf{P} \mathbf{b}_m^T \dot{\boldsymbol{\psi}}_r \tilde{\theta} \\
& + \tilde{\theta}^T \boldsymbol{\psi}_r^T \mathbf{b}_m \mathbf{P} \mathbf{b}_m^T \boldsymbol{\psi}_r \operatorname{Proj}(\boldsymbol{\tau}).
\end{aligned} \tag{A.51}$$

Recalling the properties of the projection operator and boundedness of the parameter estimates and identification errors gives

$$\begin{aligned}
\dot{V}^*_{3.5} \leqslant & -\frac{1}{2}\omega_c \omega_o \left\| \bar{x} \right\|^2 + \omega_o \left\| \bar{x} \right\| \Big(r_M k_M \left\| \omega_c \boldsymbol{\Phi}_c \boldsymbol{\Lambda}_n \boldsymbol{\Phi}_o^{-1} \right\| \\
& + r_M \Big) \left\| \bar{z} \right\| + \omega_o \left\| \bar{x} \right\| r_M \left\| \boldsymbol{\psi} - \boldsymbol{\psi}_r \right\| \theta_M \\
& + \omega_o \left\| \bar{x} \right\| r_M \left\| \boldsymbol{\psi} - \hat{\boldsymbol{\psi}} \right\| \theta_M - \frac{1}{2}\omega_o \left\| \bar{z} \right\|^2 \\
& + \omega_o \left\| \bar{z} \right\| p_M \left\| \boldsymbol{\psi} - \boldsymbol{\psi}_r \right\| \theta_M + \omega_o \left\| \bar{z} \right\| p_M \left\| \boldsymbol{\psi} - \hat{\boldsymbol{\psi}} \right\| \theta_M \\
& + \left\| \hat{\boldsymbol{\psi}} - \boldsymbol{\psi} \right\| \psi_M \theta_M^2 + \theta_M \left\| \hat{\boldsymbol{\psi}} - \boldsymbol{\psi} \right\| \left\| \bar{z} \right\| \\
& + \left\| \boldsymbol{\psi} - \boldsymbol{\psi}_r \right\| \psi_M \theta_M^2 + \theta_M \left\| \boldsymbol{\psi} - \boldsymbol{\psi}_r \right\| \left\| \bar{z} \right\| \\
& + \theta_M \psi_M \left\| \bar{z} \right\| + \omega_o \theta_M \psi_M p_M h_M \left\| \bar{z} \right\| \\
& + \omega_o \psi_M p_M \left\| \boldsymbol{\psi} - \boldsymbol{\psi}_r \right\| \theta_M^2 + \omega_o \psi_M p_M \left\| \boldsymbol{\psi} - \hat{\boldsymbol{\psi}} \right\| \theta_M^2 \\
& + \theta_M^2 \psi_M^2 p_M + \theta_M \psi_M^2 p_M \left\| \operatorname{Proj}(\boldsymbol{\tau}) \right\|.
\end{aligned} \tag{A.52}$$

By taking advantage of the explicit formula of $\boldsymbol{\tau}$, it is concluded that

$$\begin{aligned}
\left\| \operatorname{Proj}(\boldsymbol{\tau}) \right\| \leqslant & \gamma_M \left\| \hat{\boldsymbol{\psi}} - \boldsymbol{\psi} \right\| \psi_M \left\| \tilde{\theta} \right\| + \gamma_M \left\| \hat{\boldsymbol{\psi}} - \boldsymbol{\psi} \right\| \left\| \bar{z} \right\| \\
& + \gamma_M \left\| \boldsymbol{\psi} - \boldsymbol{\psi}_r \right\| \psi_M \left\| \tilde{\theta} \right\| + \gamma_M \left\| \boldsymbol{\psi} - \boldsymbol{\psi}_r \right\| \left\| \bar{z} \right\| \\
& + \gamma_M \psi_M^2 \left\| \tilde{\theta} \right\| + \gamma_M \psi_M \left\| \bar{z} \right\|.
\end{aligned} \tag{A.53}$$

It follows also from the Lipschitz property of the regressor that

$$\begin{aligned}\|\boldsymbol{\psi}-\boldsymbol{\psi}_r\| &\leqslant \|\boldsymbol{x}-\boldsymbol{x}_r\|\,\psi_L = \|\tilde{\boldsymbol{x}}\|\,\psi_L \leqslant \left\|\boldsymbol{\Phi}_c^{-1}\right\|\|\bar{\boldsymbol{x}}\|\,\psi_L,\\ \left\|\hat{\boldsymbol{\psi}}-\boldsymbol{\psi}\right\| &\leqslant \|\hat{\boldsymbol{x}}-\boldsymbol{x}\|\,\psi_L = \|\boldsymbol{\Lambda}_n\tilde{\boldsymbol{z}}\|\,\psi_L \leqslant \left\|\boldsymbol{\Lambda}_n\boldsymbol{\Phi}_o^{-1}\right\|\|\bar{\boldsymbol{z}}\|\,\psi_L.\end{aligned} \tag{A.54}$$

Embracing these notions yields

$$\begin{aligned}\dot{V}_{3.5}^{*} \leqslant\ & -\frac{1}{2}\omega_c\omega_o\|\bar{\boldsymbol{x}}\|^2 + \omega_o\|\bar{\boldsymbol{x}}\|\left(r_M k_M\left\|\omega_c\boldsymbol{\Phi}_c\boldsymbol{\Lambda}_n\boldsymbol{\Phi}_o^{-1}\right\|\right.\\ &\left.+ r_M\right)\|\bar{\boldsymbol{z}}\| + \omega_o r_M\left\|\boldsymbol{\Phi}_c^{-1}\right\|\|\bar{\boldsymbol{x}}\|^2\psi_L\theta_M\\ &+ \omega_o\|\bar{\boldsymbol{x}}\|\,r_M\left\|\boldsymbol{\Lambda}_n\boldsymbol{\Phi}_o^{-1}\right\|\|\bar{\boldsymbol{z}}\|\,\psi_L\theta_M - \frac{1}{2}\omega_o\|\bar{\boldsymbol{z}}\|^2\\ &+ \omega_o\|\bar{\boldsymbol{z}}\|\,p_M\left\|\boldsymbol{\Phi}_c^{-1}\right\|\|\bar{\boldsymbol{x}}\|\,\psi_L\theta_M\\ &+ \omega_o p_M\left\|\boldsymbol{\Lambda}_n\boldsymbol{\Phi}_o^{-1}\right\|\|\bar{\boldsymbol{z}}\|^2\psi_L\theta_M\\ &+ \left\|\boldsymbol{\Lambda}_n\boldsymbol{\Phi}_o^{-1}\right\|\|\bar{\boldsymbol{z}}\|\,\psi_L\psi_M\theta_M^2 + \theta_M\left\|\boldsymbol{\Lambda}_n\boldsymbol{\Phi}_o^{-1}\right\|\psi_L\|\bar{\boldsymbol{z}}\|^2\\ &+ \left\|\boldsymbol{\Phi}_c^{-1}\right\|\|\bar{\boldsymbol{x}}\|\,\psi_L\psi_M\theta_M^2 + \theta_M\left\|\boldsymbol{\Phi}_c^{-1}\right\|\|\bar{\boldsymbol{x}}\|\,\psi_L\|\bar{\boldsymbol{z}}\|\\ &+ \theta_M\psi_M\|\bar{\boldsymbol{z}}\| + \omega_o\theta_M\psi_M p_M h_M\|\bar{\boldsymbol{z}}\|\\ &+ \omega_o\psi_M p_M\left\|\boldsymbol{\Phi}_c^{-1}\right\|\|\bar{\boldsymbol{x}}\|\,\psi_L\theta_M^2\\ &+ \omega_o\psi_M p_M\left\|\boldsymbol{\Lambda}_n\boldsymbol{\Phi}_o^{-1}\right\|\|\bar{\boldsymbol{z}}\|\,\psi_L\theta_M^2 + \theta_M^2\psi_M^2 p_M\\ &+ \theta_M^2\psi_M^3 p_M\gamma_M\left\|\boldsymbol{\Lambda}_n\boldsymbol{\Phi}_o^{-1}\right\|\|\bar{\boldsymbol{z}}\|\,\psi_L\\ &+ \theta_M\psi_M^2 p_M\gamma_M\left\|\boldsymbol{\Lambda}_n\boldsymbol{\Phi}_o^{-1}\right\|\psi_L\|\bar{\boldsymbol{z}}\|^2\\ &+ \theta_M^2\psi_M^3 p_M\gamma_M\left\|\boldsymbol{\Phi}_c^{-1}\right\|\|\bar{\boldsymbol{x}}\|\,\psi_L\\ &+ \theta_M\psi_M^2 p_M\gamma_M\left\|\boldsymbol{\Phi}_c^{-1}\right\|\|\bar{\boldsymbol{x}}\|\,\psi_L\|\bar{\boldsymbol{z}}\| + \theta_M^2\psi_M^4 p_M\gamma_M\\ &+ \theta_M\psi_M^3 p_M\gamma_M\|\bar{\boldsymbol{z}}\|\,.\end{aligned} \tag{A.55}$$

Taking advantage of the notion that $\left\|\boldsymbol{\Phi}_c^{-1}\right\| = \omega_c^{-n+1|0}$, $\left\|\boldsymbol{\Phi}_c\omega_c\boldsymbol{\Lambda}_n\boldsymbol{\Phi}_o^{-1}\right\| = \left(\frac{\omega_c}{\omega_o}\right)^{n|1}$, $\left\|\boldsymbol{\Lambda}_n\boldsymbol{\Phi}_o^{-1}\right\| = \omega_o^{-n|-1}$ and $\omega_o\left\|\boldsymbol{\Lambda}_n\boldsymbol{\Phi}_o^{-1}\right\| = \omega_o^{-n+1|0}$ the bound of $\dot{V}_{3.5}^*(\bar{\mathbf{x}}, \bar{\mathbf{z}})$ is reformulated by grouping the suitable terms as

$$\begin{aligned}
\dot{V}_{3.5}^* \leqslant\ & \omega_o\left(-\frac{1}{2}\omega_c + r_M\omega_c^{-n+1|0}\psi_L\theta_M\right)\|\bar{\mathbf{x}}\|^2 + \Bigg(-\frac{1}{2}\omega_o \\
& + p_M\omega_o^{-n+1|0}\psi_L\theta_M + \theta_M\omega_o^{-n|-1}\psi_L \\
& + \theta_M\psi_M^2 p_M\gamma_M\omega_o^{-n|-1}\psi_L\Bigg)\|\bar{\mathbf{z}}\|^2 \\
& + \left(\omega_o\left(r_M k_M\left(\frac{\omega_c}{\omega_o}\right)^{n|1} + r_M + p_M\omega_c^{-n+1|0}\psi_L\theta_M\right)\right. \\
& + r_M\omega_o^{-n+1|0}\psi_L\theta_M + \theta_M\omega_c^{-n+1|0}\psi_L \\
& \left. + \theta_M\psi_M^2 p_M\gamma_M\omega_c^{-n+1|0}\psi_L\right)\|\bar{\mathbf{z}}\|\,\|\bar{\mathbf{x}}\| \\
& + \Big(\omega_o^{-n|-1}\psi_L\psi_M\theta_M^2 + \theta_M\psi_M + \omega_o\theta_M\psi_M p_M h_M \\
& + \psi_M p_M\omega_o^{-n+1|0}\psi_L\theta_M^2 + \theta_M^2\psi_M^3 p_M\gamma_M\omega_o^{-n|-1}\psi_L \\
& + \theta_M\psi_M^3 p_M\gamma_M\Big)\|\bar{\mathbf{z}}\| + \Big(\omega_c^{-n+1|0}\psi_L\psi_M\theta_M^2 \\
& + \omega_o\psi_M p_M\omega_c^{-n+1|0}\psi_L\theta_M^2 \\
& + \theta_M^2\psi_M^3 p_M\gamma_M\omega_c^{-n+1|0}\psi_L\Big)\|\bar{\mathbf{x}}\| + \theta_M^2\psi_M^4 p_M\gamma_M \\
& + \theta_M^2\psi_M^2 p_M.
\end{aligned} \tag{A.56}$$

Finally, invoking the Young's inequality yields

$$\begin{aligned}\dot{V}^{*}_{3.5} \leqslant \omega_o\Bigg(&-\frac{1}{2}\omega_c + r_M\psi_L\theta_M\omega_c^{-n+1|0} + \frac{1}{2\varepsilon}\Bigg(r_M k_M\left(\frac{\omega_c}{\omega_o}\right)^{n|1} \\ &+ r_M + p_M\psi_L\theta_M\omega_c^{-n+1|0}\Bigg)\Bigg)\|\bar{x}\|^2 \\ &+ \Bigg(-\frac{1}{2}\omega_o\Bigg(1-\varepsilon\Bigg(r_M k_M\left(\frac{\omega_c}{\omega_o}\right)^{n|1} + r_M \\ &+ p_M\psi_L\theta_M\omega_c^{-n+1|0}\Bigg)\Bigg) + \omega_c^{-n+1|0}p_M\psi_L\theta_M \\ &+ \omega_o^{-n|-1}\left(\theta_M\psi_L + \theta_M p_M\gamma_M\psi_M^2\psi_L\right)\Bigg)\|\bar{z}\|^2 \\ &+ \Bigg(\omega_c^{-n+1|0}r_M\psi_L\theta_M + \omega_c^{-n+1|0}\Bigg(\theta_M p_M\gamma_M\psi_L\psi_M^2 \\ &+ \theta_M\psi_L\Bigg)\Bigg)\|\bar{x}\|\,\|\bar{z}\| + \Bigg(\omega_o\theta_M\psi_M p_M h_M + \theta_M p_M\gamma_M\psi_M^3 \\ &+ \theta_M\psi_M + \omega_o^{-n+1|0}\theta_M^2\psi_M p_M\psi_L + \omega_o^{-n|-1}\Big(\theta_M^2\psi_L\psi_M \\ &+ p_M\gamma_M\psi_L\psi_M^3\theta_M^2\Big)\Bigg)\|\bar{z}\| + \omega_c^{-n+1|0}\Bigg(\omega_o\theta_M^2\psi_M p_M\psi_L \\ &+ \theta_M^2\psi_L\psi_M + p_M\gamma_M\psi_L\psi_M^3\theta_M^2\Bigg)\|\bar{x}\| + p_M\gamma_M\psi_M^4\theta_M^2\end{aligned} \tag{A.57}$$

what corresponds to the formula of (3.134) and enabled concluding about the boundedness of the tracking and estimation errors.

Consider the function given by (3.135) in the form of

$$V_{3.5}(\bar{x},\bar{z},\tilde{\theta}) = \frac{1}{2}\omega_o\bar{x}^T\mathbf{R}\bar{x} + \frac{1}{2}\bar{z}^T\mathbf{P}\bar{z} + \tilde{\theta}^T\left(\frac{1}{2}\mathbf{\Gamma}^{-1} - \mathbf{M}(t,x_r)\right)\tilde{\theta}. \tag{A.58}$$

The derivative along the trajectories of the system is expressed by

$$\begin{aligned}\dot{V}_{3.5}(\bar{x},\bar{z},\tilde{\theta}) = \omega_o\bar{x}^T\mathbf{R}\dot{\bar{x}} + \bar{z}^T\mathbf{P}\dot{\bar{z}} + \tilde{\theta}^T\mathbf{\Gamma}^{-1}\dot{\tilde{\theta}} - \tilde{\theta}^T\dot{\mathbf{M}}\tilde{\theta} \\ - 2\tilde{\theta}^T\mathbf{M}\dot{\tilde{\theta}}.\end{aligned} \tag{A.59}$$

Substituting $\dot{\bar{x}}, \dot{\bar{z}}, \dot{\tilde{\theta}}$ from (3.130) and $\dot{M}$ from Corollary 3.4 yields

$$\begin{aligned}\dot{V}_{3.5} = {} & \omega_c \omega_o \bar{x}^T \mathbf{R} \bar{\mathbf{G}} \bar{x} - \omega_o \bar{x}^T \mathbf{R} \mathbf{b}_n \left(\bar{k}^T \omega_c \mathbf{\Phi}_c \mathbf{\Lambda}_n \mathbf{\Phi}_o^{-1} + \mathbf{b}_m^T \right) \bar{z} \\ & - \omega_o \bar{x}^T \mathbf{R} \mathbf{b}_n \left(\psi - \psi_r \right) \tilde{\theta} - \omega_o \bar{x}^T \mathbf{R} \mathbf{b}_n \left(\psi - \hat{\psi} \right) \hat{\theta} \\ & + \omega_o \bar{z}^T \mathbf{P} \bar{\mathbf{H}} \bar{z} + \omega_o \bar{z}^T \mathbf{P} \mathbf{d}_m \left(\psi - \psi_r \right) \tilde{\theta} \\ & + \omega_o \bar{z}^T \mathbf{P} \mathbf{d}_m \left(\psi - \hat{\psi} \right) \hat{\theta} + \bar{z}^T \mathbf{P} \mathbf{b}_m \dot{\psi}_r \tilde{\theta} \\ & - \bar{z}^T \mathbf{P} \mathbf{b}_m \psi_r \operatorname{Proj}(\boldsymbol{\tau}) - \tilde{\theta}^T \mathbf{\Gamma}^{-1} \operatorname{Proj}(\boldsymbol{\tau}) - \tilde{\theta}^T \mathbf{M} \tilde{\theta} \\ & + \tilde{\theta}^T \psi_r^T \psi_r \tilde{\theta} + 2 \tilde{\theta}^T \mathbf{M} \operatorname{Proj}(\boldsymbol{\tau}).\end{aligned} \tag{A.60}$$

By adding and subtracting the term $\tilde{\theta}^T \mathbf{\Gamma}^{-1} \boldsymbol{\tau}$, and then substituting $\boldsymbol{\tau}$ from (3.130) leads to

$$\begin{aligned}\dot{V}_{3.5} = {} & -\frac{1}{2} \omega_c \omega_o \bar{x}^T \bar{x} - \omega_o \bar{x}^T \mathbf{R} \mathbf{b}_n \left(\bar{k}^T \omega_c \mathbf{\Phi}_c \mathbf{\Lambda}_n \mathbf{\Phi}_o^{-1} + \mathbf{b}_m^T \right) \bar{z} \\ & - \omega_o \bar{x}^T \mathbf{R} \mathbf{b}_n \left(\psi - \psi_r \right) \tilde{\theta} - \omega_o \bar{x}^T \mathbf{R} \mathbf{b}_n \left(\psi - \hat{\psi} \right) \hat{\theta} \\ & - \frac{1}{2} \omega_o \bar{z}^T \bar{z} + \omega_o \bar{z}^T \mathbf{P} \mathbf{d}_m \left(\psi - \psi_r \right) \tilde{\theta} \\ & + \omega_o \bar{z}^T \mathbf{P} \mathbf{d}_m \left(\psi - \hat{\psi} \right) \hat{\theta} + \bar{z}^T \mathbf{P} \mathbf{b}_m \dot{\psi}_r \tilde{\theta} \\ & - \bar{z}^T \mathbf{P} \mathbf{b}_m \psi_r \operatorname{Proj}(\boldsymbol{\tau}) - \tilde{\theta}^T \mathbf{\Gamma}^{-1} \left(\operatorname{Proj}(\boldsymbol{\tau}) - \boldsymbol{\tau} \right) \\ & - \tilde{\theta}^T \left(\hat{\psi}^T - \psi^T \right) \psi_r \tilde{\theta} + \tilde{\theta}^T \left(\hat{\psi}^T - \psi^T \right) \mathbf{b}_m^T \bar{z} \\ & - \tilde{\theta}^T \left(\psi^T - \psi_r^T \right) \psi_r \tilde{\theta} + \tilde{\theta}^T \left(\psi^T - \psi_r^T \right) \mathbf{b}_m^T \bar{z} \\ & - \tilde{\theta}^T \psi_r^T \psi_r \tilde{\theta} + \tilde{\theta}^T \psi_r^T \mathbf{b}_m \bar{z} - \tilde{\theta}^T \mathbf{M} \tilde{\theta} + \tilde{\theta}^T \psi_r^T \psi_r \tilde{\theta} \\ & + 2 \tilde{\theta}^T \mathbf{M} \operatorname{Proj}(\boldsymbol{\tau}).\end{aligned} \tag{A.61}$$

The terms $\tilde{\theta}^T \psi_r^T \psi_r \tilde{\theta}$ reduce each other. Recalling the characteristics of the projection operator and the boundedness of the identification errors yields

$$\begin{aligned}
\dot{V}_{3.5} \leqslant & -\frac{1}{2}\omega_c \omega_o \|\bar{x}\|^2 + \omega_o \|\bar{x}\| \left(r_M k_M \left\| \omega_c \Phi_c \Lambda_n \Phi_o^{-1} \right\| \right. \\
& \left. + r_M \right) \|\bar{z}\| + \omega_o \|\bar{x}\| r_M \|\psi - \psi_r\| \theta_M \\
& + \omega_o \|\bar{x}\| r_M \left\| \psi - \hat{\psi} \right\| \theta_M - \frac{1}{2}\omega_o \|\bar{z}\|^2 \\
& + \omega_o \|\bar{z}\| p_M \|\psi - \psi_r\| \theta_M + \omega_o \|\bar{z}\| p_M \left\| \psi - \hat{\psi} \right\| \theta_M \\
& + \|\bar{z}\| p_M \psi_M \left\| \tilde{\theta} \right\| + \|\bar{z}\| p_M \psi_M \|\mathrm{Proj}(\tau)\| \\
& + \left\| \tilde{\theta} \right\| \left\| \hat{\psi} - \psi \right\| \psi_M \theta_M + \theta_M \left\| \hat{\psi} - \psi \right\| \|\bar{z}\| \\
& + \left\| \tilde{\theta} \right\| \|\psi - \psi_r\| \psi_M \theta_M + \theta_M \|\psi - \psi_r\| \|\bar{z}\| \\
& + \left\| \tilde{\theta} \right\| \psi_M \|\bar{z}\| - \mu e^{-T_{PE}} \left\| \tilde{\theta} \right\|^2 \\
& + 2 \left\| \tilde{\theta} \right\| \psi_M^2 \|\mathrm{Proj}(\tau)\| .
\end{aligned} \tag{A.62}$$

By recalling the explicit formula of $\left\|\mathrm{Proj}(\boldsymbol{\tau})\right\|$ and taking advantage of the Lipschitz property of the regressor, it is concluded that

$$\begin{aligned}
\dot{V}_{3.5} \leqslant & -\frac{1}{2}\omega_c\omega_o \left\|\bar{x}\right\|^2 + \omega_o \left\|\bar{x}\right\| \Bigg(r_M k_M \left\|\omega_c \boldsymbol{\Phi}_c \boldsymbol{\Lambda}_n \boldsymbol{\Phi}_o^{-1}\right\| \\
& + r_M \Bigg) \left\|\bar{z}\right\| + \omega_o r_M \left\|\boldsymbol{\Phi}_c^{-1}\right\| \left\|\bar{x}\right\|^2 \psi_L \theta_M \\
& + \omega_o \left\|\bar{x}\right\| r_M \left\|\boldsymbol{\Lambda}_n \boldsymbol{\Phi}_o^{-1}\right\| \left\|\bar{z}\right\| \psi_L \theta_M - \frac{1}{2}\omega_o \left\|\bar{z}\right\|^2 \\
& + \omega_o \left\|\bar{z}\right\| p_M \left\|\boldsymbol{\Phi}_c^{-1}\right\| \left\|\bar{x}\right\| \psi_L \theta_M \\
& + \omega_o p_M \left\|\boldsymbol{\Lambda}_n \boldsymbol{\Phi}_o^{-1}\right\| \left\|\bar{z}\right\|^2 \psi_L \theta_M \\
& + \left\|\bar{z}\right\| p_M \psi_M \left\|\tilde{\theta}\right\| + p_M \psi_M^2 \gamma_M \left\|\boldsymbol{\Lambda}_n \boldsymbol{\Phi}_o^{-1}\right\| \left\|\bar{z}\right\|^2 \psi_L \theta_M \\
& + p_M \psi_M \gamma_M \left\|\boldsymbol{\Lambda}_n \boldsymbol{\Phi}_o^{-1}\right\| \psi_L \left\|\bar{z}\right\|^3 \\
& + \left\|\bar{z}\right\| p_M \psi_M^2 \gamma_M \left\|\boldsymbol{\Phi}_c^{-1}\right\| \left\|\bar{x}\right\| \psi_L \theta_M \\
& + \left\|\bar{z}\right\|^2 p_M \psi_M \gamma_M \left\|\boldsymbol{\Phi}_c^{-1}\right\| \left\|\bar{x}\right\| \psi_L + \left\|\bar{z}\right\| p_M \gamma_M \psi_M^3 \left\|\tilde{\theta}\right\| \\
& + p_M \psi_M^2 \gamma_M \left\|\bar{z}\right\|^2 + \left\|\tilde{\theta}\right\| \left\|\boldsymbol{\Lambda}_n \boldsymbol{\Phi}_o^{-1}\right\| \left\|\bar{z}\right\| \psi_L \psi_M \theta_M \\
& + \theta_M \left\|\boldsymbol{\Lambda}_n \boldsymbol{\Phi}_o^{-1}\right\| \psi_L \left\|\bar{z}\right\|^2 + \left\|\tilde{\theta}\right\| \left\|\boldsymbol{\Phi}_c^{-1}\right\| \left\|\bar{x}\right\| \psi_L \psi_M \theta_M \\
& + \theta_M \left\|\boldsymbol{\Phi}_c^{-1}\right\| \left\|\bar{x}\right\| \psi_L \left\|\bar{z}\right\| + \left\|\tilde{\theta}\right\| \psi_M \left\|\bar{z}\right\| - \mu e^{-T_{PE}} \left\|\tilde{\theta}\right\|^2 \\
& + 2\theta_M \psi_M^3 \gamma_M \left\|\boldsymbol{\Lambda}_n \boldsymbol{\Phi}_o^{-1}\right\| \left\|\bar{z}\right\| \psi_L \left\|\tilde{\theta}\right\| \\
& + 2\theta_M \psi_M^2 \gamma_M \left\|\boldsymbol{\Lambda}_n \boldsymbol{\Phi}_o^{-1}\right\| \psi_L \left\|\bar{z}\right\|^2 \\
& + 2\theta_M \psi_M^3 \gamma_M \left\|\boldsymbol{\Phi}_c^{-1}\right\| \left\|\bar{x}\right\| \psi_L \left\|\tilde{\theta}\right\| \\
& + 2\theta_M \psi_M^2 \gamma_M \left\|\boldsymbol{\Phi}_c^{-1}\right\| \left\|\bar{x}\right\| \psi_L \left\|\bar{z}\right\| \\
& + 2\psi_M^4 \gamma_M \left\|\tilde{\theta}\right\|^2 + 2\left\|\tilde{\theta}\right\| \psi_M^3 \gamma_M \left\|\bar{z}\right\| .
\end{aligned} \tag{A.63}$$

An advantage is now taken for the notion that $\left\|\bar{z}\right\| \leqslant z_M$ and $\left\|\bar{x}\right\| \leqslant x_M$ to establish quadratic bounds on the terms $p_M \psi_M \gamma_M \left\|\boldsymbol{\Lambda}_n \boldsymbol{\Phi}_o^{-1}\right\| \psi_L \left\|\bar{z}\right\|^3$ and $\left\|\bar{z}\right\|^2 p_M \psi_M \gamma_M \left\|\boldsymbol{\Phi}_c^{-1}\right\| \left\|\bar{x}\right\| \psi_L$. Moreover, the norms of the scal-

ing matrices are expressed in terms of conditional exponentiation operators and the terms are grouped accordingly to obtain

$$\begin{aligned}
\dot{V}_{3.5} \leqslant & \left(-\frac{1}{2}\omega_c\omega_o + \omega_o r_M \omega_c^{-n+1|0}\psi_L\theta_M \right) \|\bar{x}\|^2 + \Big(-\frac{1}{2}\omega_o \\
& + p_M\omega_o^{-n+1|0}\psi_L\theta_M + p_M\psi_M^2\gamma_M\omega_o^{-n|-1}\psi_L\theta_M \\
& + p_M\psi_M\gamma_M\omega_o^{-n|-1}\psi_L z_M + p_M\psi_M\gamma_M\omega_c^{-n+1|0}x_M\psi_L \\
& + p_M\psi_M^2\gamma_M + \theta_M\omega_o^{-n|-1}\psi_L \\
& + 2\theta_M\psi_M^2\gamma_M\omega_o^{-n|-1}\psi_L \Big) \|\bar{z}\|^2 + \Big(\omega_o \Big(r_M k_M \frac{\omega_c}{\omega_o}^{n|1} \\
& + r_M + p_M\omega_c^{-n+1|0}\psi_L\theta_M \Big) + r_M\omega_o^{-n+1|0}\psi_L\theta_M \\
& + p_M\psi_M^2\gamma_M\omega_c^{-n+1|0}\psi_L\theta_M + \theta_M\omega_c^{-n+1|0}\psi_L \\
& + 2\theta_M\psi_M^2\gamma_M\omega_c^{-n+1|0}\psi_L \Big) \|\bar{z}\| \, \|\bar{x}\| + \Big(p_M\psi_M \\
& + p_M\gamma_M\psi_M^3 + \omega_o^{-n|-1}\psi_L\psi_M\theta_M + \psi_M \\
& + 2\theta_M\psi_M^3\gamma_M\omega_o^{-n|-1}\psi_L + 2\psi_M^3\gamma_M \Big) \|\bar{z}\| \, \big\|\tilde{\theta}\big\| \\
& + \omega_c^{-n+1|0}\Big(\psi_L\psi_M\theta_M + 2\theta_M\psi_M^3\gamma_M\psi_L \Big) \big\|\tilde{\theta}\big\| \, \|\bar{x}\| \\
& + \Big(-\mu e^{-T_{PE}} + 2\psi_M^4\gamma_M \Big) \big\|\tilde{\theta}\big\|^2 .
\end{aligned} \tag{A.64}$$

At last, invoking the Young's inequality yields

$$\begin{aligned}\dot{V}_{3.5} \leqslant &\left(\omega_o\left(-\frac{1}{2}\omega_c+\omega_c^{-n+1|0}\theta_M r_M\psi_L+\frac{1}{2\varepsilon_1}\left(r_M\right.\right.\right.\\&\left.\left.\left.+r_M k_M\left(\frac{\omega_c}{\omega_o}\right)^{n|1}+\omega_c^{-n+1|0}p_M\theta_M\psi_L\right)\right)\\&+\frac{1}{2}\theta_M\left(\omega_c^{-n+1|0}r_M\psi_L+\omega_c^{-n+1|0}\left(p_M\gamma_M\psi_L\psi_M^2\right.\right.\\&\left.\left.+\psi_L+2\psi_M^2\gamma_M\psi_L\right)\right)+\frac{1}{2\varepsilon_2}\left(\omega_c^{-n+1|0}\left(\theta_M\psi_L\psi_M\right.\right.\\&\left.\left.+2\theta_M\gamma_M\psi_M^3\psi_L\right)\right)^2\Bigg)\|\bar{x}\|^2+\left(\frac{1}{2}\omega_o\left(-1+\varepsilon_1\left(r_M\right.\right.\right.\\&\left.\left.\left.+r_M k_M\left(\frac{\omega_c}{\omega_o}\right)^{n|1}+\omega_c^{-n+1|0}p_M\theta_M\psi_L\right)\right)\right.\\&\left.+\omega_c^{-n+1|0}p_M\theta_M\psi_L+\omega_c^{-n+1|0}x_M p_M\gamma_M\psi_M\psi_L\right.\\&\left.+\omega_o^{-n|-1}\left(p_M\gamma_M\psi_L\psi_M^2\theta_M+z_M p_M\gamma_M\psi_M\psi_L\right.\right.\\&\left.\left.+\theta_M\psi_L+2\theta_M\psi_M^2\gamma_M\psi_L\right)+p_M\gamma_M\psi_M^2\right.\\&\left.+\frac{1}{2}\left(\omega_c^{-n+1|0}\theta_M r_M\psi_L+\omega_c^{-n+1|0}\left(p_M\gamma_M\psi_L\psi_M^2\theta_M\right.\right.\right.\\&\left.\left.\left.+\theta_M\psi_L+2\theta_M\psi_M^2\gamma_M\psi_L\right)\right)+\frac{1}{2\varepsilon_3}\left(p_M\gamma_M\psi_M^3\right.\\&\left.+p_M\psi_M+\psi_M+2\gamma_M\psi_M^3+\omega_o^{-n|-1}\left(\theta_M\psi_M\psi_L\right.\right.\\&\left.\left.+2\theta_M\gamma_M\psi_M^3\psi_L\right)\right)^2\Bigg)\|\tilde{z}\|^2+\left(-\mu e^{-T_{PE}}+2\gamma_M\psi_M^4\right.\\&\left.+\frac{1}{2}\varepsilon_2+\frac{1}{2}\varepsilon_3\right)\|\tilde{\theta}\|^2\end{aligned}\tag{A.65}$$

for any $\varepsilon_1, \varepsilon_2, \varepsilon_3 \in \mathbb{R}_+$ what is consistent with the results of (3.138).

BIBLIOGRAPHY

[1] A. Abbaspour, S. Mokhtari, A. Sargolzaei, and K. K. Yen. „A survey on active fault-tolerant control systems." In: *Electronics* 9.9 (2020), p. 1513. DOI: 10.3390/electronics9091513.

[2] C. Abdallah, D. M. Dawson, P. Dorato, and M. Jamshidi. „Survey of robust control for rigid robots." In: *IEEE Control Systems Magazine* 11.2 (1991), pp. 24–30. DOI: 10.1109/37.67672.

[3] J. Ackermann, P. Blue, T. Bünte, L. Güvenc, D. Kaesbauer, M. Kordt, M. Muhler, and D. Odenthal. *Robust control: the parameter space approach*. Springer, 2002.

[4] J. Ackermann and D. Kaesbauer. „Design of robust PID controllers." In: *2001 European Control Conference (ECC)*. IEEE. 2001, pp. 522–527. DOI: 10.23919/ECC.2001.7075960.

[5] C. F. Aguilar-Ibáñez, H. J. Sira-Ramírez, and J. Á. Acosta. „Stability of active disturbance rejection control for uncertain systems: A Lyapunov perspective." In: *International Journal of Robust and Nonlinear Control* 27 (2017), pp. 4541–4553. DOI: 10.1002/rnc.3812.

[6] A. A. Amin and K. M. Hasan. „A review of fault tolerant control systems: advancements and applications." In: *Measurement* 143 (2019), pp. 58–68. DOI: 10.1016/j.measurement.2019.04.083.

[7] B. D. Anderson and A. Dehghani. „Challenges of adaptive control–past, permanent and future." In: *Annual reviews in control* 32.2 (2008), pp. 123–135. DOI: 10.1016/j.arcontrol.2008.06.001.

[8] A. M. Annaswamy and A. L. Fradkov. „A historical perspective of adaptive control and learning." In: *Annual Reviews in Control* 52 (2021), pp. 18–41. DOI: 10.1016/j.arcontrol.2021.10.014.

[9] Arduino Software. *Arduino*. https://www.arduino.cc/. [Online; accessed 25-January-2023].

[10] B. Armstrong-Helouvry. *Control of machines with friction*. Vol. 128. Springer Science & Business Media, 2012. DOI: 10.1007/978-1-4615-3972-8.

[11] J. Aseltine, A. Mancini, and C. Sarture. „A survey of adaptive control systems." In: *IRE Transactions on Automatic Control* 6.1 (1958), pp. 102–108. DOI: 10.1109/TAC.1958.1105168.

[12] W. R. Ashby. „The Set Theory of Mechanism and Homeostasis." In: *Mechanisms of Intelligence: Ashby's Writings on Cybernetics*. Intersystems Publications, 1981, pp. 20–49.

[13] R. B. Asher, D. Andrisani, and P. Dorato. „Bibliography on adaptive control systems." In: *Proceedings of the IEEE* 64.8 (1976), pp. 1226–1240. DOI: 10.1109/PROC.1976.10293.

[14] A. Astolfi, D. Karagiannis, and R. Ortega. „Towards applied nonlinear adaptive control." In: *Annual Reviews in Control* 32.2 (2008), pp. 136–148. DOI: 10.3182/20070829-3-RU-4911.00048.

[15] K. J. Åström and B. Wittenmark. *Adaptive control*. Dover Publications, 2008.

[16] K. J. Åström and B. Torsten. „Numerical identification of linear dynamic systems from normal operating records." In: *IFAC Proceedings Volumes* 2.2 (1965), pp. 96–111. DOI: 10.1016/S1474-6670(17)69024-4.

[17] J. Back and H. Shim. „Adding robustness to nominal output-feedback controllers for uncertain nonlinear systems: A nonlinear version of disturbance observer." In: *Automatica* 44.10 (2008), pp. 2528–2537. DOI: 10.1016/j.automatica.2008.02.024.

[18] B. Bandyopadhyay, S. Janardhanan, S. K. Spurgeon, et al. „Advances in sliding mode control." In: *Lecture Notes in Control and Information Sciences* 440 (2013).

[19] I. Barbalăt. „Systemes d'équations différentielles d'oscillations non linéaires." In: *Rev. Math. Pures Appl* 4.2 (1959), pp. 267–270.

[20] B. R. Barmish. „Necessary and sufficient conditions for quadratic stabilizability of an uncertain system." In: *Journal of Optimization theory and applications* 46.4 (1985), pp. 399–408. DOI: 10.1007/BF00939145.

[21] P. Bartkowiak, R. Patelski, M. Kwiatkowska, and D. Pazderski. „System Architecture for Development and Supervision of Robotic Astronomical Telescope." In: *Pomiary Automatyka Robotyka* 26.4 (2022), pp. 43–51. DOI: 10.14313/PAR_246/43.

[22] G. Bastin and M. Gevers. „Stable adaptive observers for nonlinear time-varying systems." In: *IEEE Transactions on Automatic Control* 33.7 (1988), pp. 650–658. DOI: 10.1109/9.1273.

[23] J. Baur, S. Dendorfer, J. Pfaff, C. Schütz, T. Buschmann, and H. Ulbrich. „Experimental friction identification in robot drives." In: *2014 IEEE International Conference on Robotics and Automation (ICRA)*. IEEE. 2014, pp. 6006–6011. DOI: 10.1109/ICRA.2014.6907744.

[24] J. Beerten, J. Verveckken, and J. Driesen. „Predictive direct torque control for flux and torque ripple reduction." In: *IEEE transactions on industrial electronics* 57.1 (2009), pp. 404–412. DOI: 10.1109/TIE.2009.2033487.

[25] A. Behal, D. Dawson, W. Dixon, and Y. Fang. „Tracking and regulation control of an underactuated surface vessel with nonintegrable dynamics." In: *IEEE Trans. Automat. Contr.* 47.3 (2002), pp. 495–500. DOI: 10.1109/9.989148.

[26] M. Benosman. „Model-based vs data-driven adaptive control: an overview." In: *International Journal of Adaptive Control and Signal Processing* 32.5 (2018), pp. 753–776. DOI: 10.1002/acs.2862.

[27] X. Benxian, W. Ping, D. Xueping, Z. Xingpeng, and Y. Haibin. „Study on nonlinear friction compensation for bi-axis servo system based-on ADRC." In: *International Conference on Information Science and Technology*. IEEE. 2011, pp. 788–793. DOI: 10.1109/ICIST.2011.5765100.

[28] G. Besançon. „Remarks on nonlinear adaptive observer design." In: *Systems & control letters* 41.4 (2000), pp. 271–280. DOI: 10.1016/S0167-6911(00)00065-7.

[29] G. Besançon, J. de León-Morales, and O. Huerta-Guevara. „On adaptive observers for state affine systems." In: *International journal of Control* 79.06 (2006), pp. 581–591. DOI: 10.1080/00207170600552766.

[30] S. P. Bhattacharyya, H. Chapellat, and L. H. Keel. *Robust Control: The Parametric Approach*. Prentice Hall, 1995. DOI: 10.1016/B978-0-08-042230-5.50016-5.

[31] H. W. Bode. „Variable equalizers." In: *The Bell System Technical Journal* 17.2 (1938), pp. 229–244. DOI: 10.1002/j.1538-7305.1938.tb00429.x.

[32] H. W. Bode and J. H. Cousins. *Network analysis and feedback amplifier design*. van Nostrand, 1945.

[33] B. Bona and M. Indri. „Friction compensation in robotics: an overview." In: *Proceedings of the 44th IEEE Conference on Decision and Control*. IEEE. 2005, pp. 4360–4367. DOI: 10.1109/CDC.2005.1582848.

[34] R. P. Borase, D. Maghade, S. Sondkar, and S. Pawar. „A review of PID control, tuning methods and applications." In: *International Journal of Dynamics and Control* 9.2 (2021), pp. 818–827. DOI: 10.1007/s40435-020-00665-4.

[35] S. Boyd and S. S. Sastry. „Necessary and sufficient conditions for parameter convergence in adaptive control." In: *Automatica* 22.6 (1986), pp. 629–639. DOI: 10.1016/0005-1098(86)90002-6.

[36] W. Bu, X. Tu, C. Lu, and Y. Pu. „Adaptive feedforward vibration compensation control strategy of bearingless induction motor." In: *International Journal of Applied Electromagnetics and Mechanics* 63.2 (2020), pp. 199–215. DOI: 10.3233/JAE-190092.

[37] D. Cabecinhas, P. Batista, P. Oliveira, and C. Silvestre. „Hovercraft control with dynamic parameters identification." In: *IEEE Trans. Control Syst. Technol.* 26.3 (2017), pp. 785–796. DOI: 10.1109/TCST.2017.2692733.

[38] R. Carroll and D. Lindorff. „An adaptive observer for single-input single-output linear systems." In: *IEEE Transactions on Automatic Control* 18.5 (1973), pp. 428–435. DOI: 10.1109/TAC.1973.1100367.

[39] N. Chakraborty and A. Ghosal. „Kinematics of wheeled mobile robots on uneven terrain." In: *Mechanism and machine theory* 39.12 (2004), pp. 1273–1287. DOI: 10.1016/j.mechmachtheory.2004.05.016.

[40] S. Chang, Y. Wang, and Z. Zuo. „Fixed-time active disturbance rejection control and its application to wheeled mobile robots." In: *IEEE Transactions on Systems, Man, and Cybernetics: Systems* 51.11 (2020), pp. 7120–7130. DOI: 10.1109/TSMC.2020.2966077.

[41] S. Chen, W. Bai, Y. Hu, Y. Huang, and Z. Gao. „On the conceptualization of total disturbance and its profound implications." In: *Science China Information Sciences* 63 (2020), pp. 1–3. DOI: 10.1007/s11432-018-9644-3.

[42] S. Chen, W. Bai, and Y. Huang. „ADRC for systems with unobservable and unmatched uncertainty." In: *2016 35th Chinese Control Conference (CCC)*. IEEE. 2016, pp. 337–342. DOI: 10.1109/ChiCC.2016.7553106.

[43] S. Chen, Z. Chen, and Z. Zhao. „An error-based active disturbance rejection control with memory structure." In: *Measurement and Control* 54 (5-6 2021), pp. 724–736. DOI: 10.1177/0020294020915219.

[44] S. Chen, Y. Huang, and Z. Zhao. *The necessary and sufficient condition for the uncertain control gain in active disturbance rejection control*. preprint. 2020.

[45] W. Chen. „Dynamic modeling of multi-link flexible robotic manipulators." In: *Computers & Structures* 79.2 (2001), pp. 183–195. DOI: 10.1016/S0045-7949(00)00129-2.

[46] W. Chen, F. Zhou, Y. Li, and R. Song. „The ship nonlinear course system control based on auto disturbance rejection controller." In: *2008 7th World Congress on Intelligent Control and Automation*. IEEE. 2008, pp. 6454–6458. DOI: 10.1109/WCICA.2008.4592876.

[47] X. Chen, D. Li, Z. Gao, and C. Wang. „Tuning method for second-order active disturbance rejection control." In: *Proceedings of the 30th Chinese control conference*. IEEE. 2011, pp. 6322–6327.

[48] Z. Chen, Y. Wang, M. Sun, and Q. Sun. „Convergence and stability analysis of active disturbance rejection control for first-order nonlinear dynamic systems." In: *Transactions of the Institute of Measurement and Control* 41.7 (2019), pp. 2064–2076. DOI: 10.1177/0142331218794812.

[49] Y. M. Cho and R. Rajamani. „A systematic approach to adaptive observer synthesis for nonlinear systems." In: *IEEE transactions on Automatic Control* 42.4 (1997), pp. 534–537. DOI: 10.1109/9.566664.

[50] M. Chu, G. Chen, F. J. Huang, and Q. X. Jia. „Active disturbance rejection control for trajectory tracking of manipulator joint with flexibility and friction." In: *Applied Mechanics and Materials*. Vol. 325. Trans Tech Publ. 2013, pp. 1229–1232. DOI: 10.4028/www.scientific.net/AMM.325-326.1229.

[51] M. Corless and G. Leitmann. „Continuous state feedback guaranteeing uniform ultimate boundedness for uncertain dynamic systems." In: *IEEE Transactions on Automatic Control* 26.5 (1981), pp. 1139–1144. DOI: 10.1109/TAC.1981.1102785.

[52] P. R. Dahl. *Measurement of solid friction parameters of ball bearings*. Tech. rep. Aerospace Corp El Segundo Ca Engineering Science Operations, 1977.

[53] C. C. De Wit, H. Olsson, K. J. Astrom, and P. Lischinsky. „A new model for control of systems with friction." In: *IEEE Transactions on automatic control* 40.3 (1995), pp. 419–425. DOI: 10.1109/9.376053.

[54] W. Deng and J. Yao. „Extended-state-observer-based adaptive control of electrohydraulic servomechanisms without velocity measurement." In: *IEEE/ASME Transactions on Mechatronics* 25.3 (2019), pp. 1151–1161. DOI: 10.1109/TMECH.2019.2959297.

[55] W. Dixon, I. Walker, and D. Dawson. „Fault detection for wheeled mobile robots with parametric uncertainty." In: *2001 IEEE/ASME International Conference on Advanced Intelligent Mecha-*

tronics. Proceedings. Vol. 2. IEEE. 2001, pp. 1245–1250. DOI: 10.1109/AIM.2001.936891.

[56] Q. Dong and Q. Li. „Current Control of BLDCM Based on Fuzzy Adaptive ADRC." In: *2009 Ninth International Conference on Hybrid Intelligent Systems*. Vol. 3. 2009, pp. 355–358. DOI: 10.1109/HIS.2009.285.

[57] P. Dorato. „A historical review of robust control." In: *IEEE Control Systems Magazine* 7.2 (1987), pp. 44–47. DOI: 10.1109/MCS.1987.1105273.

[58] P. Dorato, R. Tempo, and G. Muscato. „Bibliography on robust control." In: *Automatica* 29.1 (1993), pp. 201–213. DOI: 10.1016/0005-1098(93)90183-T.

[59] J. Doyle. „Robust and optimal control." In: *Proceedings of the 35th IEEE Conference on Decision and Control*. IEEE. 1996, pp. 1595–1598. DOI: 10.1109/CDC.1996.572756.

[60] V. Dragan, T. Morozan, and A.-M. Stoica. *Mathematical methods in robust control of linear stochastic systems*. Springer, 2006. DOI: 10.1007/978-1-4614-8663-3.

[61] R. Drenick and R. Shahbender. „Adaptive servomechanisms." In: *Transactions of the American Institute of Electrical Engineers, Part II: Applications and Industry* 76.5 (1957), pp. 286–292. DOI: 10.1109/TAI.1957.6367242.

[62] B. Egardt. „Lecture Notes in Control and Information Sciences." In: *Stability of adaptive controllers*. Springer-Verlag Berlin, 1979, p. 20.

[63] Espressif Systems. *ESP32*. https://www.espressif.com/en/products/socs/esp32. [Online; accessed 25-January-2023].

[64] M. S. Fadali. „On the stability of Han's ADRC." In: *2014 American Control Conference*. IEEE. 2014, pp. 3597–3601. DOI: 10.1109/ACC.2014.6859248.

[65] C. J. Fallaha, M. Saad, H. Y. Kanaan, and K. Al-Haddad. „Sliding-mode robot control with exponential reaching law." In: *IEEE Transactions on industrial electronics* 58.2 (2010), pp. 600–610. DOI: 10.1109/TIE.2010.2045995.

[66] I. Fantoni, R. Lozano, F. Mazenc, and K. Pettersen. „Stabilization of a nonlinear underactuated hovercraft." In: *Proc. of the 38th IEEE Conf. Decis. Control*. Vol. 3. IEEE. 1999, pp. 2533–2538. DOI: 10.1002/1099-1239(20000715)10:8<645::AID-RNC503>3.0.CO;2-U.

[67] R. Fareh, S. Khadraoui, M. Y. Abdallah, M. Baziyad, and M. Bettayeb. „Active disturbance rejection control for robotic systems: A review." In: *Mechatronics* 80 (2021), p. 102671. DOI: 10.1016/j.mechatronics.2021.102671.

[68] R. Fareh, M. Al-Shabi, M. Bettayeb, and J. Ghommam. „Robust active disturbance rejection control for flexible link manipulator." In: *Robotica* 38.1 (2020), pp. 118–135. DOI: 10.1017/S02635747 1900050X.

[69] G. Feng, L. Huang, and D. Zhu. „A nonlinear auto-disturbance rejection controller for induction motor." In: *IECON'98. Proceedings of the 24th Annual Conference of the IEEE Industrial Electronics Society*. Vol. 3. IEEE. 1998, pp. 1509–1514. DOI: 10.1109/IECON.1998.722875.

[70] G. Feng and Y. Liu. „An improved nonlinear control strategy for induction motor drive." In: *Canadian Conference on Electrical and Computer Engineering 2001. Conference Proceedings*. Vol. 1. IEEE. 2001, pp. 7–12. DOI: 10.1109/CCECE.2001.933630.

[71] H. Feng and B.-Z. Guo. „Active disturbance rejection control: Old and new results." In: *Annual Reviews in Control* 44 (2017), pp. 238–248. DOI: 10.1016/j.arcontrol.2017.05.003.

[72] R. P. Foundation. *Raspberry Pi 4*. https://www.raspberrypi.com/products/raspberry-pi-4-model-b/. [Online; accessed 27-January-2023].

[73] B. A. Francis and W. M. Wonham. „The internal model principle of control theory." In: *Automatica* 12.5 (1976), pp. 457–465.

[74] L. B. Freidovich and H. K. Khalil. „Performance Recovery of Feedback-Linearization-Based Designs." In: *IEEE Transactions on Automatic Control* 53.10 (2008), pp. 2324–2334. DOI: 10.1109/TAC.2008.2006821.

[75] I. B. Furtat and A. M. Tsykunov. „Adaptive control of plants of unknown relative degree." In: *Automation and Remote Control* 71.6 (2010), pp. 1076–1084. DOI: 10.1134/S0005117910060081.

[76] B. R. Gaines. „Axioms for adaptive behaviour." In: *International Journal of Man-Machine Studies* 4.2 (1972), pp. 169–199. DOI: 10.1016/S0020-7373(72)80030-0.

[77] S. Gambhire, D. R. Kishore, P. Londhe, and S. Pawar. „Review of sliding mode based control techniques for control system applications." In: *International Journal of Dynamics and Control* 9.1 (2021), pp. 363–378. DOI: 10.1007/s40435-020-00638-7.

[78] W.-C. Gan and L. Qiu. „Torque and velocity ripple elimination of AC permanent magnet motor control systems using the internal model principle." In: *IEEE/ASME Transactions on Mechatronics* 9.2 (2004), pp. 436–447. DOI: 10.1109/TMECH.2004.828626.

[79] Z. Gao. „From linear to nonlinear control means: A practical progression." In: *ISA Transactions* 41.2 (2002), pp. 177–189. DOI: 10.1016/S0019-0578(07)60077-9.

[80] Z. Gao. „Scaling and bandwidth-parameterization based controller tuning." In: *Proceedings of the 2003 American Control Conference*. Vol. 6. 2003, pp. 4989–4996. DOI: 10.1109/ACC.2003.1242516.

[81] Z. Gao. „Active Disturbance Rejection Control: A Paradigm Shift in Feedback Control System Design." In: *Proceedings of the 2006 American Control Conference*. IEEE. 2006, pp. 2399–2405. DOI: 10.1109/ACC.2006.1656579.

[82] Z. Gao. „On the centrality of disturbance rejection in automatic control." In: *ISA Transactions* 53 (4 2014), pp. 850–857. DOI: 10.1016/j.isatra.2013.09.012.

[83] Z. Gao. „Active disturbance rejection control: from an enduring idea to an emerging technology." In: *2015 10th International Workshop on Robot Motion and Control (RoMoCo)*. IEEE. 2015, pp. 269–282. DOI: 10.1109/RoMoCo.2015.7219747.

[84] Z. Gao, Y. Huang, and J. Han. „An alternative paradigm for control system design." In: *Proceedings of the 40th IEEE conference on decision and control*. Vol. 5. IEEE. 2001, pp. 4578–4585. DOI: 10.1109/CDC.2001.980926.

[85] J. E. Gaudio, T. E. Gibson, A. M. Annaswamy, M. A. Bolender, and E. Lavretsky. „Connections between adaptive control and optimization in machine learning." In: *2019 IEEE 58th Conference on Decision and Control (CDC)*. IEEE. 2019, pp. 4563–4568. DOI: 10.1109/CDC40024.2019.9029197.

[86] T. E. Gibson and A. M. Annaswamy. „Adaptive control and the definition of exponential stability." In: *2015 American Control Conference (ACC)*. IEEE. 2015, pp. 1549–1554. DOI: 10.1109/ACC.2015.7170953.

[87] K. Glover, J. Sefton, and D. McFarlane. „A tutorial on loop shaping using H-infinity robust stabilisation." In: *Transactions of the Institute of Measurement and Control* 14.3 (1992), pp. 157–168. DOI: 10.1177/014233129201400306.

[88] I. Golovin and S. Palis. „Robust control for active damping of elastic gantry crane vibrations." In: *Mechanical Systems and Signal Processing* 121 (2019), pp. 264–278. DOI: 10.1016/j.ymssp.2018.11.005.

[89] L. Grayson. „Two theorems on the second method." In: *IEEE Transactions on Automatic Control* 9.4 (1964), pp. 587–587. DOI: 10.1109/TAC.1964.1105740.

[90] B.-Z. Guo and Z.-L. Zhao. „On convergence of the nonlinear active disturbance rejection control for MIMO systems." In: *SIAM Journal on Control and Optimization* 51.2 (2013), pp. 1727–1757. DOI: 10.1137/110856824.

[91] B.-Z. Guo and Z.-l. Zhao. „On the convergence of an extended state observer for nonlinear systems with uncertainty." In: *Systems & Control Letters* 60.6 (2011), pp. 420–430. DOI: 10.1016/j.sysconle.2011.03.008.

[92] S. Gutman. „Uncertain dynamical systems–A Lyapunov min-max approach." In: *IEEE Transactions on Automatic Control* 24.3 (1979), pp. 437–443. DOI: 10.1109/TAC.1979.1102073.

[93] W. M. Haddad and D. S. Bernstein. „Robust stabilization with positive real uncertainty: Beyond the small gain theorem." In: *Systems & Control Letters* 17.3 (1991), pp. 191–208. DOI: 10.1109/CDC.1990.203985.

[94] T. Hamel and C. Samson. „Transverse function control of a motorboat." In: *Automatica* 65 (2016), pp. 132–139. DOI: 10.1016/j.automatica.2015.11.040.

[95] H. Hammouri and Z. Tmar. „Unknown input observer for state affine systems: A necessary and sufficient condition." In: *Automatica* 46.2 (2010), pp. 271–278. DOI: 10.1016/j.automatica.2009.11.004.

[96] P. Hamon, M. Gautier, and P. Garrec. „Dynamic identification of robots with a dry friction model depending on load and velocity." In: *2010 IEEE/RSJ international conference on intelligent robots and systems*. IEEE. 2010, pp. 6187–6193. DOI: 10.1109/IROS.2010.5649189.

[97] J. Han. „Nonlinear tracking-differentiator." In: *Journal of Systems Science and Mathematical Sciences* 14 (1994). In Chinese, pp. 177–183.

[98] J. Han. „Auto-disturbances-rejection controller." In: *Proceedings of 2nd Asian Control Conference*. Vol. 3. In Chinese. ACA. 1997, pp. 567–570.

[99] J. Han. „A class of extended state observers for uncertain systems." In: *Control and decision* 10.1 (1995). In Chinese, pp. 85–88.

[100] J. Han. „Auto-disturbances-rejection Controller and It's Applications." In: *Control and decision* 13.1 (1998). In Chinese, pp. 19–23.

[101] J. Han. „Nonlinear design methods for control systems." In: *IFAC Proceedings Volumes* 32.2 (1999), pp. 1531–1536. DOI: 10.1016/S1474-6670(17)56259-X.

[102] J. Han. „From PID to Active Disturbance Rejection Control." In: *IEEE Transactions on Industrial Electronics* 56.3 (2009), pp. 900–906. DOI: 10.1109/TIE.2008.2011621.

[103] L. Hao, C. Xiang, M. E. Giannaccini, H. Cheng, Y. Zhang, S. Nefti-Meziani, and S. Davis. „Design and control of a novel variable stiffness soft arm." In: *Advanced Robotics* 32.11 (2018), pp. 605–622. DOI: 10.1080/01691864.2018.1476179.

[104] K. Harrington and J. K. Bennet. *Servo Library for ESP32*. https://github.com/madhephaestus/ESP32Servo. [Online; accessed 25-January-2023].

[105] D. J. Hill. „A generalization of the small-gain theorem for nonlinear feedback systems." In: *Automatica* 27.6 (1991), pp. 1043–1045. DOI: 10.1016/0005-1098(91)90140-W.

[106] Y. Hong and H. Li. „Nonlinear H infinity control and related problems of homogeneous systems." In: *International Journal of Control* 71.1 (1998), pp. 79–92. DOI: 10.1080/002071798221939.

[107] R. A. Horn and C. R. Johnson. *Topics in matrix control*. Cambridge University Press, 1991.

[108] M. Hou. „Estimation of sinusoidal frequencies and amplitudes using adaptive identifier and observer." In: *IEEE transactions on automatic control* 52.3 (2007), pp. 493–499. DOI: 10.1109/TAC.2006.890389.

[109] Y. Hou, Z. Gao, F. Jiang, and B. T. Boulter. „Active disturbance rejection control for web tension regulation." In: *Proceedings of the 40th IEEE Conference on Decision and Control*. Vol. 5. IEEE. 2001, pp. 4974–4979. DOI: 10.1109/CDC.2001.980997.

[110] Z.-G. Hou, Y. Huang, and J.-Q. Han. „Active noise cancellation with a nonlinear control mechanism." In: *Proceedings of the 37th IEEE Conference on Decision and Control*. Vol. 2. IEEE. 1998, pp. 1577–1578. DOI: 10.1109/CDC.1998.758516.

[111] C. Huang and L. Guo. „Control of a class of nonlinear uncertain systems by combining state observers and parameter estimators." In: *Proceedings of the 10th world congress on intelligent control and automation*. IEEE. 2012, pp. 2054–2059. DOI: 10.1109/WCICA.2012.6358214.

[112] H. Huang, L. Wu, J. Han, G. Feng, and Y. Lin. „A new synthesis method for unit coordinated control system in thermal power plant-ADRC control scheme." In: *2004 International Conference on Power System Technology, 2004. PowerCon 2004.* Vol. 1. IEEE. 2004, pp. 133–138. DOI: 10.1109/ICPST.2004.1459980.

[113] S. Huang, W. Liang, and K. K. Tan. „Intelligent friction compensation: A review." In: *IEEE/ASME Transactions on Mechatronics* 24.4 (2019), pp. 1763–1774. DOI: 10.1109/TMECH.2019.2916665.

[114] Y. Huang and J. Han. „Analysis and design for the second order nonlinear continuous extended states observer." In: *Chinese science bulletin* 45.21 (2000), pp. 1938–1944. DOI: 10.1007/BF02909682.

[115] Y. Huang, K. Xu, J. Han, and J. Lam. „Flight control design using extended state observer and non-smooth feedback." In: *Proceedings of the 40th IEEE Conference on Decision and Control*. Vol. 1. IEEE. 2001, pp. 223–228. DOI: 10.1109/CDC.2001.980102.

[116] Y. Huang and W. Xue. „Active disturbance rejection control: Methodology and theoretical analysis." In: *ISA transactions* 53.4 (2014), pp. 963–976. DOI: 10.1016/j.isatra.2014.03.003.

[117] A. J. Humaidi, H. M. Badr, and A. R. Ajil. „Design of active disturbance rejection control for single-link flexible joint robot manipulator." In: *2018 22nd International Conference on System Theory, Control and Computing (ICSTCC)*. IEEE. 2018, pp. 452–457. DOI: 10.1109/ICSTCC.2018.8540652.

[118] Institute of Electrical and Electronics Engineers. *IEEE Xplore*. https://ieeexplore.ieee.org/. [Online; accessed 25-January-2023].

[119] P. Ioannou and J. Sun. „Theory and design of robust direct and indirect adaptive-control schemes." In: *International Journal of Control* 47.3 (1988), pp. 775–813. DOI: 10.1080/00207178808906054.

[120] P. Ioannou and S. Baldi. „Robust adaptive control." In: *The Control System Handbook*. CRC Press, 2011. DOI: 10.1201/b10384-41.

[121] P. A. Ioannou and P. V. Kokotovic. *Adaptive systems with reduced models*. Springer, 1983. DOI: 10.1007/BFb0006357.

[122] P. A. Ioannou and J. Sun. *Robust adaptive control*. Prentice Hall, 1996.

[123] A. Isidori and W. Kang. „H_∞ control via measurement feedback for general nonlinear systems." In: *IEEE Transactions on Automatic Control* 40.3 (1995), pp. 466–472. DOI: 10.1002/rnc.4590040409.

[124] R. A. Jarvis. „Optimization strategies in adaptive control: a selective survey." In: *IEEE Transactions on Systems, Man, and Cybernetics* 1 (1975), pp. 83–94. DOI: 10.1109/TSMC.1975.5409158.

[125] S. Jeong and D. Chwa. „Coupled multiple sliding-mode control for robust trajectory tracking of hovercraft with external disturbances." In: *IEEE Trans. Ind. Electron.* 65.5 (2017), pp. 4103–4113. DOI: 10.1109/TIE.2017.2774772.

[126] T. Jiang, C. Huang, and L. Guo. „Control of uncertain nonlinear systems based on observers and estimators." In: *Automatica* 59 (2015), pp. 35–47. DOI: 10.1016/j.automatica.2015.06.012.

[127] Z.-P. Jiang and T. Liu. „Small-gain theory for stability and control of dynamical networks: A survey." In: *Annual Reviews in Control* 46 (2018), pp. 58–79. DOI: 10.1016/j.arcontrol.2018.09.001.

[128] N. H. Jo, Y. Joo, and H. Shim. „A study of disturbance observers with unknown relative degree of the plant." In: *Automatica* 50.6 (2014), pp. 1730–1734. DOI: 10.1016/j.automatica.2014.04.015.

[129] C. Johnson. „Accomodation of external disturbances in linear regulator and servomechanism problems." In: *IEEE Transactions on automatic control* 16.6 (1971), pp. 635–644. DOI: 10.1109/TAC.1971.1099830.

[130] G. Joshi and G. Chowdhary. „Deep model reference adaptive control." In: *2019 IEEE 58th Conference on Decision and Control (CDC)*. IEEE. 2019, pp. 4601–4608. DOI: 10.1109/CDC40024.2019.9029173.

[131] G. Joshi, J. Virdi, and G. Chowdhary. „Asynchronous deep model reference adaptive control." In: *Conference on Robot Learning*. PMLR. 2021, pp. 984–1000.

[132] S. M. Joshi and S. Gupta. „On a class of marginally stable positive-real systems." In: *IEEE Transactions on Automatic Control* 41.1 (1996), pp. 152–155. DOI: 10.1109/9.481623.

[133] T. Kaczorek, A. Dzieliński, W. Dąbrowski, and R. Łopatka. *Podstawy teorii sterowania*. In Polish. Wydawnictwo WNT, 2020.

[134] R. E. Kalman. „Design of a self-optimizing control system." In: *Transactions of the American Society of Mechanical Engineers* 80.2 (1958), pp. 468–477. DOI: 10.1115/1.4012407.

[135] M. Karkoub and K. Tamma. „Modelling and μ-synthesis control of flexible manipulators." In: *Computers & Structures* 79.5 (2001), pp. 543–551. DOI: 10.1016/S0045-7949(00)00155-3.

[136] A. Kelkar and S. Joshi. „Robust control of non-passive systems via passification [for passification read passivation]." In: *Proceedings of the 1997 American Control Conference*. Vol. 5. IEEE. 1997, pp. 2657–2661. DOI: 10.1109/ACC.1997.611938.

[137] H. K. Khalil. *Nonlinear Control, 3rd Edition*. Prentice Hall Upper Saddle River, NJ, 2002.

[138] F. Khani and A. Yazdizadeh. „Boiler-turbine unit controller design based on the extended state observer." In: *2009 IEEE International Conference on Control and Automation*. 2009, pp. 2066–2071. DOI: 10.1109/ICCA.2009.5410201.

[139] V. L. Kharitonov. „Robust stability analysis of time delay systems: A survey." In: *Annual Reviews in Control* 23 (1999), pp. 185–196. DOI: 10.1016/S1367-5788(99)00021-8.

[140] P. V. Kokotović. „Applications of singular perturbation techniques to control problems." In: *SIAM review* 26.4 (1984), pp. 501–550. DOI: 10.1137/1026104.

[141] H. Komurcugil, S. Biricik, S. Bayhan, and Z. Zhang. „Sliding mode control: Overview of its applications in power converters." In: *IEEE Industrial Electronics Magazine* 15.1 (2020), pp. 40–49. DOI: 10.1109/MIE.2020.2986165.

[142] M. Korotina, J. G. Romero, S. Aranovskiy, A. Bobtsov, and R. Ortega. „A new on-line exponential parameter estimator without persistent excitation." In: *Systems & Control Letters* 159 (2022), p. 105079. DOI: 10.1016/j.sysconle.2021.105079.

[143] K. Kozlowski, D. Pazderski, B. Krysiak, T. Jedwabny, J. Piasek, S. Kozlowski, S. Brock, D. Janiszewski, and K. Nowopolski. „High precision automated astronomical mount." In: *Automation 2019: Progress in Automation, Robotics and Measurement Techniques*. Springer, 2019, pp. 299–315. DOI: 10.1007/978-3-030-13273-6_29.

[144] K. Kozłowski. „Application on Non-Linear Techniques in Robot Control." In: *Journal of Intelligent & Robotic Systems* 85.3-4 (2017), p. 411. DOI: 10.1007/s10846-016-0406-4.

[145] K. Kozłowski, W. Kowalczyk, B. Krysiak, M. Kiełczewski, and T. Jedwabny. „Modular architecture of the multi-robot system for teleoperation and formation control purposes." In: *9th International Workshop on Robot Motion and Control*. IEEE. 2013, pp. 19–24. DOI: 10.1109/RoMoCo.2013.6614578.

[146] K. Kozłowski and D. Pazderski. „Modeling and control of a 4-wheel skid-steering mobile robot." In: *International journal of applied mathematics and computer science* 14.4 (2004), pp. 477–496.

[147] S. Kozłowski, D. Pazderski, B. Krysiak, R. Patelski, T. Jedwabny, K. Kozłowski, and M. Sybis. „SkyLab: Research and development facility for ground-based observations." In: *Ground-based and Airborne Telescopes VIII*. Vol. 11445. SPIE. 2020, pp. 1399–1408. DOI: 10.1117/12.2576332.

[148] G. Kreisselmeier. „Adaptive observers with exponential rate of convergence." In: *IEEE Transactions on Automatic Control* 22.1 (1977), pp. 2–8. DOI: 10.1109/TAC.1977.1101401.

[149] G. Kreisselmeier and K. Narendra. „Stable model reference adaptive control in the presence of bounded disturbances." In: *IEEE Transactions on Automatic Control* 27.6 (1982), pp. 1169–1175. DOI: 10.1109/TAC.1982.1103093.

[150] M. Krstic, P. V. Kokotovic, and I. Kanellakopoulos. *Nonlinear and adaptive control design*. John Wiley & Sons, Inc., 1995.

[151] B. Krysiak, D. Pazderski, S. Kozłowski, and K. Kozłowski. „High Efficiency Direct-drive Mount for Space Surveillance and NEO Applications." In: *Publications of the Astronomical Society of the Pacific* 132.1015 (2020), p. 095002. DOI: 10.1088/1538-3873/ab9cc5.

[152] I. D. Landau. *Adaptive Control: The Model Reference Approach*. Marcel Dekker, 1979.

[153] I. Landau. „From robust control to adaptive control." In: *Control Engineering Practice* 7.9 (1999), pp. 1113–1124. DOI: 10.1016/S0967-0661(99)00076-3.

[154] E. Lavretsky, T. E. Gibson, and A. M. Annaswamy. *Projection Operator in Adaptive Systems*. 2012.

[155] E. Lavretsky and K. A. Wise. „Robust and Adaptive Control with Output Feedback." In: *Robust and Adaptive Control: With Aerospace Applications*. Springer-Verlag London, 2013. Chap. 14, pp. 417–449.

[156] T. E. Lechekhab, S. Manojlovic, M. Stankovic, R. Madonski, and S. Simic. „Robust error-based active disturbance rejection control of a quadrotor." In: *Aircraft Engineering and Aerospace Technology* (2020). DOI: 10.1108/AEAT-12-2019-0266.

[157] C.-H. Lee. „A survey of PID controller design based on gain and phase margins." In: *International Journal of Computational Cognition* 2.3 (2004), pp. 63–100.

[158] T. H. Lee, K. K. Tan, and S. Huang. „Adaptive friction compensation with a dynamical friction model." In: *IEEE/ASME transactions on mechatronics* 16.1 (2010), pp. 133–140. DOI: 10.1109/TMECH.2009.2036994.

[159] G. Leitmann. „On one approach to the control of uncertain systems." In: *Proceedings of 1994 33rd IEEE Conference on Decision and Control*. IEEE. 1994, pp. 2112–2116. DOI: 10.1115/1.2899077.

[160] A. Levant. „Higher-order sliding modes, differentiation and output-feedback control." In: *International journal of Control* 76.9-10 (2003), pp. 924–941. DOI: 10.1080/0020717031000099029.

[161] F. Lewis, S. Jagannathan, and A. Yesildirak. *Neural network control of robot manipulators and non-linear systems*. CRC press, 2020. DOI: 10.1201/9781003062714.

[162] S. Li and Z. Liu. „Adaptive speed control for permanent-magnet synchronous motor system with variations of load inertia." In: *IEEE transactions on industrial electronics* 56.8 (2009), pp. 3050–3059. DOI: 10.1109/TIE.2009.2024655.

[163] S. Li, J. Yang, W.-H. Chen, and X. Chen. *Disturbance observer-based control: methods and applications*. CRC press, 2014. DOI: 10.1201/b16570.

[164] X. Li, Z. Gao, W. Ai, and S. Tian. „On the Equivalence between PID-like controller and LADRC for second-order systems." In: *2020 IEEE 9th Data Driven Control and Learning Systems Conference (DDCLS)*. 2020, pp. 1003–1008. DOI: 10.1109/DDCLS49620.2020.9275160.

[165] X. Li, W. Zhou, D. Jia, J. Qian, J. Luo, P. Jiang, and W. Ma. „A Decoupling Synchronous Control Method of Two Motors for Large Optical Telescope." In: *IEEE Transactions on Industrial Electronics* 69.12 (2022), pp. 13405–13416. DOI: 10.1109/TIE.2022.3142407.

[166] A. Liu, H. Zhao, T. Song, Z. Liu, H. Wang, and D. Sun. „Adaptive control of manipulator based on neural network." In: *Neural Computing and Applications* 33.9 (2021), pp. 4077–4085. DOI: 10.1007/s00521-020-05515-0.

[167] D. Liu, Q. Gao, Z. Chen, and Z. Liu. „Linear active disturbance rejection control of a two-degrees-of-freedom manipulator." In: *Mathematical Problems in Engineering* 2020 (2020). DOI: 10.1155/2020/6969207.

[168] R. Liu, F. Nageotte, P. Zanne, M. de Mathelin, and B. Dresp-Langley. „Deep reinforcement learning for the control of robotic manipulation: a focussed mini-review." In: *Robotics* 10.1 (2021), p. 22. DOI: 10.3390/robotics10010022.

[169] Y. Liu, Z. Zhu, and D. Howe. „Direct torque control of brushless DC drives with reduced torque ripple." In: *IEEE Transactions on Industry Applications* 41.2 (2005), pp. 599–608. DOI: 10.1109/TIA.2005.844853.

[170] L. Ljung. „Consistency of the least-squares identification method." In: *IEEE Transactions on Automatic Control* 21.5 (1976), pp. 779–781. DOI: 10.1109/TAC.1976.1101344.

[171] A. Loria, E. Panteley, and M. Maghenem. „Strict Lyapunov functions for model-reference adaptive control based on the Mazenc construction." In: *Congreso Nacional de Control Automático (CNCA 2019)*. Asociación de México de Control Automático. 2019, pp. 407–412.

[172] A. Loría, R. Kelly, and A. R. Teel. „Uniform parametric convergence in the adaptive control of mechanical systems." In: *European Journal of Control* 11.2 (2005), pp. 87–100. DOI: 10.3166/ejc.11.87-100.

[173] A. Loría and E. Panteley. „Uniform exponential stability of linear time-varying systems: revisited." In: *Systems & Control Letters* 47.1 (2002), pp. 13–24. DOI: 10.1016/S0167-6911(02)00165-2.

[174] A. Loría, E. Panteley, and A. Teel. „A new notion of persistency-of-excitation for UGAS of NLTV systems: Application to stabilisation of nonholonomic systems." In: *1999 European Control Conference (ECC)*. IEEE. 1999, pp. 1363–1368. DOI: 10.23919/ECC.1999.7099501.

[175] N. Lozada-Castillo, A. Luviano-Juárez, and I. Chairez. „Robust control of uncertain feedback linearizable systems based on adaptive disturbance estimation." In: *ISA transactions* 87 (2019), pp. 1–9. DOI: 10.1016/j.isatra.2018.10.003.

[176] G. Luders and K. Narendra. „An adaptive observer and identifier for a linear system." In: *IEEE Transactions on Automatic Control* 18.5 (1973), pp. 496–499. DOI: 10.1109/TAC.1973.1100369.

[177] G. Luders and K. Narendra. „A new canonical form for an adaptive observer." In: *IEEE Transactions on Automatic Control* 19.2 (1974), pp. 117–119. DOI: 10.1109/TAC.1974.1100499.

[178] A. M. Lyapunov. „The general problem of the stability of motion." In Russian. PhD thesis. Moscow University, 1892.

[179] K. Łakomy and M. M. Michałek. „The VFO path-following kinematic controller for robotic vehicles moving in a 3D space." In: *2017 11th International Workshop on Robot Motion and Control (RoMoCo)*. IEEE. 2017, pp. 263–268. DOI: 10.1109/RoMoCo.2017.8003923.

[180] K. Łakomy, R. Patelski, and D. Pazderski. „ESO architectures in the trajectory tracking ADR controller for a mechanical system: a comparison." In: *Advanced, contemporary control*. Springer, 2020, pp. 1323–1335.

[181] R. Madonski, M. Ramirez-Neria, M. Stanković, S. Shao, Z. Gao, J. Yang, and S. Li. „On vibration suppression and trajectory tracking in largely uncertain torsional system: An error-based ADRC approach." In: *Mechanical Systems and Signal Processing* 134 (2019), p. 106300. DOI: 10.1016/j.ymssp.2019.106300.

[182] R. Madonski, K. Łakomy, and J. Yang. „Comparative study of output-based and error-based ADRC schemes in application to buck converter-fed DC motor system." In: *2020 59th IEEE Conference on Decision and Control (CDC)*. IEEE. 2020, pp. 2744–2749. DOI: 10.1109/CDC42340.2020.9304198.

[183] R. Madonski, M. Stanković, S. Shao, Z. Gao, J. Yang, and S. Li. „Active disturbance rejection control of torsional plant with unknown frequency harmonic disturbance." In: *Control Engineering Practice* 100 (2020), p. 104413. DOI: 10.1016/j.conengprac.2020.104413.

[184] R. Madonski, S. Shao, H. Zhang, Z. Gao, J. Yang, and S. Li. „General error-based active disturbance rejection control for swift industrial implementations." In: *Control Engineering Practice* 84 (2019), pp. 218–229. DOI: 10.1016/j.conengprac.2018.11.021.

[185] R. Madoński. „On active disturbance rejection in robotic motion control." PhD thesis. Poznan University of Technology, 2016.

[186] R. Madoński, Z. Gao, and K. Łakomy. „Towards a turnkey solution of industrial control under the active disturbance rejection paradigm." In: *2015 54th Annual Conference of the Society of Instrument and Control Engineers of Japan (SICE)*. IEEE. 2015, pp. 616–621. DOI: 10.1109/SICE.2015.7285478.

[187] R. Madoński, M. Przybyła, M. Kordasz, and P. Herman. „Application of active disturbance rejection control to a reel-to-reel system seen in tire industry." In: *2011 IEEE International Conference on Automation Science and Engineering*. IEEE. 2011, pp. 274–278. DOI: 10.1109/CASE.2011.6042407.

[188] I. M. Mareels, B. D. Anderson, R. R. Bitmead, M. Bodson, and S. S. Sastry. „Revisiting the MIT rule for adaptive control." In: *Adaptive Systems in Control and Signal Processing 1986*. Elsevier, 1987, pp. 161–166. DOI: 10.1016/B978-0-08-034085-2.50031-6.

[189] R. Marine, G. L. Santosuosso, and P. Tomei. „Robust adaptive observers for nonlinear systems with bounded disturbances." In: *IEEE Transactions on automatic control* 46.6 (2001), pp. 967–972. DOI: 10.1109/9.928609.

[190] R. Marino. „Adaptive observers for single output nonlinear systems." In: *IEEE Transactions on Automatic Control* 35.9 (1990), pp. 1054–1058. DOI: 10.1109/9.58536.

[191] D. L. Martinez-Vazquez, A. Rodriguez-Angeles, and H. Sira-Ramirez. „Robust GPI observer under noisy measurements." In: *2009 6th International Conference on Electrical Engineering, Computing Science and Automatic Control (CCE)*. 2009, pp. 1–5. DOI: 10.1109/ICEEE.2009.5393403.

[192] MathWorks, Inc. *MATLAB*. https://www.mathworks.com/products/matlab.html. [Online; accessed 25-January-2023].

[193] J. C. Maxwell. „On governors." In: *Proceedings of the Royal Society of London* 16 (1868), pp. 270–283. DOI: 10.1017/CBO9780511710377.009.

[194] F. Mazenc. „Strict Lyapunov functions for time-varying systems." In: *Automatica* 39.2 (2003), pp. 349–353. DOI: 10.1016/S0005-1098(02)00233-9.

[195] F. Mazenc, M. De Queiroz, and M. Malisoff. „Uniform global asymptotic stability of a class of adaptively controlled nonlinear systems." In: *IEEE Transactions on Automatic Control* 54.5 (2009), pp. 1152–1158. DOI: 10.1109/TAC.2009.2013053.

[196] M. M. Michałek. „Robust trajectory following without availability of the reference time-derivatives in the control scheme with active disturbance rejection." In: *2016 American Control Conference (ACC)*. IEEE. 2016, pp. 1536–1541. DOI: 10.1109/ACC.2016.7525134.

[197] E. A. Misawa. „Robust nonlinear control system design: An overview." In: *1992 American Control Conference*. IEEE. 1992, pp. 1819–1823. DOI: 10.23919/ACC.1992.4792426.

[198] R. Mishkov and S. Darmonski. „Exact parameter estimation without persistent excitation in nonlinear adaptive control systems." In: *Seventh National Conference with International Participation" Process Automation in the Food and Biotechnology Industries"*,

2013/Scientific Works" Food Science, Engineering and Technologies 2013", Vol. LX, No. 2. Vol. 60. 2. 2013, pp. 100–106.

[199] Z. Mohamed, J. Martins, M. Tokhi, J. S. Da Costa, and M. Botto. „Vibration control of a very flexible manipulator system." In: *Control Engineering Practice* 13.3 (2005), pp. 267–277. DOI: 10.1016/j.conengprac.2003.11.014.

[200] R. V. Monopoli and L. Grayson. „Discussion on "Two theorems on the second method"." In: *IEEE Transactions on Automatic Control* 11.1 (1966), pp. 140–141. DOI: 10.1109/TAC.1966.1098272.

[201] R. Morales, H. Sira-Ram'ırez, and J. Somolinos. „Linear active disturbance rejection control of the hovercraft vessel model." In: *Ocean Engineering* 96 (2015), pp. 100–108. DOI: 10.1016/j.oceaneng.2014.12.031.

[202] P. Morin and C. Samson. „Control with transverse functions and a single generator of underactuated mechanical systems." In: *Proc. of the 45th IEEE Conf. Decis. Control*. Jan. 2007, pp. 6110–6115. DOI: 10.1109/CDC.2006.377277.

[203] K. Narendra. „The maturing of adaptive control." In: *Foundations of Adaptive Control*. Springer, 1991, pp. 1–36. DOI: 10.1007/BFb0044772.

[204] K. S. Narendra. „Parameter adaptive control-the end... or the beginning?" In: *Proceedings of 1994 33rd IEEE Conference on Decision and Control*. Vol. 3. IEEE. 1994, pp. 2117–2125. DOI: 10.1109/CDC.1994.411420.

[205] K. S. Narendra and A. M. Annaswamy. „Persistent excitation in adaptive systems." In: *International Journal of Control* 45.1 (1987), pp. 127–160. DOI: 10.1080/00207178708933715.

[206] K. S. Narendra and A. M. Annaswamy. *Stable adaptive systems*. Dover Publications, 2005.

[207] K. S. Narendra and Z. Han. „The changing face of adaptive control: the use of multiple models." In: *Annual reviews in control* 35.1 (2011), pp. 1–12. DOI: 10.1016/j.arcontrol.2011.03.010.

[208] K. S. Narendra and L. S. Valavani. „Direct and indirect adaptive control." In: *IFAC Proceedings Volumes* 11.1 (1978), pp. 1981–1987. DOI: 10.1016/S1474-6670(17)66174-3.

[209] I. NaturalPoint. *OptiTrack*. https://optitrack.com/. [Online; accessed 27-January-2023].

[210] M. Nowicki, R. Madoński, and K. Kozłowski. „First look at conditions on applicability of ADRC." In: *2015 10th International Workshop on Robot Motion and Control (RoMoCo)*. 2015, pp. 294–299. DOI: 10.1109/RoMoCo.2015.7219750.

[211] H. Nyquist. „Regeneration theory." In: *Bell system technical journal* 11.1 (1932), pp. 126–147. DOI: 10.1115/1.4015084.

[212] A. O'Dwyer. „PI and PID controller tuning rules: an overview and personal perspective." In: (2006). DOI: 10.1049/cp:20060431.

[213] W. Oelen, H. Berghuis, H. Nijmeijer, and C. C. De Wit. „Hybrid stabilizing control on a real mobile robot." In: *IEEE Robotics & Automation Magazine* 2.2 (1995), pp. 16–23. DOI: 10.1109/100.392415.

[214] V. A. Oliveira, L. V. Cossi, M. C. Teixeira, and A. M. Silva. „Synthesis of PID controllers for a class of time delay systems." In: *Automatica* 45.7 (2009), pp. 1778–1782. DOI: 10.1016/j.automatica.2009.03.018.

[215] H. Olsson, K. J. Åström, C. C. De Wit, M. Gäfvert, and P. Lischinsky. „Friction models and friction compensation." In: *Eur. J. Control* 4.3 (1998), pp. 176–195. DOI: 10.1016/S0947-3580(98)70113-X.

[216] R. Ortega, A. Bobtsov, A. Pyrkin, and S. Aranovskiy. „A parameter estimation approach to state observation of nonlinear systems." In: *Systems & Control Letters* 85 (2015), pp. 84–94. DOI: 10.1016/j.sysconle.2015.09.008.

[217] R. Ortega, V. Nikiforov, and D. Gerasimov. „On modified parameter estimators for identification and adaptive control. A unified framework and some new schemes." In: *Annual Reviews in Control* 50 (2020), pp. 278–293. DOI: 10.1016/j.arcontrol.2020.06.002.

[218] Palaform Ltd. *Model hovercraft*. https://modelhovercraft.co.uk/product/hovercraft-kits/sirius-600-radio-controlled-hovercraft-kit/. [Online; accessed 24-January-2023].

[219] S. I. Palomino-Resendiz, N. B. Lozada-Castillo, D. A. Flores-Hernández, O. O. Gutiérrez-Frías, and A. Luviano-Juárez. „Adaptive active disturbance rejection control of solar tracking systems with partially known model." In: *Mathematics* 9.22 (2021), p. 2871. DOI: 10.3390/math9222871.

[220] W. Pan and F. Chen. „Design of Ship Main Engine Speed Controller Based on Fuzzy Adaptive Active Disturbance Rejection Technique." In: *2010 International Conference on Intelligent System Design and Engineering Application*. Vol. 1. 2010, pp. 586–589. DOI: 10.1109/ISDEA.2010.295.

[221] Y. Pan, C. Yang, L. Pan, and H. Yu. „Integral sliding mode control: performance, modification, and improvement." In: *IEEE Transactions on Industrial Informatics* 14.7 (2017), pp. 3087–3096. DOI: 10.1109/TII.2017.2761389.

[222] E. Panteley, A. Loria, and A. Teel. „Relaxed persistency of excitation for uniform asymptotic stability." In: *IEEE Transactions on Automatic Control* 46.12 (2001), pp. 1874–1886. DOI: 10.1109/9.975471.

[223] P. Parks. „Liapunov redesign of model reference adaptive control systems." In: *IEEE Transactions on Automatic Control* 11.3 (1966), pp. 362–367. DOI: 10.1109/TAC.1966.1098361.

[224] R. Patelski, P. Bartkowiak, and D. Pazderski. *AST Communication Module*. https://github.com/rpatelski/AST-Communication-Module. [Online; accessed 27-January-2023; private].

[225] R. Patelski and P. Dutkiewicz. „On the stability of ADRC for manipulators with modelling uncertainties." In: *ISA transactions* 102 (2020), pp. 295–303. DOI: 10.1016/j.isatra.2020.02.027.

[226] R. Patelski and D. Pazderski. „Algorytm sterowania ruchem osi zrobotyzowanego montażu teleskopu." In: *Prace Naukowe Politechniki Warszawskiej. Elektronika*. In Polish. 2018.

[227] R. Patelski and D. Pazderski. „Tracking control for a cascade perturbed control system using the active disturbance rejection paradigm." In: *Archives of Control Sciences* 29.2 (2019), pp. 387–408. DOI: 10.24425/acs.2019.129387.

[228] R. Patelski and D. Pazderski. „Improving the active disturbance rejection controller tracking quality by the input-gain underestimation for a second-order plant." In: *Electronics* 10.8 (2021), p. 907. DOI: 10.3390/electronics10080907.

[229] R. Patelski and D. Pazderski. „Extended State Observer Based Parameter Identification of the Hovercraft System." In: *2022 26th International Conference on Methods and Models in Automation and Robotics (MMAR)*. IEEE. 2022, pp. 330–335. DOI: 10.1109/MMAR55195.2022.9874346.

[230] R. Patelski and D. Pazderski. „Identyfikacja modelu robota mobilnego z użyciem adaptacyjnego obserwatora ESO." In: *Prace Naukowe Politechniki Warszawskiej. Elektronika*. In Polish. 2022.

[231] R. Patelski and D. Pazderski. „Novel Adaptive Extended State Observer for Dynamic Parameter Identification with Asymptotic Convergence." In: *Energies* 15.10 (2022), p. 3602. DOI: 10.3390/en15103602.

[232] R. Patelski and D. Pazderski. „Parameter Identifying Disturbance Rejection Control with Asymptotic Error Convergence." In review. 2023.

[233] D. Pazderski, R. Patelski, B. Krysiak, and K. Kozłowski. „Analysis of an impact of inertia parameter in active disturbance rejection control structures." In: *Electronics* 9.11 (2020), p. 1801. DOI: 10.3390/electronics9111801.

[234] I. R. Petersen and R. Tempo. „Robust control of uncertain systems: Classical results and recent developments." In: *Automatica* 50.5 (2014), pp. 1315–1335. DOI: 10.1016/j.automatica.2014.02.042.

[235] K. Y. Pettersen and O. Egeland. „Exponential stabilization of an underactuated surface vessel." In: *Proc. of 35th IEEE Conf. Decis. Control*. Vol. 1. 1996, pp. 967–972. DOI: 10.1109/CDC.1996.574602.

[236] J. Piasek, R. Patelski, D. Pazderski, and K. Kozłowski. „Identification of a dynamic friction model and its application in a precise tracking control." In: *Acta Polytechnica Hungarica* 16.10 (2019), pp. 83–99. DOI: 10.12700/APH.16.10.2019.10.6.

[237] H. A. Pierson and M. S. Gashler. „Deep learning in robotics: a review of recent research." In: *Advanced Robotics* 31.16 (2017), pp. 821–835. DOI: 10.1080/01691864.2017.1365009.

[238] L. Praly and Z.-P. Jiang. „Further results on robust semiglobal stabilization with dynamic input uncertainties." In: *Proceedings of the 37th IEEE Conference on Decision and Control*. Vol. 1. 1998, 891–896 vol.1. DOI: 10.1109/CDC.1998.760806.

[239] J. Preminger and J. Rootenberg. „Some considerations relating to control systems employing the invariance principle." In: *IEEE Transactions on Automatic Control* 9.3 (1964), pp. 209–215. DOI: 10.1109/TAC.1964.1105722.

[240] M. Przybyła, M. Kordasz, R. Madoński, P. Herman, and P. Sauer. „Active Disturbance Rejection Control of a 2DOF manipulator with significant modeling uncertainty." In: *Bulletin of the Polish Academy of Sciences: Technical Sciences* (2012), pp. 509–520. DOI: 10.2478/v10175-012-0064-z.

[241] Z. Pu, R. Yuan, J. Yi, and X. Tan. „A class of adaptive extended state observers for nonlinear disturbed systems." In: *IEEE Transactions on Industrial Electronics* 62.9 (2015), pp. 5858–5869. DOI: 10.1109/TIE.2015.2448060.

[242] X. Qi, J. Li, Y. Xia, and Z. Gao. „On the Robust Stability of Active Disturbance Rejection Control for SISO Systems." In: *Circuits Syst. Signal Process.* 36.1 (2017), pp. 65–81. DOI: 10.1007/s00034-016-0302-y.

[243] X. Qi, J. Li, Y. Xia, and Z. Gao. „On the robust stability of active disturbance rejection control for SISO systems." In: *Circuits, Systems, and Signal Processing* 36.1 (2017), pp. 65–81. DOI: 10.1007/s00034-016-0302-y.

[244] M. S. Raafat and R. Akmeliawati. „Survey on robust control of precision positioning systems." In: *Recent patents on mechanical engineering* 5.1 (2012), pp. 55–68. DOI: 10.2174/2212797611205010055.

[245] R. Raible. „Comments on "An approach to self-adaptive control based on the use of time moment and a model reference"." In: *IEEE Transactions on Automatic Control* 8.3 (1963), pp. 270–270. DOI: 10.1109/TAC.1963.1105585.

[246] N. Rao Sripada and D. Grant Fisher. „Improved least squares identification." In: *International Journal of Control* 46.6 (1987), pp. 1889–1913. DOI: 10.1080/00207178708934023.

[247] H. D. Rojas and J. Cortés-Romero. „On the equivalence between Generalized Proportional Integral Observer and Disturbance Observer." In: *ISA Transactions* (2022). DOI: 10.1016/j.isatra.2022.06.032.

[248] S. B. Roy. „Relaxing persistence of excitation for parameter convergence in adaptive control: an initial excitation based approach." PhD thesis. IIT, Delhi, 2019.

[249] J. Ruan and Y. Li. „ADRC based ship course controller design and simulations." In: *2007 IEEE International Conference on Automation and Logistics*. IEEE. 2007, pp. 2731–2735. DOI: 10.1109/ICAL.2007.4339044.

[250] J. Ruan, F. Yang, R. Song, and Y. Li. „Study on ADRC-based intelligent vehicle lateral locomotion control." In: *2008 7th World Congress on Intelligent Control and Automation*. IEEE. 2008, pp. 2619–2624. DOI: 10.1109/WCICA.2008.4593336.

[251] M. G. Safonov. „Origins of robust control: Early history and future speculations." In: *Annual Reviews in Control* 36.2 (2012), pp. 173–181. DOI: 10.3182/20120620-3-DK-2025.00179.

[252] H. Sage, M. De Mathelin, and E. Ostertag. „Robust control of robot manipulators: a survey." In: *International Journal of control* 72.16 (1999), pp. 1498–1522. DOI: 10.1080/002071799220137.

[253] C. Samson. „Stability analysis of adaptively controlled systems subject to bounded disturbances." In: *Automatica* 19.1 (1983), pp. 81–86. DOI: 10.1016/0005-1098(83)90077-8.

[254] E. Sariyildiz and K. Ohnishi. „A guide to design disturbance observer." In: *Journal of Dynamic Systems, Measurement, and Control* 136.2 (2014), p. 021011. DOI: 10.1115/1.4025801.

[255] S. Sastry and M. Bodson. *Adaptive control: stability, convergence, and robustness*. 1989.

[256] D. Seborg, T. Edgar, and S. Shah. „Adaptive control strategies for process control: a survey." In: *AIChE Journal* 32.6 (1986), pp. 881–913. DOI: 10.1002/aic.690320602.

[257] B. Shackcloth and R. B. Chart. „Synthesis of model reference adaptive systems by Liapunov's second method." In: *IFAC Proceedings Volumes* 2.2 (1965), pp. 145–152. DOI: 10.1016/S1474-6670(17)69028-1.

[258] S. Shao and Z. Gao. „On the conditions of exponential stability in active disturbance rejection control based on singular perturbation analysis." In: *International Journal of Control* 90.10 (2017), pp. 2085–2097. DOI: 10.1080/00207179.2016.1236217.

[259] H. Shim, G. Park, Y. Joo, J. Back, and N. H. Jo. „Yet another tutorial of disturbance observer: robust stabilization and recovery of nominal performance." In: *Control Theory and Technology* 14.3 (2016), pp. 237–249. DOI: 10.1007/s11768-016-6006-9.

[260] Y. Shtessel, C. Edwards, L. Fridman, A. Levant, et al. *Sliding mode control and observation*. Vol. 10. Springer, 2014. DOI: 10.1007/978-0-8176-4893-0.

[261] N. Sidek and N. Sarkar. „Dynamic modeling and control of nonholonomic mobile robot with lateral slip." In: *Third International Conference on Systems (icons 2008)*. IEEE. 2008, pp. 35–40. DOI: 10.1109/ICONS.2008.22.

[262] G. J. Silva, A. Datta, and S. P. Bhattacharyya. *PID controllers for time-delay systems*. Vol. 43. Springer, 2005. DOI: 10.1201/9781420019612-9.

[263] L. Simoni, M. Beschi, G. Legnani, and A. Visioli. „Friction modeling with temperature effects for industrial robot manipulators." In: *2015 IEEE/RSJ international conference on intelligent robots and systems (IROS)*. IEEE. 2015, pp. 3524–3529. DOI: 10.1109/IROS.2015.7353869.

[264] A. Singh and A. Singla. „Kinematic modeling of robotic manipulators." In: *Proceedings of the national academy of sciences, India section A: physical sciences* 87.3 (2017), pp. 303–319. DOI: 10.1007/s40010-016-0285-x.

[265] H. Sira-Ramírez, C. López-Uribe, and M. Velasco-Villa. „Linear observer-based active disturbance rejection control of the omnidirectional mobile robot." In: *Asian Journal of Control* 15.1 (2013), pp. 51–63. DOI: 10.1002/asjc.523.

[266] H. Sira-Ramírez and E. Zurita-Bustamante. „On the equivalence between ADRC and Flat Filter based controllers: A frequency domain approach." In: *Control Engineering Practice* 107 (2021), p. 104656. DOI: 10.1016/j.conengprac.2020.104656.

[267] H. Sira-Ramírez. „Dynamic second-order sliding mode control of the hovercraft vessel." In: *IEEE Trans. Control Syst. Technol.* 10.6 (2002), pp. 860–865. DOI: 10.1109/TCST.2002.804134.

[268] H. Sira-Ramírez and C. A. Ibáñez. „On the control of the hovercraft system." In: *Dynamics and Control* 10.2 (2000), pp. 151–163. DOI: 10.1023/A:1008343807817.

[269] H. Sira-Ramírez and C. A. Ibáñez. „The control of the hovercraft system: a flatness based approach." In: *Proc. of the IEEE International Conf. on Control Applications*. IEEE. 2000, pp. 692–697. DOI: 10.1109/CCA.2000.897513.

[270] H. Sira-Ramírez, E. W. Zurita-Bustamante, and C. Huang. „Equivalence Among Flat Filters, Dirty Derivative-Based PID Controllers, ADRC, and Integral Reconstructor-Based Sliding Mode Control." In: *IEEE Transactions on Control Systems Technology* 28.5 (2020), pp. 1696–1710. DOI: 10.1109/TCST.2019.2919822.

[271] O. A. Somefun, K. Akingbade, and F. Dahunsi. „The dilemma of PID tuning." In: *Annual Reviews in Control* 52 (2021), pp. 65–74. DOI: 10.1016/j.arcontrol.2021.05.002.

[272] G. Sommerhoff. *Analytical Biology*. Oxford University Press, 1950.

[273] R. Song, Y. Li, W. Yu, F. Wang, and J. Ruan. „Study on adrc based lateral control for tracked mobile robots on stairs." In: *2008 IEEE International Conference on Automation and Logistics*. IEEE. 2008, pp. 2048–2052. DOI: 10.1109/ICAL.2008.4636500.

[274] M. W. Spong. „Modeling and Control of Elastic Joint Robots." In: *Journal of Dynamic Systems, Measurement, and Control* 109.4 (1987), pp. 310–318. DOI: 10.1115/1.3143860.

[275] M. R. Stanković, M. R. Rapaić, S. M. Manojlović, S. T. Mitrović, S. M. Simić, and M. B. Naumović. „Optimised active disturbance rejection motion control with resonant extended state observer." In: *International Journal of Control* 92.8 (2019), pp. 1815–1826. DOI: 10.1080/00207179.2017.1414308.

[276] STMicroelectronics. *STM32 32-bit Arm Cortex MCUs*. https://www.st.com/en/microcontrollers-microprocessors/stm32-32-bit-arm-cortex-mcus.html. [Online; accessed 27-January-2023].

[277] P. R. Stromer. „Adaptive or self-optimizing control systems — a bibliography." In: *IRE Transactions on Automatic control* 1 (1959), pp. 65–68. DOI: 10.1109/TAC.1959.6429404.

[278] W. Su and L. Xie. „Robust control of nonlinear feedback passive systems." In: *Systems & control letters* 28.2 (1996), pp. 85–93. DOI: 10.1016/0167-6911(96)00011-4.

[279] Y.-R. Su, Q. Wang, F.-B. Yan, and Y.-M. Huang. „Friction compensation for an m-Level telescope based on high-precision LuGre parameters identification." In: *Research in Astronomy and Astrophysics* 21.1 (2021), p. 019. DOI: 10.1088/1674-4527/21/1/19.

[280] N. Sünderhauf, O. Brock, W. Scheirer, R. Hadsell, D. Fox, J. Leitner, B. Upcroft, P. Abbeel, W. Burgard, M. Milford, et al. „The limits and potentials of deep learning for robotics." In: *The International journal of robotics research* 37.4-5 (2018), pp. 405–420. DOI: 10.1177/0278364918770733.

[281] R. S. Sutton, A. G. Barto, and R. J. Williams. „Reinforcement learning is direct adaptive optimal control." In: *IEEE control systems magazine* 12.2 (1992), pp. 19–22. DOI: 10.23919/ACC.1991.4791776.

[282] S. E. Talole and S. B. Phadke. „Extended state observer based control of flexible joint system." In: *2008 IEEE International Symposium on Industrial Electronics*. IEEE. 2008, pp. 2514–2519. DOI: 10.1109/ISIE.2008.4677013.

[283] Z. Tao, W. Shu, W. Lei, and Z. Yang. „Active Disturbance Rejection Control of Servo Systems with Friction." In: *2009 IITA International Conference on Control, Automation and Systems Engineering (case 2009)*. IEEE. 2009, pp. 558–561. DOI: 10.1109/CASE.2009.119.

[284] S. Thrun, W. Burgard, and D. Fox. *Probabilistic Robotics*. The MIT Press, 2006. DOI: 10.1145/504729.504754.

[285] G. Tian and Z. Gao. „Frequency response analysis of active disturbance rejection based control system." In: *2007 IEEE international conference on control applications*. IEEE. 2007, pp. 1595–1599. DOI: 10.1109/CCA.2007.4389465.

[286] G. Tian and Z. Gao. „From poncelet's invariance principle to active disturbance rejection." In: *2009 American Control Conference*. IEEE. 2009, pp. 2451–2457. DOI: 10.1109/ACC.2009.5160285.

[287] T. N. Truong, H.-J. Kang, and A. T. Vo. „An active disturbance rejection control method for robot manipulators." In: *International Conference on Intelligent Computing*. Springer. 2020, pp. 190–201. DOI: 10.1007/978-3-030-60796-8_16.

[288] J. G. Truxal. „Adaptive control." In: *IFAC Proceedings Volumes* 1.2 (1963), pp. 386–392. DOI: 10.1016/S1474-6670(17)69711-8.

[289] S. G. Tzafestas. „Mobile robot control and navigation: A global overview." In: *Journal of Intelligent & Robotic Systems* 91.1 (2018), pp. 35–58. DOI: 10.1007/s10846-018-0805-9.

[290] V. A. Ugrinovskii. „Robust H_∞ infinity control in the presence of stochastic uncertainty." In: *International Journal of Control* 71.2 (1998), pp. 219–237. DOI: 10.1080/002071798221849.

[291] T. Umeno and Y. Hori. „Robust speed control of DC servomotors using modern two degrees-of-freedom controller design." In: *IEEE Transactions on industrial electronics* 38.5 (1991), pp. 363–368. DOI: 10.1109/41.97556.

[292] V. Utkin. „Variable structure systems with sliding modes." In: *IEEE Transactions on Automatic control* 22.2 (1977), pp. 212–222. DOI: 10.1109/TAC.1977.1101446.

[293] V. Utkin, A. Poznyak, Y. Orlov, and A. Polyakov. „Conventional and high order sliding mode control." In: *Journal of the Franklin Institute* 357.15 (2020), pp. 10244–10261. DOI: 10.1016/j.jfranklin.2020.06.018.

[294] M. Vakil, R. Fotouhi, and P. Nikiforuk. „Energy-based approach for friction identification of robotic joints." In: *Mechatronics* 21.3 (2011), pp. 614–624. DOI: 10.1016/j.mechatronics.2010.12.007.

[295] N. Van Quyen, N. P. Quang, et al. „Dynamic model with a new formulation of Coriolis/centrifugal matrix for robot manipulators." In: *Journal of Computer Science and Cybernetics* 36.1 (2020), pp. 89–104. DOI: 10.15625/1813-9663/1/1/14557.

[296] R. Vilanova, V. Alfaro, O. Arrieta, and C. Pedret. „Analysis of the claimed robustness for PI/PID robust tuning rules." In: *18th Mediterranean Conference on Control and Automation, MED'10*. IEEE. 2010, pp. 658–662. DOI: 10.1109/MED.2010.5547796.

[297] D. Wang, H. He, and D. Liu. „Adaptive critic nonlinear robust control: A survey." In: *IEEE transactions on cybernetics* 47.10 (2017), pp. 3429–3451. DOI: 10.1109/TCYB.2017.2712188.

[298] S. Wang and J. Na. „Parameter estimation and adaptive control for servo mechanisms with friction compensation." In: *IEEE Transactions on Industrial Informatics* 16.11 (2020), pp. 6816–6825. DOI: 10.1109/TII.2020.2971056.

[299] Y. Wang, Z. Chen, M. Sun, Q. Sun, and M. Piao. „On Sign Projected Gradient Flow Optimized Extended State Observer Design for a Class of Systems with Uncertain Control Gain." In: *IEEE Transactions on Industrial Electronics* (2022). DOI: 10.1109/TIE.2022.3150096.

[300] Y. Wang, J. Liu, Z. Chen, M. Sun, and Q. Sun. „On the stability and convergence rate analysis for the nonlinear uncertain systems based upon active disturbance rejection control." In: *International Journal of Robust and Nonlinear Control* 30.14 (2020), pp. 5728–5750. DOI: 10.1002/rnc.5103.

[301] Y. Wang, H. Tong, and H. Ren. „NESO-Based Path Following Control for Underactuated Hovercrafts with Unknown Nonlinear Uncertainties and a Safety Limit Constraint." In: *Applied Sciences* 10.15 (2020), p. 5287. DOI: 10.3390/app10155287.

[302] A. Weinmann. *Uncertain models and robust control*. Springer Science & Business Media, 2012. DOI: 10.1007/978-3-7091-6711-3.

[303] H. P. Whitaker, J. Yamron, and A. Kezer. *Design of model-reference adaptive control systems for aircraft*. Massachusetts Institute of Technology, Instrumentation Laboratory, 1958.

[304] B. Widrow. „Pattern recognition and adaptive control." In: *IEEE Transactions on Applications and Industry* 83.74 (1964), pp. 269–277. DOI: 10.1109/TAI.1964.5407756.

[305] B. Wie and D. S. Bernstein. „Benchmark problems for robust control design." In: *Journal of Guidance, Control, and Dynamics* 15.5 (1992), pp. 1057–1059. DOI: 10.2514/3.20949.

[306] R. L. Williams, B. E. Carter, P. Gallina, and G. Rosati. „Dynamic model with slip for wheeled omnidirectional robots." In: *IEEE transactions on Robotics and Automation* 18.3 (2002), pp. 285–293. DOI: 10.1109/TRA.2002.1019459.

[307] World Robotics. *World Robotics 2021 Industrial Robots*. VDMA Verlag, 2021.

[308] World Robotics. *World Robotics 2021 Service Robots*. VDMA Verlag, 2021.

[309] A.-G. Wu and G.-R. Duan. „Design of Generalized PI Observers for Descriptor Linear Systems." In: *IEEE Transactions on Circuits and Systems I: Regular Papers* 53.12 (2006), pp. 2828–2837. DOI: 10.1109/TCSI.2006.885695.

[310] M. Wu, Y. He, and J.-H. She. *Stability analysis and robust control of time-delay systems*. Springer, 2010. DOI: 10.1007/978-3-642-03037-6.

[311] W. Xie, D. Cabecinhas, R. Cunha, and C. Silvestre. „Robust motion control of an underactuated hovercraft." In: *IEEE Trans. Control Syst. Technol.* 27.5 (2018), pp. 2195–2208. DOI: 10.1109/TCST.2018.2862861.

[312] S. Xu and T. Chen. „Robust H_∞ control for uncertain stochastic systems with state delay." In: *IEEE transactions on automatic control* 47.12 (2002), pp. 2089–2094. DOI: 10.1109/TAC.2002.805670.

[313] W. Xue, W. Bai, S. Yang, K. Song, Y. Huang, and H. Xie. „ADRC with adaptive extended state observer and its application to air–fuel ratio control in gasoline engines." In: *IEEE Transactions on Industrial Electronics* 62.9 (2015), pp. 5847–5857. DOI: 10.1109/TIE.2015.2435004.

[314] W. Xue and Y. Huang. „Comparison of the DOB based control, a special kind of PID control and ADRC." In: *Proceedings of the 2011 American control conference*. IEEE. 2011, pp. 4373–4379. DOI: 10.1109/ACC.2011.5991310.

[315] W. Xue and Y. Huang. „The active disturbance rejection control for a class of MIMO block lower-triangular system." In: *Proceedings of the 30th Chinese control conference*. IEEE. 2011, pp. 6362–6367.

[316] W. Xue and Y. Huang. „On frequency-domain analysis of ADRC for uncertain system." In: *2013 American Control Conference*. IEEE. 2013, pp. 6637–6642. DOI: 10.1109/ACC.2013.6580881.

[317] W. Xue and Y. Huang. „On performance analysis of ADRC for nonlinear uncertain systems with unknown dynamics and discontinuous disturbances." In: *Proceedings of the 32nd chinese control conference*. IEEE. 2013, pp. 1102–1107.

[318] W. Xue and Y. Huang. „On performance analysis of ADRC for a class of MIMO lower-triangular nonlinear uncertain systems." In: *ISA transactions* 53.4 (2014), pp. 955–962. DOI: 10.1016/j.isatra.2014.02.002.

[319] W. Xue and Y. Huang. „Performance analysis of 2-DOF tracking control for a class of nonlinear uncertain systems with discontinuous disturbances." In: *nternational Journal of Robust and Nonlinear Control* 28 (4 2018), pp. 1456–1473. DOI: 10.1002/rnc.3972.

[320] W. Xue, Y. Huang, and Z. Gao. „On ADRC for non-minimum phase systems: canonical form selection and stability conditions." In: *Control Theory and Technology*. Springer. 2016, pp. 199–208. DOI: 10.1007/s11768-016-6041-6.

[321] A. S. Yamashita. „A review on the uncertainty and disturbance estimator, its applications and extensions." In: *International Journal of Automation and Control* 11.4 (2017), pp. 384–410. DOI: 10.1504/IJAAC.2017.087053.

[322] X. Yang and Y. Huang. „Capabilities of extended state observer for estimating uncertainties." In: *2009 American control conference*. IEEE. 2009, pp. 3700–3705. DOI: 10.1109/ACC.2009.5160642.

[323] B. Yao and M. Tomizuka. „Smooth robust adaptive sliding mode control of manipulators with guaranteed transient performance." In: *Proceedings of 1994 American Control Conference - ACC '94*. Vol. 1. 1994, 1176–1180 vol.1. DOI: 10.1109/ACC.1994.751934.

[324] J. Yao, W. Deng, and Z. Jiao. „Adaptive control of hydraulic actuators with LuGre model-based friction compensation." In: *IEEE Transactions on Industrial Electronics* 62.10 (2015), pp. 6469–6477. DOI: 10.1109/TIE.2015.2423660.

[325] J. Yao, Z. Jiao, and D. Ma. „Adaptive robust control of DC motors with extended state observer." In: *IEEE transactions on industrial electronics* 61.7 (2013), pp. 3630–3637. DOI: 10.1109/TIE.2013.2281165.

[326] B. Yu, S. Kim, and J. Suk. „Robust control based on ADRC and DOBC for small-scale helicopter." In: *IFAC-PapersOnLine* 52.12 (2019), pp. 140–145. DOI: 10.1016/j.ifacol.2019.11.183.

[327] X. Yu, Y. Feng, and Z. Man. „Terminal sliding mode control–An overview." In: *IEEE Open Journal of the Industrial Electronics Society* 2 (2020), pp. 36–52. DOI: 10.1109/OJIES.2020.3040412.

[328] L. Zadeh. „On the definition of adaptivity." In: *Proceedings of the IEEE* 51.3 (1963), pp. 469–470. DOI: 10.1109/PROC.1963.1852.

[329] A. Zakai. „Emscripten: an LLVM-to-JavaScript compiler." In: *Proceedings of the ACM international conference companion on Object oriented programming systems languages and applications companion*. 2011, pp. 301–312. DOI: 10.1145/2048147.2048224.

[330] A. Zakai, D. Schuff, H. Ahn, G. Chen, and T. Lively. *Emscripten*. https://emscripten.org/. [Online; accessed 27-January-2023].

[331] G. Zames. „Functional analysis applied to nonlinear feedback systems." In: *IEEE Transactions on Circuit Theory* 10.3 (1963), pp. 392–404. DOI: 10.1109/TCT.1963.1082162.

[332] M. Zdancewicz, ed. *Politechnika Poznańska*. Broszura Informacyjna, Politechnika Poznańska, Dom Wydawniczy Netter. 2014.

[333] C. Zhang and X. Zhou. „The auto-disturbances rejection control of TCSC." In: *Control Engineering Practice* 7.2 (1999), pp. 195–199. DOI: 10.1016/S0967-0661(98)00186-5.

[334] D. Zhang and B. Wei. „A review on model reference adaptive control of robotic manipulators." In: *Annual Reviews in Control* 43 (2017), pp. 188–198. DOI: 10.1016/j.arcontrol.2017.02.002.

[335] D. Zhang, Q. Wu, and X. Yao. „Bandwidth Based Stability Analysis of Active Disturbance Rejection Control for Nonlinear Uncertain Systems." In: *Journal of Systems Science & Complexity* 31.6 (2018), pp. 49–68. DOI: 10.1007/s11424-018-7073-4.

[336] H. Zhang. „Information Driven Control Design: A Case for PMSM Control." PhD thesis. Cleveland State University, 2017.

[337] C. Zhao. „Capability of ADRC for minimum-phase plants with unknown orders and uncertain relative degrees." In: *Proceedings of the 29th Chinese Control Conference*. IEEE. 2010, pp. 6121–6126.

[338] C. Zhao and Y. Huang. „ADRC based input disturbance rejection for minimum-phase plants with unknown orders and/or uncertain relative degrees." In: *Journal of Systems Science and Complexity* 25.4 (2012), pp. 625–640. DOI: 10.1007/s11424-012-1022-4.

[339] C. Zhao and D. Li. „Control design for the SISO system with the unknown order and the unknown relative degree." In: *ISA transactions* 53.4 (2014), pp. 858–872. DOI: 10.1016/j.isatra.2013.10.001.

[340] C. Zhao, D. Li, J. Cui, and L. Tian. „Decentralized low-order ADRC design for MIMO system with unknown order and relative degree." In: *Personal and Ubiquitous Computing* 22.5 (2018), pp. 987–1004. DOI: 10.1007/s00779-018-1158-x.

[341] S. Zhao and Z. Gao. „Active disturbance rejection control for non-minimum phase systems." In: *Proceedings of the 29th Chinese control conference*. IEEE. 2010, pp. 6066–6070.

[342] Y. Zhao, L. Zhao, and H. Gao. „Vibration control of seat suspension using H_∞ reliable control." In: *Journal of Vibration and Control* 16.12 (2010), pp. 1859–1879. DOI: 10.1177/1077546309349852.

[343] Y. Zhao and X. Wang. „A review of low-frequency active vibration control of seat suspension systems." In: *Applied Sciences* 9.16 (2019), p. 3326. DOI: 10.3390/app9163326.

[344] Z.-L. Zhao and B.-Z. Guo. „On convergence of nonlinear active disturbance rejection control for MIMO systems." In: *Proceedings of the 31st Chinese Control Conference*. 2012, pp. 434–441.

[345] Z.-L. Zhao and B.-Z. Guo. „On convergence of nonlinear active disturbance rejection control for SISO nonlinear systems." In: *Journal of Dynamical and Control Systems* 22.2 (2016), pp. 385–412. DOI: 10.1007/s10883-015-9304-5.

[346] Q. Zheng. „On Active Disturbance Rejection Control: Stability Analysis and Applications in Disturbance Decoupling Control." PhD thesis. Cleveland State University, 2009.

[347] Q. Zheng, L. Q. Gaol, and Z. Gao. „On stability analysis of active disturbance rejection control for nonlinear time-varying plants with unknown dynamics." In: *2007 46th IEEE Conference on Decision and Control*. 2007, pp. 3501–3506. DOI: 10.1109/CDC.2007.4434676.

[348] K. Zhou and J. C. Doyle. *Essentials of robust control*. Prentice Hall Upper Saddle River, NJ, 1998.

[349] K. Zhou, P. P. Khargonekar, J. Stoustrup, and H. H. Niemann. „Robust stability and performance of uncertain systems in state space." In: *Proceedings of the 31st IEEE Conference on Decision and Control*. IEEE. 1992, pp. 662–667. DOI: 10.1109/CDC.1992.371646.

[350] W. Zhou, S. Shao, and Z. Gao. „A Stability Study of the Active Disturbance Rejection Control Problem by a Singular Perturbation Approach." In: *Applied Mathematical Sciences* 3 (2009), pp. 491–508.

[351] S. A. Zimmermann, T. F. Berninger, J. Derkx, and D. J. Rixen. „Dynamic modeling of robotic manipulators for accuracy evaluation." In: *2020 IEEE International Conference on Robotics and Automation (ICRA)*. IEEE. 2020, pp. 8144–8150. DOI: 10.1109/ICRA40945.2020.9197304.